Development of A Microbial Electrochemical Biosensor for Detection of Oil Sands Naphthenic Acids

by

Tae Hyun Chung

A thesis submitted in partial fulfillment of the requirements for the degree of

Master of Science

in

Environmental Engineering

Department of Civil and Environmental Engineering
University of Alberta

Abstract

With a large number of oil deposits in Canada, Alberta oil sands industries are currently conducting bitumen extraction processes using hot water. In oil sands process water (OSPW) from these oil sands operations, naphthenic acids (NAs) are identified as one of the primary sources of acute toxicity and were assessed for their endocrine-disrupting potentials. Hence, the monitoring of NAs in aqueous environmental matrices is crucial for oil sands-related industries. Commonly used analytical methods for NAs, such as Fourier transform infrared spectroscopy and high-performance liquid chromatography, are time-consuming, expensive, and samples must be sent to an analytical lab for analysis. Therefore, this study aims to develop a microbial electrochemical biosensor (MXC) for the detection of NAs in water samples. First, experiments were conducted to develop an optimal calibration method for the MXC biosensor by comparing different approaches (closed-circuit operation vs. charging-discharging operation) using a single model NA compound (cyclohexane carboxylic acid). The charging-discharging operation significantly increased the peak currents by 90-124 folds higher than that observed for closed-circuit operation. Besides, a strong linear relationship between model NA concentrations and the peak currents ($R^2 = 0.96$) was observed. Second, experiments were conducted to evaluate the impact of different environmental parameters on biosensor performance. The results revealed that this MXC biosensor would be sensitive to salinity levels and temperature changes; however, once calibrated, it can be used for measurement of NA concentrations. The method was further validated with a complex model NA compound (mixtures of alkylated cyclopentane carboxylic acid, CNA). Interestingly, enriching the anode biofilm with salt content (1500 mg/L) significantly reduced the performance of the MXC biosensor applied for CNA detection. Furthermore, the presence of other organics, such as polycyclic aromatic hydrocarbons (e.g., 2-

methylnaphalene and pyrene) in OSPW, can greatly interfere with the current output produced by CNA. However, still a linear relationship has been observed between CNA concentrations and current from the MXC biosensor. Overall, the results of this study demonstrated that with further development, MXC biosensors could be used as a simple bioanalytical tool for monitoring NA concentrations in OSPW.

Preface

Chapter 2 is under review as T.H. Chung, M.N.A. Meshref, B.R. Dhar (2020), "*A review and roadmap for developing electrochemical cell-based biosensors for recalcitrant environmental contaminants, emphasis on aromatic compounds*" in Chemical Engineering Journal. I was responsible for data curation, visualization, and writing the original draft including review and editing. M.N.A., Meshref was responsible for reviewing and editing the original draft. B.R., Dhar was responsible for supervision as well as editing and reviewing the original draft.

Chapter 3 has been published as T.H. Chung, M.N.A. Meshref, B.R. Dhar (2020), "*Microbial electrochemical biosensor for rapid detection of naphthenic acid in aqueous solution*", in the Journal of Electroanalytical Chemistry, vol. 873, 114405. I was responsible for conceptualization, methodology, formal analysis, data curation, visualization, and writing the original draft including review and editing. M.N.A., Meshref was responsible for formal analysis, data curation, visualization, and reviewing and editing the original draft. B.R., Dhar planned and supervised the study, including editing and reviewing the original draft.

Chapter 4 will be submitted as T.H. Chung, M.N.A. Meshref, B.R. Dhar (2020) in a peer-reviewed journal. I was responsible for conceptualization, methodology, formal analysis, data curation, visualization, and writing the original draft including review and editing. M.N.A., Meshref was responsible for formal analysis, data curation, visualization, and reviewing and editing the original draft. B.R., Dhar planned and supervised the study, including editing and reviewing the original draft.

Dedication

This work is wholeheartedly dedicated to my father, mother, other relatives, and my dear friends who have been the source of inspiration and gave me strength when I thought of giving up, who continually provide their moral, spiritual, emotional, and financial support, who shared their words of advice and encouragement to finish this study.

And I also dedicated this work to the Almighty God, thank you for the guidance, power of mind, protection, skills and strength, and for giving me a healthy life.

Acknowledgments

First and foremost, praise and thank God for His showers of blessings throughout my graduate studies to complete the thesis research successfully.

I would like to express my sincere gratitude to my supervisor, Dr. Bipro Dhar, for giving me the opportunity to further my studies in graduate school and pursue research that I find to be important and meaningful. His caring, friendship, empathy, dynamism, sincerity, vision, and motivation have deeply inspired me and have helped me to build my strength and career in the field of research. It was a great privilege and honor to work and study under his guidance. Words cannot describe how extremely grateful I am for meeting him and what he has offered me over the past two years.

I would also like to express my appreciation to the current and former lab members of Dhar lab, Basem Zakaria, Sajib Barua, John Ryue, and especially, Mohamed Meshref for their amazing guidance and mentorship as well as invaluable assistance and input.

I also greatly thank the donors of the scholarships and awards (Alberta Innovates Graduate Student Scholarship, Westmoreland Coal Company Graduate Student Scholarship, University of Alberta Graduate Fellowship, and Korean-Canadian Scholarships) that I have received during my Master's program at the University of Alberta. I also thank the Natural Sciences and Engineering Research Council of Canada (NSERC) and Imperial Oil to support this research project. Special thanks go to our collaborators from Imperial's Breakthrough & Innovation Team (Calgary, AB) for their review and valuable comments to improve manuscripts.

Finally, special thanks are also owed to my father Joong Ha Alex Chung, mother Jin Goo Choi, brother Jae Hyun Jack Chung, sister-in-law Sera Pyo, and dear friends Felix Jihoon Park,

Gloria Hyunsu Cho, Gimoon Wang, Alex (Dowook) Kim, Jun-Kyu Kwak, and especially, Anqi Mou for their indescribable, steadfast, and unfailing love and support during my graduate studies. Their kind and lovely words always kept me motivated and brought me so many joys.

Table of Contents

List of Tables

List of Figures

List of Abbreviations and Acronyms

2-MN	2-Methylnaphthalene
3D	Three-Dimensional
4-NP	4-Nitrophenol
AD	Anaerobic Digestion
AEF	Acid-Extractable Fraction
AEM	Anion-Exchange Membrane
ANN	Artificial Neural Networks
BE	Benzoylecgonine
BOD	Biochemical Oxygen Demand
BTEX	Benzene, Toluene, Ethylbenzene, Xylene
CC	Closed-Circuit
CD	Charging-Discharging
CEM	Cation-Exchange Membrane
CHA	Cyclohexane Carboxylic Acid
c-NA	Classical Naphthenic Acid
CNA	Commercial Naphthenic Acid
COD	Chemical Oxygen Demand
CY	Columbic Yields
DAQ	Data Acquisition
EAB	Electroactive Bacteria
EET	Extracellular Electron Transfer

EPEA	Environmental Protection and Enhancement Act
FTICR-MS	Fourier Transform Ion Cyclotron Resonance Mass Spectrometry
FTIR	Fourier Transform Infrared
GC-MS	Gas Chromatography Mass Spectrometry
HPLC	High-Performance Liquid Chromatography
HPLC-UHRMS	High-Performance Liquid Chromatography Ultra-Resolution Mass Spectrometry
IEM	Ion-Exchange Membrane
LCMS	Liquid Chromatography Mass Spectrometry
MDC	Microbial Desalination Cell
MEC	Microbial Electrolysis Cell
MFC	Microbial Fuel Cell
MFT	Matured Fine Tailings
MS	Mass Spectrometry
MXC	Microbial Electrochemical Cell
NA	Naphthenic Acid
OSPW	Oil Sands Process-Affected Water
oxy-NA	Oxygenated Naphthenic Acid
PAH	Polycyclic Aromatic Hydrocarbon
PB	Prussian Blue
PCB	Polychlorinated Biphenyls
PNP	P-Nitrophenol
SFS	Synchronous Fluorescence Spectroscopy

SHE	Standard Hydrogen Electrode
SPEEK	Sulfonated Polyether ketone
UPLC-QTOF-MS	Ultra-High-Performance Liquid Chromatography-Quadrupole Time of Flight Mass Spectrometry
UPLC-TOF-MS	Ultra-High-Performance Liquid Chromatography Time of Flight Mass Spectrometry
VOC	Volatile Organic Carbon

Chapter 1 – Extended Background on the Oil Sands Naphthenic Acids

1-1. Background and Motivation

Canada's oil sands are proven to be one of the largest crude oil deposits in the world (Allen, 2008) with the total volume of recoverable oil stored in northern Alberta oil sands estimated to be 170 billion barrels of bitumen (Zhang et al., 2018). These oil sands resources are approximately composed of 1-8 weight percent (wt%) water, 6-16 wt% bitumen, and 80-87 wt% sand, silt, and clay (Kannel & Gan, 2012). During the surface mining operation, the estimates of the production of oil sands bitumen and heavy oil will be increased to 4 million barrels per day by 2024 in comparison to 2 million barrels a day in 2014 (Bari & Kindzierski, 2018). In addition, approximately, 4 m^3 of tailings are being generated per m^3 of processed oil sands (Holowenko et al., 2002; Scott et al., 2008b). The most concerning aspect of Alberta oil sands is the production of a large volume of oil sands tailings and oil sands process-affected water (OSPW) during the hot water bitumen extraction process (Benally et al., 2018) by oil sands-related industries (Barrow et al., 2015; Wu et al., 2019).

Due to Alberta's zero-discharge regulation, the discharged OSPW is stored in engineered on-site settling basins, which are widely known as oil sands tailings ponds (Allen, 2008; Xue et al., 2018) and the part of this OSPW is recycled back into the extraction processes (Wu et al., 2019). Generally, 2-4 barrels of fresh water are typically required to produce a barrel of bitumen (Brisbois et al., 2019; Headley et al., 2013b; Zubot, 2010). The freshwater withdrawals can be reduced by significant recycling of tailings. The recycling back in the extraction processes can be up to a certain extent, approximately 18 times, and the recycled OSPW should be safely stored again in the oil sands tailing ponds (Barrow et al., 2015). Despite the recycling of overlying water into the extraction process, a large volume of OSPW (~170,000 m^3) is still being continuously

accumulated and stored in the tailing ponds (Barrow et al., 2015; Fennell & Arciszewski, 2019; Redman et al., 2018). Additionally, greater than 1 billion m^3 of mature fine tailings are expected to be stored in the oil-sand tailings ponds near the oil sands region of northern Alberta by 2025 (Martin, 2015; Rogers et al., 2002b; Wu et al., 2019). Despite the heavy recycling of OSPW for reuse in the extraction processes, this growing inventory-volume of tailings ponds (approximately covering >170 km^2) (Martin et al., 2008; Sohrabi et al., 2013; Wiseman et al., 2013; Wu et al., 2019) necessitate the urgent need for extensive remediation and appropriate monitoring. Particularly, the presence of various water-soluble organics from bitumen in OSPW poses a significant threat to the aquatic ecosystem and wildlife (Garcia-Garcia et al., 2011; Hagen et al., 2014). Numerous studies have confirmed that the toxicity of OSPW is primarily attributed to the presence of various naphthenic acids (NAs) that are natural components of petroleum (El-Din et al., 2011; Mahaffey & Dubé, 2016; Pérez-Estrada et al., 2011; Shi et al., 2017). Hence, the management of these large volumes of the OSPW containing NAs is crucial as one of the major environmental challenges faced by many oil sands mining companies in Alberta. Ultimately, the monitoring of OSPW, especially the NAs became essential due to its infiltration into groundwater and a similar potential influence on the surface water bodies through the OSPW seepage (Fennell & Arciszewski, 2019; Huang et al., 2018).

1-1.1 Oil sands process-affected water (OSPW)

OSPW frequently contains problematic constituents that require treatment before discharge into the receiving aquatic ecosystem (Allen, 2008; McQueen et al., 2017). It consists of suspended solids, various organic compounds, including unrecovered bitumen and hydrocarbons, inorganic compounds, salts, and trace metals (Allen, 2008; El-Din et al., 2011; Fu et al., 2017; Headley et al., 2013b; Mahaffey & Dubé, 2016; Xue et al., 2017). Furthermore, the organic compounds

present in OSPW are mixtures of benzene, humic and fulvic acids, naphthenic acids (NAs), phenols, and polycyclic aromatic hydrocarbons (PAHs) (Wang et al., 2013). In terms of toxicity, the presence of various water-soluble organics, such as NAs from bitumen in OSPW induces an adverse impact (e.g., narcosis, endocrine disruption, immunotoxicity, and carcinogenicity) on both the aquatic ecosystem and wildlife (Garcia-Garcia et al., 2011; Hagen et al., 2014). Risks of human health are also have been attributed to the organic fractions of OSPW (Hodson, 2013; Huang et al., 2016; Kim et al., 2012; Kurek et al., 2013; Zhang et al., 2016). For instance, specific types of NAs found in OSPW have been determined to be carcinogenic; hence, estrogenic and androgenic activities of specific NAs and exposure to these NAs can also potentially disrupt the human reproductive system (Mahaffey & Dubé, 2016; Martin, 2015; Pérez-Estrada et al., 2011).

Wu et al. (2019) have stated NAs are contributing to the primary toxicity in OSPW and they are known to be the most persistent organics. NAs found in OSPW are also known to be corrosive to the oil sands process equipment, and they will eventually affect the quality of the extracted crude oil (Clemente & Fedorak, 2005). OSPW mixtures do not encompass NAs only as constituents of concerns, but also other organic and inorganic matters such as suspended solids, hydrocarbons, and unrecovered bitumen, salts, trace metals as well as inorganic compounds (El-Din et al., 2011; Headley et al., 2013b; Mahaffey & Dubé, 2016). However, several studies have confirmed that the toxicity of OSPW is primarily associated with the presence of various NAs that are natural components of petroleum (El-Din et al., 2011; Mahaffey & Dubé, 2016; Pérez-Estrada et al., 2011; Shi et al., 2015). Moreover, Morandi et al. (2015) have reported that the NA isomer classes are confirmed to be the most toxic among other isomer classes present in OSPW. Hence, the characterization of OSPW should be based on salt content, metals, and organic compounds, which are primarily naphthenic acid fraction compounds (NAFCs) (see Section 1.2) (Crowe et al.,

2001; Headley et al., 2009a). In OSPW, various NAs exist as complex heterogeneous mixtures, with a typical concentration in the range of 20 to 120 mg/L (Pérez-Estrada et al., 2011; Shi et al., 2015). The general characteristics of OSPW are shown in Table 1.1.

Table 1-1. General Characterization of Oil Sands Process-Affected Water (Zhang, 2016).

Parameter	Range
pH	7.8 – 8.5
Conductivity (μS/cm)	3459 – 4500
Total suspended solids (TSS) (mg/L)	97 – 221
Total dissolved solids (TDS) (mg/L)	2477 – 2859
Alkalinity (mg/L)	609.3 – 776.9
Chloride (mg/L)	641.0 – 715.7
Sulfate (mg/L)	274.7 – 602.6
Sodium (mg/L)	840.6 – 846.7
Potassium (mg/L)	14.7 – 17.0
Magnesium (mg/L)	8.6 – 15.1
Calcium (mg/L)	10.1 – 25.3
Organic Parameters	
Chemical oxygen demand (COD) (mg/L)	204 – 302.2
Total organic carbon (TOC) (mg/L)	48.3 – 75.0
Biochemical oxygen demand (BOD_5) (mg/L)	2.7 – 3.30
Polycyclic aromatic hydrocarbons (PAH) (mg/L)	0.01
Total naphthenic acids (NAs) (mg/L)	8.92 – 39.2 In some cases, can be up to 130 mg/L (Grewer et al., 2010)

1-1.2 Naphthenic acids (NAs)

NAs are known as the most problematic among all the contaminants present in OSPW (Xue et al., 2018). From the surface mining of oil sands, most NAs end up in the tailings-ponds (Wu et al., 2019) and it has been demonstrated that there are >200,000 different NA species present in oil sands (Anderson et al., 2012; Rowland et al., 2011a). Approximately, 200 mg of NAs are found per 1 kg of oil sands (Clemente & Fedorak, 2004), and 15% are partitioned into the OSPW during extraction processes (Scott et al., 2008b). As discussed in the previous section, NAs can be present in the surrounding surface waters and groundwaters (e.g., Athabasca river and aquifers) through potential infiltration (Fennell & Arciszewski, 2019) or naturally in the water, and also by other industrial activities and natural processes, such as effluent discharge, groundwater mixing, crude oil spills, or erosion of riverbank oil sands deposits (Headley et al., 2007). The concentrations of NAs in these water bodies are relatively small in quantities (e.g., <1 mg/L in surface water sources in the Athabasca oil sands region and 2-5 mg/L in near-surface aquifers (Janfada et al., 2006; Regional Aquatics Monitoring Program, 2011) compared with the NA concentration found in the tailings ponds (e.g., total NA concentration as high as 68 mg/L (Allen, 2008) and sometimes, it can reach up to 130 mg/L in Steam-Assisted Gravity Drainage produced water (Grewer et al., 2010)). Despite the low concentrations present, the potential seepage of NAs in groundwaters is still a concern (Wu et al., 2019).

1-1.2.1 NA types, structures, and chemical properties

NAs are identified as a cluster of aliphatic and alicyclic, alkyl-substituted carboxylic acids with a generalized formula of $C_nH_{2n+z}O_x$ (Han et al., 2008; Xue et al., 2018). The carboxylic group is usually bonded or attached to a side chain instead of to the cycloaliphatic ring (Wu et al., 2019). The commonly-used term used to describe the compounds present in OSPW is naphthenic acid

fraction compounds (NAFCs) (Fennell & Arciszewski, 2019), which refers to the sum of classical NAs ($C_nH_{2n+z}O_2$) (c-NAs), oxidized NAs (oxy-NAs), and S- and N-containing (heteroatoms) NAs, termed heteroatomic NAs (Headley et al., 2009a; Islam et al., 2015; Meshref et al., 2017; Yue et al., 2016). Hence, NAFCs are known to be diverse heteroatom compounds in OSPW, which are expressed as a chemical formula $C_nH_{2n+z}O_xN_\beta S_\gamma$. The subscript "n" represents the number of carbons (numbers between 7 to 30) (Zhu et al., 2018), "x" is a representation of the oxygen (e.g., equal to two for c-NAs with two oxygen atom; and three or more for oxidized NAs (oxy-NAs) formed after the oxidation of c-NAs (Huang et al., 2018; Kannel & Gan, 2012; Meshref et al., 2017)), "Z" is either value of zero or negative even-numbered integer, can be up to -12 (e.g., Z=0 indicates no ring, Z=-2 indicated one ring, Z=-4 indicates two rings, etc.) (Zhu et al., 2018), representing hydrogen deficiency through the formation of rings or the presence of double bonds equivalents (DBE), and "β" and "γ" represents nitrogen and sulfur numbers, respectively (Headley et al., 2013b; Headley et al., 2014; Rogers et al., 2002a).

Furthermore, the molecular weight can be another distinguishing factor for NA structures. The molecular weights of NA have a general range of 100 to 500 g mol^{-1} (Clemente et al., 2003a; Clemente et al., 2003b), and sometimes it can be as high as 1200 g mol^{-1} (Mohammed & Sorbie, 2009). NAs with low molecular weights include both cyclopentane and cyclohexane carboxylic acid, and NAs with high molecular weights contain 4 carboxylic acids and 4 to 8 unsaturated rings (Mohammed & Sorbie, 2009). In OSPW, rings with 5 or 6 carbons are the predominant structures, contributing to ~95%, and the majority of NAs generally have 2 to 3 rings, meaning Z=-4 and Z=-6, respectively (Clemente et al., 2003a; Del Rio et al., 2006). Monocyclic acids are the main structures for other structures of NAs, such as 7 to 12 carbons (Brient et al., 1995). Furthermore, the majority of the NAs are c-NAs, contributing to ~50% of the acid extractable organic fraction

(Grewer et al., 2010) with a concentration range of 20 – 120 mg/L (Toor et al., 2013). NAs are soluble in water at neutral or alkaline pH (e.g., having dissociation constant ranging from ~10^{-5} to 10^{-6} (Xu et al., 2017)) and their solubility is more influenced by pH than temperature (e.g., NA is more soluble in water with alkaline pH (Janfada et al., 2006)).

Of note, before the implementations of more sophisticated and advanced analytical methods, such as high-performance liquid chromatography ultra-resolution mass spectrometry (HPLC-UHRMS), it was believed that the acid extractable organics in OSPW was primarily comprised of c-NAs (Scott et al., 2020). However, these acid extractable organics were further evidenced to contain more complex mixtures and different compounds, such as oxy-NAs and heteroatomic NAs, other than the c-NAs (Grewer et al., 2010; Headley et al., 2013a; Headley et al., 2013b). This finding was assisted by enhanced characterization methods like UPLC-UHRMS (Pereira & Martin, 2015; Pereira et al., 2013). In fact, both c-NAs and some oxy-NAs (O_3 and O_4-species) were the dominant species in OSPW, with the O_2 species still being distinctly the primary group (Ajaero et al., 2017; Huang et al., 2017; Xue et al., 2017), because the oxy-NAs are likely the oxidation products of c-NAs through oxidation and biodegradation (Ajaero et al., 2017). More importantly, the concentrations, compositions, as well as structures of these NAs may change over time (Pérez-Estrada et al., 2011; Shi et al., 2015) and with the source of crude oil (Wu et al., 2019). Figure 1.1 below illustrates the general structures of NAs found in OSPW.

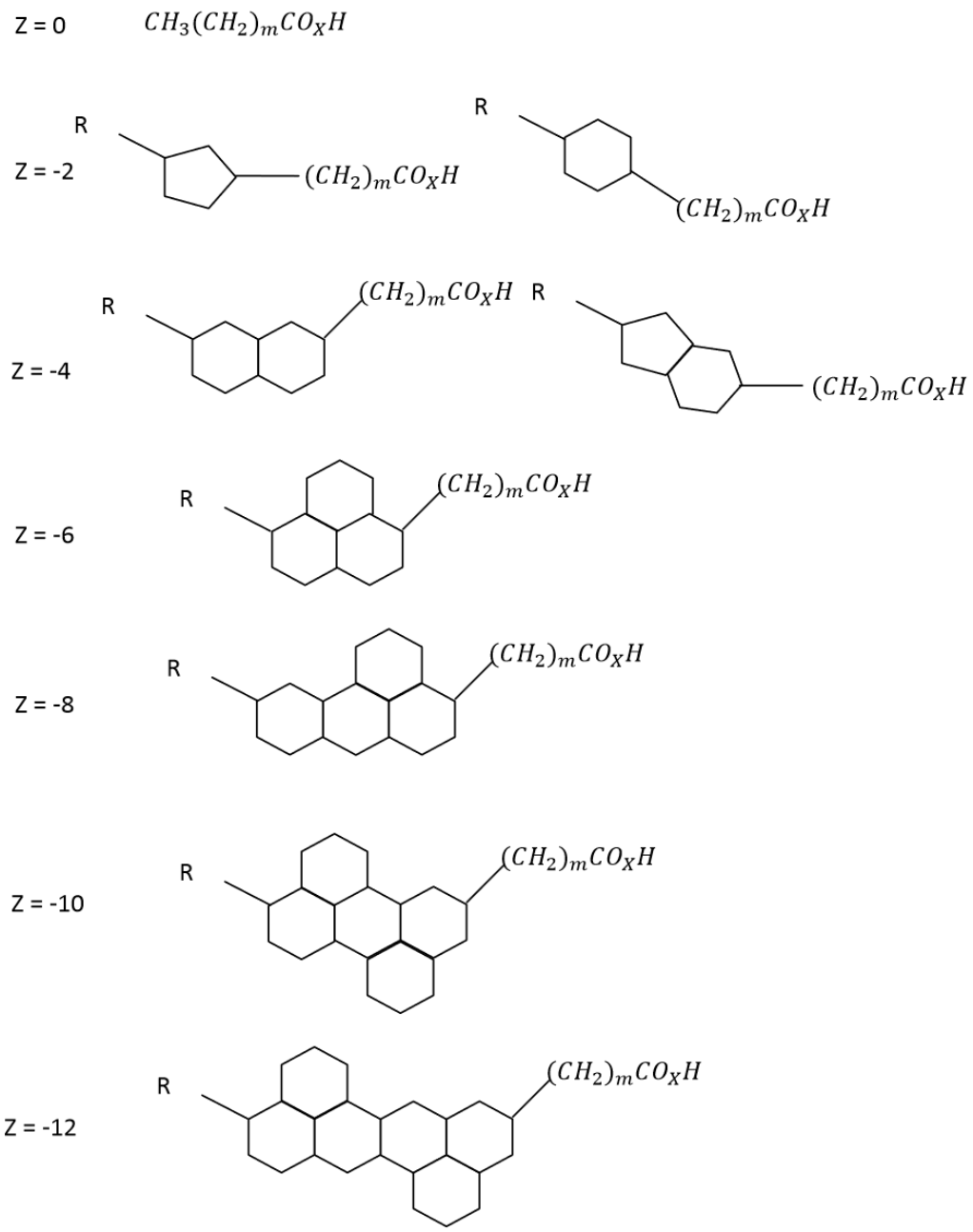

Figure 1-1. General structures of NAs for Z=0 to -12. R represents the alkyl groups, m is the length of the alkyl chain (number of CH_2 units), x is the number of oxygen atoms where x=2 is for c-NAs, and x ≥ 3 is for oxy-NAs. Note. This figure was adopted from Islam (2014).

1-1.2.2 NAs and their correlation to biodegradation

Compared to other processes, biodegradation has been known to be the major pathway of the natural degradation of OSPW NAs (Quagraine et al., 2005; Xue et al., 2018). Hence, it is crucial to understand the correlation between NAs and biodegradation as well as to engineer biological processes to enhance the biodegradation of NAs (Xue et al., 2018) to aid both removal and monitoring processes. When it comes to a correlation between cyclicity and biodegradation of NAs, multiple studies have observed and agreed that NAs with higher Z numbers were less biodegradable (Han et al., 2008; Huang et al., 2015; Wang et al., 2013; Xue et al., 2017; Xue et al., 2016). Scott et al. (2005) also have reported NAs with more branched and complex structures are harder to degrade compared to the NAs with simpler structures. On the other hand, less cyclic and acyclic NAs are not only less persistent, but they are also likely more hydrophobic, in which higher hydrophobicity may further increase the biodegradation (Pourrezaei, 2013). More importantly, the NAs are the most persistent organic compounds found in OSPW (Wu et al., 2019) and they are extremely recalcitrant, having an estimated half-life of ~13 years in the tailings ponds (Han et al., 2009) and difficult to be biodegraded naturally (Scott et al., 2005). Hence, continuous monitoring of NAs has not become the only significant concern for both the public and the government but also having appropriate analysis techniques (i.e., the practical analytical procedure) is crucial.

1-1.2.3 The importance of NA monitoring

The effect of NAs on the environment and human health has been discussed earlier in Section 1.1. Besides the environmental concerns and the adverse effects of NAs on oil processing, NAs have been reported as important raw materials in chemical industries. For instance, NAs can be used as antiseptics, paint drying reagents, additives in petroleum fluids, and many more (Shao et al., 2017).

Furthermore, salts of naphthenic acid, known as naphthenate salts, can be used as catalysts, corrosion inhibitors, emulsifiers, dispersants as well as preservatives (Wang et al., 2006). Hence, NA monitoring is important as it greatly assists in the environment and human health protection, oil quality improvement, transportation, and refining processes, as well as recovery of valuable raw materials.

1-1.3 Identification, characterization, and analytical methods of NAs

Environmental monitoring of NAs became important as it is an integral part of sustainable environmental management in the oil sands industries. Thus, previous research studies on the identification and quantification of NA compounds in OSPW have drawn the interests of many oil-sands mining-related companies in Alberta. According to Alberta's Environmental Protection and Enhancement Act (EPEA), development of an oil sands project requires submission of environmental impact assessment reports, where background concentrations of NAs in surface and ground waters near the proposed mining site must be included. Therefore, in addition to OSPW samples, oil sands operators are required to routinely monitor NAs in water samples from surrounding surface freshwater and groundwater wells for a potential OSPW seepage into them (Fennell & Arciszewski, 2019; Huang et al., 2018).

Many different analytical techniques have been used for characterization and quantification of the OSPW NAs, such as chemical oxygen demand (COD) (Huang et al., 2015), Fourier transform infrared spectroscopy (FTIR) (El-Din et al., 2011; MacKinnon & Boerger, 1986; Rogers et al., 2002a), gas chromatography coupled with mass-spectrometry (GC-MS) (Holowenko et al., 2002; Scott et al., 2008a), ultra-performance liquid chromatography coupled with high resolution mass spectrometry (UPLC/HRMS) (Martin et al., 2010; Sun et al., 2014), ultra-performance liquid

chromatography time of flight mass spectrometry (UPLC-TOF-MS) (Headley et al., 2016; Kovalchik et al., 2017; Sun et al., 2014; Wang et al., 2013), Fourier transform ion cyclotron resonance mass spectrometry (FTICR-MS) (Ajaero et al., 2017), synchronous fluorescence spectroscopy (SFS) (Martin et al., 2014), and Orbitrap mass spectrometry (Pereira et al., 2013) reviewed by Brown et al. (2015), Xue et al. (2018), and Fennell and Arciszewski (2019). Detail reviews on different analytical methods for NAs can be found elsewhere (Brown & Ulrich, 2015; Clemente & Fedorak, 2005; Headley et al., 2009b; Hughes et al., 2017; Sun et al., 2014). Due to the high complexity of the organic matrix in OSPW, currently, no single absolute analytical method exists for detection and quantification of mining-related NAs and other individual compounds existing in OSPW (Fennell & Arciszewski, 2019; Headley et al., 2016; Kovalchik et al., 2017; Xue et al., 2018). Furthermore, most of these commonly-used analytical techniques still face challenges due to extremely complex distributions of NAs in OSPW. Mainly, the analysis of NAs with these techniques listed above are expensive, involve time-consuming methodologies, and are lab-based analyses (Ajaero et al., 2017; Huang et al., 2018; Ripmeester & Duford, 2019). Some analytical methods, such as GC-MS and FTIR spectroscopy can even lead to misclassifications of compounds (Hughes et al., 2017; Merlin et al., 2007). For instance, GC-MS methods are only suitable to quantify the c-NAs with a derivatization method based on its unit mass resolution (Hughes et al., 2017). Furthermore, GC-MS can also overestimate the total NA measurement due to its low mass resolution (e.g., the measurement of total NAs may contain other organic compounds with the same nominal mass that cannot be resolved from NAs) (Hughes et al., 2017; Kovalchik et al., 2017) Hence, development of a low-cost and fast analytical method that can be deployed on-site for reliable real-time monitoring of NAs will help to address such analytical challenges.

1-1.4 Commonly-used analytical methods of NAs

1-1.4.1 FTIR spectroscopy

Fourier transform infrared (FTIR) spectroscopy is known as the oil sands industry's standard quantification method developed by Syncrude Canada Ltd. (Clemente & Fedorak, 2005), which measures monomer and dimer absorbances associated with the carbonyl group of the carboxylic acids. For analysis with FTIR, filtered OSPW samples are acidified and extracted with dichloromethane (DCM); then, absorbances of the monomeric and dimeric forms of the carboxylic groups are measured after concentrating the acid extractable organics (Brown & Ulrich, 2015; El-Din et al., 2011). Hence, this process can be quite time-consuming. FTIR spectroscopy is not specific to individual NAs and it is unable to resolve carbon numbers or Z families for specific NAs. This is possibly due to the presence of contaminants, such as polycyclic aromatic hydrocarbons and phthalates contaminating the NA mixtures upon extraction (Holowenko et al., 2002). Furthermore, the FTIR may trigger inaccurate measurements of NA concentrations by detecting other organic compounds that are similar in structures, such as fatty acids in OSPW (Brown & Ulrich, 2015; Brunswick et al., 2016; Fennell & Arciszewski, 2019; Grewer et al., 2010; Headley et al., 2013b; Headley et al., 2016; Kovalchik et al., 2017; Merlin et al., 2007). For instance, bias towards higher total NA concentrations measured by FTIR was widely reported (Han et al., 2009; Hughes et al., 2017); where the FTIR determines the total acid-extractable fraction (AEF), which includes all –CO, -CHO, and –COOH groups overestimating the concentrations of NAs (Grewer et al., 2010). However, FTIR may be suitable for some specific cases, such as evaluating the performance of OSPW treatment systems (Zubot et al., 2012). In summary, FTIR can quantify OSPW NAs, but it is a time-consuming and lab-based analysis, which may also lack reliability.

1-1.4.2 GC-MS

Gas-chromatography-mass spectrometry (GC-MS) is another commonly used analytical method for NAs detection. GC-MS determines the relative abundance of specific NA isomers in a complex NA mixture after NA derivatization (e.g., using methylation step to make esters or making *tert*-butyldimethylsilyl derivatives of the NAs) (Bowman et al., 2020; Holowenko et al., 2002; John et al., 1998; Miles et al., 2020). Using GC-MS, the percent composition of each eluting component within the NAs mixture based on carbon and Z numbers can be obtained (Holowenko et al., 2002). However, there are several drawbacks of using GC-MS as an analytical method of NAs. GC-MS is sensitive and it suffers from few matrix effects, associated with a formation of moieties from the volatile derivatives, which complicates the mass spectral interpretation, and finally, the method is time-consuming (Bataineh et al., 2006). GC-MS sometimes has inadequate resolving power and can include other organics when estimating the total NA concentrations (e.g., overestimating) (Hughes et al., 2017). Furthermore, it can also overestimate the relative proportions of low molecular weight (MW) acids (Clemente & Fedorak, 2004). Similar to FTIR, GC-MS is also a time-consuming and lab-based analysis, which may be unreliable to quantify OSPW NAs, especially when identifying for an OSPW seepage (Fennell & Arciszewski, 2019).

1-1.4.3 FTICR-MS and SFS

Fourier transform ion cyclotron resonance-mass spectrometry (FTICR-MS) is another analytical method for NAs with an enhanced mass accuracy and resolution compared to other analytical techniques; giving better performance in the mass assignments (Ajaero et al., 2017; Barrow et al., 2003). FTICR-MS operates based on a cyclotron (e.g., a type of particle accelerator), where the electrons are captured in orbits by a strong magnetic field, while being accelerated by an applied voltage field; then, the cyclotron frequency is related to m/z (Mellon, 2003). Regarding the NA

detection, the FTICR-MS is known to provide identification of individual NAs (Barrow et al., 2004). Synchronous fluorescence spectroscopy (SFS) also has been utilized for the monitoring of NAs (Kavanagh et al., 2009). SFS is suitable for multicomponent analysis, which produces spectra through simultaneous scanning of the excitation and the emission monochromators of a spectrofluorimeter, with a fixed wavelength difference between them. However, similar to the common analytical methods, all of these methods are time-consuming (e.g., sample preparations, transportation of samples), expensive (e.g., using high-resolution spectrometry, very large in size), and lab-based analyses, which are not available for on-site quantification of OSPW NAs (Ajaero et al., 2017; Huang et al., 2018; Ripmeester & Duford, 2019; Zubarev & Makarov, 2013).

1-1.4.4 UPLC/QTOF-MS and Orbitrap-MS

Up to date, in contrast to the analytical methods mentioned above, ultra-high performance liquid chromatography-quadrupole time-of-flight mass spectrometry (UHPLC/QTOF-MS) and Orbitrap-mass spectrometry (Orbitrap-MS) have been recognized as the typical approaches in many chemical fingerprinting and toxicological studies (Frank et al., 2014; Hughes et al., 2017). UHPLC/QTOF-MS analysis is a high-resolution analytical method that combines high specificity, sensitivity, and quantitative capabilities, which can detect transformation products. In the case of analyzing model NA compounds such as cyclohexane carboxylic acid (CHA), the transformation intermediate compounds and by-products can be detected in liquid chromatography-mass spectrometry (LCMS) setup (Abdalrhman et al., 2020; Drzewicz et al., 2010). It is worth noting that UHPLC/QTOF-MS separates NAs based on their carbon numbers, degree of cyclization, and the extent of alkyl branching; therefore, providing increased analytical sensitivity with additional specificity (Bataineh et al., 2006). However, a complete quantification UHPLC/QTOF-MS method for NAs is not available in the meantime due to the lack of standard compounds for individual NA

in OSPW. Given this fact, the various NA compounds can display variations in sensitivity within mass spectrometry detection (Huang et al., 2019; Sun et al., 2014). Instead, the Orbitrap-MS has been implemented for the characterization of OSPW NAs (Headley et al., 2013b; Hughes et al., 2017). Orbitrap-MS is an ion trap mass analyzer, in which, the image current from the trapped ions is detected and converted to a mass spectrum using the Fourier transform of the frequency signal (Hecht et al., 2006; Zubarev & Makarov, 2013); hence, providing very high-resolution mass spectrum (Hu et al., 2005). Specifically, the Orbitrap-MS uses electrodes and radial electric fields to circulate the injected ions, where the outer electrodes are used as receiver plates to generate image current (e.g., meaning it relies on the mass-to-charge ratio, m/z) (Hecht et al., 2006; Zubarev & Makarov, 2013). More importantly, the Orbitrap-MS delivers highly-sensitive analysis (e.g., allowing very accurate measurement of mass) to a level similar to FTICR-MS with low cost (e.g., 10 cm or a size of a coin, very small in size), and simple in operation and maintenance (e.g., indestructible, very long-life time) (Hecht et al., 2006; Zubarev & Makarov, 2013).

With regards to NA detection, these two techniques are very advantageous as they can specifically distinguish the c-NAs from other compounds, such as heteroatoms, bicyclic acids, aromatics as well as oxygenated acids (Barrow et al., 2015; Grewer et al., 2010; Headley et al., 2009b; Kovalchik et al., 2017; Lengger et al., 2015; Rowland et al., 2014; Rowland et al., 2011a; Rowland et al., 2011b; Rowland et al., 2011c; Wilde et al., 2015). However, precise identification of NA structures is still not possible due to the complicated OSPW matrix in addition to being a lab-based analysis involving an expensive high-resolution spectrometry and sample preparation.

1-1.4.5 Sensor-based analytical methods of NAs

To date, there have been significant efforts to develop sensor-based techniques for on-site quantification of NAs concentrations. For instance, Taschuk et al. (2010) developed a prototype of a sensor (8.5 kg in weight) combining ultraviolet light-emitting diodes and a charge-coupled device spectrometer that can measure NA concentration below 10 mg/L. A similar attempt by Kaur et al. (2013) while they developed a disposable peptide-based sensor that can detect NAs at low concentration (~5 mg/L) using a fluorescence-based competitive binding method. De Corby (2013) integrated a micro-spectrometer into a silicon-based optofluidic sensor for the detection of NAs. Interestingly, all these approaches primarily focus on fluorescence characterization of NAs deploying spectrometer, which is still expensive and requires external energy input. Furthermore, these methods are not suitable for real-time monitoring of NAs. Therefore, the development of a sensor for online detection and in other reclamation systems, such as constructed wetlands, end pit lakes, etc., could be the current underdevelopment efforts, dedication, and commitment by oil sands companies. Implementation of an efficient and effective-early warning system is crucial to trace the existence, and to mitigate the impact of contamination, which guarantees the public health as well as the water environmental security (Liu et al., 2016).

1-1.5 Overview of NA monitoring and potential solutions to analytical challenges

As demonstrated by Frank et al. (2014), applying multiple methods is also common; and using different ionization methods has also gained attraction recently in environmental measurements (Headley et al., 2016). Despite these novel developments of more sophisticated approaches and methods for OSPW NAs, major challenges, such as lack of a single standard method for NA measurement and absence of reference materials, are still unsolved issues (Tanna et al., 2019). Moreover, they are not widely available in commercial labs, requiring high-skilled hands (e.g.,

specialized to operate) and interpretation of results is more challenging compared to low-resolution analytical techniques (Hughes et al., 2017).

Therefore, it is anticipated that the development of a low-cost and fast analytical method for on-site quantification and monitoring of NAs will help to address these analytical challenges. Recently, the development of microbial electrochemical biosensors (MXC biosensors) for organic contaminants or toxicants monitoring has received significant momentum (Chung et al., 2020; Jiang et al., 2018; Sun et al., 2015). MXC biosensors produce an electrical signal in response to the presence of a target contaminant; the electrical signal can be correlated to the concentration of the contaminant (Adekunle, 2018; Jiang et al., 2018; Kim et al., 2007; Sun et al., 2015). MXC biosensor can be operated in self-powered mode, and its size can be fabricated to a μL-scale to reduce fabrication costs (Xiao et al., 2020; Yang et al., 2016).

1-2. Specific Objectives

This research focuses on the detection of OSPW NAs using MXC biosensor. The demonstrations of preliminary MXC-biosensor proof-of-concept tests by Dr. Dhar's research group have been successful (Barua et al., 2018a; Barua et al., 2018b). The currents produced from the oxidation of model NAs were correlated to the concentrations of model NAs. Therefore, further research is warranted to bring this biosensor a step forward towards field-scale application. The specific objectives of my research are:

1) To develop a quick and reliable method for calibration of MXC biosensor for the detection of NA for a practical field-scale application.
2) To understand the interactions between multiple NAs and environmental parameters.

3) To understand the effects of other organics, such as polycyclic aromatic hydrocarbons present in OSPW on MXC biosensor's response.

Initially, the optimal calibration method for this MXC biosensor was developed by comparing various calibration methods in terms of quickness, precision, and reproducibility. With the developed calibration method, the effects of various environmental conditions on MXC biosensor's performance were investigated. Furthermore, the impacts of commercial NAs (e.g., mixtures of different NAs) and polycyclic aromatic hydrocarbons (e.g., which are other organics found in OSPW) on the biosensor performance was investigated, which is necessary before implementing the MXC biosensors for NA detections in real OSPW. Ultimately, the outcomes from these proposed research objectives can demonstrate that the development of MXC-biosensor could enable fast, reliable, and on-site measurements of NA concentrations in real OSPW.

1-3. Thesis Outline

This thesis is divided into five chapters. Chapter 1 highlights the extended background and motivation of the topic under investigation and summarizes the specific objectives of the proposed research. Chapter 2 presents a comprehensive literature review (in an article format) related to the proposed research (MXC biosensors for the detection of recalcitrant environmental contaminants similarly structured to NAs). Chapters 3, and 4 present the findings from this thesis research in article format. Chapter 5 summarizes the results with their scientific and engineering implications and provides recommendations for future research.

1-4. References

Abdalrhman, A.S., Wang, C., How, Z.T., El-Din, M.G. 2020. Degradation of cyclohexanecarboxylic acid as a model naphthenic acid by the UV/chlorine process: Kinetics and by-products identification. *Journal of Hazardous Materials*, **402**, 123476.

Adekunle, A. 2018. Development of an Autonomous Biobattery/biosensor System for Remote Applications, McGill University Libraries.

Ajaero, C., McMartin, D.W., Peru, K.M., Bailey, J., Haakensen, M., Friesen, V., Martz, R., Hughes, S.A., Brown, C., Chen, H., McKenna, A.M., Corilo, Y.E., Headley, J.V. 2017. Fourier Transform Ion Cyclotron Resonance Mass Spectrometry Characterization of Athabasca Oil Sand Process-Affected Waters Incubated in the Presence of Wetland Plants. *Energy & Fuels*, **31**(2), 1731-1740.

Allen, E.W. 2008. Process water treatment in Canada's oil sands industry: I. Target pollutants and treatment objectives. *Journal of Environmental Engineering and Science*, **7**(2), 123-138.

Anderson, J., Wiseman, S., Wang, N., Moustafa, A., Perez-Estrada, L., Gamal El-Din, M., Martin, J., Liber, K., Giesy, J.P. 2012. Effectiveness of ozonation treatment in eliminating toxicity of oil sands process-affected water to Chironomus dilutus. *Environmental science & technology*, **46**(1), 486-493.

Bari, M.A., Kindzierski, W.B. 2018. Ambient volatile organic compounds (VOCs) in communities of the Athabasca oil sands region: Sources and screening health risk assessment. *Environmental Pollution*, **235**, 602-614.

Barrow, M.P., Headley, J.V., Peru, K.M., Derrick, P.J. 2004. Fourier transform ion cyclotron resonance mass spectrometry of principal components in oilsands naphthenic acids. *Journal of chromatography A*, **1058**(1-2), 51-59.

Barrow, M.P., McDonnell, L.A., Feng, X., Walker, J., Derrick, P.J. 2003. Determination of the nature of naphthenic acids present in crude oils using nanospray Fourier transform ion cyclotron resonance mass spectrometry: The continued battle against corrosion. *Analytical chemistry*, **75**(4), 860-866.

Barrow, M.P., Peru, K.M., Fahlman, B., Hewitt, L.M., Frank, R.A., Headley, J.V. 2015. Beyond Naphthenic Acids: Environmental Screening of Water from Natural Sources and the Athabasca Oil Sands Industry Using Atmospheric Pressure Photoionization Fourier Transform Ion Cyclotron Resonance Mass Spectrometry. *J Am Soc Mass Spectrom*, **26**(9), 1508-21.

Barua, S., Zakaria, B.S., Dhar, B.R. 2018a. Development of a self-powered biosensor for real-time monitoring of naphthenic acids. *Canada's Oil Sands Innovation Alliance (COSIA) Innovation Summit*, Calgary, AB, Canada.

Barua, S., Zakaria, B.S., Dhar, B.R. 2018b. Development of bioelectrochemical sensing device for naphthenic acids. *53rd Central Canadian Symposium on Water Quality Research*, Toronto, ON, Canada.

Bataineh, M., Scott, A., Fedorak, P., Martin, J. 2006. Capillary HPLC/QTOF-MS for characterizing complex naphthenic acid mixtures and their microbial transformation. *Analytical Chemistry*, **78**(24), 8354-8361.

Benally, C., Li, M., El-Din, M.G. 2018. The effect of carboxyl multiwalled carbon nanotubes content on the structure and performance of polysulfone membranes for oil sands process-affected water treatment. *Separation and purification Technology*, **199**, 170-181.

Bowman, D.T., Warren, L.A., Slater, G.F. 2020. Isomer-specific monitoring of naphthenic acids at an oil sands pit lake by comprehensive two-dimensional gas chromatography–mass spectrometry. *Science of The Total Environment*, **746**, 140985.

Brient, J., Wessner, P., Doyle, M. 1995. Kirk-Othmer Encyclopedia of Chemical Technology Naphthenic acids, John Wiley and Sons, New York.

Brisbois, M.C., Morris, M., de Loë, R. 2019. Augmenting the IAD framework to reveal power in collaborative governance–An illustrative application to resource industry dominated processes. *World Development*, **120**, 159-168.

Brown, L., Ulrich, A. 2015. Protocols for measurement of naphthenic acids in aqueous samples. in: *Hydrocarbon and Lipid Microbiology Protocols*, Springer, pp. 201-216.

Brunswick, P., Hewitt, L.M., Frank, R.A., van Aggelen, G., Kim, M., Shang, D. 2016. Specificity of high resolution analysis of naphthenic acids in aqueous environmental matrices. *Analytical Methods*, **8**(37), 6764-6773.

Chung, T.H., Meshref, M.N., Dhar, B.R. 2020. Microbial electrochemical biosensor for rapid detection of naphthenic acid in aqueous solution. *Journal of Electroanalytical Chemistry*, 114405.

Clemente, J.S., Fedorak, P.M. 2004. Evaluation of the analyses of tert-butyldimethylsilyl derivatives of naphthenic acids by gas chromatography–electron impact mass spectrometry. *Journal of Chromatography A*, **1047**(1), 117-128.

Clemente, J.S., Fedorak, P.M. 2005. A review of the occurrence, analyses, toxicity, and biodegradation of naphthenic acids. *Chemosphere*, **60**(5), 585-600.

Clemente, J.S., Prasad, N., MacKinnon, M.D., Fedorak, P.M. 2003a. A statistical comparison of naphthenic acids characterized by gas chromatography–mass spectrometry. *Chemosphere*, **50**(10), 1265-1274.

Clemente, J.S., Yen, T.-W., Fedorak, P.M. 2003b. Development of a high performance liquid chromatography method to monitor the biodegradation of naphthenic acids. *Journal of Environmental Engineering and Science*, **2**(3), 177-186.

Crowe, A., Han, B., Kermode, A., Bendell-Young, L., Plant, A. 2001. Effects of oil sands effluent on cattail and clover: photosynthesis and the level of stress proteins. *Environmental Pollution*, **113**(3), 311-322.

De Corby, R. 2013. Development of Silicon-Based Optofluidic Sensors for Oil Sands Environmental Monitoring. OSRIN Report No. TR-41. 19 pp. http://hdl. handle. net/10402/era. 36936.

Del Rio, L., Hadwin, A., Pinto, L., MacKinnon, M., Moore, M. 2006. Degradation of naphthenic acids by sediment micro-organisms. *Journal of Applied Microbiology*, **101**(5), 1049-1061.

Drzewicz, P., Afzal, A., El-Din, M.G., Martin, J.W. 2010. Degradation of a model naphthenic acid, cyclohexanoic acid, by vacuum UV (172 nm) and UV (254 nm)/H2O2. *The Journal of Physical Chemistry A*, **114**(45), 12067-12074.

El-Din, M.G., Fu, H., Wang, N., Chelme-Ayala, P., Pérez-Estrada, L., Drzewicz, P., Martin, J.W., Zubot, W., Smith, D.W. 2011. Naphthenic acids speciation and removal during petroleum-coke adsorption and ozonation of oil sands process-affected water. *Science of the Total Environment*, **409**(23), 5119-5125.

Fennell, J., Arciszewski, T.J. 2019. Current knowledge of seepage from oil sands tailings ponds and its environmental influence in northeastern Alberta. *Science of the total environment*.

Frank, R.A., Roy, J.W., Bickerton, G., Rowland, S.J., Headley, J.V., Scarlett, A.G., West, C.E., Peru, K.M., Parrott, J.L., Conly, F.M. 2014. Profiling oil sands mixtures from industrial developments and natural groundwaters for source identification. *Environmental science & technology*, **48**(5), 2660-2670.

Fu, L., Li, C., Lillico, D.M., Phillips, N.A., Gamal El-Din, M., Belosevic, M., Stafford, J.L. 2017. Comparison of the acute immunotoxicity of nonfractionated and fractionated oil sands process-affected water using mammalian macrophages. *Environmental science & technology*, **51**(15), 8624-8634.

Garcia-Garcia, E., Ge, J.Q., Oladiran, A., Montgomery, B., El-Din, M.G., Perez-Estrada, L.C., Stafford, J.L., Martin, J.W., Belosevic, M. 2011. Ozone treatment ameliorates oil sands process water toxicity to the mammalian immune system. *Water Res*, **45**(18), 5849-57.

Grewer, D.M., Young, R.F., Whittal, R.M., Fedorak, P.M. 2010. Naphthenic acids and other acid-extractables in water samples from Alberta: what is being measured? *Science of the Total Environment*, **408**(23), 5997-6010.

Hagen, M.O., Katzenback, B.A., Islam, M.D., Gamal El-Din, M., Belosevic, M. 2014. The analysis of goldfish (Carassius auratus L.) innate immune responses after acute and subchronic exposures to oil sands process-affected water. *Toxicol Sci*, **138**(1), 59-68.

Han, X., MacKinnon, M.D., Martin, J.W. 2009. Estimating the in situ biodegradation of naphthenic acids in oil sands process waters by HPLC/HRMS. *Chemosphere*, **76**(1), 63-70.

Han, X., Scott, A.C., Fedorak, P.M., Bataineh, M., Martin, J.W. 2008. Influence of molecular structure on the biodegradability of naphthenic acids. *Environmental science & technology*, **42**(4), 1290-1295.

Headley, J., Peru, K., Fahlman, B., Colodey, A., McMartin, D. 2013a. Selective solvent extraction and characterization of the acid extractable fraction of Athabasca oils sands process waters by Orbitrap mass spectrometry. *International Journal of Mass Spectrometry*, **345**, 104-108.

Headley, J., Peru, K., Mohamed, M., Frank, R., Martin, J., Hazewinkel, R., Humphries, D., Gurprasad, N., Hewitt, L., Muir, D. 2013b. Chemical fingerprinting of naphthenic acids and oil sands process waters—A review of analytical methods for environmental samples. *Journal of Environmental Science and Health, Part A*, **48**(10), 1145-1163.

Headley, J.V., Kumar, P., Dalai, A., Peru, K.M., Bailey, J., McMartin, D.W., Rowland, S.M., Rodgers, R.P., Marshall, A.G. 2014. Fourier transform ion cyclotron resonance mass spectrometry characterization of treated Athabasca oil sands processed waters. *Energy & Fuels*, **29**(5), 2768-2773.

Headley, J.V., Peru, K.M., Armstrong, S.A., Han, X., Martin, J.W., Mapolelo, M.M., Smith, D.F., Rogers, R.P., Marshall, A.G. 2009a. Aquatic plant-derived changes in oil sands naphthenic acid signatures determined by low-, high-and ultrahigh-resolution mass spectrometry. *Rapid Communications in Mass Spectrometry: An International Journal Devoted to the Rapid Dissemination of Up-to-the-Minute Research in Mass Spectrometry*, **23**(4), 515-522.

Headley, J.V., Peru, K.M., Barrow, M.P. 2016. Advances in mass spectrometric characterization of naphthenic acids fraction compounds in oil sands environmental samples and crude oil—a review. *Mass spectrometry reviews*, **35**(2), 311-328.

Headley, J.V., Peru, K.M., Barrow, M.P. 2009b. Mass spectrometric characterization of naphthenic acids in environmental samples: a review. *Mass spectrometry reviews*, **28**(1), 121-134.
Headley, J.V., Peru, K.M., Barrow, M.P., Derrick, P.J. 2007. Characterization of naphthenic acids from Athabasca oil sands using electrospray ionization: the significant influence of solvents. *Analytical chemistry*, **79**(16), 6222-6229.
Hecht, E.S., Scigelova, M., Eliuk, S., Makarov, A. 2006. Fundamentals and Advances of Orbitrap Mass Spectrometry. *Encyclopedia of Analytical Chemistry: Applications, Theory and Instrumentation*, 1-40.
Hodson, P.V. 2013. History of environmental contamination by oil sands extraction. *Proceedings of the National Academy of Sciences*, **110**(5), 1569-1570.
Holowenko, F.M., MacKinnon, M.D., Fedorak, P.M. 2002. Characterization of naphthenic acids in oil sands wastewaters by gas chromatography-mass spectrometry. *Water research*, **36**(11), 2843-2855.
Hu, Q., Noll, R.J., Li, H., Makarov, A., Hardman, M., Graham Cooks, R. 2005. The Orbitrap: a new mass spectrometer. *Journal of mass spectrometry*, **40**(4), 430-443.
Huang, C., Shi, Y., El-Din, M.G., Liu, Y. 2015. Treatment of oil sands process-affected water (OSPW) using ozonation combined with integrated fixed-film activated sludge (IFAS). *Water research*, **85**, 167-176.
Huang, C., Shi, Y., Xue, J., Zhang, Y., El-Din, M.G., Liu, Y. 2017. Comparison of biomass from integrated fixed-film activated sludge (IFAS), moving bed biofilm reactor (MBBR) and membrane bioreactor (MBR) treating recalcitrant organics: importance of attached biomass. *Journal of hazardous materials*, **326**, 120-129.
Huang, R., Chen, Y., Meshref, M.N., Chelme-Ayala, P., Dong, S., Ibrahim, M.D., Wang, C., Klamerth, N., Hughes, S.A., Headley, J.V. 2018. Characterization and determination of naphthenic acids species in oil sands process-affected water and groundwater from oil sands development area of Alberta, Canada. *Water research*, **128**, 129-137.
Huang, R., McPhedran, K.N., Sun, N., Chelme-Ayala, P., El-Din, M.G. 2016. Investigation of the impact of organic solvent type and solution pH on the extraction efficiency of naphthenic acids from oil sands process-affected water. *Chemosphere*, **146**, 472-477.
Huang, R., Qin, R., Chelme-Ayala, P., Wang, C., El-Din, M.G. 2019. Assessment of ozonation reactivity of aromatic and oxidized naphthenic acids species separated using a silver-ion solid phase extraction method. *Chemosphere*, **219**, 313-320.
Hughes, S.A., Huang, R., Mahaffey, A., Chelme-Ayala, P., Klamerth, N., Meshref, M.N., Ibrahim, M.D., Brown, C., Peru, K.M., Headley, J.V. 2017. Comparison of methods for determination of total oil sands-derived naphthenic acids in water samples. *Chemosphere*, **187**, 376-384.
Islam, M.S. 2014. Combined Adsorption and Biodegradation Processes for Oil Sands Process-Affected Water Treatment.
Islam, M.S., Zhang, Y., McPhedran, K.N., Liu, Y., El-Din, M.G. 2015. Granular activated carbon for simultaneous adsorption and biodegradation of toxic oil sands process-affected water organic compounds. *Journal of environmental management*, **152**, 49-57.
Janfada, A., Headley, J.V., Peru, K.M., Barbour, S. 2006. A laboratory evaluation of the sorption of oil sands naphthenic acids on organic rich soils. *Journal of Environmental Science and Health, Part A*, **41**(6), 985-997.

Jiang, Y., Yang, X., Liang, P., Liu, P., Huang, X. 2018. Microbial fuel cell sensors for water quality early warning systems: Fundamentals, signal resolution, optimization and future challenges. *Renewable and Sustainable Energy Reviews*, **81**, 292-305.

John, W.P.S., Rughani, J., Green, S.A., McGinnis, G.D. 1998. Analysis and characterization of naphthenic acids by gas chromatography–electron impact mass spectrometry of tert.-butyldimethylsilyl derivatives. *Journal of Chromatography A*, **807**(2), 241-251.

Kannel, P.R., Gan, T.Y. 2012. Naphthenic acids degradation and toxicity mitigation in tailings wastewater systems and aquatic environments: a review. *Journal of Environmental Science and Health, Part A*, **47**(1), 1-21.

Kaur, A., Kim, J.R., Michie, I., Dinsdale, R.M., Guwy, A.J., Premier, G.C., Sustainable Environment Research, C. 2013. Microbial fuel cell type biosensor for specific volatile fatty acids using acclimated bacterial communities. *Biosens Bioelectron*, **47**, 50-5.

Kavanagh, R.J., Burnison, B.K., Frank, R.A., Solomon, K.R., Van Der Kraak, G. 2009. Detecting oil sands process-affected waters in the Alberta oil sands region using synchronous fluorescence spectroscopy. *Chemosphere*, **76**(1), 120-126.

Kim, E.-S., Liu, Y., Gamal El-Din, M. 2012. Evaluation of membrane fouling for in-line filtration of oil sands process-affected water: the effects of pretreatment conditions. *Environmental science & technology*, **46**(5), 2877-2884.

Kim, M., Hyun, M.S., Gadd, G.M., Kim, H.J. 2007. A novel biomonitoring system using microbial fuel cells. *Journal of environmental monitoring*, **9**(12), 1323-1328.

Kovalchik, K.A., MacLennan, M.S., Peru, K.M., Headley, J.V., Chen, D.D. 2017. Standard method design considerations for semi-quantification of total naphthenic acids in oil sands process affected water by mass spectrometry: A review. *Frontiers of Chemical Science and Engineering*, **11**(3), 497-507.

Kurek, J., Kirk, J.L., Muir, D.C., Wang, X., Evans, M.S., Smol, J.P. 2013. Legacy of a half century of Athabasca oil sands development recorded by lake ecosystems. *Proceedings of the National Academy of Sciences*, **110**(5), 1761-1766.

Lengger, S.K., Scarlett, A.G., West, C.E., Frank, R.A., Hewitt, L.M., Milestone, C.B., Rowland, S.J. 2015. Use of the distributions of adamantane acids to profile short-term temporal and pond-scale spatial variations in the composition of oil sands process-affected waters. *Environmental Science: Processes & Impacts*, **17**(8), 1415-1423.

Liu, S., Li, R., Smith, K., Che, H. 2016. Why conventional detection methods fail in identifying the existence of contamination events. *Water research*, **93**, 222-229.

MacKinnon, M.D., Boerger, H. 1986. Description of two treatment methods for detoxifying oil sands tailings pond water. *Water Quality Research Journal*, **21**(4), 496-512.

Mahaffey, A., Dubé, M. 2016. Review of the composition and toxicity of oil sands process-affected water. *Environmental Reviews*, **25**(1), 97-114.

Martin, J.W. 2015. The Challenge: Safe release and reintegration of oil sands process-affected water. *Environmental toxicology and chemistry*, **34**(12), 2682-2682.

Martin, J.W., Barri, T., Han, X., Fedorak, P.M., El-Din, M.G., Perez, L., Scott, A.C., Jiang, J.T. 2010. Ozonation of oil sands process-affected water accelerates microbial bioremediation. *Environmental science & technology*, **44**(21), 8350-8356.

Martin, J.W., Han, X., Peru, K.M., Headley, J.V. 2008. Comparison of high-and low-resolution electrospray ionization mass spectrometry for the analysis of naphthenic acid mixtures in oil sands process water. *Rapid Communications in Mass Spectrometry: An International*

Journal Devoted to the Rapid Dissemination of Up-to-the-Minute Research in Mass Spectrometry, **22**(12), 1919-1924.
Martin, N., Burkus, Z., McEachern, P., Yu, T. 2014. Naphthenic acids quantification in organic solvents using fluorescence spectroscopy. *Journal of Environmental Science and Health, Part A*, **49**(3), 294-306.
McQueen, A.D., Kinley, C.M., Hendrikse, M., Gaspari, D.P., Calomeni, A.J., Iwinski, K.J., Castle, J.W., Haakensen, M.C., Peru, K.M., Headley, J.V., Rodgers, J.H., Jr. 2017. A risk-based approach for identifying constituents of concern in oil sands process-affected water from the Athabasca Oil Sands region. *Chemosphere*, **173**, 340-350.
Mellon, F. 2003. Mass Spectrometry| Principles and Instrumentation.
Merlin, M., Guigard, S.E., Fedorak, P.M. 2007. Detecting naphthenic acids in waters by gas chromatography–mass spectrometry. *Journal of Chromatography A*, **1140**(1-2), 225-229.
Meshref, M.N., Chelme-Ayala, P., El-Din, M.G. 2017. Fate and abundance of classical and heteroatomic naphthenic acid species after advanced oxidation processes: Insights and indicators of transformation and degradation. *Water research*, **125**, 62-71.
Miles, S.M., Asiedu, E., Balaberda, A.-l., Ulrich, A.C. 2020. Oil sands process affected water sourced Trichoderma harzianum demonstrates capacity for mycoremediation of naphthenic acid fraction compounds. *Chemosphere*, 127281.
Mohammed, M.A., Sorbie, K.S. 2009. Naphthenic acid extraction and characterization from naphthenate field deposits and crude oils using ESMS and APCI-MS. *Colloids and Surfaces A: Physicochemical and Engineering Aspects*, **349**(1-3), 1-18.
Morandi, G.D., Wiseman, S.B., Pereira, A., Mankidy, R., Gault, I.G., Martin, J.W., Giesy, J.P. 2015. Effects-directed analysis of dissolved organic compounds in oil sands process-affected water. *Environmental Science & Technology*, **49**(20), 12395-12404.
Pereira, A., Martin, J. 2015. Exploring the complexity of oil sands process-affected water by high efficiency supercritical fluid chromatography/orbitrap mass spectrometry. *Rapid Communications in Mass Spectrometry*, **29**(8), 735-744.
Pereira, A.S., Bhattacharjee, S., Martin, J.W. 2013. Characterization of oil sands process-affected waters by liquid chromatography orbitrap mass spectrometry. *Environmental science & technology*, **47**(10), 5504-5513.
Pérez-Estrada, L.A., Han, X., Drzewicz, P., Gamal El-Din, M., Fedorak, P.M., Martin, J.W. 2011. Structure–reactivity of naphthenic acids in the ozonation process. *Environmental science & technology*, **45**(17), 7431-7437.
Pourrezaei, P. 2013. Physico-Chemical Processes for Oil Sands Process-Affected Water Treatment.
Quagraine, E., Peterson, H., Headley, J. 2005. In situ bioremediation of naphthenic acids contaminated tailing pond waters in the Athabasca oil sands region—demonstrated field studies and plausible options: a review. *Journal of Environmental Science and Health*, **40**(3), 685-722.
Redman, A., Parkerton, T., Butler, J., Letinski, D., Frank, R., Hewitt, L., Bartlett, A., Gillis, P., Marentette, J., Parrott, J. 2018. Application of the target lipid model and passive samplers to characterize the toxicity of bioavailable organics in oil sands process-affected water. *Environmental science & technology*, **52**(14), 8039-8049.
Regional Aquatics Monitoring Program. 2011. Query water quality data. Regional Aquatics Monitoring Program.

Ripmeester, M.J., Duford, D.A. 2019. Method for routine "naphthenic acids fraction compounds" determination in oil sands process-affected water by liquid-liquid extraction in dichloromethane and Fourier-Transform Infrared Spectroscopy. *Chemosphere*, **233**, 687-696.

Rogers, V.V., Liber, K., MacKinnon, M.D. 2002a. Isolation and characterization of naphthenic acids from Athabasca oil sands tailings pond water. *Chemosphere*, **48**(5), 519-527.

Rogers, V.V., Wickstrom, M., Liber, K., MacKinnon, M.D. 2002b. Acute and subchronic mammalian toxicity of naphthenic acids from oil sands tailings. *Toxicological Sciences*, **66**(2), 347-355.

Rowland, S., Pereira, A., Martin, J., Scarlett, A., West, C., Lengger, S., Wilde, M., Pureveen, J., Tegelaar, E., Frank, R. 2014. Mass spectral characterisation of a polar, esterified fraction of an organic extract of an oil sands process water. *Rapid Communications in Mass Spectrometry*, **28**(21), 2352-2362.

Rowland, S.J., Scarlett, A.G., Jones, D., West, C.E., Frank, R.A. 2011a. Diamonds in the rough: identification of individual naphthenic acids in oil sands process water. *Environmental science & technology*, **45**(7), 3154-3159.

Rowland, S.J., West, C.E., Jones, D., Scarlett, A.G., Frank, R.A., Hewitt, L.M. 2011b. Steroidal aromatic 'naphthenic acids' in oil sands process-affected water: structural comparisons with environmental estrogens. *Environmental science & technology*, **45**(22), 9806-9815.

Rowland, S.J., West, C.E., Scarlett, A.G., Jones, D., Frank, R.A. 2011c. Identification of individual tetra-and pentacyclic naphthenic acids in oil sands process water by comprehensive two-dimensional gas chromatography/mass spectrometry. *Rapid communications in mass spectrometry*, **25**(9), 1198-1204.

Scott, A.C., Mackinnon, M.D., Fedorak, P.M. 2005. Naphthenic acids in Athabasca oil sands tailings waters are less biodegradable than commercial naphthenic acids. *Environmental science & technology*, **39**(21), 8388-8394.

Scott, A.C., Young, R.F., Fedorak, P.M. 2008a. Comparison of GC–MS and FTIR methods for quantifying naphthenic acids in water samples. *Chemosphere*, **73**(8), 1258-1264.

Scott, A.C., Zubot, W., Davis, C.W., Brogly, J. 2020. Bioaccumulation potential of naphthenic acids and other ionizable dissolved organics in oil sands process water (OSPW)–A review. *Science of The Total Environment*, **712**, 134558.

Scott, A.C., Zubot, W., MacKinnon, M.D., Smith, D.W., Fedorak, P.M. 2008b. Ozonation of oil sands process water removes naphthenic acids and toxicity. *Chemosphere*, **71**(1), 156-160.

Shao, X., Liu, G., Yang, J., Xu, X. 2017. Research on the synthesis of ionic liquids/layered double hydroxides intercalation composites and their application on the removal of naphthenic acid from oil. *Energy & Fuels*, **31**(10), 10718-10726.

Shi, Y., Huang, C., El-Din, M.G., Liu, Y. 2017. Optimization of moving bed biofilm reactors for oil sands process-affected water treatment: The effect of HRT and ammonia concentrations. *Science of the Total Environment*, **598**, 690-696.

Shi, Y., Huang, C., Rocha, K.C., El-Din, M.G., Liu, Y. 2015. Treatment of oil sands process-affected water using moving bed biofilm reactors: with and without ozone pretreatment. *Bioresource technology*, **192**, 219-227.

Sohrabi, V., Ross, M., Martin, J., Barker, J. 2013. Potential for in situ chemical oxidation of acid extractable organics in oil sands process affected groundwater. *Chemosphere*, **93**(11), 2698-2703.

Sun, J.-Z., Peter Kingori, G., Si, R.-W., Zhai, D.-D., Liao, Z.-H., Sun, D.-Z., Zheng, T., Yong, Y.-C. 2015. Microbial fuel cell-based biosensors for environmental monitoring: a review. *Water Science and Technology*, **71**(6), 801-809.

Sun, N., Chelme-Ayala, P., Klamerth, N., McPhedran, K.N., Islam, M.S., Perez-Estrada, L., Drzewicz, P., Blunt, B.J., Reichert, M., Hagen, M. 2014. Advanced analytical mass spectrometric techniques and bioassays to characterize untreated and ozonated oil sands process-affected water. *Environmental science & technology*, **48**(19), 11090-11099.

Tanna, R.N., Redman, A.D., Frank, R.A., Arciszewski, T.J., Zubot, W.A., Wrona, F.J., Brogly, J.A., Munkittrick, K.R. 2019. Overview of Existing Science to Inform Oil Sands Process Water Release: A Technical Workshop Summary. *Integrated environmental assessment and management*, **15**(4), 519-527.

Taschuk, M., Wang, Q., Drake, S., Ewanchuk, A., Gupta, M., Alostaz, M., Ulrich, A., Sego, D., Tsui, Y. 2010. Portable Naphthenic Acid Sensor for Oil Sands Applications. *IN: Proceedings of the Second International Oil Sands Tailings Conference. Sego, D. and N. Beier (Eds.)*. Citeseer. pp. 213-221.

Toor, N.S., Han, X., Franz, E., MacKinnon, M.D., Martin, J.W., Liber, K. 2013. Selective biodegradation of naphthenic acids and a probable link between mixture profiles and aquatic toxicity. *Environmental toxicology and chemistry*, **32**(10), 2207-2216.

Wang, N., Chelme-Ayala, P., Perez-Estrada, L., Garcia-Garcia, E., Pun, J., Martin, J.W., Belosevic, M., Gamal El-Din, M. 2013. Impact of ozonation on naphthenic acids speciation and toxicity of oil sands process-affected water to Vibrio fischeri and mammalian immune system. *Environmental science & technology*, **47**(12), 6518-6526.

Wang, Y., Chu, Z., Qiu, B., Liu, C., Zhang, Y. 2006. Removal of naphthenic acids from a vacuum fraction oil with an ammonia solution of ethylene glycol. *Fuel*, **85**(17-18), 2489-2493.

Wilde, M.J., West, C.E., Scarlett, A.G., Jones, D., Frank, R.A., Hewitt, L.M., Rowland, S.J. 2015. Bicyclic naphthenic acids in oil sands process water: Identification by comprehensive multidimensional gas chromatography–mass spectrometry. *Journal of Chromatography A*, **1378**, 74-87.

Wiseman, S.B., He, Y., Gamal-El Din, M., Martin, J.W., Jones, P.D., Hecker, M., Giesy, J.P. 2013. Transcriptional responses of male fathead minnows exposed to oil sands process-affected water. *Comparative Biochemistry and Physiology Part C: Toxicology & Pharmacology*, **157**(2), 227-235.

Wu, C., De Visscher, A., Gates, I.D. 2019. On naphthenic acids removal from crude oil and oil sands process-affected water. *Fuel*, **253**, 1229-1246.

Xiao, N., Wu, R., Huang, J.J., Selvaganapathy, P.R. 2020. Development of a xurographically fabricated miniaturized low-cost, high-performance microbial fuel cell and its application for sensing biological oxygen demand. *Sensors and Actuators B: Chemical*, **304**, 127432.

Xu, X., Pliego, G., Zazo, J.A., Sun, S., García-Muñoz, P., He, L., Casas, J.A., Rodriguez, J.J. 2017. An overview on the application of advanced oxidation processes for the removal of naphthenic acids from water. *Critical Reviews in Environmental Science and Technology*, **47**(15), 1337-1370.

Xue, J., Huang, C., Zhang, Y., Liu, Y., El-Din, M.G. 2018. Bioreactors for oil sands process-affected water (OSPW) treatment: A critical review. *Science of the Total Environment*, **627**, 916-933.

Xue, J., Zhang, Y., Liu, Y., El-Din, M.G. 2017. Dynamics of naphthenic acids and microbial community structures in a membrane bioreactor treating oil sands process-affected water: impacts of supplemented inorganic nitrogen and hydraulic retention time. *RSC Advances*, **7**(29), 17670-17681.

Xue, J., Zhang, Y., Liu, Y., El-Din, M.G. 2016. Treatment of raw and ozonated oil sands process-affected water under decoupled denitrifying anoxic and nitrifying aerobic conditions: a comparative study. *Biodegradation*, **27**(4-6), 247-264.

Yang, W., Wei, X., Fraiwan, A., Coogan, C.G., Lee, H., Choi, S. 2016. Fast and sensitive water quality assessment: a μL-scale microbial fuel cell-based biosensor integrated with an air-bubble trap and electrochemical sensing functionality. *Sensors and Actuators B: Chemical*, **226**, 191-195.

Yue, S., Ramsay, B.A., Wang, J., Ramsay, J.A. 2016. Biodegradation and detoxification of naphthenic acids in oil sands process affected waters. *Science of the Total Environment*, **572**, 273-279.

Zhang, L., Zhang, Y., El-Din, M.G. 2018. Degradation of recalcitrant naphthenic acids from raw and ozonated oil sands process-affected waters by a semi-passive biofiltration process. *Water research*, **133**, 310-318.

Zhang, Y. 2016. Development and application of Fenton and UV-Fenton processes at natural pH using chelating agents for the treatment of oil sands process-affected water.

Zhang, Y., Xue, J., Liu, Y., El-Din, M.G. 2016. Treatment of oil sands process-affected water using membrane bioreactor coupled with ozonation: a comparative study. *Chemical Engineering Journal*, **302**, 485-497.

Zhu, S., Li, M., El-Din, M.G. 2018. The roles of pH and draw solute on forward osmosis process treating aqueous naphthenic acids. *Journal of Membrane Science*, **549**, 456-465.

Zubarev, R.A., Makarov, A. 2013. Orbitrap mass spectrometry, ACS Publications.

Zubot, W., MacKinnon, M.D., Chelme-Ayala, P., Smith, D.W., Gamal El-Din, M. 2012. Petroleum coke adsorption as a water management option for oil sands process-affected water. *Sci Total Environ*, **427-428**, 364-72.

Zubot, W.A. 2010. Removal of naphthenic acids from oil sands process water using petroleum coke, University of Alberta.

Chapter 2 – A review and roadmap for developing microbial electrochemical cell-based biosensors for recalcitrant environmental contaminants, emphasis on aromatic compounds

This chapter contains an extensive review of literature introducing the concept of a microbial electrochemical cell-based (MXC) biosensor and its applications for the detection of recalcitrant and persistent toxicants (e.g., oil, phenolic compounds, hydrocarbons, etc.) with emphasis on aromatic compounds, which are similar in chemical structures/compositions compared with naphthenic acids.

A version of this chapter currently under review in Chemical Engineering Journal (manuscript number: CEJ-D-20-20198).

2-1. Introduction

The microbial electrochemical cells (MXCs) are unique biosystems that use electroactive bacteria as biocatalysts to convert the chemical energy in organic matters into bioenergy, such as bio-electricity in microbial fuel cell (MFC) (Logan, 2008), bio-hydrogen in microbial electrolysis cell (MEC) (Logan et al., 2008; Wagner et al., 2009), bio-methane in microbial electrolysis cell assisted anaerobic digester (MEC-AD) (Huang et al., 2020; Zakaria & Dhar, 2019), and water desalination in microbial desalination cell (MDC) (Al-Mamun et al., 2018; Jafary et al., 2020). MXCs have also been implemented for the applications of nutrient recovery (Barua et al., 2019; Zou et al., 2017) and production of chemicals, such as hydrogen peroxide (Chung et al., 2020b; Rozendal et al., 2009) from waste and wastewater. Due to the extensive studies since the early 2000s, several studies have been implemented for scaling up the energy-generating MXCs (Dhar et al., 2016; Heidrich et al., 2014; Liang et al., 2018; Sim et al., 2018a). However, MXCs still face challenges, in the design and configuration of the reactor such as determination of an optimal electrode spacing. This requires further investigations before their implementations in full-scale applications and commercialization (Heidrich et al., 2014; Sim et al., 2018a; Zakaria & Dhar, 2019).

Despite these research gaps and scale-up challenges, the MXCs have shown great potentials and interests as a biosensing tool over other energy and resource recovery applications. Over the last decades, the MXC biosensors have been demonstrated to be a feasible approach for rapid monitoring of water quality parameters, such as biochemical oxygen demand (BOD) (Guo & Liu, 2020), chemical oxygen demand (COD) (Jia et al., 2017), microbial activities (Tront et al., 2008), single organic substrates, such as acetate (Tront et al., 2008), and presence of toxicants, such as formaldehyde (Jiang et al., 2018a) and heavy metals (Yi et al., 2019a). Furthermore, MXC biosensors for organic contaminants or toxicants monitoring have emerged due to various

advantages over conventional biosensors and other analytical tools (Do et al., 2020; Peixoto et al., 2011; Stein et al., 2012b; Sun et al., 2015; Yang et al., 2016). For instance, MXC biosensors do not require a transducer to translate biological response to a quantitative electrical signal, which is crucial for traditional biosensors that use enzymes, antibody, and pigment molecules as bioreceptor. Due to the unique metabolic features of electroactive bacteria (EAB), MXC biosensors can be operated in an intermittent mode, where the EAB can survive for several days (e.g., ~11 days) despite the lack of substrate (Ruiz et al., 2015). This feature can allow us to use the MXC biosensor as a portable biosensor. Moreover, their deployment in MFC mode can provide a 'self-powered' operation (Davila et al., 2011; Sun et al., 2015), which further simplifies their management and maintenance. MXC biosensors can also be manufactured to microliter scales (Xiao et al., 2020b; Xu et al., 2015; Yang et al., 2016), significantly lowing the fabrication costs. A detailed comparison with other analytical methods is described in the literature (Chu et al., 2020). Due to these attractive features, MXC biosensors have already been commercialized for water quality monitoring (Jiang et al., 2018b).

Among various environmental contaminants, aromatic compounds are considered as recalcitrant and the most persistent in the environment (Seo et al., 2009). Aromatic compounds are classified as organic compounds containing one or more aromatic rings, such as benzene rings (Seo et al., 2009), which include polycyclic aromatic hydrocarbons (PAHs), alkylated PAH derivatives, heterocyclic compounds containing one or more N, S, or O atoms within the aromatic ring, and many more (Ahad et al., 2020). These aromatic compounds are also ubiquitous (Wallace et al., 2020) and recalcitrant (Zhang et al., 2020a). More importantly, some of these aromatic compounds have been confirmed to be carcinogenic (e.g., PAH) (Menzie et al., 1992) and highly-toxic (e.g., heterocyclic compounds derived from crude oils and shale oils) (Tsuda et al., 1982)

ever since back in the 1900s. Therefore, the detection of these aromatic compounds became critical to protect the environment (e.g., aquatic species including fish and invertebrates and wildlife) as well as the public health (e.g., severe symptoms and bioaccumulation effects) from their potential exposures (Pv et al., 2020; Wallace et al., 2020). Many expensive and time-consuming analytical instruments and tools (e.g., mass-spectrometry- and chromatography-based) have been widely implemented for the detection of such aromatic compounds and other recalcitrant contaminants, often with the requirement of highly skillful hands and samples' pre-treatment and preparation (Ahmad et al., 2019; Do et al., 2020; Zhang et al., 2019). Nonetheless, despite their high-quality performances (e.g., high sensitivity and selectivity), they still face a major limitation of being lab-based analysis, which is unsuitable for *in situ* field applications. Therefore, the development of a rapid and inexpensive *in situ* monitoring methods for these toxicants is crucial for minimizing environmental risks.

In recent years, extensive research activities conducted on the biosensors based on the principle of MXC (Davila et al., 2011; Sun et al., 2015; Zhou et al., 2017a). Previous studies also demonstrated that MXC-based biosensors could be a promising bioanalytical tool for next-generation environmental monitoring of various recalcitrant and persistent contaminants, including aromatic compounds (Chouler & Di Lorenzo, 2019; Chung et al., 2020a; Dai et al., 2019; Kim et al., 2007; Liu et al., 2014). Multiple recent review articles have been published for supporting the applications of MXCs for monitoring water quality parameters (e.g., COD, BOD), chemical and biological toxicants (Do et al., 2020; Jiang et al., 2018b; Sun et al., 2015; Zhou et al., 2017a). Bioelectrochemical degradations (e.g., using MFCs and MECs) of aromatic compounds have been discussed earlier (Yang et al., 2020). Moreover, the applications of MXC

biosensors for aromatic compounds have been investigated in a few studies (discussed in details later).

To the best of the author's knowledge, there are no related review articles mainly focusing on detecting recalcitrant environmental contaminants, such as aromatic compounds (e.g., phenols and their derivatives), pesticides, formaldehyde, heavy metals, etc. using MXC biosensors. Hence, this review article provides a comprehensive review of published reports on detecting recalcitrant contaminants, especially the aromatic compounds using MXC biosensors, including their challenges and prospects. We critically reviewed and discussed the detection of various types of recalcitrant contaminants, especially the aromatic compounds using MXC biosensors, along with various performance metrics, operating conditions, and calibration methods. Moreover, we discussed the challenges and prospects of MXC biosensors on the detection of the toxicants mentioned above.

2-2. Biosensing mechanisms in MXCs

Unlike many other applications of MXCs, the MXC biosensors do not focus on producing high current densities, but instead, they focus on changes in the electrical signal (i.e., current, voltage) under various concentrations of target analytes (Jiang et al., 2018b). In a typical MXC biosensor, the biofilm of specialized bacteria, called electroactive bacteria (EAB), serves as the sensing and transducing element (Sun et al., 2015; Zhou et al., 2017a). The presence or change in the concentration of target analytes (i.e., contaminants) in water would affect their metabolic activities, such as substrate oxidation rates and subsequent electron transfer rates, and ultimately, the electrical response (e.g., current, voltage) (Chung et al., 2020a; Dai et al., 2019; Sun et al., 2015). Figure 2-1 illustrates different biosensing pathways for an MXC biosensor.

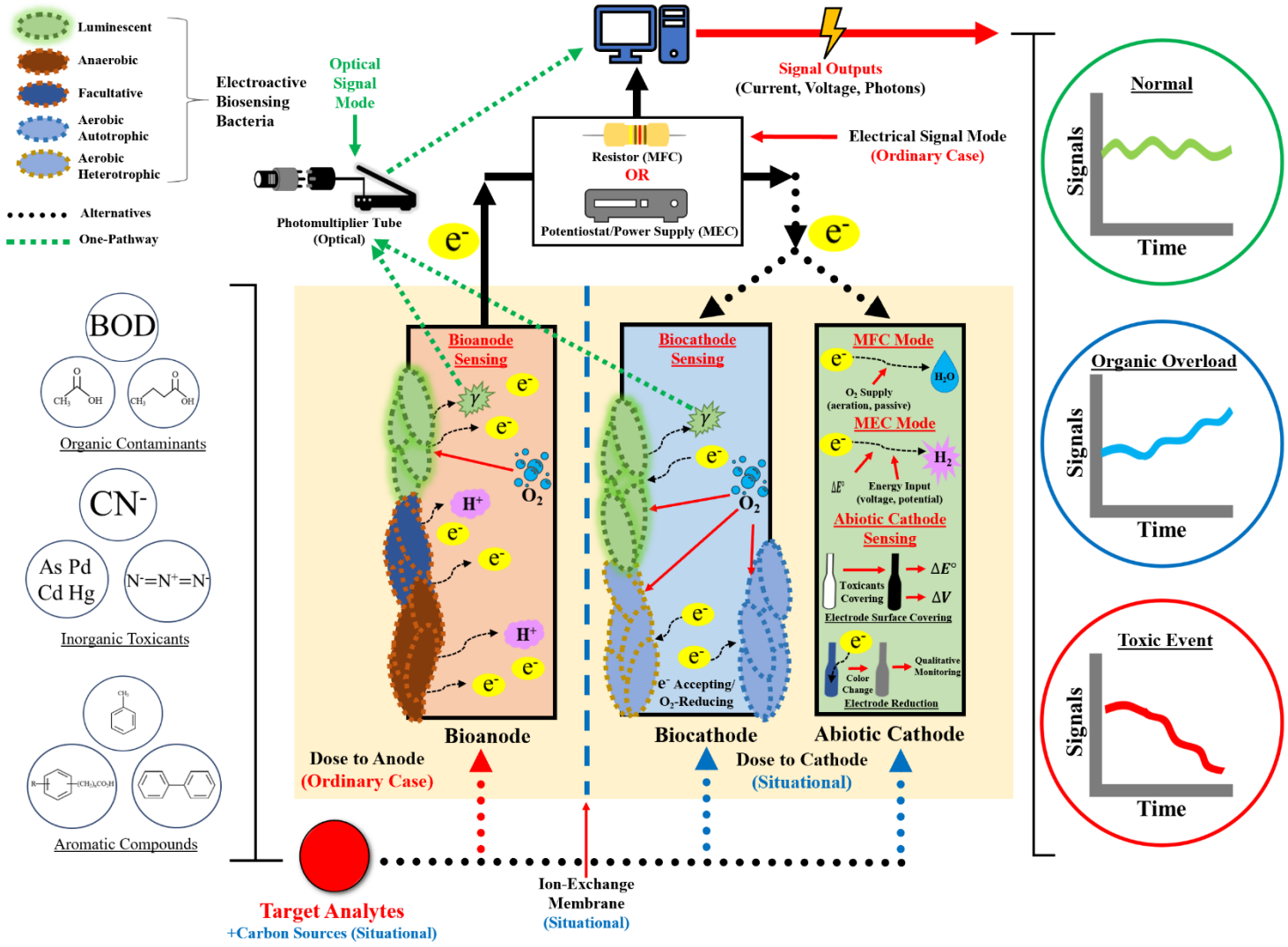

Figure 2-1. Potential pathways of MXC biosensing mechanism emphasizing on the main pathway, the anode dosage, such as MFC and MEC biosensor modes

The typical MXC biosensors, organic analytes are dosed to the anode chamber. Once the organic analytes enter the anode chamber, anaerobic or facultative EAB produces the electrons via microbial oxidation; then, the released electrons are further transferred to the anode electrode by a process called extracellular electron transport (Jiang et al., 2014; Lovley & Nevin, 2011). Then, the electrons further move from anode to the cathode through an external circuit driven by the potential gradient between the two electrodes (Sun et al., 2015). Thus, MXC biosensors produce an electrical signal output, such as voltage and current as a function of the oxidation rate of organic analytes (Kaur et al., 2013; Zhou et al., 2017a). The levels of electrical signals generated will depend on the concentration of the organic analytes; thus, the electrical signal can be correlated to the concentrations of organic contaminant (Kaur et al., 2013; Zhou et al., 2017a). Moreover, the signal outputs from MXCs proportionally increases or decreases in response to the concentration of organic matters and toxicants (e.g., inhibition of microbial activities occurs when toxicant concentrations exceed a specified value (Kim et al., 2007)), respectively (Adekunle, 2018; Sonawane et al., 2020; Sun et al., 2015; Zhou et al., 2017a). In the case of inorganic contaminants, such as heavy metals, additional carbon sources are added to drive the anodic microbial oxidation, which are required as part of the MXC biosensing mechanism (Table 2-1). Detailed explanations regarding the main MXC biosensing mechanism (e.g., bioanode sensing) and signal processing (e.g., inhibition ratio) can be found elsewhere (Adekunle, 2018; Jiang et al., 2018b; Sonawane et al., 2020; Sun et al., 2015; Zhou et al., 2017a).

Table 2-1. The construction and performance of MXC biosensor for detection of aromatic compounds, recalcitrant and persistent toxicants.

Note CEM (cation-exchange membrane), AEM (anion-exchange membrane), IEM (ion-exchange membrane)

Sensed Analyte	Detection Limit, Linear Range	Other Sources Added	Inoculum Sources	Working Volume (mL): Anode (left) Cathode (right)		Electrode Type: Anode (left) Cathode (right)		Electron Acceptor	Type	Chamber Type	Operating Condition			Time (min) Response, Exposure	Signal Processing [control mode]	Signal Outputs		References
											Temp (°C)	pH	Operating Mode			Initial	Final	
AROMATIC COMPOUNDS																		
BTEX	50 mg/L (Toluene)	Glucose (1.5% w/w)	*E. coli*	126		Carbon felt	Titanium wire coil	-	MFC	Single	-	-	-	5	Current [Constant Potential]	Refer to the literature		(Santoro et al., 2016)
Hydrocarbons	0.04 – 1% gasoline (v/v)	Glucose (30 - 500 mg COD/L)	Microalgae (*C. vulgaris*), Anaerobic sludge	60	60	Carbon cloth	Carbon cloth	O_2	MFC	Dual with CEM	-	-	Semi-continuous	-	Voltage [External Resistance]	Refer to the literature		(Nandimandalam & Gude, 2019)
Naphthenic acid (CHA model)	40 – 200 mg COD/L	-	Mature fine tailings	80	40	Carbon fiber	Stainless-steel mesh	-	MXC	Dual with AEM	Room temp.	8.1 ± 0.2	Batch	220	Current [Constant Potential]	Refer to the literature		(Chung et al., 2020a)
Oil (engine oil)	0.5 – 3.0 mL/ 100 mL	Acetate (720 mg/L)	Anoxic sludge	100	50	Carbon cloth	Carbon fiber	O_2	MFC	Dual	24.9 ± 1.6	-	Batch	103.5 – 729.0	Voltage [External Resistance]	0 mV	-37.5 – -118.1 mV	(Dai et al., 2019)
PCB	1.0 mg/L	Glucose-glutamic acid, Glucose (150 mg BOD/L)	Activated sludge	-	-	-	-	-	MFC	Dual	35.0	7.0 ± 0.2	Semi-continuous	-	Inhibition ratio, Columbic yield [External Resistance]	Inhibition Ratio = 38%		(Kim et al., 2007)
Pesticide	0.05 ppm (Atrazine)	Acetate (0.1 – 200 mM)	Anaerobic sludge	0.128		Carbon cloth	Carbon cloth	O_2	MFC	Single	10 - 40	6.3 – 12.5	Continuous	30	Sensitivity, Current [External Resistance]	1.39 $ppm^{-1}cm^2$		(Chouler & Di Lorenzo, 2019)
	0.5 µM (Diuron)	BG11, sunlight (-)	*Synechocystis* PCC6803	-		Carbon nanotube	Pt wire	-	Photo-MXC sensor	-	22.0 ± 2.0	-	Batch	-	Photocurrent, Inhibition ratio [Constant Potential]	91% ± 4%		(Tucci et al., 2019)
	10 µM (Atrazine)															76% ± 7%		
	0.5 – 10 µM (Paraquat)														Photocurrent [Constant Potential]	203% ± 3%		
PNP	9 mg/L	-	*Pseudomonas monteilii* LZU-3	240	240	Carbon felt	Carbon felt	KCN	MFC	Dual with CEM	30.0	7.8	Batch	30	Voltage [External Resistance]	Maximum voltage (mV) = 0.0.7508(PNP, mg/L) + 40.4735		(Chen et al., 2016)
4-NP	10 – 150 mg/L	Glucose glutamic acid (600 mg/L)	MFC effluent	10		Carbon cloth	Pt gas diffusion electrode	O_2	MFC	Single	-	-	Semi-continuous	-	Current density [External Resistance]	Refer to the literature		(Spurr et al., 2020)
RECALCITRANT AND PERSISTENT TOXICANTS																		
Azide	0.02 mM	Lactate (900 mg/L)	Primary wastewater	-		-	-	-	MFC	Single	35.0	-	Continuous	24	Current [Constant Potential]	Refer to the literature		(Ahn & Schröder, 2015)

BE (real urine)	627 ng/mL	-	Domestic wastewater	6		Carbon cloth	Carbon cloth	O_2	MFC	Single	32.0 ± 2.0	9.0	Batch	-	Power, Current density [External Resistance]	16 mW/m^2, 0.15 A/m^2	(Catal et al., 2019)
BE (synthetic urine)	100 ng/mL	Acetate (979 mg/L)	Domestic wastewater	6		Carbon cloth	Carbon cloth	O_2	MFC	Single	32.0 ± 2.0	7.4	Batch	-	Power, Current density [External Resistance]	96 mW/m^2, 0.37 A/m^2	(Catal et al., 2019)
Cyanide	10.4 mg/L	Lactate (900 mg/L)	Primary WW	-		-	-	-	MFC	Single	35.0	-	Continuous	24	Current [Constant Potential]	Refer to the literature	(Ahn & Schröder, 2015)
Diazinon	1.0 mg/L	Glucose-glutamic acid, Glucose (150 mg BOD/L)	Activated sludge	-		-	-	-	MFC	Dual	35.0	7.0 ± 0.2	Semi-continuous	-	Inhibition Ratio [External Resistance]	28%	(Kim et al., 2007)
Formaldehyde (liquid form)	0.0005%	Acetate (720 mg/L)	-	7	7	-	Gas diffusion electrode	O_2	MFC	Dual	-	-	Continuous	-	Current [External Resistance]	0.011 mA	(Jiang et al., 2018a)
	0.0005%	Acetate (590 mg/L)	MFC effluent	7	7	Graphite felt	Graphite felt	O_2	Bioanode MFC	Dual with CEM	25.0 ± 1.0	-	Continuous	NA	Sensitivity, Current [Constant Potential]	3.4 – 5.5 mA%$^{-1}$cm^{-2}	(Jiang et al., 2017b)
									Bicathode MFC							7.4 – 67.5 mA%$^{-1}$cm^{-2}	
	0.00148%	-	Lake sediment	56		Carbon fiber brushes	Platinum plate	-	MFC	Single	25.0 ± 1.0	-	Batch	-	Response ratio [Constant Potential]	1600 – 5000 A %$^{-1}$ m^{-3}	(Liao et al., 2018)
	0.001 – 0.1%	Yeast extract (5 g/L)	*S. oneidensis*	0.14		Carbon cloth	Air-cathode	O_2	MFC	Dual with CEM	30	-	Continuous	80>	Current [Constant Potential]	Refer to the literature	(Yang et al., 2016)
	0.01%	Acetate (1180 mg/L)	*Geobacter sulfurreducens*	180		Carbon paper	Graphite rod	-	MFC	Single	-	-	-	-	Columbic yield [Constant Potential]	Refer to the literature	(Li et al., 2016)
	0.01%	Lactate (200 mM)	*S. oneidensis*	120		Graphite rod	Platinum	-	MFC	Single	30.0 ± 1.0	-	-	582	Current [Constant Potential]	Refer to the literature	(Wang et al., 2013)
	0.1%	-	-	100		Chitosan-coated multi-layered electrode (cellulose fiber, carbon nanofibers, and graphite powder)		O_2	MFC	Single (with an edge connector)	-	7.5 ± 0.1	-	10 – 200	Current [-]	0.6 µA (-0.021 µA/min)	(Chouler et al., 2018)
	0.1%	Acetate (-)	Geobacter *sulfurreducens*	0.144	0.144	Photolithograhpy, DRIE coated with Ti/Ni/Au		-	MFC	Dual with CEM	-	7.0	-	-	Power, Voltage [Fixed Current]	Refer to the literature	(Davila et al., 2011)
	1 mg/L	CO_2 (10% v/v)	Soil, sludge	100		Graphite rod	Pt spiral wires	O_2	MXC	Single	28.0 ± 2	7.8 ± 0.2	Batch	-	Current [-]	Refer to the literature	(Prévoteau et al., 2019)
Formaldehyde (gas form)	~35 ppm	Acetate (720 mg/L)	-	7	7	-	Gas diffusion electrode	O_2	MFC	Dual	-		Continuous	60	Inhibition ratio [External Resistance]	27% (20 ppm formaldehyde), 45.8% (35 ppm formaldehyde)	(Jiang et al., 2018a)
HEAVY METALS																	
As^{3+}	0.33 mg/L	Yeast extract, tryptone (5000, 10000 mg/L)	*E. cloacae*	-	-	Carbon felt	Pt-coated carbon cloth	O_2	MFC	Dual with CEM	-	-	-	-	Polarization [Open Circuit]	Refer to the literature	(Rasmussen & Minteer, 2015)

	3 mg/L	Lactate (1800 mg/L)	Mutant *S. oneidensis*	100		Graphite rod	Graphite rod	Fe-$C_6H_5O_7$	MFC	Single	-	-	Continuous	120	Current [Constant Potential]	Current (μA) = 0.29(Aresenic, μL) + 10.42	(Webster et al., 2014)
As^{5+}	3.45 mg/L	Yeast extract, tryptone (5000, 10000 mg/L)	*E. cloacae*	-	-	Carbon felt	Pt-coated carbon cloth	O_2	MFC	Dual with CEM	-	-	-	-	Polarization [Open Circuit]	Refer to the literature	(Rasmussen & Minteer, 2015)
Cd^{2+}	0.001 mg/L	Acetate (11.8 – 590 mg/L)	MFC effluent	2		Carbon cloth	Carbon cloth	O_2	MFC	Single	20.0 ± 3.0	-	Continuous	6	Current [External Resistance]	Refer to the literature	(Di Lorenzo et al., 2014)
	0.5 mg/L	$C_8H_{18}N_2O_4S$ (7200 mg/)	*S. loihica PV-4*	50	50	Carbon clot	Pt-loaded carbon paper	-	MFC	Dual with CEM	25.0	-	Continuous	30	Columbic yield [Constant Potential]	171.1 mC/2400s	(Yi et al., 2019b)
															Columbic yield [External Resistance]	232.0 mC/2400s	
	1.0 mg/L	Glucose (1 g/L)	Cultured sludge, medium solution	14.1	14.1	Titanium wire	Titanium wire	$K_3Fe(CN)_6$	MFC	Dual with CEM	-	-	Batch	-	Inhibition absorbance [External Resistance]	28.4%	(Yu et al., 2020)
	1.5 mg/L	Acetate (59 mg/L)	Acetate-fed MFC effluent	13	25	Carbon cloth	Carbon paper	O_2	MFC	Dual with CEM	25.0 ± 0.5	-	Continuous	60	Inhibition ratio [External Resistance]	22.8%	(Yi et al., 2019a)
	2 mg/L	Glucose (1000 mg/L)	Anaerobic sludge	14.13	21.2	Graphite felt	Graphite felt	KCN	MFC	Dual with CEM	30.0 ± 1.0	7.0	Batch	-	Inhibition ratio [External Resistance]	9.29%	(Yu et al., 2017)
Co^{2+}	1.0 mg/L	Glucose (1 g/L)	Cultured sludge, medium solution	14.1	14.1	Titanium wire	Titanium wire	$K_3Fe(CN)_6$	MFC	Dual with CEM	-	-	Batch	-	Inhibition absorbance [External Resistance]	11.0%	(Yu et al., 2020)
Cr^{3+}	2 mg/L	Glucose (1000 mg/L)	Anaerobic sludge	14.13	21.2	Graphite felt	Graphite felt	KCN	MFC	Dual with CEM	30.0 ± 1.0	7.0	Batch	-	Inhibition ratio [External Resistance]	1.95%	(Yu et al., 2017)
Cr^{6+}	1 mg/L	Acetate (200 mg/L)	Wastewater	30		Carbon cloth	Carbon cloth	O_2	MFC	Single	-	-	-	NA	Voltage [External Resistance]	-350 – -398 mV / -298 mV	(Liu et al., 2014)
	1 mg/L	CO_2 (10% v/v)	Soil, sludge	100		Graphite rod	Pt spiral wires	O_2	MXC	Single	28.0 ± 2	7.8 ± 0.2	Batch	1	Current [-]	Refer to the literature	(Prévoteau et al., 2019)
	2.4 mg/L	Glucose (20 mM)	*P. veronii* 2E	60		Carbon felt	Air-breathing activated carbon	O_2	MFC	Single	-	7.0	Contunous	-	Sensitivity [External Resistance]	0.31 ± 0.02 μA/cm² /mg Cr (VI)/L	(Lazzarini Behrmann et al., 2020)
	2.5 mg/L	-	*E.aestuarii* YC211	170	170	Graphite felt	Graphite felt	Cr^{6+}	MFC	Dual with CEM	30.0	7.0	Batch	15 – 30	Power density [External Resistance]	98.3 mW/m² (maximum; others NA)	(Wu et al., 2017)
															Voltage [External Resistance]	Voltage (mV) = 517.15 - 2.3265(Cr^{6+} mg/L) (for 2.5 – 60 mg/L range)	
	10 mg/L	Acetate (250 mg COD/L)	-	30		Carbon ink-coated filter paper	4-layer-PTFE, Pt-coated carbon cloth	O_2	MFC	Single	-	-	Batch	8 – 120	Power [External Resistance]	0.35 mW / 0.08 mW	(Xu et al., 2016)

	10 mg/L	Wastewater (-)	WW fed- MFC effluent	0.2		Carbon ink	Carbon ink	-	MFC	-	-	-	-	6 – 180	Voltage [External Resistance]	0.18 V	0.04 V	(Xu et al., 2015b)
Cu^{2+}	0.01 mg/L	Acetate (88 mg/L)	Primary WW	70	50	Graphite rod	Graphite rod	$K_3Fe(CN)_6$	Planktonic MFC	Dual with CEM	Room temp.	6.8	Continuous	120	Current [External Resistance]	NA		(Patil et al., 2010)
	0.3 – 100 mg/L	Acetate (1 g/L)	MFC effluent	14	14	Graphite felt	Graphite felt	$K_3Fe(CN)_6$	MFC	Dual with CEM	23.0 ± 3.0	-	Continuous	<60 - 960	Inhibition ratio [External Resistance]	0 – 5% (1 h) 60 – 80% (20 h)		(Xing et al., 2020)
	1 mg/L	Glucose (1 g/L)	Cultured sludge, medium solution	14.1	14.1	Titanium wire	Titanium wire	$K_3Fe(CN)_6$	MFC	Dual with CEM	-	-	Batch	-	Inhibition absorbance [External Resistance]	66.6%		(Yu et al., 2020)
	1 – 6 mg/L	-	Luminescent bacteria (*Vibrio fischeri*)	15	15	Carbon felt	Pt sheet	O_2	MXC	Dual	Room temp.	-	-	-	Current, Optical signal [Constant Potential]	Refer to the literature		(Qi et al., 2019)
	2 mg/L	Glucose (1000 mg/L)	Anaerobic sludge	14.13	21.2	Graphite felt	Graphite felt	KCN	MFC	Dual with CEM	30.0 ± 1.0	7.0	Batch	-	Inhibition ratio [Constant Potential]	12.56%		(Yu et al., 2017)
	2 mg/L	Acetate (590 mg/L)	Acetate-fed MFC effluent	6.7	28	Graphite felt	Carbon-fiber brush	-	MFC	Dual with CEM	30.0 ± 1.0	-	-	120	Current [Constant Potential]	0.76 – 1.55 mA (flow-through) 0.02 – 0.06 mA (flow-by)		(Jiang et al., 2015)
	2 – 6 mg/L	Acetate (295 mg/L)	Acetate-fed MFC effluent	1.4 per chamber	28	Graphite felt	Carbon fiber	O_2	MFC	Dual with CEM	25.0 ± 1.0	-	Batch	5 – 25	Inhibition ratio [External Resistance]	Inhibition ratio (%) = 18.04(Cu^{2+}, mg/L) – 19.35		(Jiang et al., 2017c)
	5 mg/L	Domestic wastewater (300 – 400 mg COD/L)	DWW	28	28	Carbon cloth	Carbon cloth	O_2	MFC	Dual with CEM	-	-	Continuous	> 120	Voltage [External Resistance]	60%		(Shen et al., 2013)
	>6 mg/L	Acetate (590 mg/L)	Primary WW	120		Graphite rod	Graphite rod	$K_3Fe(CN)_6$	MFC	Single	Room temp.	6.8	Continuous	120	Current [Constant Potential]	Refer to the literature		(Patil et al., 2010)
	85 mg/L	Acetate (29.5 – 1180 mg/L)	MFC effluent	33	33	-	-	$K_3Fe(CN)_6$, $K_4Fe(CN)_6$	MFC	Dual with CEM	30.0	7.0	Continuous	< 50	Current change [Constant Potential]	69.8%, 44.4%, 15.8% (anode potential, respectively)		(Stein et al., 2010)
	300 mg/L	Acetate (500 mg COD/L)	DWW	43.2		Carbon cloth	Pt-loaded carbon cloth	O_2	MFC	Single with CEM	Room temp.	7.0 ± 0.2	Continuous	120	Current [External Resistance]	65%	15%	(Tan et al., 2018)
Fe^{2+}	167.5 mg/L	Acetate, Lactate (47.2 – 153 mg/L)	Natural mud	96	96	Graphite rod, graphite granules		O_2	MFC	Dual	25.0 ± 3.0	7.0	Batch	-	Current [External Resistance]	Refer to the literature		(Tran et al., 2015)
	400 mg/L	Acetate (108 mg/L)	Anaerobic sludge	50		Carbon felt	Mn-based catalyzed carbon E4	O_2	MFC	Single	23.0	7.0-7.5	Continuous	-	Current [External Resistance]	Refer to the literature		(Adekunle et al., 2019)
							Carbon paper with Ni	-	MEC									
$Fe3^{+}$	2.8 mg/L	Acetate (1180 mg/L)	*Geobacter sulfurreducens*	180		Carbon paper	Graphite rod	Fe-$C_6H_5O_7$	MFC	Single	-	-	-	-	Columbic yield [Constant Potential]	Refer to the literature		(Li et al., 2016)
	8 mg/L	Acetate (200 mg/L)	DWW	30		Non-PTFE treated carbon cloth	4-layer PTFE/Pt-coated carbon cloth	O_2	MFC	Single	-	-	-	NA	Voltage [External Resistance]	-350 – -398 mV		(Liu et al., 2014)

Hg^{2+}	0.5 mg/L	CO_2 (10% v/v)	Mix of soil and sludge	100		Graphite rod	Pt spiral wires	O_2	MXC	Single	28.0 ± 2	7.8 ± 0.2	Batch	1	Current [-]	Refer to the literature	(Prévoteau et al., 2019)
	1.0 mg/L	Lactate (1 mM)	*S. loihica* PV-4	20	40	Carbon cloth	Pt loaded carbon paper	-	MFC with baffles	Dual with CEM	25.0 ± 0.5	-	Continuous	~30	Sensitivity [External Resistance]	52.3%	(Yi et al., 2020)
	1.0 mg/L	Glucose-glutamic acid, Glucose (150 mg BOD/L)	Activated sludge	-	-	-	-	-	MFC	Dual	35.0	7.0 ± 0.2	Semi-continuous	-	Inhibition ratio, Columbic yield [External Resistance]	IR = 28% CY = NA	(Kim et al., 2007)
	1.5 mg/L	Acetate (59 mg/L, 118 mg/L)	-	28	28	Carbon cloth	Carbon cloth	O_2	SAB-MFC	Dual with CEM	25.0 ± 0.5	-	Continuous	30	Current [External Resistance]	Refer to the literature	(Zhao et al., 2019)
	2.0 mg/L	Glucose (1000 mg/L)	Anaerobic sludge	14.13	21.2	Graphite felt	Graphite felt	KCN	MFC	Dual with CEM	30.0 ± 1.0	7.0	Batch	-	Inhibition ratio [External Resistance]	13.99%	(Yu et al., 2017)
Mg^{2+}	100 mg/L	Acetate (108 mg/L)	Anaerobic sludge	50		Carbon felt	Mn-based catalyzed carbon E4	O_2	MFC	Single	23.0	7.0-7.5	Continuous	-	Current [External Resistance]	Refer to the literature	(Adekunle et al., 2019)
							Carbon paper with Ni	-	MEC								
Ni^{2+}	10 mg/L	-	MFC effluent	-	-	Non-porous graphite plate	Non-porous graphite plate	-	MFC	Dual with CEM	-	-	Continuous	120	Polarization [Constant Potential]	Refer to the literature	(Stein et al., 2012a)
	13.2 mg/L	-	MFC effluent	-	-	Various graphite types	-	-	MFC	Dual with various IEM	30.0	-	Continuous	120	Current [Constant Potential]	Refer to the literature	(Stein et al., 2012c)
	20 mg/L	Wastewater (-)	WW fed-MFC effluent	0.2		Carbon ink	Carbon ink	-	Membrane-based MFC	Single	-	-	-	6 – 180	Voltage [External Resistance]	0.18 V 0.15 V	(Xu et al., 2015b)
Pb^{2+}	0.1 – 1.2 mg/L	Acetate (300 mg/L)	MWW	28		Carbon felt, Indium tin oxide	-	O_2	MFC	Single	-	-	Semi-continuous	-	Inhibition ratio [External Resistance]	~100%	(Li et al., 2019)
	1.0 mg/L	Glucose-glutamic acid, Glucose (150 mg BOD/L)	Activated sludge	-	-	-	-	-	MFC	Dual	35.0	7.0 ± 0.2	Semi-continuous	-	Inhibition ratio [External Resistance]	Inhibition ratio = 46%	(Kim et al., 2007)
	1.0 mg/L	Glucose (1 g/L)	Cultured sludge, medium solution	14.1	14.1	Titanium wire	Titanium wire	$K_3Fe(CN)_6$	MFC	Dual with CEM	-	-	Batch	-	Inhibition absorbance [External Resistance]	33.8%	(Yu et al., 2020)
	1.5 mg/L	Acetate (59 mg/L)	Acetate-fed MFC effluent	13	25	Carbon cloth	Carbon paper	O_2	MFC	Dual with CEM	25.0 ± 0.5	-	Continuous	60	Inhibition ratio [External Resistance]	21.8%	(Yi et al., 2019a)
	2.0 mg/L	Glucose (1000 mg/L)	Anaerobic sludge	14.13	21.2	Graphite felt	Graphite felt	KCN	MFC	Dual with CEM	30.0 ± 1.0	7.0	Batch	-	Inhibition ratio [External Resistance]	5.59%	(Yu et al., 2017)
	>10 mg/L	CO_2 (10% v/v)	Soil, sludge	100		Graphite rod	Pt spiral wires	O_2	MXC	Single	28.0 ± 2	7.8 ± 0.2	Batch	-	Current [-]	Refer to the literature	(Prévoteau et al., 2019)
Zn^{2+}	0 – 400 µM	Synthetic wastewater (-)	*E. Coli* BL21	240	240	Carbon felt	Carbon felt	$K_3Fe(CN)_6$	MFC	Dual with CEM	37.0	9.0	Batch	-	Voltage [External Resistance]	160 – 342 mV	(Khan et al., 2020)
	2.0 mg/L	Glucose (1000 mg/L)	Anaerobic sludge	14.13	21.2	Graphite felt	Graphite felt	KCN	MFC	Dual with CEM	30.0 ± 1.0	7.0	Batch	-	Inhibition ratio [External Resistance]	8.81%	(Yu et al., 2017)

As shown in Figure 2-1, there are other biosensing pathways for the MXC biosensor. For instance, luminescent bacteria can also be used as the anodic biosensing element (Qi et al., 2019). In response to the target analytes, luminescent bacteria produce electrons as well as photons. Thus, both electrical and optical signal outputs can be simultaneously generated with luminescent bacteria. Moreover, the use of luminescent bacteria as the cathodic biosensing element (e.g., as an electron acceptor) was also successful in producing optical signals (Qi et al., 2019). The use of a cathode chamber for toxicant monitoring has recently gained interest due to its several benefits, such as improved system robustness due to protection of anode biofilm (Dai et al., 2019), ability to handle both aerobic and anaerobic conditions (Jiang et al., 2018a), and enhanced sensitivity (Jiang et al., 2017b; Liao et al., 2018). Besides, cathode-based sensing can be accomplished in abiotic (Dai et al., 2019) or biotic conditions (Jiang et al., 2017b). Especially, for biotic mode, electrotrophic (e.g., electron-accepting) heterotrophic or autotrophic bacteria are used as biocatalysts for O_2-reducing processes, which can be inhibited by the presence of toxicants (e.g., formaldehyde), resulting in the decreased signal outputs (Jiang et al., 2018a; Jiang et al., 2017b). For abiotic cathode sensing mode, the presence of toxicants can eventually cover the cathode electrode, leading to the change in signal outputs and potentials due to suppression of cathodic reduction (Dai et al., 2019). In addition, MXC biosensors can provide quick qualitative monitoring of organics and toxicants using the combination of both anode and cathode. For instance, a specific cathode electrode, such as Prussian Blue electrode, can change color (e.g., blue to transparent by Fe-reduction) in response to the number of electrons transferred from the anode to facilitate a quick qualitative monitoring method (Yu et al., 2020). Hence, when the injected toxicants inhibit the microbial activities in the anode, the reduction reaction of Fe (III) to Fe (II) is decreased, and there will not be a significant color change (vice versa for the organic matter). More in-depth discussions

on other sensing pathways of MXC biosensors are elucidated later in Section 2-4.2.5. Given such multiple demonstrated biosensing pathways by MXC biosensors, this evidence their high potentials for the detection of aromatic compounds.

2-3. MXC biosensor for monitoring of aromatic compounds and other recalcitrant, persistent, and ubiquitous environmental pollutants

Most of the analytical methods used for detecting recalcitrant contaminants like aromatic compounds are expensive and time-consuming due to the requirement of samples pre-treatment and preparation (Ahmad et al., 2019; Peixoto et al., 2011; Ripmeester & Duford, 2019; Zhang et al., 2019). To address such challenges, studies have explored MXC biosensor as an alternative. For instance, MXC biosensors have been applied to recalcitrant aromatic compounds, such as hydrocarbons (Nandimandalam & Gude, 2019), oil (Dai et al., 2019), mining-related naphthenic acids (Chung et al., 2020a), polychlorinated biphenyls (Kim et al., 2007), pesticides (Chouler & Di Lorenzo, 2019), phenolic compounds (Chen et al., 2016; Spurr et al., 2020), and toluene (Santoro et al., 2016). Studies also have confirmed the capability of MXC biosensors on other recalcitrant contaminants, such as heavy metals, surfactants, toxic volatile organic compounds (VOCs), and many more (Table 2-1).

2-3.1 MXC biosensors for aromatic compounds

2-3.1.1 BTEX

BTEX, a short form for benzene, toluene, ethylbenzene, and xylene, is classified as mono-aromatic hydrocarbons, which is produced from a variety of oil derivatives including gasoline (Weelink et al., 2010; Xue et al., 2018). Compared to other crude oil compounds, such as aliphatic hydrocarbons, BTEX has a high solubility in water (1600 - 1750 mg/L, 500 mg/L, ~150 mg/L, and

~150 mg/L for benzene, toluene, ethylbenzene, and xylene, respectively), which typically accounts for ~90% of the dissolved contaminants in groundwater (Palma et al., 2018).

Before the applications of MXC biosensor on BTEX, studies have confirmed the degradation of BTEX in traditional MXCs targeting their microbial oxidation and subsequent electrons recovery (Daghio et al., 2018; Zhang et al., 2018). Furthermore, Friman et al. (2012) have confirmed that EAB (e.g., *Pseudomonas putida* F1) could use toluene as the sole carbon and energy source to generate current using a MEC. Based on the authors' knowledge, Santoro et al. (2016) first proposed the detection of toluene (e.g., one of BTEX) using MXC biosensor. In their study, toluene was introduced to the anode biofilm enriched with *E. Coli.* After the current was stabilized without any toluene at 17 h mark, the changes in current output caused by different toluene concentrations (e.g., 50 – 1000 mg/L and >1000 mg/L) were observed. Toluene concentration, as low as 50 mg/L was detected within a 5-min interval. On the other hand, at a very high concentration of toluene (>1,000 mg/L), the anode biofilm was permanently damaged, suggesting the need for alternative approaches to detect high concentrations of toluene. Moreover, their study did not explicitly reveal the applicability of MXC biosensor on BTEX, as their findings were more on the VOC determination (e.g., combined effect of simultaneous addition of two VOCs and the corresponding synergistic effect). However, more studies are still warranted to further confirm the applicability of MXC biosensors for other BTEX compounds.

2-3.1.2 Naphthenic acids

Out of various hydrocarbon contaminants present in the oil sands process affected water (OSPW) and tailings porewater, naphthenic acids (NAs) have been identified as one of the primary sources of acute toxicity (El-Din et al., 2011; Mahaffey & Dubé, 2016). These oil sands NAs are partially

aromatic (Abdalrhman et al., 2019), and their toxicity and recalcitrance pose a significant threat to the aquatic ecosystem and wildlife (El-Din et al., 2011; Mahaffey & Dubé, 2016). After the bitumen extraction processes, OSPW containing various NAs is stored in engineered on-site basins, known as oil sand tailings ponds (Allen, 2008). However, potential seepage of OSPW into the surrounding water bodies, such as groundwater and surface water (Fennell & Arciszewski, 2019), substantiated the importance of oil sands NA monitoring. Commonly used analytical tools for the detection of NAs include Fourier transform infrared (FTIR) spectroscopy, gas chromatography-mass spectrometry (GC-MS), and high-performance liquid chromatography (HPLC) (Fennell & Arciszewski, 2019; Ripmeester & Duford, 2019). However, these methods are expensive, require time-consuming sample preparation. Also, samples must be taken to an analytical laboratory for quantification and characterization (Ripmeester & Duford, 2019). Before the implementation of an MXC biosensor, a few studies have confirmed NA degradation using MXCs (Choi & Liu, 2014; Jiang et al., 2013). Recently, Chung et al. (2020a) have investigated the first attempt of the detection of a model NA compound (cyclohexane carboxylic acid) in water samples using a dual-chamber MXC biosensor. In their study, the model NA compound was injected into the anode chamber, which was enriched with oil sands matured fine tailings. Their MXC biosensor, first, faced challenges due to low peak current output (μA) and low precision (R^2 = 0.64) under the closed-circuit operation. However, when the charging-discharging operation was applied, the peak currents significantly increased to a milli-ampere scale with high precision (R^2 = 0.96). NA was successfully detected in a short time (<3 h) with a low detection limit (40 mg COD/L). However, further research is required to reveal more insights about the feasibility of MXC biosensors regarding complicated water matrices such as real OSPW.

2-3.1.3 Crude Oil and hydrocarbons

The monitoring of crude oil and hydrocarbons in environmental samples became significantly crucial due to the growing concerns regarding the environmental damages caused by accidental leakage during processing, storing, and transportation of petroleum products (Dai et al., 2019; Nandimandalam & Gude, 2019). Aromatic hydrocarbons in leaked oil are known to be persistent in the environment (Jha et al., 2008), which induces adverse impacts on the soil ecosystem and wildlife as well as threatening human health (Cheng et al., 2016; Gmurek et al., 2017). A release of even small quantities of hydrocarbons can still have long-lasting impacts on the environment (Brown et al., 2017; Willie et al., 2017). Various analytical methods, employing physical properties (e.g., pressure, sound wave, flow, temperature) (Bown et al., 1987) and monitoring tools (e.g., visible, infrared, ultraviolet, laser-acoustic, laser-fluorescence) (Fingas, 2016) have been implemented for oil detection. However, these methods suffered from high cost (Fingas & Brown, 2005) and performance interference due to various weather conditions (Fingas & Brown, 2014; Zhang, 1997).

In response to these challenges, the MXC biosensors have been explored to detect oil and hydrocarbons. The applicability of MXCs on oil and hydrocarbons has been investigated by multiple previous studies (Liu et al., 2019; Morris et al., 2009; Zhao et al., 2019a), showing promising results. Dai et al. (2019) first implemented an upward open-channel (UOC) MFC biosensor for the detection of oil. The authors introduced engine oil into the cathode chamber of the UOC-MFC biosensor and allowed the oil to cover the surface of the cathode electrode. Then, the drop in the potential and power density resulting from the inhibition of cathodic oxygen reduction reaction by the oil layer was examined. Their approach could detect the engine oil concentration as low as 0.5 mL (per 100 mL of electrolyte solution; the details of electrolyte

solution is described in their literature). Despite the presence of other compounds like heavy metals in the oil samples, the results showed great potential. The separation between two chambers in their UOC-MFC biosensor could ensure robustness and stability of anode biofilm (no exposure to oil), and the rapid (~2.3 h) recovery of abiotic cathode after the oil shock events.

Nandimandalam and Gude (2019) have compared the feasibility of using both anode and cathode biofilms for biosensing hydrocarbons. Both anode (enriched with anaerobic sludge) and cathode (enriched with microalgae) biofilms were exposed to various concentrations of the gasoline (simulated hydrocarbons) for a comparison. When the hydrocarbons were dosed to the anode, the inhibition of anode biofilm led to a reduction in the output voltages. Similarly, the growth of microalgae biocathode was inhibited when the gasoline was introduced in the cathode chamber. Their study showed that both anode and cathode could be used as sensing elements to quantify the hydrocarbons in the range between 0.04 – 1% v/v, which further suggested the potential applicability of MXC biosensors for petroleum-related products.

2-3.1.4 Pesticides

Pesticides are widely used to control pests in agricultural developing countries like China (Zhao et al., 2018). Many of these pesticides are known to be toxic with high solubility (Lin et al., 2020) and recalcitrance (Zhang et al., 2020a), resulting in high COD, and low BOD in the pesticide-contaminated water bodies (García-Mancha et al., 2017). Hence, the biological treatment of pesticide wastewater usually needs a long retention time as well as specific functional groups of microbes (Geed et al., 2017). With some of the pesticides (e.g., triazines derivative pesticides and chlorinated pesticides) being aromatic and persistent in the environment (Bilal et al., 2019; Gonçalves-Filho et al., 2020; Zhang et al., 2020b), the implementation of a rapid early-warning

system for pesticides detection/monitoring in water and wastewater are crucial to support the environmental management.

Analytical techniques, such as GC-MS, have been implemented to trace pesticides (Lin et al., 2020); however, they cannot provide a rapid field monitoring of pesticides in water matrices. Up to date, various MXCs have been applied to the treatment of pesticide wastewater, demonstrating their applicability (Cao et al., 2017; Lin et al., 2020). A recent study has confirmed the MXC's biosensing application on detecting pesticides using a single-chambered miniature (128 μL) MFC enriched with anaerobic sludge (Chouler & Di Lorenzo, 2019). A model pesticide, atrazine, was detected in synthetic wastewater containing acetate based on the drop in current output. After 30 minutes of exposure time, atrazine concentration as low as 0.05 ppm was detected. Their MXC biosensor system was able to recover in a short time frame (e.g., 44 min). Moreover, a photo-bioelectrochemical sensor was also developed for the detection of various pesticides (Tucci et al., 2019). Similar to current output by conventional MXC biosensors, photocurrent was used as the indicator, where an increase or a decrease in photocurrent determined the presence of pesticides. In their study, three different pesticides (e.g., diuron, atrazine, and paraquat) were compared based on the changes in photocurrent. Diuron at a very low concentration (0.5 μM) significantly inhibited the biosensor system (e.g., achieving the inhibition ratio of 91%), whereas a high concentration of atrazine (10 μM) was not as sensitive (inhibition ratio = 76%). In contrast, paraquat (0.5 – 10 μM) increased the photocurrent output by ~2 folds. Hence, this study clearly demonstrated that the sensitivity and signal output of MXC biosensors, such as in photo-bioelectrochemical sensor, can significantly vary depending on the types of pesticides. Nonetheless, with more involvement of in-depth future studies, MXC biosensors can potentially be used for the monitoring of various types of pesticides.

2-3.1.5 Phenolic compounds

Phenolic compounds have been widely adopted in many industries, such as explosives, fertilizers, paints, plastics, textiles, rubbers, among others (Raza et al., 2019). Phenols are considered as aromatic compounds (Jun et al., 2019; Raza et al., 2019). Exposures to phenols and their derivatives even at low concentrations pose significant threats to the wildlife and aquatic living organisms (Gmurek et al., 2017; Jun et al., 2019) and human health causing cancer and leading to severe symptoms, such as respiratory and lung problems, and damage to the immune system (Busca et al., 2008; Gami et al., 2014). The phenolic compounds are further known to be recalcitrant and persistent, especially they are refractory to conventional water treatment (Brandão et al., 2013). Therefore, monitoring phenols and their derivatives in water samples became important to further protect the environment and human health.

Similar to other aromatic compounds, commonly-used analytical methods, such as ultraviolet spectrometry, GC, and HPLC (Chauhan et al., 2000; Yao et al., 1991), for phenolic compounds have several analytical limitations (Raut et al., 2012) as discussed earlier. To address these challenges, various investigations were conducted to trace phenolic compounds using MXC biosensors (Chen et al., 2016; Spurr et al., 2020). Previous studies have confirmed the biodegradation of phenols using MXCs (Shen et al., 2012; Zhu & Ni, 2009). Following those studies, Chen et al. (2016) have developed an aerobic bioanode MFC biosensor to monitor *p*-nitrophenol (PNP). This MFC biosensor was able to rapidly detect PNP in 30 min and its concentrations as low as 9 mg/L in wastewater. Specifically, in their study, the pure culture PNP-degrading aerobic EAB (*Pseudomonas monteilii* LZU-3) was used to form an anode biofilm, and they were able to produce voltage using PNP as a sole substrate. Similarly, Spurr et al. (2020) were also successful in detecting 4-nitrophenol using MFC biosensors. In their study, three MFC

biosensors were operated in a series, where they highlighted selective monitoring of 4-nitrophenol in wastewaters containing other organic matters. In conclusion, these two recent studies have demonstrated the feasibility of *in situ* selective monitoring of phenolic compounds.

2-3.1.6 PCBs

Natural degradation of polychlorinated biphenyls (PCBs) is often a challenge as biodegradation processes involving plants and bacteria are very slow or even can be prevented due to the absence of a terminal electron acceptor (Wu et al., 2019b). PCBs are identified as one of the persistent organic pollutants due to their low biodegradation and bioaccumulation. PCBs can accumulate in soils and sediments, posing a significant adverse impact on the environment due to their toxicity to living organisms and human health (e.g., carcinogenic) (Reddy et al., 2019; Zeng et al., 2013; Zhang et al., 2019). Therefore, the development of a novel *in situ* monitoring method for PCBs in water bodies, such as groundwater and surface water, is required.

A wide variety of techniques (e.g., GC-MS and extraction methods) have been developed for the detection of PCBs, but they encountered many limitations, such as requirement of skilled personnel, time-consuming analysis, high costs (Ahmad et al., 2019; Zhang et al., 2019). Based on an extensive and thorough review of literature, Kim et al. (2007) presented the first study to apply MXC biosensor for the detection of PCBs. In their study, PCBs were added to the simulated wastewater and fed to the anode chamber of a dual-chamber MFC biosensor, which was inoculated with activated sludge. Then, they observed the inhibition ratio obtained from the MXC biosensor's operation with PCBs. Their inhibition ratio (e.g., $[CY_{Normal} - CY_{Toxic}]/CY_{Normal}$) was determined by calculating the columbic yields (CY) from pre- and post-toxic events, where the columbic yield is a sum of integration of peak currents over time. Higher concentrations of toxicants will suppress

the anodic microbial activities, which will aggravate the inhibition ratio. Furthermore, the use of inhibition ratio can be beneficial over other signal outputs, such as current and voltage for toxicant detection. It provides a single-term value, which reflects on the MXC biosensor inhibition caused by toxicants. The MFC biosensor developed by the authors could detect PCB concentration (1 mg/L) within one hour, indicated by an inhibition ratio (38%). Their study led to more applications of MXCs on PCBs, such as bioremediation (Hennebel et al., 2011; Wu et al., 2019b).

2-3.2 Other recalcitrant contaminants

Besides above-mentioned contaminants (mostly aromatic compounds), studies have correspondingly reported the applications of MXC biosensors for other recalcitrant pollutants, which include azide (Ahn & Schröder, 2015), cyanide (Ahn & Schröder, 2015), diazinon (Kim et al., 2007), formaldehyde (Chouler et al., 2018; Jiang et al., 2018a; Liao et al., 2018), various metal ions (Yi et al., 2019a; Yi et al., 2019b; Yu et al., 2020), and urine (Catal et al., 2019) (see Table 2-1). Many of these toxicants, such as heavy metals and formaldehyde are considered as highly-toxic, recalcitrant and persistent, which can induce a significant adverse impact on both environment and human health (Na et al., 2019; Zhang et al., 2020b).

MXC applications to these toxicants, such as heavy metals, were validated by previous studies (Ali et al., 2020; Colantonio & Kim, 2016). Based on previous studies, MXC biosensors can be applied for rapid identification (e.g., 1 min), quantification (Prévoteau et al., 2019), as well as sensitive monitoring (e.g., detecting the target analyte to a very low limit) of heavy metal concentrations (~1 μg/L) (Adekunle et al., 2019b; Di Lorenzo et al., 2014). Similarly, the detection of formaldehyde concentrations as low as 5 ppm (0.0005 %) (Jiang et al., 2018a) in a short time (e.g., 10 min) (Chouler et al., 2018) was also feasible using MXC biosensors. Thus, MXC

biosensors also have tremendous potential for the detection of these recalcitrant toxicants. More fundamentals and discussions regarding the applications of MXC biosensors on these recalcitrant, persistent, and ubiquitous toxicants and pollutants can be found in the literature (Chu et al., 2020; Jiang et al., 2018b; Zhou et al., 2017a).

2-4. Challenges and roadmap for future development

Based on the discussions in the previous sections (2-1 to 2-3), MXC biosensors have potential to provide a rapid *in situ* monitoring of the aromatic compounds and other recalcitrant contaminants. However, there are still some analytical challenges faced by MXC biosensors that must be addressed before they can be further implemented for field applications.

Specifically, recalcitrant pollutants like aromatic compounds may lead to low electrical output and the potential for longer response time due to the complexity of the analyte structures. Furthermore, improving the sensitivity of the MXC biosensor is one of the important factors to attain accurate interpretation of the data during environmental monitoring (Adekunle, 2018). There are also uncertainties in the selection for an optimal MXC biosensor (e.g., MFC vs. MEC, different configurations, types of operations, etc.) as there are many pros and cons associated with each type of MXC biosensor for different types of toxicants and pollutants. More importantly, the selective monitoring of target analytes with MXC biosensors is still an unresolved issue. Thus, the above-mentioned concerns about MXC biosensors necessitate more research to further enhance the performance (e.g., sensitivity and selectivity) and to avoid any masking of valuable information (e.g., cases of false positive-alarm). Therefore, in this section, challenges, recommendations, and future outlooks associated with applications of MXC biosensors on recalcitrant and toxicants with the emphasis on aromatic compounds are thoroughly discussed.

2-4.1 MFC vs. MEC biosensors: Which mode should be selected for recalcitrant pollutants?

The selection of MXC type is critical for detecting recalcitrant contaminants due to more analytical challenges over the monitoring of readily biodegradable organics or typical water quality parameters, such as acetate and BOD. MXC biosensors can be largely classified into two types: (i) MFC-based biosensor; and (ii) MEC-based biosensor. Briefly, MFC biosensors are autonomous due to the usage of oxygen as the terminal electron acceptor, which does not require an external power supply to operate. On the other hand, MEC biosensors require an additional power supply in the form of applied voltage or potential. Up to date, both MFC (>40 studies) and MEC (~20 studies) biosensors have been extensively used to detect various recalcitrant contaminants, including aromatics (Table 1). However, it is still unknown which type of MXC biosensor is touted as a better biosensing tool for the aforementioned toxicants.

MXC biosensors can be operated with an external resistance (MFC mode) or the constant potential/voltage (MEC mode). The use of a fixed external resistance (MFC mode) is advantageous due to its low cost and simplicity (Adekunle, 2018). However, the use of MFC biosensors may lead to poor signal stability due to the changes in electrode potentials, resulting in potential false positives (Stein et al., 2010). Alternatively, MEC can facilitate a much more stable background signal and better sensitivity than MFC mode (Adekunle, 2018; Jiang et al., 2015; Shen et al., 2013). Concerning the selection between two configurations, two recent studies have compared MFC and MEC biosensors. For readily biodegradable organics, such as volatile fatty acids (VFAs) in anaerobic digesters, Wu et al. (2019a) stated MEC biosensors had shown higher accuracy with a short response time than MFC biosensors. However, in the same year, Adekunle et al. (2019a) have proposed a contradicting result. They found that the MFC biosensor is more suitable for both organic and inorganic compounds, such as acetate, ammonium, and metal sulfates, than the MEC

biosensor. The MFC biosensor showed a faster response time, higher sensitivity, and faster recovery time after the toxic spike events. However, currently, no studies have systematically investigated MFC vs. MEC biosensors for detecting recalcitrant compounds reviewed in this article. Therefore, more comprehensive studies are required for the selection of an optimum MXC biosensor configuration for recalcitrant compounds.

Notably, the selection between MFC and MEC biosensors is critical due to their effects on the stability, sensitivity, recovery time as well as biosensor's operation. MFC mode does not require a power supply or potentiostat, significantly reducing operating costs. Notably, compared to potentiostat mode, it allows an exemption of using a miniaturized reference electrode, which is often difficult to maintain when constructing miniaturized MXC biosensors (Jiang et al., 2018b). However, the MFC biosensors face poor signal stability (Adekunle, 2018) as the electrical signal is affected by both the anodic and cathodic conditions, leading to potential false warnings (Jiang et al., 2018b; Yang et al., 2016). For instance, the anode potential will change when the toxicants are introduced to EAB; thus, ultimately altering the background signals of the MFC biosensor. Nevertheless, maintaining a constant cathode condition during the operation is also often a challenge (Jiang et al., 2018b). To overcome such issues, MEC mode using the potentiostat will be necessary, or alternatively, the usage of a lower external resistance can be another option. For instance, several studies have suggested a lower resistance can significantly increase the MFC's sensitivity, such as an increase in power output (Stein et al., 2012b) can be achieved by controlling EAB growth and maturing of the biofilm (Do et al., 2020). However, MEC vs. MFC mode with lower external resistance has not been studied for monitoring of recalcitrant contaminants, including aromatics.

In MFC mode, the leakage of oxygen (i.e., diffusion through a membrane/separator) from the cathode to the anode chamber can lower coulombic efficiency and subsequently the biosensor's signal output (Do et al., 2020). Many studies have applied air-cathode MFC biosensors for recalcitrant contaminants (Table 1). When the oxygen molecules intrude from cathode to anode, the growth of aerobic heterotrophic bacteria in the anode biofilm is stimulated (Feng et al., 2013; Xiao et al., 2020a). Furthermore, these diffused oxygens may hinder the growth of obligate anaerobes or even results in a loss of entire obligate anaerobic microbial consortia (Feng et al., 2013; Liu et al., 2011b). To overcome this drawback, Ayyaru and Dharmalingam (2014) investigated an MFC equipped with sulfonated polyether ketone (SPEEK) membrane for BOD biosensing application. Their study showed a 62.5% higher sensing range as well as lower oxygen permeability with the SPEEK membrane compared with the MFC utilizing the standard Nafion proton exchange membrane. This finding highlighted the potential to improve the performance of the air-cathode MFC biosensor, which should be investigated for the detection of aromatics and other recalcitrant toxicants. Alternatively, MEC biosensors can be another option over the air-cathode MFC biosensors to completely eliminate this issue. Given these facts, MEC biosensors are more robust to environmental interruptions, mainly due to the use of potentiostat or power supply (Adekunle, 2018; Wu et al., 2019a) to further assist in the stable environmental monitoring of recalcitrant contaminants. However, still, the remote powering of MEC biosensors would be challenging for potential field deployment.

2-4.2 Design and operation of MXC biosensors: an outlook for recalcitrant contaminants

Figure 2-2 illustrates different environmental, operating, and design parameters affecting the MXC biosensor's performance as well as their process optimization when the biosensors are implemented for the detection of various recalcitrant contaminants, including aromatics.

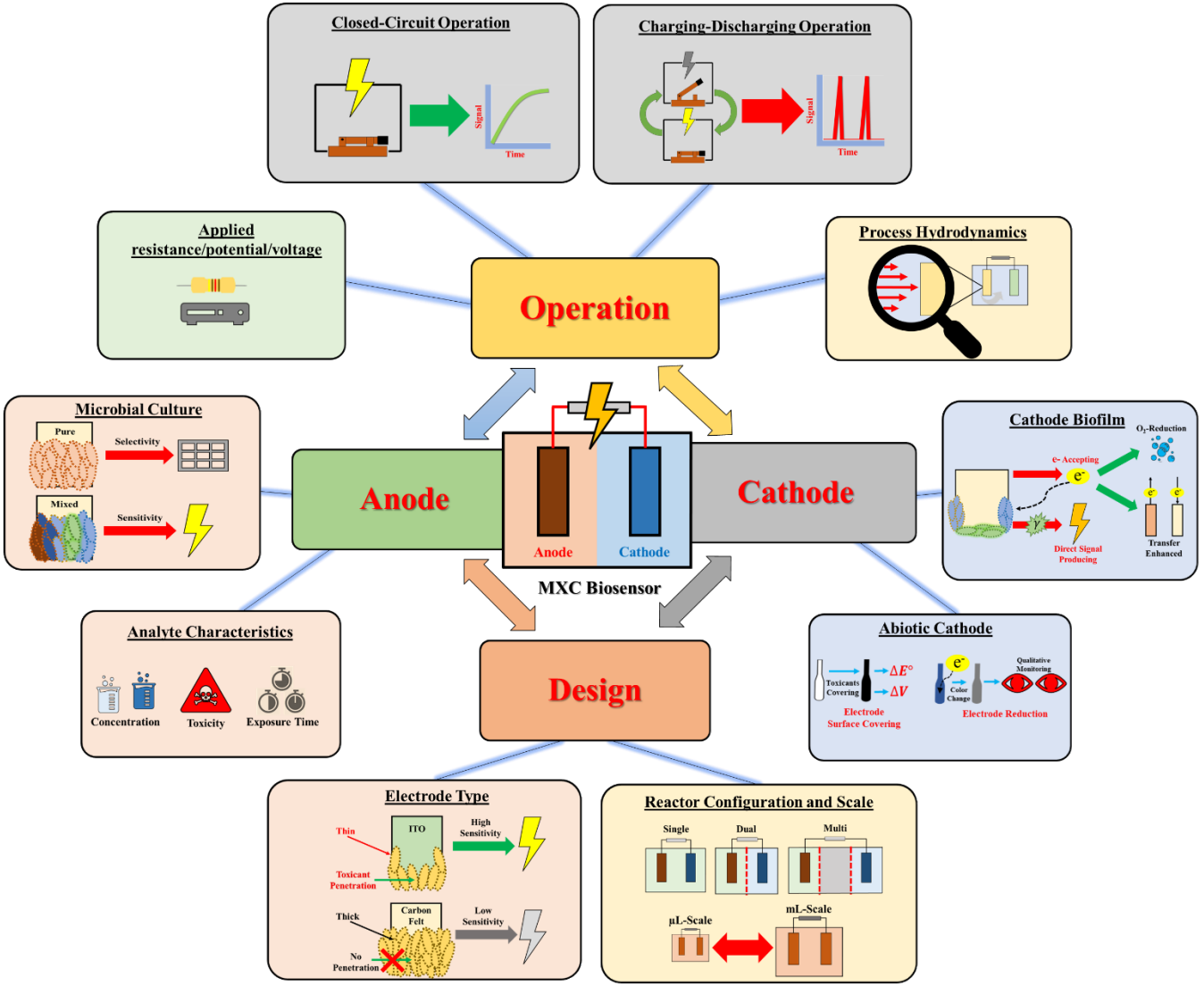

Figure 2-2. Parameters affecting MXC biosensor's performance and their optimization.

2-4.2.1 Significance of design and scales

Several factors, such as differences in designs and scales, can affect MXC biosensor's signal output and sensitivity. First, MXC biosensors can be operated under single- or multi-chamber (mostly dual-chamber) configurations with the presence of ion-exchange membranes. Depending on the monitoring types and purposes, both single- and multi-chamber MXC biosensors can be implemented. Design of a membrane-less single-chamber MXC biosensor was found to be better than the multi-chamber design due to the higher power output, faster response, low construction costs, improved sensitivity as well as simplicity in miniaturization, reducing the capital cost (Davila et al., 2011; Yang et al., 2013; Zhang et al., 2014). Despite the benefits of using a single-chamber, several studies have used multi-chamber biosensors (see Table 1). Particularly, a multi-chamber design can protect the anode biofilm from highly-toxic compounds, such as oil (Dai et al., 2019). Also, the use of cathode as a sensing element can provide selective monitoring of a target recalcitrant compound without disturbing anode biofilm (Jin et al., 2017; Sun et al., 2019b).

Furthermore, the reactor size, mainly the anode volume, can significantly affect the MXC biosensor's sensitivity (Ahn & Schröder, 2015; Davila et al., 2011; Yang et al., 2016). As shown in Table 1, various working volumes were used, ranging from milliliter to microliter scales. Davila et al. (2011) and Di Lorenzo et al. (2014) have reported that smaller-scale (milliliter scales) MXC biosensors result in an enhanced sensitivity (e.g., higher power densities) compared to a larger scale (microliter scales) MXC biosensor. Moon et al. (2004) also have found the response time can substantially be shortened (e.g., from 36 min to 5 min) by decreasing the anodic working volume from 25 mL to 5 mL. Constructing a small scale MXC biosensor can provide a significant reduction in capital cost. For example, it can be fabricated as small as 1.8 μL (Xiao et al., 2020b). However, Uría et al. (2012) have reported that an excessively small anode compartment can be

difficult to fabricate. Also, a miniaturized anode chamber can affect the effective area of the ion-exchange membrane and the ratio between anode to cathode, deteriorating the MXC biosensor's performance (Yi et al., 2020).

A few studies reported that 3D printing could be used for precise and low-cost fabrication of reactor bodies for miniaturized MXC biosensors (Di Lorenzo et al., 2014; López-Hincapié et al., 2020; Theodosiou et al., 2020). For instance, Di Lorenzo et al. (2014) developed a 3D printed miniaturized MFC biosensor (anode volume of 2 cm^3) that could provide rapid detection of COD (30-132 minutes) compared to earlier studies utilizing MFC biosensors with relatively larger anode volumes (2.8 vs. 12.6-73 cm^3). Furthermore, their biosensor showed adequate sensitivity to cadmium as a model toxicant compound (detection range of 1-50 µg/L with 12 minutes response time). To date, 3D printing was mostly used to fabricate the body of MXC biosensors (Di Lorenzo et al., 2014; López-Hincapié et al., 2020; Theodosiou et al., 2020). However, a few recent studies demonstrated that 3D printing could be used for manufacturing of other components of MXCs, such as electrodes and membranes (Bian et al., 2018a; Bian et al., 2018b; Philamore et al., 2015; You et al., 2017; Zhou et al., 2017b). Notably, fabrication of porous anode electrode with 3D printing followed by surface modification (e.g., via carbonization, modification with metals) could generate higher voltage compared to conventional electrode materials, such as carbon cloth and copper mesh (Bian et al., 2018a; Bian et al., 2018b). Interestingly, a most recent study by Freyman et al. (2020) demonstrated 3D printing of bioanode by mixing printing ink and model EAB (*Shewanella Oneidensis* MR-1), which could produce a stable current for almost 93 hours. Such an innovative approach can considerably reduce biofilm development for biosensing applications. Thus, 3D printing of electrodes should be further explored for enhancing the sensitivity and portability of MXC biosensors for recalcitrant compounds monitoring.

However, micro-scale or miniaturized MXC biosensors are often vulnerable to the invasion of bubbles because they can even be sensitive to the tiny air bubbles (e.g., micro-bubbles) (Fraiwan et al., 2013). For instance, the performance of MXC biosensors can be reduced by 33% and resulting in a longer recovery time (>4 days) (Fraiwan et al., 2013). Despite these flaws faced by micro-scale MXC biosensors, they still perform better as biosensors (Davila et al., 2011; Di Lorenzo et al., 2014). For instance, issues regarding microbubble intrusion can be resolved by introducing air-bubble traps (Liu et al., 2011a; Sung & Shuler, 2009). Without interfering with the sensor's functionality, Yang et al. (2016) have demonstrated the prevention of micro-air bubbles by integrating a microscale air bubble trap with an MFC biosensor. With such preventive approaches, smaller-scale MXC biosensors should be further investigated for recalcitrant compounds. Many studies have utilized various configurations and sizes of MXC biosensors for the detection of recalcitrant contaminants, including various aromatic compounds (see Table 1). It was apparent that microliter scale membrane-less single-chamber MXC biosensors equipped with baffles in the anode may provide superior performance over other designs (Davila et al., 2011; Xiao et al., 2020b; Yang et al., 2013; Yi et al., 2020; Zhang et al., 2014).

Studies also have shown the importance of the effective flow, such as velocity distribution at the anode surface (Kim et al., 2014), on the performance of MXC biosensors (Massaglia et al., 2017; Yi et al., 2020). Thus, optimizing the shape of the anode chamber, including various inlet and outlet settings, can potentially increase the biosensor's performance and sensitivity (Massaglia et al., 2017; Yi et al., 2020). This can be attributed to the significant influence of the anode chamber configuration on the fluid dynamic characteristics (Logan et al., 2015). For instance, Massaglia et al. (2017) have reported higher sensitivity and more rapid response using a drop-like shape anode compartment over the squared shape due to having a larger percentage of the effective exposed

area, illustrated by computational fluid dynamics. Furthermore, Jiang et al. (2015) also have reported higher sensitivity (e.g., ~15 – 41 times) for Cu (II) ion detection using the flow-through electrode over a flow-by electrode as the mass transport of Cu (II) ions was enhanced, highlighting the importance of anode hydrodynamics on the sensor's performance. More recently, Yi et al. (2020) have investigated the anodic flow field and hydrodynamic characteristics of MFC biosensor by comparing two different anode configurations; for instance, the presence vs. absence of baffles. In their study, the orthogonal anode design (with baffles) exhibited higher voltage output (42 - 52.3%) due to the reduction in the dead zone (e.g., the region where the flow velocity is < 5% of the maximum velocity; Vesvikar and Al-Dahhan (2005)) by 14% and due to the improved flow velocity at electrode surface (by 334.6%) and its uniformity (by 24.8%) compared with the original design.

2-4.2.2 Electrochemical operation: closed circuit vs. charging-discharging operation

In presence of recalcitrant contaminants, MXC biosensors generate low signal output. Thus, increasing the sensitivity of MXC biosensor is important for the detection of such compounds (Chung et al., 2020a). Another critical factor that significantly influences MXC biosensor sensitivity would be the mode of electrochemical operation. To date, most studies have used closed-circuit operation, where the electrons were continuously being transferred from anode to cathode, for the detection of contaminants via continuous monitoring of electrical signal (see Table 2-1). Nonetheless, Jiang et al. (2017a) introduced an alternation of external resistor connection and disconnection (e.g., transient-state connection mode) in an MFC biosensor, where the sensitivity was significantly increased by up to 247% for heavy metals than the control biosensor constantly connected with the external resistor. Their study also concluded that the external resistance connection phase could be better for monitoring the organic matter, while the disconnection phase

of external resistance can be more suitable for toxicity monitoring. For instance, the output voltage produced by an external resistance disconnection rapidly reached saturation for organic matter, making the biosensor unable to differentiate different concentrations of organics; thus, the use of external resistance connection was better for organic monitoring due to the enhanced sensitivity. However, the output voltage obtained using external resistance disconnection resulted in a higher signal output during toxicity monitoring. Hence, these previous studies indicated that the changes in electrochemical operation methods could substantially impact the MXC biosensor's performance.

Moreover, recently, the implementation of charging-discharging operation has gained interest mainly due to enhanced sensitivity, faster response time, and lower energy input compared with the MXCs operated under continuous closed-circuit operation (Chung et al., 2020a; Sim et al., 2018b; Zakaria & Dhar, 2020). Charging-discharging operation is a process of alternating an open-circuit (electron charging) and a closed-circuit (electron discharging) operation, where the electrons are accumulated onto the anode electrode, then rapidly transferred to the cathode, creating a transient peak current (Chung et al., 2020a; Sim et al., 2018b). Based on the authors' knowledge, Sim et al. (2018b) first applied charging-discharging operation for BOD monitoring in wastewater samples, where the BOD concentrations were rapidly measured (e.g., 2 min). With this validation, Chung et al. (2020a) have successfully detected a model NA compound using charging-discharging cycles (an alternation between open-circuit and closed-circuit) using an MXC biosensor. In their study, the use of charging-discharging cycles substantially enhanced the sensitivity (e.g., increase in current output from microampere to milliampere range). Also, it led to faster response time (< 3.5 h) over the closed-circuit operation, highlighting the significance of

optimizing electrochemical operation method for the detection of recalcitrant contaminants like aromatic naphthenic acid.

2-4.2.3 Implications of anode biofilm composition and morphology

Another key factor that can substantially affect the overall performance of MXC biosensor is the community composition and morphology of anodic microbial consortia (Li et al., 2019; Prévoteau et al., 2019; Xiao et al., 2020a). Anode biofilm activity can be affected by the electrode types, inoculum, nutrients, presence of non-EAB like aerobic bacteria, concentrations and complexity of substrate, and toxicity levels. These factors will ultimately influence the signal output of MXC biosensors (Li et al., 2019; Xiao et al., 2020a; Yi et al., 2018).

Although the enrichment of EAB on the anode is known to be critical for bioanode-based sensing in MXC biosensors, EAB may need syntrophic partners (e.g., fermentative bacteria) for generating an electrical signal from aromatic compounds (e.g., naphthenic acids) (Chung et al., 2020a). A recent review by Do et al. (2020) also has suggested future studies of MXC biosensors should reflect more on the selection of effective EAB that is capable of metabolizing various types of organic substances. For instance, Qi et al. (2019) have shown enhanced sensitivity as well as faster response time using an MXC biosensor enriched with luminescent bacteria (*Vibrio fischeri*) over the common types of EAB, such as *Geobacter* species for the detection of Cu (II).

Li et al. (2019) have reported 3.9 times higher sensitivity using indium tin oxide (ITO) electrode over carbon felt electrode for the detection of Pb^{2+} as a toxicant. This was attributed to the differences in biofilm morphologies. The biofilm grown on carbon felt electrode was non-uniform and thick. In contrast, relatively uniform and thin biofilm grown on the ITO electrode facilitated efficient toxicant exposure within the biofilm (Li et al., 2019). Thus, tailoring biofilm

morphology by selecting an optimum electrode material should be considered for anode-based monitoring of recalcitrant compounds. Regarding the effects of different inoculum, Yi et al. (2018) have compared two different inoculums (e.g., *Shewanella loihica* PV-4, pure culture vs. mixed culture MFC effluent) on biosensor's sensitivity. In their study, the MFC biosensor enriched with a mixed culture has resulted in higher voltage output than the one enriched with pure culture for organic compound detection. Nevertheless, the pure culture produced higher sensitivity for toxicity compound monitoring due to lower extracellular polymeric substances (EPS) content in biofilms; toxicants could easily diffuse within the loose biofilm (i.e., less EPS content).

2-4.2.4 Toxicity level and exposure time

The toxicity level of recalcitrant analytes like aromatic compounds can be another factor of concern. Santoro et al. (2016) have confirmed that more toxic VOCs (e.g., toluene and n-cyclohexyl-pyrrolidone) led to higher inhibition of anode biofilm in MXC biosensor compared with other lower toxic VOCs (e.g., butanol, 1-methyl-2-pyrrolidone, n,n-dimethylacetamide, dimethyl sulfide, n-methyl succinimide, cyclopentanone). Additionally, this study further compared the effects of individual and combined toxicity on the biosensor's performance. For instance, the combined effect of simultaneous addition of two VOCs (e.g., toluene and n-cyclohexyl-pyrrolidone) showed a synergistic effect (e.g., greater inhibition than the sum of individual toxicities on MXC biosensor performance) at low concentrations (e.g., <2,000 mg/L), but the combined toxicity was lower than the sum of individual toxicities at high concentrations (e.g., 2,000 – 10,000 mg/L). In most cases, aromatic compounds are highly toxic. Hence, the time for incubation in the presence of toxicity can also significantly alter the anode biofilm and subsequently influence biosensor performance (Do et al., 2020). A longer toxicant exposure will be riskier for the anode biofilm (e.g., biofilm recovery and stabilizing baseline), resulting in a

higher inhibition ratio. Therefore, identifying the optimal exposure time is crucial for the toxicity biosensors (Yang et al., 2018).

2-4.2.5 Impact of pH, anode potential, and overpotential on baseline current

Maintaining a stable anodic condition in MXC biosensors is critical because environmental factors, such as anode potential and pH, can substantially impact the overpotential toward the measured current and the baseline current as well as the biosensing pathway (Do et al., 2020). A baseline current, known as the constant current output, is required to prevent false positive-alarms caused by changes in anode potential and pH than a toxicant present in the anolyte (Do et al., 2020). Thus, the pH and the overpotential control became essential parts of producing and maintaining a stable baseline current in MXC biosensors (Modin & Wilén, 2012; Stein et al., 2010). Controlling the anode potential in an MXC biosensor can simply be achieved by using a potentiostat. In some aquatic environments, such as groundwater, containing a majority of the aromatic compounds and other recalcitrant contaminants, may have a low buffering capacity with a risk of acidification due to the geochemical conditions (Mossmark et al., 2008).

To maintain a stable pH, Modin and Wilén (2012) have utilized a membrane-less MXC biosensor to eliminate the pH gradient between the anode and the cathode. However, the pH gradient within the anode biofilm still remains as one of the unresolved issues in the operation of MXCs (Dhar et al., 2017; Torres et al., 2008). Thus, it would be challenging to deploy MXC biosensors for monitoring water quality parameters in low buffer-capacity wastewaters, containing many different types of aromatic compounds. Thus, further studies should evaluate the anodic parameters and their impacts on the performance of MXC biosensor applied to aromatic compounds and other recalcitrant contaminants.

2-4.2.6 Cathode as a sensing element

The toxicity monitoring with anodic EAB has several limitations, such as (1) requirement of biodegradable organics to produce signal output; (2) variations in the organic substrate below saturation level may result in alteration of baseline current and ultimately imply false-positive toxicity; (3) hindered performance via protons accumulation due to the low buffer content in a water sample; (4) irreversible inhibition of anode biofilm by toxic compounds (Prévoteau et al., 2019; Xiao et al., 2020a; Zeng et al., 2016). Therefore, such challenges may restrict the applicability of using the anode biofilm as a biosensing element. Therefore, the approach of using cathode as the sensing element in MXC biosensors has received significant momentum (Dai et al., 2019; Jiang et al., 2018a; Jiang et al., 2017b; Liao et al., 2018) (see Table 1). For instance, Dai et al. (2019) have successfully monitored aromatic hydrocarbons (e.g., engine oil) by dosing analytes into the abiotic cathode compartment. Thus, using an abiotic cathode as a sensing element can eliminate the toxicity contact with the anode biofilm (Dai et al., 2019).

Moreover, biocathode can also serve as a biosensing element (Jiang et al., 2018a). For instance, studies have highlighted the advantages of using biocathode over the anode biofilm. It can help prevent signal interferences because cathode biofilms hold a diverse redox potential depending on the biosensing mechanisms (i.e., electrochemical and/or biochemical reaction pathways) and ions flow direction (Jafary et al., 2015; Si et al., 2015). Biocathode is not only limited to anaerobic conditions. It can be used in various environmental conditions, such as aerobic and anoxic environments, for toxicity monitoring (e.g., formaldehyde) (Jiang et al., 2018a). Furthermore, biocathode can be combined with the gas diffusion electrode to detect both the liquid and gas phase of toxicants (Jiang et al., 2018a). Liao et al. (2018) also have successfully detected formaldehyde using a novel autotrophic biocathode as the sensing element. This study further

highlighted that the autotrophic phylum (e.g., *Nitrospirae*) contributed to the highest responsivity compared to other species (e.g., anaerobic heterotrophs in anode biofilm), in which biocathode can be more promising for specific toxicity monitoring over the anode biofilm.

Jiang et al. (2017b) studied bioanode vs. biocathode as a biosensing element for toxicity monitoring. Their study has shown that the detection of lower concentrations of formaldehyde was not suitable using bioanode because of its low sensitivity and unsuccessful in background signal recovery due to washing out of soluble electron carriers, such as the endogenous shuttle during the continuous flow of water sample. On the other hand, detection of the lower concentrations of formaldehyde was possible due to the production of high background signal using biocathode as a sensing element. Similarly, Prévoteau et al. (2019) have introduced O_2-reducing electroautotrophic bacteria on the cathode to detect heavy metals (e.g., mercury (II), chromium (VI), and lead (II)) and formaldehyde. Their study demonstrated that the electroautotrophs in the cathode were grown in tap water, and they survived for at least 8 months as well as having a response time as short as 1 min, showing the potentials for a rapid and robust method to detect toxicants.

However, Qi et al. (2019) have found a better performance of the bioanode than the biocathode using luminescent bacteria (*Vibrio fischeri*) in MXC biosensors. Their study highlighted that the luminescent biofilm in the cathode was not able to produce synchronous optical and electrical signals. This was due to the requirement of both organic matters and dissolved oxygen by the luminescent bacteria as an electron acceptor for both current and optical signal generation. Thus, more studies are still required to evaluate the benefits of using the cathode as the sensing element over the anode biofilm for the applications of aromatic compounds. As discussed earlier, the monitoring process of aromatic compounds with an anode as a sensing

element can be challenging and inconvenient. Therefore, despite a study by Qi et al. (2019), using the cathode as the sensing element should still be considered in future research for the detection of recalcitrant and persistent environmental contaminants, including aromatic compounds.

Nonetheless, the cathode could play a complementary role to further improve MXC biosensor performance, where anode still served as the biosensing element. For instance, Nandimandalam and Gude (2019) have introduced microalgae in the cathode chamber to enhance the biosensor's sensitivity by promoting electron transfer processes as the microalgae produce *in situ* oxygen (an extra electron acceptor) (Arana & Gude, 2018; Kokabian et al., 2018). In response to more convenient on-line monitoring, Yu et al. (2020) have proposed an MFC biosensor to detect heavy metals through visual color change of Prussian Blue (PB) cathode, which represents a simple qualitative method for the on-line monitoring of toxicants. For instance, the PB electrode can change in color depending on the absence or presence of toxicants in the anode. When the organic matter without any toxicants is introduced to the anode, microbial oxidation occurs and the reduction of Fe (III) to Fe (II) in PB, turning the PB color transparent. However, when the toxicants are dosed, the microbial activities are inhibited, which the reduction of Fe (III) to Fe (II) is also limited, resulting in less decoloration. Figure 2-3 illustrates the working principle of the MXC biosensor using a PB as a cathode electrode. Furthermore, the PB has an appropriate reduction initiation potential of 0.4 V (bioanode potential of MFC biosensor is approximately -0.2 V), making the MFC biosensor self-charging and still autonomous by creating a sufficient potential gradient. The benefit of this study is that the approach of using PB cathode as a sensing element can be used for quick qualitative monitoring of toxicants. Moreover, relying on visual color change can alleviate the requirement of a Data Acquisition (DAQ) system for the monitoring of electrical response, which can sometimes be challenging for field applications. Hence, the use of the PB

electrode on biosensing applications can lead to the development of MXC biosensor applications for more convenient on-line monitoring of recalcitrant toxicants, where quantitative measurement is not critical.

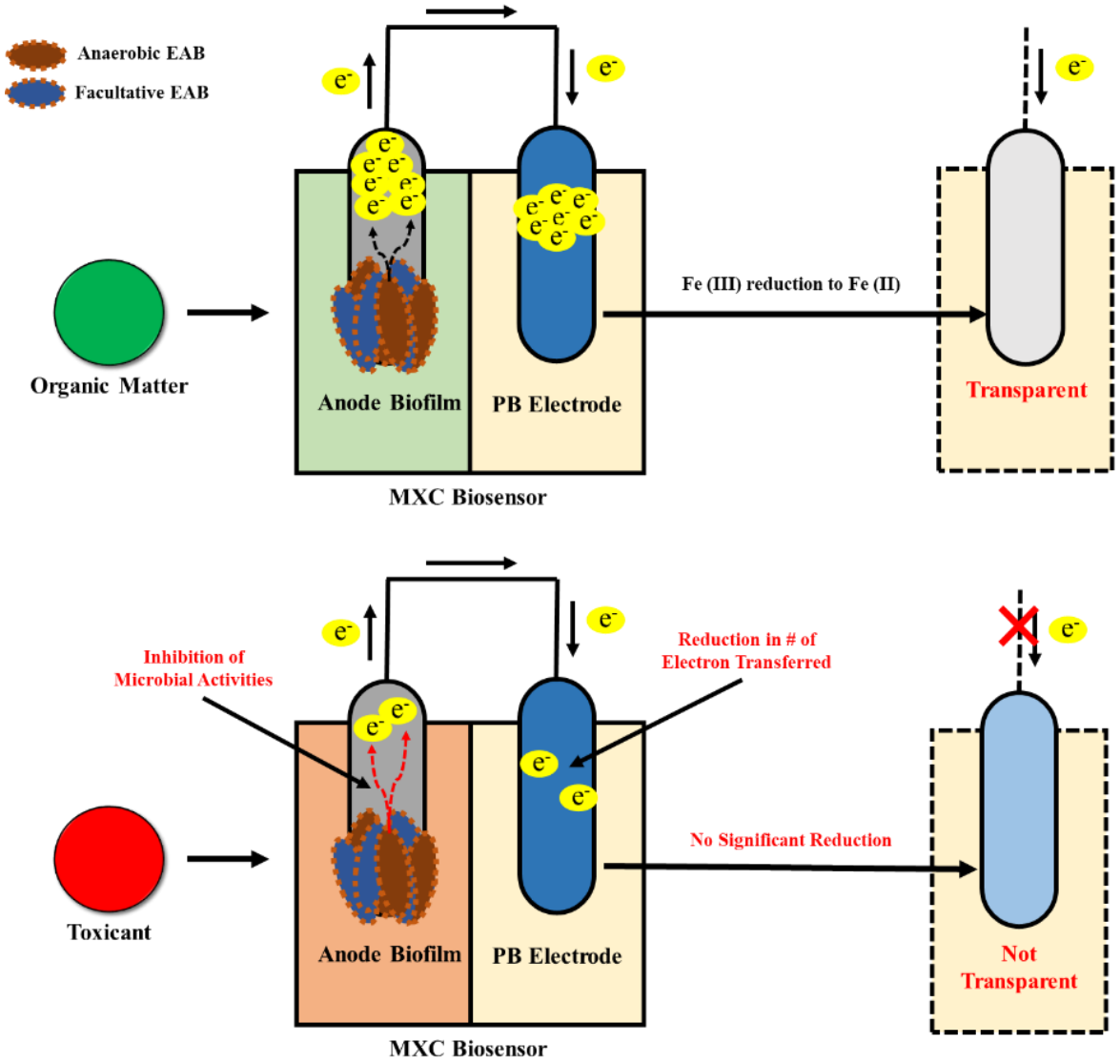

Figure 2-3. MXC biosensor equipped with a PB electrode for organic and toxicant monitoring.

2-4.3 Significance of complex water matrices on selectivity

Selectivity in biosensors represents the ability of a bioreceptor to detect a specific analyte in a sample containing contaminants and other admixtures; thus, selectivity can be considered as a critical factor towards developing MXC biosensors (Nikhil et al., 2016). Although MXC biosensors have shown tremendous potentials, it is still uncertain whether MXC biosensors can perform selective detection of specific recalcitrant compounds (Do et al., 2020; Spurr et al., 2020). During the monitoring process, a drop in signal outputs can be due to various reasons, such as lowering organic content (e.g., BOD), toxicants, growth of aerobic bacteria, nutrient limitations, and many more (Spurr et al., 2020; Xiao et al., 2020a). Thus, the MXC biosensor may not clearly distinguish the exact reason for the changes in signal output (Spurr et al., 2020). For instance, if the MXC biosensor is fed with a water/wastewater sample containing a various mixture of toxicants, it would be questionable whether it is possible to quantify and characterize individual toxicants or target analyte (e.g., detecting copper ions in a mixture of heavy metals) present in a given water matrix (Do et al., 2020).

Many studies, including the recent ones, only have dosed analytes to MXC biosensors individually, not as a mixture, and lack information regarding the individual concentration of toxicants (Adekunle et al., 2019a; Xing et al., 2020; Yu et al., 2020). For instance, Yu et al. (2017) have explored various heavy metals, but in their study, each heavy metal was dosed separately, lacking to show selectivity in MXC biosensor. On the other hand, Adekunle et al. (2019b) have tested a mixture of heavy metals in mining rock drainage water, but their study only showed the correlation of total heavy metal concentration, lacking information on the correlation of individual heavy metal concentrations present in mining rock drainage to the signal output.

Previous studies have focused on enhancing the selectivity in MXC biosensors. Spurr et al. (2020) have operated three MFC biosensors in a series that can clearly distinguish the current drop caused by a decrease in BOD or a presence of toxicants. When the water sample containing BOD entered the system, the first MFC biosensor produced a higher current than the second and the third ones due to the substrate degradation during each stage. However, when the water sample containing toxicants (4-nitrophenol) was introduced, all three biosensors were exhibiting hindered performance, in which selective monitoring of 4-nitrophenol was feasible. Figure 2-4 shows a conceptual schematic of selective monitoring using MXC biosensors operated in-series. However, a modular design would be necessary to deploy such an idea in the field.

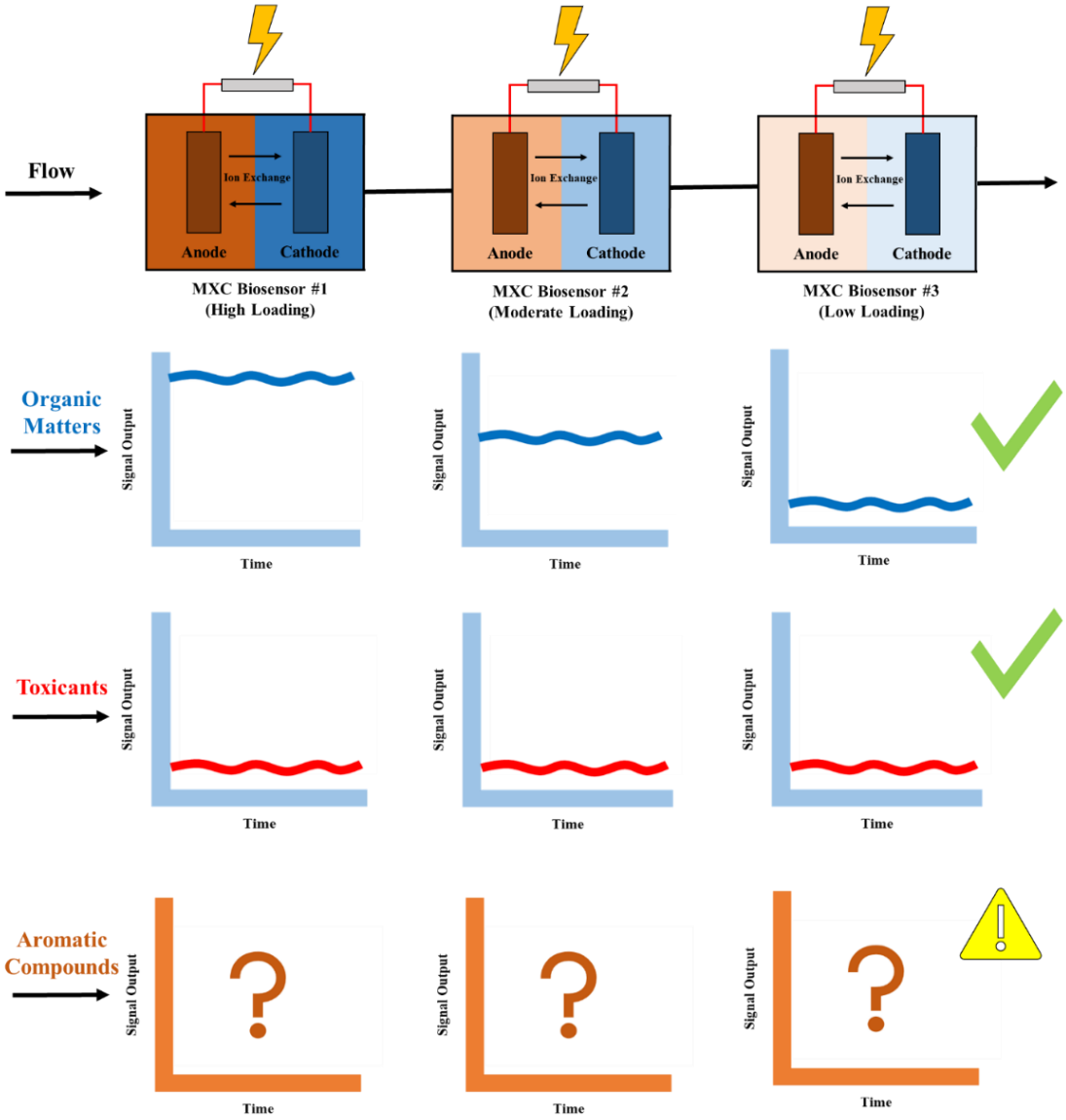

Figure 2-4. Selective monitoring of organics and toxicants using MXC biosensors operated in-series.

To further enhance the selectivity of MXC biosensors, Sun et al. (2019a) and Jin et al. (2016) have proposed three-chamber MXC biosensors (along with using cathode chamber of MXC biosensor (Jin et al., 2017)) to ensure target analyte selectivity. In their studies, anaerobic digester (AD) effluent, containing VFAs and other complex organics (e.g., proteins and lipids), was dosed to the additional chamber (or cathode chamber) separated by ion-exchange membranes (See Figure 2-5a, c). This way, VFAs can be completely separated from other complex organics and hence, can be selectively detected. However, these studies still were not able to identify individual VFAs (e.g., acetate), which is feasible in other analytical tools, such as GC-MS. To address this issue, Sun et al. (2019b) have investigated a dual-chamber MFC biosensor, in which the anode biofilm was enriched with acetate as the sole carbon source, to selectively detect acetate. Similar to the above studies, the AD effluents were injected into the cathode chamber and allowed only VFAs to pass through the anion-exchange membrane towards the anode, but the key point was in the matured EAB biofilm enriched with the only acetate, where the interference from other VFAs was very limited. Thus, their study selectively detected acetate from other VFAs, highlighting the importance of the anode biofilm enrichment process. The ion exchange membrane separation and selective monitoring for aromatic compounds or mixtures are yet to be demonstrated using MXC biosensors (see Figures 2-4 and -5 b, d). However, previous studies demonstrated ion exchange membrane separation of aromatic compounds (Goering et al., 2000; Sungpet et al., 2002), suggesting the potentials to perform selective monitoring using ion-exchange membranes in MXC biosensors. Hence, further research would be needed to assess the feasibility of incorporating such an approach in MXC biosensors.

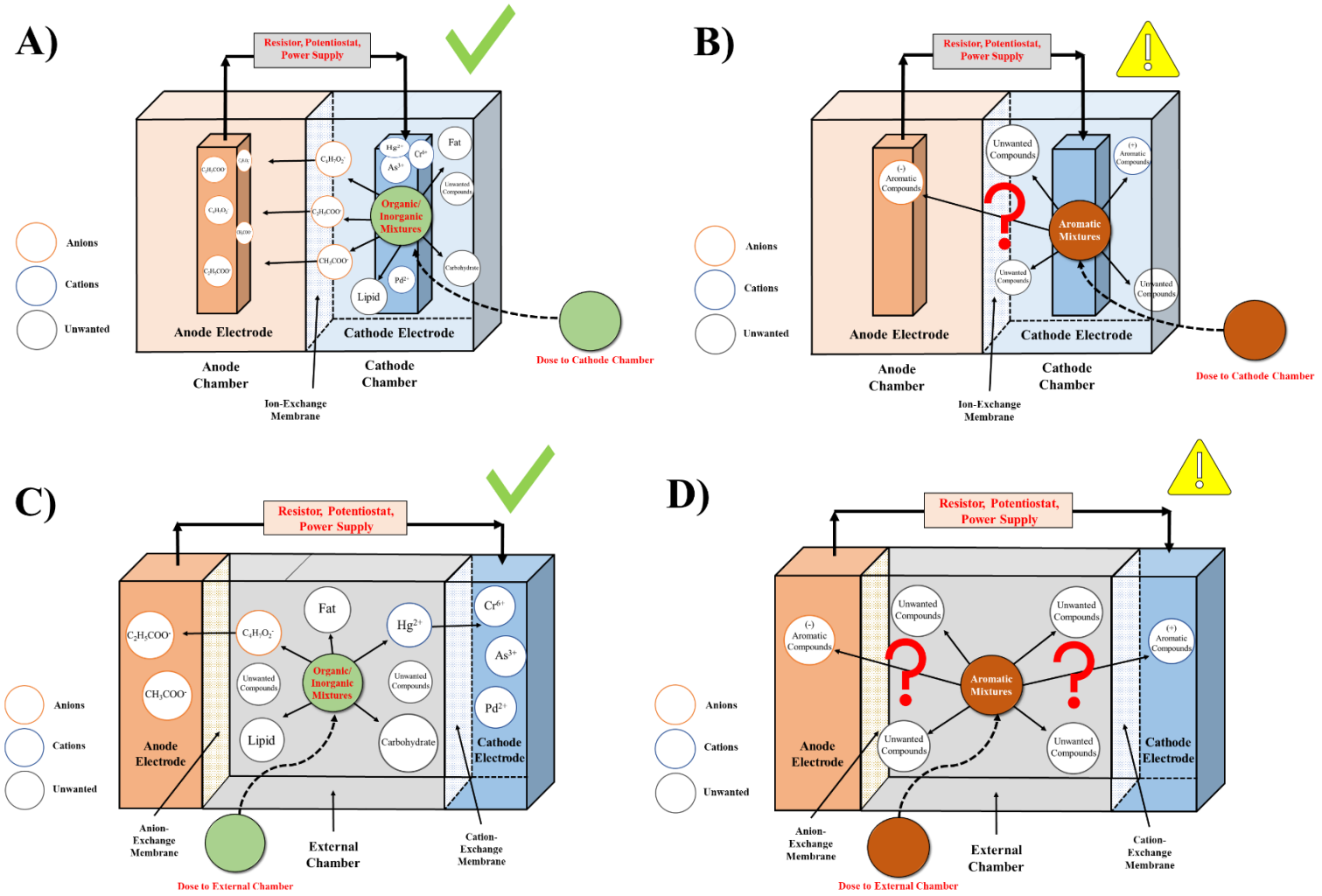

Figure 2-5. Separation and selective monitoring of a target analyte in MXC biosensor using cathode or a middle chamber; a) organic/inorganic mixtures in cathode; b) aromatic mixtures in cathode; c) organic/inorganic mixtures in a middle chamber; d) aromatic mixtures in a middle chamber.

As highlighted by Sun et al. (2019b), microbial communities or biofilms enrichment processes can affect the selectivity of MXC biosensor. Do et al. (2020) have suggested using MXC biosensors with pure culture over mixed culture biofilms to increase the selectivity. For instance, Chen et al. (2016) successfully performed the selective monitoring of PNP in wastewater samples containing other aromatic compounds and metal ions using an anode biofilm enriched with pure culture (*Pseudomonas monteilii* LZU-3). However, on-line monitoring of complex organic contaminants like aromatic compounds using a single strain is still challenging as the microbial oxidation of complex compounds often requires syntrophy of mixed cultures (see Table 1). Additionally, as discussed in Section 2-4.2.3 and the literature Yi et al. (2018), an increase in the selectivity using pure cultures may result in a decrease in the sensitivity. Therefore, more investigations are required to support the relationship between the bacterial consortia and the selectivity of MXC biosensor.

Due to the above challenges, future studies should pay attention to improving the MXC biosensor's selectivity because various wastewater and water samples contain many different organic and inorganic compounds/toxicants, not only containing the target analyte. Especially, in some water bodies, like groundwater, they can contain mixtures of aromatic compounds (Jensen et al., 1988) and various toxicants, including heavy metals (Adekunle et al., 2019b). Thus, for instance, if the MXC biosensor was used to monitor this groundwater matrix, it would not be possible to justify whether the signal output was altered by either aromatic compounds or heavy metals. Therefore, it would be useful to investigate how to substantially improve selectivity in MXC biosensors that are applied to mixtures of various aromatic compounds and other toxicants.

2-4.4 Field applicability of MXC biosensor

To date, the field applicability of MXC biosensors for recalcitrant organic compounds have rarely been investigated. A few studies demonstrated field application of MFC biosensors for monitoring water quality parameters (e.g., COD) (Feng & Harper Jr, 2013; Velasquez-Orta et al., 2017) mainly due to their autonomous and self-powered properties. For instance, MFC biosensors can be operated for up to 10-11 days without any carbon sources (Ruiz et al., 2015). MFC biosensors were capable of measuring water quality parameters for field samples (Feng & Harper Jr, 2013), as well as *in situ* monitoring of water bodies, such as shallow and deep groundwaters (e.g., electrodes can be embedded in the soil sediment) (Velasquez-Orta et al., 2017). Compared to MFC biosensors, the field applicability of MEC biosensors remains uncertain, mainly due to the energy requirement in the form of applied voltage/potential. However, for remote powering of MEC biosensors, MEC and MFC biosensors can be combined. For instance, Adekunle (2018) has developed an integrated biosensor configuration, MFC, and MEC biosensor connected in a series, where an MFC acted as a biobattery, which served as a power source for the MEC biosensor operation. In their previous studies, MFCs have been optimized to produce a stable power production over a fairly long period (>9 months) (Adekunle et al., 2017) as well as ensuring the maximum power generation during > 1-year operation (Adekunle et al., 2019c). Even though previous studies primarily focused on water quality parameters monitoring, such lessons learned as well as techniques developed from these studies can be valuable for further development of MXC biosensors for recalcitrant compounds.

Alleviating the discrepancy between field and lab performance of MXC biosensor was also reported in the literature (Feng & Harper Jr, 2013). Compared to the lab-scale sensor, irregular and relatively lower electrical signals were generated during field monitoring of water quality

parameters (Feng & Harper Jr, 2013). The authors addressed this challenge by developing artificial neural networks (ANN) model trained with lab and field data. It was then implemented to generate ANN-derived correlations and R^2 values related to influent characteristics (e.g., COD concertation) for a different data set. Their study demonstrated that ANN could accurately predict COD concentration for field samples. Recently ANN model was also implemented to predict optimum design parameters for MXCs (e.g., anode angle, inlet flow rate, and flow direction, etc.) (de Ramón-Fernández et al., 2020; Jaeel et al., 2016). A few recent studies showed that advanced machine learning models could help to predict microbial communities and feed substrates for MFCs (Cai et al., 2019; Lesnik & Liu, 2017). Therefore, advanced machine learning methods should be considered in developing smart MXC biosensors, such as optimizing biosensor design and predicting the interference of various environmental factors on biosensor's performance for field applications. Notably, the optimization of the design and operating parameters for MXC biosensors can be time-consuming. Combining machine learning with 3D printing can provide unique opportunities in reducing the time lag for innovation in predicting biosensor performance, understanding the relative importance of various design parameters, and ultimately an optimized design (Fig. 2-6).

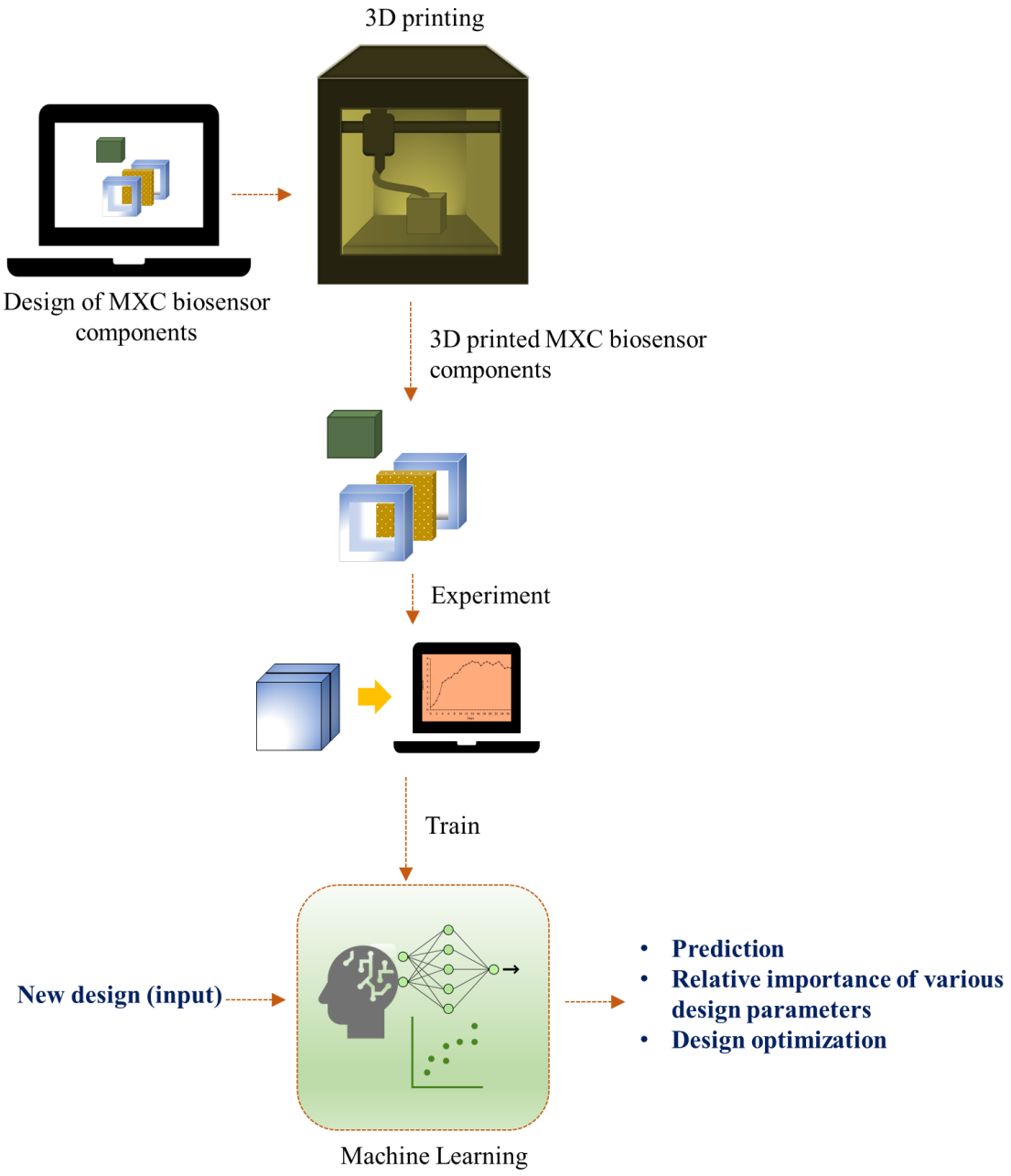

Figure 2-6. A conceptual schematic showing how 3D printing and machine learning can be combined for MXC biosensor design improvement and optimization.

2-5. Conclusions

This paper highlights the applications of MXC biosensors for various recalcitrant environmental pollutants. Previous studies have confirmed that MXC biosensors can provide simple and rapid detection of different recalcitrant contaminants, including aromatic compounds and their derivatives. The results of earlier studies suggested that MXC biosensors could address many challenges associated with conventional lab-based analytical methods. Though the results were promising, MXC biosensors have been tested in laboratory settings. Thus, further research is warranted to make a compelling case for their field deployment as a practical detection technique for recalcitrant contaminants, including aromatics. In this article, a number of research gaps were highlighted for further research. Notably, it became apparent that the field-application may present a particular challenge in terms of selectivity when biosensors are exposed to complex environmental matrices. This article outlines previous efforts to overcome such challenges encountered during the detection of readily biodegradable substrates and typical water quality parameters and provides perspectives on how these strategies can be adopted for recalcitrant pollutants. Based on the appraisal of previous studies, we propose that future research focus on the miniaturization of design and fabrication with 3D printing technologies to achieve better sensitivity from MXC biosensors. Furthermore, for facilitating field application, the integration of machine learning should be considered for the smart biosensing of complex recalcitrant contaminants. Thus, with the support of more future studies, MEC biosensors can potentially be deployed on-site as an efficient and affordable system/technique for monitoring aromatics and other recalcitrant toxic compounds in the field.

2-6. References

Abdalrhman, A.S., Ganiyu, S.O., El-Din, M.G. 2019. Degradation kinetics and structure-reactivity relation of naphthenic acids during anodic oxidation on graphite electrodes. *Chemical Engineering Journal*, **370**, 997-1007.

Adekunle, A. 2018. Development of an Autonomous Biobattery/biosensor System for Remote Applications, McGill University Libraries.

Adekunle, A., Raghavan, V., Tartakovsky, B. 2017. Carbon source and energy harvesting optimization in solid anolyte microbial fuel cells. *Journal of Power Sources*, **356**, 324-330.

Adekunle, A., Raghavan, V., Tartakovsky, B. 2019a. A comparison of microbial fuel cell and microbial electrolysis cell biosensors for real-time environmental monitoring. *Bioelectrochemistry*, **126**, 105-112.

Adekunle, A., Raghavan, V., Tartakovsky, B. 2019b. On-line monitoring of heavy metals-related toxicity with a microbial fuel cell biosensor. *Biosens Bioelectron*, **132**, 382-390.

Adekunle, A., Raghavan, V., Tartakovsky, B. 2019c. Real-Time Performance Optimization and Diagnostics during Long-Term Operation of a Solid Anolyte Microbial Fuel Cell Biobattery. *Batteries*, **5**(1), 9.

Ahad, J.M., Macdonald, R., Parrot, J., Yang, Z., Zhang, Y., Siddique, T., Kuznetsova, A., Rauert, C., Galarneau, E., Studabaker, W. 2020. Polycyclic aromatic compounds (PACs) in the Canadian environment: A review of sampling techniques, strategies and instrumentation. *Environmental Pollution*, 114988.

Ahmad, I., Weng, J., Stromberg, A., Hilt, J., Dziubla, T. 2019. Fluorescence based detection of polychlorinated biphenyls (PCBs) in water using hydrophobic interactions. *Analyst*, **144**(2), 677-684.

Ahn, Y., Schröder, U. 2015. Microfabricated, continuous-flow, microbial three-electrode cell for potential toxicity detection. *BioChip Journal*, **9**(1), 27-34.

Al-Mamun, A., Ahmad, W., Baawain, M.S., Khadem, M., Dhar, B.R. 2018. A review of microbial desalination cell technology: configurations, optimization and applications. *Journal of Cleaner Production*, **183**, 458-480.

Ali, J., Wang, L., Waseem, H., Djellabi, R., Oladoja, N., Pan, G. 2020. FeS@ rGO nanocomposites as electrocatalysts for enhanced chromium removal and clean energy generation by microbial fuel cell. *Chemical Engineering Journal*, **384**, 123335.

Allen, E.W. 2008. Process water treatment in Canada's oil sands industry: I. Target pollutants and treatment objectives. *Journal of Environmental Engineering and Science*, **7**(2), 123-138.

Arana, T.J., Gude, V.G. 2018. A microbial desalination process with microalgae biocathode using sodium bicarbonate as an inorganic carbon source. *International biodeterioration & biodegradation*, **130**, 91-97.

Ayyaru, S., Dharmalingam, S. 2014. Enhanced response of microbial fuel cell using sulfonated poly ether ether ketone membrane as a biochemical oxygen demand sensor. *Analytica chimica acta*, **818**, 15-22.

Barua, S., Zakaria, B.S., Chung, T., Hai, F.I., Haile, T., Al-Mamun, A., Dhar, B.R. 2019. Microbial electrolysis followed by chemical precipitation for effective nutrients recovery from digested sludge centrate in WWTPs. *Chemical Engineering Journal*, **361**, 256-265.

Bian, B., Shi, D., Cai, X., Hu, M., Guo, Q., Zhang, C., Wang, Q., Sun, A.X., Yang, J. 2018a. 3D printed porous carbon anode for enhanced power generation in microbial fuel cell. *Nano Energy*, **44**, 174-180.

Bian, B., Wang, C., Hu, M., Yang, Z., Cai, X., Shi, D., Yang, J. 2018b. Application of 3D printed porous copper anode in microbial fuel cells. *Frontiers in Energy Research*, **6**, 50.

Bilal, M., Iqbal, H.M., Barceló, D. 2019. Persistence of pesticides-based contaminants in the environment and their effective degradation using laccase-assisted biocatalytic systems. *Science of The Total Environment*, **695**, 133896.

Bown, J., Bianchini, M., Ligthart, M., du Payrat, C.N., Whitmore, J. 1987. Methods of prevention, detection and control of spillages in west European oil pipelines. *Quarterly journal of technical papers*, **1**.

Brandão, Y., Teodosio, J., Dias, F., Eustáquio, W., Benachour, M. 2013. Treatment of phenolic effluents by a thermochemical oxidation process (DiCTT) and modelling by artificial neural networks. *Fuel*, **110**, 185-195.

Brown, D.M., Bonte, M., Gill, R., Dawick, J., Boogaard, P.J. 2017. Heavy hydrocarbon fate and transport in the environment. *Quarterly Journal of Engineering Geology and Hydrogeology*, **50**(3), 333-346.

Busca, G., Berardinelli, S., Resini, C., Arrighi, L. 2008. Technologies for the removal of phenol from fluid streams: a short review of recent developments. *Journal of Hazardous Materials*, **160**(2-3), 265-288.

Cai, W., Lesnik, K.L., Wade, M.J., Heidrich, E.S., Wang, Y., Liu, H. 2019. Incorporating microbial community data with machine learning techniques to predict feed substrates in microbial fuel cells. *Biosensors and Bioelectronics*, **133**, 64-71.

Cao, X., Yu, C., Wang, H., Zhou, F., Li, X. 2017. Simultaneous degradation of refractory organic pesticide and bioelectricity generation in a soil microbial fuel cell with different conditions. *Environmental technology*, **38**(8), 1043-1050.

Catal, T., Kul, A., Atalay, V.E., Bermek, H., Ozilhan, S., Tarhan, N. 2019. Efficacy of microbial fuel cells for sensing of cocaine metabolites in urine-based wastewater. *Journal of Power Sources*, **414**, 1-7.

Chauhan, A., Chakraborti, A.K., Jain, R.K. 2000. Plasmid-encoded degradation of p-nitrophenol and 4-nitrocatechol by Arthrobacter protophormiae. *Biochemical and biophysical research communications*, **270**(3), 733-740.

Chen, Z., Niu, Y., Zhao, S., Khan, A., Ling, Z., Chen, Y., Liu, P., Li, X. 2016. A novel biosensor for p-nitrophenol based on an aerobic anode microbial fuel cell. *Biosens Bioelectron*, **85**, 860-868.

Cheng, M., Zeng, G., Huang, D., Lai, C., Xu, P., Zhang, C., Liu, Y. 2016. Hydroxyl radicals based advanced oxidation processes (AOPs) for remediation of soils contaminated with organic compounds: a review. *Chemical Engineering Journal*, **284**, 582-598.

Choi, J., Liu, Y. 2014. Power generation and oil sands process-affected water treatment in microbial fuel cells. *Bioresource technology*, **169**, 581-587.

Chouler, J., Cruz-Izquierdo, A., Rengaraj, S., Scott, J.L., Di Lorenzo, M. 2018. A screen-printed paper microbial fuel cell biosensor for detection of toxic compounds in water. *Biosens Bioelectron*, **102**, 49-56.

Chouler, J., Di Lorenzo, M. 2019. Pesticide detection by a miniature microbial fuel cell under controlled operational disturbances. *Water Science and Technology*, **79**(12), 2231-2241.

Chu, N., Liang, Q., Hao, W., Jiang, Y., Liang, P., Zeng, R.J. 2020. Microbial electrochemical sensor for water biotoxicity monitoring. *Chemical Engineering Journal*, 127053.

Chung, T.H., Meshref, M.N., Dhar, B.R. 2020a. Microbial electrochemical biosensor for rapid detection of naphthenic acid in aqueous solution. *Journal of Electroanalytical Chemistry*, 114405.

Chung, T.H., Meshref, M.N., Hai, F.I., Al-Mamun, A., Dhar, B.R. 2020b. Microbial electrochemical systems for hydrogen peroxide synthesis: Critical review of process optimization, prospective environmental applications, and challenges. *Bioresource Technology*, 123727.

Colantonio, N., Kim, Y. 2016. Cadmium (II) removal mechanisms in microbial electrolysis cells. *Journal of hazardous materials*, **311**, 134-141.

Daghio, M., Tofalos, A.E., Leoni, B., Cristiani, P., Papacchini, M., Jalilnejad, E., Bestetti, G., Franzetti, A. 2018. Bioelectrochemical BTEX removal at different voltages: assessment of the degradation and characterization of the microbial communities. *Journal of hazardous materials*, **341**, 120-127.

Dai, Z., Xu, Z., Wang, T., Fan, Y., Liu, Y., Yu, R., Zhu, G., Lu, X., Li, B. 2019. In-situ oil presence sensor using simple-structured upward open-channel microbial fuel cell (UOC-MFC). *Biosensors and Bioelectronics: X*, **1**, 100014.

Davila, D., Esquivel, J., Sabate, N., Mas, J. 2011. Silicon-based microfabricated microbial fuel cell toxicity sensor. *Biosensors and Bioelectronics*, **26**(5), 2426-2430.

de Ramón-Fernández, A., Salar-García, M., Fernández, D.R., Greenman, J., Ieropoulos, I. 2020. Evaluation of artificial neural network algorithms for predicting the effect of the urine flow rate on the power performance of microbial fuel cells. *Energy*, **213**, 118806.

Dhar, B.R., Ryu, H., Santo Domingo, J.W., Lee, H.-S. 2016. Ohmic resistance affects microbial community and electrochemical kinetics in a multi-anode microbial electrochemical cell. *Journal of Power Sources*, **331**, 315-321.

Dhar, B.R., Sim, J., Ryu, H., Ren, H., Santo Domingo, J.W., Chae, J., Lee, H.-S. 2017. Microbial activity influences electrical conductivity of biofilm anode. *Water research*, **127**, 230-238.

Di Lorenzo, M., Thomson, A.R., Schneider, K., Cameron, P.J., Ieropoulos, I. 2014. A small-scale air-cathode microbial fuel cell for on-line monitoring of water quality. *Biosensors and Bioelectronics*, **62**, 182-188.

Do, M.H., Ngo, H.H., Guo, W., Chang, S.W., Nguyen, D.D., Liu, Y., Varjani, S., Kumar, M. 2020. Microbial fuel cell-based biosensor for online monitoring wastewater quality: A critical review. *Science of the Total Environment*, **712**, 135612.

El-Din, M.G., Fu, H., Wang, N., Chelme-Ayala, P., Pérez-Estrada, L., Drzewicz, P., Martin, J.W., Zubot, W., Smith, D.W. 2011. Naphthenic acids speciation and removal during petroleum-coke adsorption and ozonation of oil sands process-affected water. *Science of the Total Environment*, **409**(23), 5119-5125.

Feng, Y., Barr, W., Harper Jr, W. 2013. Neural network processing of microbial fuel cell signals for the identification of chemicals present in water. *Journal of environmental management*, **120**, 84-92.

Feng, Y., Harper Jr, W.F. 2013. Biosensing with microbial fuel cells and artificial neural networks: laboratory and field investigations. *Journal of environmental management*, **130**, 369-374.

Fennell, J., Arciszewski, T.J. 2019. Current knowledge of seepage from oil sands tailings ponds and its environmental influence in northeastern Alberta. *Science of the total environment*.
Fingas, M. 2016. *Oil spill science and technology*. Gulf professional publishing.
Fingas, M., Brown, C. 2014. Review of oil spill remote sensing. *Marine pollution bulletin*, **83**(1), 9-23.
Fingas, M., Brown, C. 2005. An update on oil spill remote sensors. *Proc. 28th Arctic and Marine Oil Spill Program (AMOP) Tech. Seminar*. pp. 7-9.
Fraiwan, A., Sundermier, S., Han, D., Steckl, A., Hassett, D., Choi, S. 2013. Enhanced Performance of Micro-Electro-Mechanical-Systems (MEMS) Microbial Fuel Cells Using Electrospun Microfibrous Anode and Optimizing Operation. *Fuel Cells*, **13**(3), 336-341.
Freyman, M.C., Kou, T., Wang, S., Li, Y. 2020. 3D printing of living bacteria electrode. *Nano Research*, **13**(5), 1318-1323.
Friman, H., Schechter, A., Nitzan, Y., Cahan, R. 2012. Effect of external voltage on Pseudomonas putida F1 in a bio electrochemical cell using toluene as sole carbon and energy source. *Microbiology*, **158**(2), 414-423.
Gami, A., Shukor, M., Khalil, K.A., Dahalan, F., Khalid, A., Ahmad, S. 2014. Phenol and its toxicity. *Journal of Environmental Microbiology and Toxicology*, **2**(1), 11-24.
García-Mancha, N., Monsalvo, V., Puyol, D., Rodriguez, J., Mohedano, A. 2017. Enhanced anaerobic degradability of highly polluted pesticides-bearing wastewater under thermophilic conditions. *Journal of hazardous materials*, **339**, 320-329.
Geed, S., Shrirame, B., Singh, R., Rai, B. 2017. Assessment of pesticides removal using two-stage Integrated Aerobic Treatment Plant (IATP) by Bacillus sp. isolated from agricultural field. *Bioresource technology*, **242**, 45-54.
Gmurek, M., Olak-Kucharczyk, M., Ledakowicz, S. 2017. Photochemical decomposition of endocrine disrupting compounds–A review. *Chemical Engineering Journal*, **310**, 437-456.
Goering, R., Bowman, C., Koval, C., Noble, R., Ashley, M. 2000. Complexation structure and transport mechanism of 1, 5-hexadiene and 1-hexene through silver facilitated transport membranes. *Journal of Membrane Science*, **172**(1-2), 49-57.
Gonçalves-Filho, D., Silva, C.C.G., De Souza, D. 2020. Pesticides determination in foods and natural waters using solid amalgam-based electrodes: challenges and trends. *Talanta*, **212**, 120756.
Guo, F., Liu, H. 2020. Impact of heterotrophic denitrification on BOD detection of the nitrate-containing wastewater using microbial fuel cell-based biosensors. *Chemical Engineering Journal*, 125042.
Heidrich, E.S., Edwards, S.R., Dolfing, J., Cotterill, S.E., Curtis, T.P. 2014. Performance of a pilot scale microbial electrolysis cell fed on domestic wastewater at ambient temperatures for a 12 month period. *Bioresource technology*, **173**, 87-95.
Hennebel, T., Benner, J., Clauwaert, P., Vanhaecke, L., Aelterman, P., Callebaut, R., Boon, N., Verstraete, W. 2011. Dehalogenation of environmental pollutants in microbial electrolysis cells with biogenic palladium nanoparticles. *Biotechnology letters*, **33**(1), 89-95.
Huang, Q., Liu, Y., Dhar, B.R. 2020. A critical review of microbial electrolysis cells coupled with anaerobic digester for enhanced biomethane recovery from high-strength feedstocks. *Critical Reviews in Environmental Science and Technology*, 1-40.

Jaeel, A.J., Al-wared, A.I., Ismail, Z.Z. 2016. Prediction of sustainable electricity generation in microbial fuel cell by neural network: effect of anode angle with respect to flow direction. *Journal of Electroanalytical Chemistry*, **767**, 56-62.

Jafary, T., Al-Mamun, A., Alhimali, H., Baawain, M.S., Rahman, M.S., Rahman, S., Dhar, B.R., Aghbashlo, M., Tabatabaei, M. 2020. Enhanced power generation and desalination rate in a novel quadruple microbial desalination cell with a single desalination chamber. *Renewable and Sustainable Energy Reviews*, **127**, 109855.

Jafary, T., Daud, W.R.W., Ghasemi, M., Kim, B.H., Jahim, J.M., Ismail, M., Lim, S.S. 2015. Biocathode in microbial electrolysis cell; present status and future prospects. *Renewable and Sustainable Energy Reviews*, **47**, 23-33.

Jensen, B.K., Arvin, E., Gundersen, A.T. 1988. Biodegradation of nitrogen-and oxygen-containing aromatic compounds in groundwater from an oil-contaminated aquifer. *Journal of contaminant hydrology*, **3**(1), 65-75.

Jha, M.N., Levy, J., Gao, Y. 2008. Advances in remote sensing for oil spill disaster management: state-of-the-art sensors technology for oil spill surveillance. *Sensors*, **8**(1), 236-255.

Jia, H., Yang, G., Ngo, H.-H., Guo, W., Zhang, H., Gao, F., Wang, J. 2017. Enhancing simultaneous response and amplification of biosensor in microbial fuel cell-based upflow anaerobic sludge bed reactor supplemented with zero-valent iron. *Chemical Engineering Journal*, **327**, 1117-1127.

Jiang, Y., Liang, P., Huang, X., Ren, Z.J. 2018a. A novel microbial fuel cell sensor with a gas diffusion biocathode sensing element for water and air quality monitoring. *Chemosphere*, **203**, 21-25.

Jiang, Y., Liang, P., Liu, P., Miao, B., Bian, Y., Zhang, H., Huang, X. 2017a. Enhancement of the sensitivity of a microbial fuel cell sensor by transient-state operation. *Environmental Science: Water Research & Technology*, **3**(3), 472-479.

Jiang, Y., Liang, P., Liu, P., Wang, D., Miao, B., Huang, X. 2017b. A novel microbial fuel cell sensor with biocathode sensing element. *Biosens Bioelectron*, **94**, 344-350.

Jiang, Y., Liang, P., Liu, P., Yan, X., Bian, Y., Huang, X. 2017c. A cathode-shared microbial fuel cell sensor array for water alert system. *International Journal of Hydrogen Energy*, **42**(7), 4342-4348.

Jiang, Y., Liang, P., Zhang, C., Bian, Y., Yang, X., Huang, X., Girguis, P.R. 2015. Enhancing the response of microbial fuel cell based toxicity sensors to Cu(II) with the applying of flow-through electrodes and controlled anode potentials. *Bioresour Technol*, **190**, 367-72.

Jiang, Y., Su, M., Li, D. 2014. Removal of sulfide and production of methane from carbon dioxide in microbial fuel cells–microbial electrolysis cell (MFCs–MEC) coupled system. *Applied biochemistry and biotechnology*, **172**(5), 2720-2731.

Jiang, Y., Ulrich, A.C., Liu, Y. 2013. Coupling bioelectricity generation and oil sands tailings treatment using microbial fuel cells. *Bioresource technology*, **139**, 349-354.

Jiang, Y., Yang, X., Liang, P., Liu, P., Huang, X. 2018b. Microbial fuel cell sensors for water quality early warning systems: Fundamentals, signal resolution, optimization and future challenges. *Renewable and Sustainable Energy Reviews*, **81**, 292-305.

Jin, X., Angelidaki, I., Zhang, Y. 2016. Microbial Electrochemical Monitoring of Volatile Fatty Acids during Anaerobic Digestion. *Environ Sci Technol*, **50**(8), 4422-9.

Jin, X., Li, X., Zhao, N., Angelidaki, I., Zhang, Y. 2017. Bio-electrolytic sensor for rapid monitoring of volatile fatty acids in anaerobic digestion process. *Water research*, **111**, 74-80.

Jun, L.Y., Yon, L.S., Mubarak, N., Bing, C.H., Pan, S., Danquah, M.K., Abdullah, E., Khalid, M. 2019. An overview of immobilized enzyme technologies for dye and phenolic removal from wastewater. *Journal of Environmental Chemical Engineering*, **7**(2), 102961.

Kaur, A., Kim, J.R., Michie, I., Dinsdale, R.M., Guwy, A.J., Premier, G.C., Centre, S.E.R. 2013. Microbial fuel cell type biosensor for specific volatile fatty acids using acclimated bacterial communities. *Biosensors and Bioelectronics*, **47**, 50-55.

Khan, A., Salama, E.-S., Chen, Z., Ni, H., Zhao, S., Zhou, T., Pei, Y., Sani, R.K., Ling, Z., Liu, P. 2020. A novel biosensor for zinc detection based on microbial fuel cell system. *Biosensors and Bioelectronics*, **147**, 111763.

Kim, J., Kim, H., Kim, B., Yu, J. 2014. Computational fluid dynamics analysis in microbial fuel cells with different anode configurations. *Water science and technology*, **69**(7), 1447-1452.

Kim, M., Hyun, M.S., Gadd, G.M., Kim, H.J. 2007. A novel biomonitoring system using microbial fuel cells. *Journal of environmental monitoring*, **9**(12), 1323-1328.

Kokabian, B., Gude, V.G., Smith, R., Brooks, J.P. 2018. Evaluation of anammox biocathode in microbial desalination and wastewater treatment. *Chemical Engineering Journal*, **342**, 410-419.

Lazzarini Behrmann, I.C., Grattieri, M., Minteer, S.D., Ramirez, S.A., Vullo, D.L. 2020. Online self-powered Cr (VI) monitoring with autochthonous Pseudomonas and a bio-inspired redox polymer. *Analytical and Bioanalytical Chemistry*, 1-9.

Lesnik, K.L., Liu, H. 2017. Predicting microbial fuel cell biofilm communities and bioreactor performance using artificial neural networks. *Environmental science & technology*, **51**(18), 10881-10892.

Li, F., Zheng, Z., Yang, B., Zhang, X., Li, Z., Lei, L. 2016. A laminar-flow based microfluidic microbial three-electrode cell for biosensing. *Electrochimica Acta*, **199**, 45-50.

Li, J., Hu, J., Yang, C., Pu, W., Hou, H., Xu, J., Liu, B., Yang, J. 2019. Enhanced detection of toxicity in wastewater using a 2D smooth anode based microbial fuel cell toxicity sensor. *RSC advances*, **9**(15), 8700-8706.

Liang, P., Duan, R., Jiang, Y., Zhang, X., Qiu, Y., Huang, X. 2018. One-year operation of 1000-L modularized microbial fuel cell for municipal wastewater treatment. *Water research*, **141**, 1-8.

Liao, C., Wu, J., Zhou, L., Li, T., Du, Q., An, J., Li, N., Wang, X. 2018. Optimal set of electrode potential enhances the toxicity response of biocathode to formaldehyde. *Sci Total Environ*, **644**, 1485-1492.

Lin, S., Lu, Y., Ye, B., Zeng, C., Liu, G., Li, J., Luo, H., Zhang, R. 2020. Pesticide wastewater treatment using the combination of the microbial electrolysis desalination and chemical-production cell and Fenton process. *Frontiers of Environmental Science & Engineering*, **14**(1), 12.

Liu, B., Lei, Y., Li, B. 2014. A batch-mode cube microbial fuel cell based "shock" biosensor for wastewater quality monitoring. *Biosens Bioelectron*, **62**, 308-14.

Liu, B., Zhai, H., Liang, Y., Ji, M., Wang, R. 2019. Increased power production and removal efficiency of polycyclic aromatic hydrocarbons by plant pumps in sediment microbial electrochemical systems: A preliminary study. *Journal of hazardous materials*, **380**, 120896.

Liu, C., Thompson, J.A., Bau, H.H. 2011a. A membrane-based, high-efficiency, microfluidic debubbler. *Lab on a Chip*, **11**(9), 1688-1693.

Liu, Z., Liu, J., Zhang, S., Xing, X.-H., Su, Z. 2011b. Microbial fuel cell based biosensor for in situ monitoring of anaerobic digestion process. *Bioresource technology*, **102**(22), 10221-10229.
Logan, B.E. 2008. *Microbial fuel cells*. John Wiley & Sons.
Logan, B.E., Call, D., Cheng, S., Hamelers, H.V., Sleutels, T.H., Jeremiasse, A.W., Rozendal, R.A. 2008. Microbial electrolysis cells for high yield hydrogen gas production from organic matter. *Environmental science & technology*, **42**(23), 8630-8640.
Logan, B.E., Wallack, M.J., Kim, K.-Y., He, W., Feng, Y., Saikaly, P.E. 2015. Assessment of microbial fuel cell configurations and power densities. *Environmental Science & Technology Letters*, **2**(8), 206-214.
López-Hincapié, J.D., Picos-Benítez, A.R., Cercado, B., Rodríguez, F., Rodríguez-García, A. 2020. Improving the configuration and architecture of a small-scale air-cathode single chamber microbial fuel cell (MFC) for biosensing organic matter in wastewater samples. *Journal of Water Process Engineering*, **38**, 101671.
Lovley, D.R., Nevin, K.P. 2011. A shift in the current: new applications and concepts for microbe-electrode electron exchange. *Current opinion in Biotechnology*, **22**(3), 441-448.
Mahaffey, A., Dubé, M. 2016. Review of the composition and toxicity of oil sands process-affected water. *Environmental Reviews*, **25**(1), 97-114.
Massaglia, G., Gerosa, M., Agostino, V., Cingolani, A., Sacco, A., Saracco, G., Margaria, V., Quaglio, M. 2017. Fluid dynamic modeling for microbial fuel cell based biosensor optimization. *Fuel Cells*, **17**(5), 627-634.
Menzie, C.A., Potocki, B.B., Santodonato, J. 1992. Exposure to carcinogenic PAHs in the environment. *Environmental science & technology*, **26**(7), 1278-1284.
Modin, O., Wilén, B.-M. 2012. A novel bioelectrochemical BOD sensor operating with voltage input. *Water research*, **46**(18), 6113-6120.
Moon, H., Chang, I.S., Kang, K.H., Jang, J.K., Kim, B.H. 2004. Improving the dynamic response of a mediator-less microbial fuel cell as a biochemical oxygen demand (BOD) sensor. *Biotechnology letters*, **26**(22), 1717-1721.
Morris, J.M., Jin, S., Crimi, B., Pruden, A. 2009. Microbial fuel cell in enhancing anaerobic biodegradation of diesel. *Chemical Engineering Journal*, **146**(2), 161-167.
Mossmark, F., Hultberg, H., Ericsson, L.O. 2008. Recovery from groundwater extraction in a small catchment area with crystalline bedrock and thin soil cover in Sweden. *Science of the total environment*, **404**(2-3), 253-261.
Na, C.-J., Yoo, M.-J., Tsang, D.C., Kim, H.W., Kim, K.-H. 2019. High-performance materials for effective sorptive removal of formaldehyde in air. *Journal of hazardous materials*, **366**, 452-465.
Nandimandalam, H., Gude, V.G. 2019. Indigenous biosensors for in situ hydrocarbon detection in aquatic environments. *Marine Pollution Bulletin*, **149**, 110643.
Nikhil, B., Pawan, J., Nello, F., Pedro, E. 2016. Introduction to biosensors. *Essays in Biochemistry*, **60**(1), 1-8.
Palma, E., Daghio, M., Tofalos, A.E., Franzetti, A., Viggi, C.C., Fazi, S., Papini, M.P., Aulenta, F. 2018. Anaerobic electrogenic oxidation of toluene in a continuous-flow bioelectrochemical reactor: Process performance, microbial community analysis, and biodegradation pathways. *Environmental Science: Water Research & Technology*, **4**(12), 2136-2145.

Patil, S., Harnisch, F., Schröder, U. 2010. Toxicity response of electroactive microbial biofilms—a decisive feature for potential biosensor and power source applications. *ChemPhysChem*, **11**(13), 2834-2837.
Peixoto, L., Min, B., Martins, G., Brito, A.G., Kroff, P., Parpot, P., Angelidaki, I., Nogueira, R. 2011. In situ microbial fuel cell-based biosensor for organic carbon. *Bioelectrochemistry*, **81**(2), 99-103.
Philamore, H., Rossiter, J., Walters, P., Winfield, J., Ieropoulos, I. 2015. Cast and 3D printed ion exchange membranes for monolithic microbial fuel cell fabrication. *Journal of Power Sources*, **289**, 91-99.
Prévoteau, A., Clauwaert, P., Kerckhof, F.-M., Rabaey, K. 2019. Oxygen-reducing microbial cathodes monitoring toxic shocks in tap water. *Biosensors and Bioelectronics*, **132**, 115-121.
Pv, H., Sj, W., de Solla, S., Ja, H., Slj, H., Jl, P., Pj, T., Berthiaume, A., Langlois, V. 2020. Polycyclic aromatic compounds (PACs) in the Canadian environment: The challenges of ecological risk assessments. *Environmental Pollution*, 115165.
Qi, X., Liu, P., Liang, P., Hao, W., Li, M., Huang, X. 2019. Dual-signal-biosensor based on luminescent bacteria biofilm for real-time online alert of Cu (II) shock. *Biosensors and Bioelectronics*, **142**, 111500.
Rasmussen, M., Minteer, S.D. 2015. Long-term arsenic monitoring with an Enterobacter cloacae microbial fuel cell. *Bioelectrochemistry*, **106**, 207-212.
Raut, N., O'Connor, G., Pasini, P., Daunert, S. 2012. Engineered cells as biosensing systems in biomedical analysis. *Analytical and bioanalytical chemistry*, **402**(10), 3147-3159.
Raza, W., Lee, J., Raza, N., Luo, Y., Kim, K.-H., Yang, J. 2019. Removal of phenolic compounds from industrial waste water based on membrane-based technologies. *Journal of industrial and engineering chemistry*, **71**, 1-18.
Reddy, A.V.B., Moniruzzaman, M., Aminabhavi, T.M. 2019. Polychlorinated biphenyls (PCBs) in the environment: Recent updates on sampling, pretreatment, cleanup technologies and their analysis. *Chemical Engineering Journal*, **358**, 1186-1207.
Ripmeester, M.J., Duford, D.A. 2019. Method for routine "naphthenic acids fraction compounds" determination in oil sands process-affected water by liquid-liquid extraction in dichloromethane and Fourier-Transform Infrared Spectroscopy. *Chemosphere*, **233**, 687-696.
Rozendal, R.A., Leone, E., Keller, J., Rabaey, K. 2009. Efficient hydrogen peroxide generation from organic matter in a bioelectrochemical system. *Electrochemistry Communications*, **11**(9), 1752-1755.
Ruiz, Y., Ribot-Llobet, E., Baeza, J.A., Guisasola, A. 2015. Conditions for high resistance to starvation periods in bioelectrochemical systems. *Bioelectrochemistry*, **106**, 328-334.
Santoro, C., Mohidin, A.F., Grasso, L.L., Seviour, T., Palanisamy, K., Hinks, J., Lauro, F.M., Marsili, E. 2016. Sub-toxic concentrations of volatile organic compounds inhibit extracellular respiration of Escherichia coli cells grown in anodic bioelectrochemical systems. *Bioelectrochemistry*, **112**, 173-177.
Seo, J.-S., Keum, Y.-S., Li, Q.X. 2009. Bacterial degradation of aromatic compounds. *International journal of environmental research and public health*, **6**(1), 278-309.
Shen, J., Feng, C., Zhang, Y., Jia, F., Sun, X., Li, J., Han, W., Wang, L., Mu, Y. 2012. Bioelectrochemical system for recalcitrant p-nitrophenol removal. *Journal of hazardous materials*, **209**, 516-519.

Shen, Y., Wang, M., Chang, I.S., Ng, H.Y. 2013. Effect of shear rate on the response of microbial fuel cell toxicity sensor to Cu (II). *Bioresource technology*, **136**, 707-710.
Si, R.-W., Zhai, D.-D., Liao, Z.-H., Gao, L., Yong, Y.-C. 2015. A whole-cell electrochemical biosensing system based on bacterial inward electron flow for fumarate quantification. *Biosensors and Bioelectronics*, **68**, 34-40.
Sim, J., Reid, R., Hussain, A., An, J., Lee, H.-S. 2018a. Hydrogen peroxide production in a pilot-scale microbial electrolysis cell. *Biotechnology Reports*, **19**, e00276.
Sim, J., Reid, R., Hussain, A., Lee, H.-S. 2018b. Semi-continuous measurement of oxygen demand in wastewater using biofilm-capacitance. *Bioresource Technology Reports*, **3**, 231-237.
Sonawane, J.M., Ezugwu, C.I., Ghosh, P.C. 2020. Microbial fuel cell-based biological oxygen demand sensors for monitoring wastewater: State-of-the-art and practical applications. *ACS sensors*, **5**(8), 2297-2316.
Spurr, M.W., Eileen, H.Y., Scott, K., Head, I.M. 2020. A microbial fuel cell sensor for unambiguous measurement of organic loading and definitive identification of toxic influents. *Environmental Science: Water Research & Technology*, **6**(3), 612-621.
Stein, N.E., Hamelers, H.M., van Straten, G., Keesman, K.J. 2012a. On-line detection of toxic components using a microbial fuel cell-based biosensor. *Journal of Process Control*, **22**(9), 1755-1761.
Stein, N.E., Hamelers, H.V., Buisman, C.N. 2012b. The effect of different control mechanisms on the sensitivity and recovery time of a microbial fuel cell based biosensor. *Sensors and Actuators B: Chemical*, **171**, 816-821.
Stein, N.E., Hamelers, H.V., Buisman, C.N. 2012c. Influence of membrane type, current and potential on the response to chemical toxicants of a microbial fuel cell based biosensor. *Sensors and Actuators B: Chemical*, **163**(1), 1-7.
Stein, N.E., Hamelers, H.V., Buisman, C.N. 2010. Stabilizing the baseline current of a microbial fuel cell-based biosensor through overpotential control under non-toxic conditions. *Bioelectrochemistry*, **78**(1), 87-91.
Sun, H., Angelidaki, I., Wu, S., Dong, R., Zhang, Y. 2019a. The potential of bioelectrochemical sensor for monitoring of acetate during anaerobic digestion: Focusing on novel reactor design. *Frontiers in microbiology*, **9**, 3357.
Sun, H., Zhang, Y., Wu, S., Dong, R., Angelidaki, I. 2019b. Innovative operation of microbial fuel cell-based biosensor for selective monitoring of acetate during anaerobic digestion. *Science of the Total Environment*, **655**, 1439-1447.
Sun, J.-Z., Peter Kingori, G., Si, R.-W., Zhai, D.-D., Liao, Z.-H., Sun, D.-Z., Zheng, T., Yong, Y.-C. 2015. Microbial fuel cell-based biosensors for environmental monitoring: a review. *Water Science and Technology*, **71**(6), 801-809.
Sung, J.H., Shuler, M.L. 2009. Prevention of air bubble formation in a microfluidic perfusion cell culture system using a microscale bubble trap. *Biomedical microdevices*, **11**(4), 731-738.
Sungpet, A., Pimsert, A., Jiraratananon, R., Way, J. 2002. Facilitated transport of unsaturated hydrocarbons through crosslinked-poly (sulfonated styrene). *Chemical Engineering Journal*, **87**(3), 321-328.
Tan, Y.C., Kharkwal, S., Chew, K.K.W., Alwi, R., Mak, S.F.W., Ng, H.Y. 2018. Enhancing the robustness of microbial fuel cell sensor for continuous copper(II) detection against

organic strength fluctuations by acetate and glucose addition. *Bioresour Technol*, **259**, 357-364.
Theodosiou, P., Greenman, J., Ieropoulos, I.A. 2020. Developing 3D-Printable Cathode Electrode for Monolithically Printed Microbial Fuel Cells (MFCs). *Molecules*, **25**(16), 3635.
Torres, C.I., Lee, H.-S., Rittmann, B.E. 2008. Carbonate species as OH− carriers for decreasing the pH gradient between cathode and anode in biological fuel cells. *Environmental science & technology*, **42**(23), 8773-8777.
Tran, P.H.N., Luong, T.T.T., Nguyen, T.T.T., Nguyen, H.Q., Van Duong, H., Kim, B.H. 2015. Possibility of using a lithotrophic iron-oxidizing microbial fuel cell as a biosensor for detecting iron and manganese in water samples. *Environmental Science: Processes & Impacts*, **17**(10), 1806-1815.
Tront, J.M., Fortner, J., Plötze, M., Hughes, J., Puzrin, A.M. 2008. Microbial fuel cell biosensor for in situ assessment of microbial activity. *Biosensors and Bioelectronics*, **24**(4), 586-590.
Tsuda, H., Hagiwara, A., Shibata, M., Ohshima, M., Ito, N. 1982. Carcinogenic effect of carbazole in the liver of (C57BL/6N× C3H/HeN) F1 mice. *journal of the National Cancer Institute*, **69**(6), 1383-1389.
Tucci, M., Bombelli, P., Howe, C.J., Vignolini, S., Bocchi, S., Schievano, A. 2019. A storable mediatorless electrochemical biosensor for herbicide detection. *Microorganisms*, **7**(12), 630.
Uría, N., Sánchez, D., Mas, R., Sánchez, O., Muñoz, F.X., Mas, J. 2012. Effect of the cathode/anode ratio and the choice of cathode catalyst on the performance of microbial fuel cell transducers for the determination of microbial activity. *Sensors and Actuators B: Chemical*, **170**, 88-94.
Velasquez-Orta, S.B., Werner, D., Varia, J.C., Mgana, S. 2017. Microbial fuel cells for inexpensive continuous in-situ monitoring of groundwater quality. *Water Res*, **117**, 9-17.
Vesvikar, M.S., Al-Dahhan, M. 2005. Flow pattern visualization in a mimic anaerobic digester using CFD. *Biotechnology and Bioengineering*, **89**(6), 719-732.
Wagner, R.C., Regan, J.M., Oh, S.-E., Zuo, Y., Logan, B.E. 2009. Hydrogen and methane production from swine wastewater using microbial electrolysis cells. *water research*, **43**(5), 1480-1488.
Wallace, S., de Solla, S., Head, J., Hodson, P., Parrott, J., Thomas, P., Berthiaume, A., Langlois, V. 2020. Polycyclic aromatic compounds (PACs) in the Canadian environment: Exposure and effects on wildlife. *Environmental Pollution*, 114863.
Wang, X., Gao, N., Zhou, Q. 2013. Concentration responses of toxicity sensor with Shewanella oneidensis MR-1 growing in bioelectrochemical systems. *Biosensors and Bioelectronics*, **43**, 264-267.
Webster, D.P., TerAvest, M.A., Doud, D.F., Chakravorty, A., Holmes, E.C., Radens, C.M., Sureka, S., Gralnick, J.A., Angenent, L.T. 2014. An arsenic-specific biosensor with genetically engineered Shewanella oneidensis in a bioelectrochemical system. *Biosensors and Bioelectronics*, **62**, 320-324.
Weelink, S.A., Van Eekert, M.H., Stams, A.J. 2010. Degradation of BTEX by anaerobic bacteria: physiology and application. *Reviews in Environmental Science and Bio/Technology*, **9**(4), 359-385.

Willie, M., Esler, D., Boyd, W.S., Molloy, P., Ydenberg, R.C. 2017. Spatial variation in polycyclic aromatic hydrocarbon exposure in Barrow's goldeneye (Bucephala islandica) in coastal British Columbia. *Marine Pollution Bulletin*, **118**(1-2), 167-179.

Wu, D., Li, L., Zhao, X., Peng, Y., Yang, P., Peng, X. 2019a. Anaerobic digestion: a review on process monitoring. *Renewable and Sustainable Energy Reviews*, **103**, 1-12.

Wu, L.-C., Tsai, T.-H., Liu, M.-H., Kuo, J.-L., Chang, Y.-C., Chung, Y.-C. 2017. A Green microbial fuel cell-based biosensor for in situ chromium (VI) measurement in electroplating wastewater. *Sensors*, **17**(11), 2461.

Wu, M., Xu, X., Lu, K., Li, X. 2019b. Effects of the presence of nanoscale zero-valent iron on the degradation of polychlorinated biphenyls and total organic carbon by sediment microbial fuel cell. *Science of The Total Environment*, **656**, 39-44.

Xiao, N., Selvaganapathy, P.R., Wu, R., Huang, J.J. 2020a. Influence of wastewater microbial community on the performance of miniaturized microbial fuel cell biosensor. *Bioresource technology*, **302**, 122777.

Xiao, N., Wu, R., Huang, J.J., Selvaganapathy, P.R. 2020b. Development of a xurographically fabricated miniaturized low-cost, high-performance microbial fuel cell and its application for sensing biological oxygen demand. *Sensors and Actuators B: Chemical*, **304**, 127432.

Xing, F., Xi, H., Yu, Y., Zhou, Y. 2020. A sensitive, wide-ranging comprehensive toxicity indicator based on microbial fuel cell. *Science of The Total Environment*, **703**, 134667.

Xu, Z., Liu, B., Dong, Q., Lei, Y., Li, Y., Ren, J., McCutcheon, J., Li, B. 2015. Flat microliter membrane-based microbial fuel cell as "on-line sticker sensor" for self-supported in situ monitoring of wastewater shocks. *Bioresour Technol*, **197**, 244-51.

Xu, Z., Liu, Y., Williams, I., Li, Y., Qian, F., Zhang, H., Cai, D., Wang, L., Li, B. 2016. Disposable self-support paper-based multi-anode microbial fuel cell (PMMFC) integrated with power management system (PMS) as the real time "shock" biosensor for wastewater. *Biosens Bioelectron*, **85**, 232-239.

Xue, Y., Lu, S., Fu, X., Sharma, V.K., Mendoza-Sanchez, I., Qiu, Z., Sui, Q. 2018. Simultaneous removal of benzene, toluene, ethylbenzene and xylene (BTEX) by CaO2 based Fenton system: Enhanced degradation by chelating agents. *Chemical Engineering Journal*, **331**, 255-264.

Yang, G.-X., Sun, Y.-M., Kong, X.-Y., Zhen, F., Li, Y., Li, L.-H., Lei, T.-Z., Yuan, Z.-H., Chen, G.-Y. 2013. Factors affecting the performance of a single-chamber microbial fuel cell-type biological oxygen demand sensor. *Water science and technology*, **68**(9), 1914-1919.

Yang, K., Ji, M., Liang, B., Zhao, Y., Zhai, S., Ma, Z., Yang, Z. 2020. Bioelectrochemical degradation of monoaromatic compounds: Current advances and challenges. *Journal of Hazardous Materials*, 122892.

Yang, W., Wei, X., Fraiwan, A., Coogan, C.G., Lee, H., Choi, S. 2016. Fast and sensitive water quality assessment: a μL-scale microbial fuel cell-based biosensor integrated with an air-bubble trap and electrochemical sensing functionality. *Sensors and Actuators B: Chemical*, **226**, 191-195.

Yang, Y., Wang, Y.-Z., Fang, Z., Yu, Y.-Y., Yong, Y.-C. 2018. Bioelectrochemical biosensor for water toxicity detection: generation of dual signals for electrochemical assay confirmation. *Analytical and bioanalytical chemistry*, **410**(4), 1231-1236.

Yao, S., Meyer, A., Henze, G. 1991. Comparison of amperometric and UV-spectrophotometric monitoring in the HPLC analysis of pesticides. *Fresenius' journal of analytical chemistry*, **339**(4), 207-211.

Yi, Y., Xie, B., Zhao, T., Li, Z., Stom, D., Liu, H. 2019a. Effect of external resistance on the sensitivity of microbial fuel cell biosensor for detection of different types of pollutants. *Bioelectrochemistry*, **125**, 71-78.
Yi, Y., Xie, B., Zhao, T., Liu, H. 2018. Comparative analysis of microbial fuel cell based biosensors developed with a mixed culture and Shewanella loihica PV-4 and underlying biological mechanism. *Bioresource technology*, **265**, 415-421.
Yi, Y., Xie, B., Zhao, T., Qian, Z., Liu, H. 2020. The effect of anode hydrodynamics on the sensitivity of microbial fuel cell based biosensors and the biological mechanism. *Bioelectrochemistry*, **132**, 107351.
Yi, Y., Xie, B., Zhao, T., Qian, Z., Liu, H. 2019b. Effect of control mode on the sensitivity of a microbial fuel cell biosensor with Shewanella loihica PV-4 and the underlying bioelectrochemical mechanism. *Bioelectrochemistry*, **128**, 109-117.
You, J., Preen, R.J., Bull, L., Greenman, J., Ieropoulos, I. 2017. 3D printed components of microbial fuel cells: Towards monolithic microbial fuel cell fabrication using additive layer manufacturing. *Sustainable Energy Technologies and Assessments*, **19**, 94-101.
Yu, D., Bai, L., Zhai, J., Wang, Y., Dong, S. 2017. Toxicity detection in water containing heavy metal ions with a self-powered microbial fuel cell-based biosensor. *Talanta*, **168**, 210-216.
Yu, D., Zhang, H., Bai, L., Fang, Y., Liu, C., Zhang, H., Li, T., Han, L., Yu, Y., Yu, H. 2020. Visual detection of the toxicity of wastewater containing heavy metal ions using a microbial fuel cell biosensor with a Prussian blue cathode. *Sensors and Actuators B: Chemical*, **302**, 127177.
Zakaria, B.S., Dhar, B.R. 2020. An intermittent power supply scheme to minimize electrical energy input in a microbial electrolysis cell assisted anaerobic digester. *Bioresource Technology*, 124109.
Zakaria, B.S., Dhar, B.R. 2019. Progress towards catalyzing electro-methanogenesis in anaerobic digestion process: Fundamentals, process optimization, design and scale-up considerations. *Bioresource technology*, 121738.
Zeng, S., Gan, N., Weideman-Mera, R., Cao, Y., Li, T., Sang, W. 2013. Enrichment of polychlorinated biphenyl 28 from aqueous solutions using Fe3O4 grafted graphene oxide. *Chemical engineering journal*, **218**, 108-115.
Zeng, X., Borole, A.P., Pavlostathis, S.G. 2016. Inhibitory effect of furanic and phenolic compounds on exoelectrogenesis in a microbial electrolysis cell bioanode. *Environmental science & technology*, **50**(20), 11357-11365.
Zhang, C., Li, Y., Shen, H., Shuai, D. 2020a. Simultaneous coupling of photocatalytic and biological processes: A promising synergistic alternative for enhancing decontamination of recalcitrant compounds in water. *Chemical Engineering Journal*, 126365.
Zhang, D., Wang, Y., Li, C., Zhang, X. 2019. Polychlorinated biphenyl detection in organic solvents with paper-based analytical devices. *Environmental Technology*, 1-6.
Zhang, H., Yuan, X., Xiong, T., Wang, H., Jiang, L. 2020b. Bioremediation of co-contaminated soil with heavy metals and pesticides: influence factors, mechanisms and evaluation methods. *Chemical Engineering Journal*, 125657.
Zhang, J. 1997. Designing a cost-effective and reliable pipeline leak-detection system. *Pipes and Pipelines International*, **42**(1), 20-26.

Zhang, S., You, J., An, N., Zhao, J., Wang, L., Cheng, Z., Ye, J., Chen, D., Chen, J. 2018. Gaseous toluene powered microbial fuel cell: Performance, microbial community, and electron transfer pathway. *Chemical Engineering Journal*, **351**, 515-522.

Zhang, X., Xia, X., Ivanov, I., Huang, X., Logan, B.E. 2014. Enhanced activated carbon cathode performance for microbial fuel cell by blending carbon black. *Environmental science & technology*, **48**(3), 2075-2081.

Zhao, L., Deng, J., Hou, H., Li, J., Yang, Y. 2019a. Investigation of PAH and oil degradation along with electricity generation in soil using an enhanced plant-microbial fuel cell. *Journal of Cleaner Production*, **221**, 678-683.

Zhao, L., Wang, C., Gu, H., Yue, C. 2018. Market incentive, government regulation and the behavior of pesticide application of vegetable farmers in China. *Food Control*, **85**, 308-317.

Zhao, T., Xie, B., Yi, Y., Liu, H. 2019b. Sequential flowing membrane-less microbial fuel cell using bioanode and biocathode as sensing elements for toxicity monitoring. *Bioresour Technol*, **276**, 276-280.

Zhou, T., Han, H., Liu, P., Xiong, J., Tian, F., Li, X. 2017a. Microbial fuels cell-based biosensor for toxicity detection: A review. *Sensors*, **17**(10), 2230.

Zhou, Y., Tang, L., Liu, Z., Hou, J., Chen, W., Li, Y., Sang, L. 2017b. A novel anode fabricated by three-dimensional printing for use in urine-powered microbial fuel cell. *Biochemical Engineering Journal*, **124**, 36-43.

Zhu, X., Ni, J. 2009. Simultaneous processes of electricity generation and p-nitrophenol degradation in a microbial fuel cell. *Electrochemistry Communications*, **11**(2), 274-277.

Zou, S., Qin, M., Moreau, Y., He, Z. 2017. Nutrient-energy-water recovery from synthetic sidestream centrate using a microbial electrolysis cell-forward osmosis hybrid system. *Journal of Cleaner Production*, **154**, 16-25.

Chapter 3 – Microbial Electrochemical Biosensor for a Rapid Detection of a Naphthenic Acid Model Compound in Water Samples

From the literature review in the previous chapter, it is evident that MXC biosensor can be applied to detect aromatic compounds. Hence, the applicability of MXC biosensor on a single model naphthenic acid compound (cyclohexane carboxylic acid) was first investigated. Specifically, an optimal operating method (e.g., calibration) was determined for the identification of a model compound. In addition, different environmental parameters (e.g., salinity and temperature) were examined to partially mimic the conditions of real OSPW.

A version of this chapter was published in Journal of Electroanalytical Chemistry (2020); 873: 114405.

3-1. Introduction

Canada (Alberta)'s oil sands are proven to be one of the largest oil deposits in the world (Allen, 2008). The oil sands mining operation in Northern Alberta produces a large volume of oil sands process-affected water (OSPW) through their hot water bitumen extraction process (Barrow et al., 2015). OSPW consists of suspended solids, various complex organic compounds, including unrecovered bitumen and hydrocarbons, inorganic compounds, salts, and trace metals (El-Din et al., 2011; Mahaffey & Dubé, 2016). Due to Alberta's "zero-discharge" policy, OSPW is stored in engineered on-site settling basins, which are widely known as oil sands tailing ponds (Allen, 2008). Currently, >1 billion m^3 of OSPW are stored in tailing ponds in the oil sands region of Northern Alberta (Martin, 2015). Management of this large volume of OSPW is one of the major environmental challenges faced by oil sands mining companies (Allen, 2008). Particularly, the presence of various water-soluble organics from bitumen in OSPW poses a significant threat to the aquatic ecosystem and wildlife (McQueen et al., 2017). Numerous studies have confirmed that the toxicity of OSPW is primarily attributed to the presence of various naphthenic acids (NAs) that are natural components of petroleum (El-Din et al., 2011; Mahaffey & Dubé, 2016). Due to these environmental-threatening features, there is a growing concern over NAs intrusion into the surrounding surface and groundwater, which can result in a subsequent adverse impact on the aquatic ecosystem and environment. Numerous studies also revealed the estrogenic and androgenic activity of these NAs and suggested that exposure to these NAs can potentially disrupt the human reproductive system (Leclair et al., 2015; Reinardy et al., 2013). Hence, NA concentrations have been routinely monitored in OSPW and surface waters (Ripmeester & Duford, 2019; Ross et al., 2012).

The monitoring of NAs in water samples is the major analytical challenge faced by oil-mining companies. Currently, no single absolute analytical method exists for the detection and quantification of mining-related NAs (Headley et al., 2016). Commonly used analytical methods for NAs include Fourier transform infrared spectroscopy, gas chromatography-mass spectrometry, and high-performance liquid chromatography (Headley et al., 2016). However, the analysis of NAs with these methods is time-consuming and expensive, and samples need to be sent to an analytical laboratory (Ripmeester & Duford, 2019). Hence, the development of a low-cost, fast, and on-site analytical method for rapid detection and quantification of NAs will help to address these analytical challenges.

In recent years, microbial electrochemical cells (MXCs) biosensors have demonstrated great potential to be the next generation real-time environmental monitoring tool (Davila et al., 2011; Kaur et al., 2013; Yu et al., 2017). To briefly describe the working principle of MXC biosensors, biofilms of electroactive bacteria serve as the biorecognition element on the anode (Sun et al., 2015). The electrons released via microbial oxidation of organic analytes are transferred to the intermediate redox carriers; then, they are further transferred to the anode electrode through the extracellular electron transfer (EET) process (Lovley & Nevin, 2011). Finally, electrons move to the cathode through an external circuit driven by the potential gradient between the two electrodes. Thus, MXC biosensors can continuously generate electrical signals in response to the presence of targeted organic analytes; and usually, levels of produced electrical signals depend on the concentrations of organic electron donors (Kaur et al., 2013). Also, MXC biosensors' size can be manipulated to a miniature scale (i.e., μL) (Davila et al., 2011) to lower the fabrication costs. Therefore, MXC biosensors have been extensively studied for monitoring microbial activities, organics, and other contaminants in various wastewater treatment systems (Sun et al.,

2015). Previous studies have confirmed anaerobic biodegradation of OSPW; however, the complete biodegradation was a pitfall (Choi & Liu, 2014; Jiang et al., 2013; Labrada & Nemati, 2017). Rather than targetting OSPW treatments, MXCs can better serve as a biosensing tool for detecting NA concentrations in OSPW. To date, no studies have investigated the feasibility of measuring NAs concentrations with MXC biosensors.

The present study, thus, evaluates the applicability of MXC biosensor for quantification of NA concentration in water samples. Firstly, we investigated whether steady currents generated by an MXC biosensor could be linearly correlated with corresponding NA concentrations. Secondly, we optimized a calibration method to further improve analytical performance in terms of precision, time-efficiency, sensitivity, and reproducibility. Finally, we explored the effects of salinity levels and water temperature on the sensitivity of the biosensor. We also characterized the bacterial communities to get more insights into the biosensing mechanism. To the best of authors' knowledge, this work is first to prove that MXC biosensor could be applied for the detection of NAs concentrations.

3-2. Materials and Methods

3-2.1 Microbial electrochemical biosensor

A dual-chamber MXC biosensor was constructed with plexiglass**.** The biosensor consisted of an anode and a cathode separated by an anion exchange membrane (AMI-7001, Membranes International Inc., USA). High-density carbon fibers (2293-A, 24A Carbon Fiber, Fibre Glast Development Corp., Ohio, USA) integrated with a stainless-steel frame with a surface area of 122.57 cm^2 was used as the anode and a stainless-steel mesh (T304, McMaster-Carr, USA) was used as the cathode (see Fig. 3-1a).

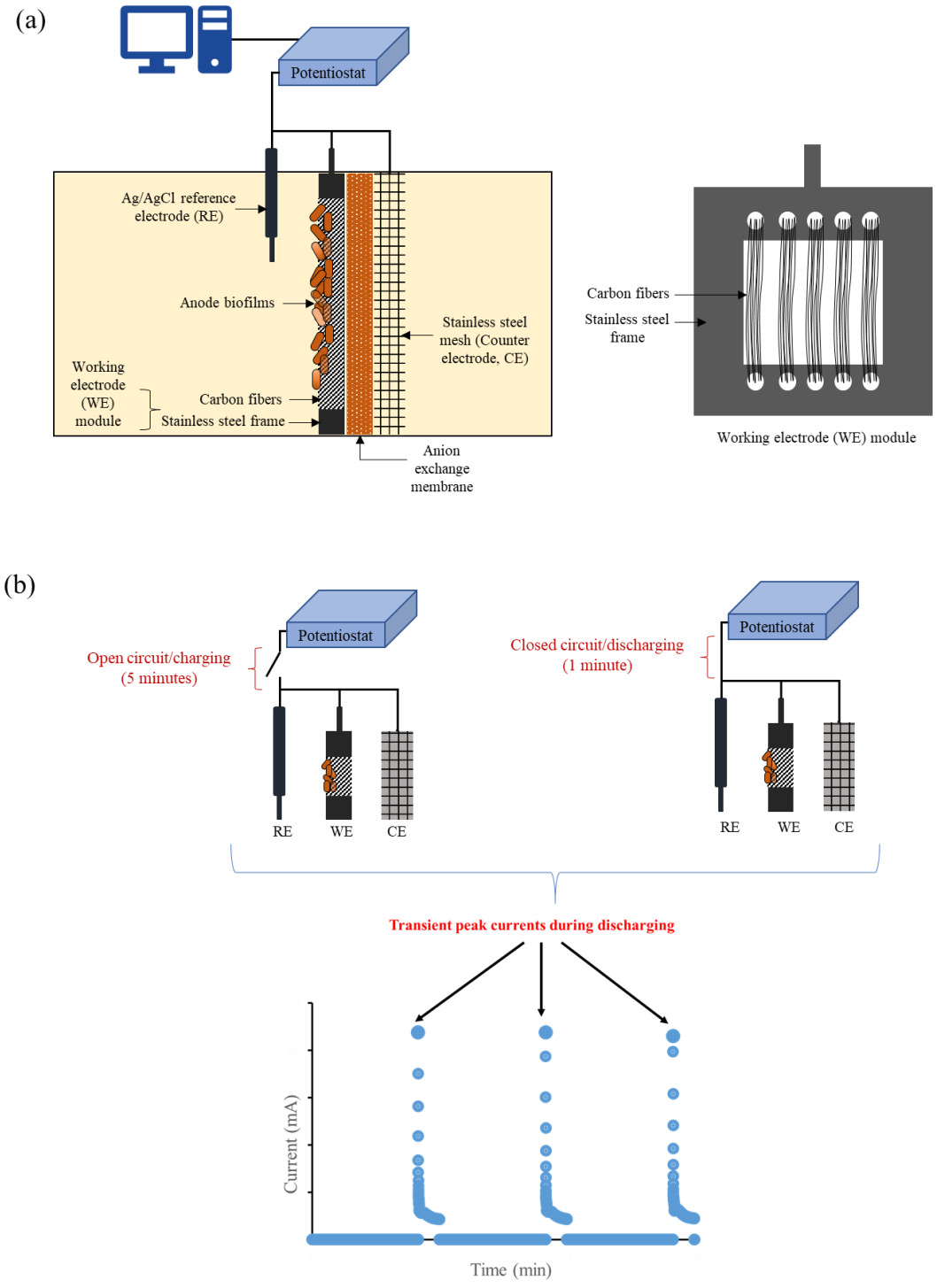

Figure 3-1. Schematic diagram showing (a) configuration of microbial electrochemical biosensor, and (b) charging-discharging operation of microbial electrochemical biosensor.

The cathode chamber was filled with tap water and the anode chamber was filled with an NA-containing media. Since this study is in a developing stage, decently larger working volumes of the anode (80 mL) and the cathode (40 mL) were selected. The anode chamber was equipped with an Ag/AgCl reference electrode (MF-2052, Bioanalytical System Inc., USA), which was < 1 cm away from the anode electrode. During the experiment, anode potential was set at -0.2 V vs. standard hydrogen electrode (SHE) by a potentiostat system (Squidstat Prime, Admiral Instruments, Arizona, USA). The anolyte was stirred at 250 rpm with a magnetic stirrer. During the entire operating period, the substrate medium was injected into the anode chamber under anaerobic conditions. Also, the extended gas outlet tubes from both chambers were placed in a jar filled with tap water.

Previous studies already have demonstrated the biodegradation of OSPW with MXCs, which were inoculated with matured fine tailings (MFT) deposits from oil sands tailings reservoir (Choi & Liu, 2014; Jiang et al., 2013). Therefore, the biosensor was inoculated with pre-enriched biofilms collected from a mother MXC reactor that was originally inoculated with MFT from oil sands tailings pond located in Northern Alberta and fed with a mixture of acetate and various model naphthenic acids. NA is a mixture of different cyclopentyl and cyclohexyl carboxylic acids (Han et al., 2008); and of note, cyclohexane carboxylic acid ($C_6H_{11}CO_2H$) (CHA) has frequently been used as a model NA for investigation of various fundamental aspects in OSPW related studies (Afzal et al., 2012; Drzewicz et al., 2012). Therefore, CHA (CAS: 98-89-5, New Jersey, USA) was chosen as a model NA to explore the biosensing capability of this MXC. During the inoculation of the biosensor, the composition of the substrate medium was (per L of deionized water) 131.25 mg $C_6H_{11}CO_2H$ (CHA), 588 mg $NaHCO_3$ (sodium bicarbonate), and trace minerals. The detailed composition of the trace minerals can be found in the literature

(Dhar et al., 2013). The typical pH values in OSPW ranged from 7.8 to 8.5 (Zhang, 2016); hence, the average pH value of 8.1±0.2 was maintained throughout the experiments. After reaching steady-state current in repetitive fed-batch cycles, experiments were performed for biosensor calibration and studying the effects of salinity levels and different temperatures on biosensor's sensitivity. All the experimental runs were performed in a batch mode. Before each experimental run, the anolyte was completely evacuated from the anode chamber and washed with 500 mL-mineral of media lacking any CHA with a peristaltic pump operated at a flow rate of 311.4 mL/min to remove any residual organics from the previous cycle. At the end of each experimental cycle, the anode chamber was fed with CHA medium containing 300 mg COD/L for >12 hours to ensure that the current and the anode biofilm could be fully recovered before the next experimental cycle.

3-2.2 Experiments

Initially, calibration of the biosensor was performed with different CHA concentrations (50, 100, 150, 200, and 250 as mg COD/L) and a fixed bicarbonate buffer concentration of 7 mmol/L for comparing two different calibration methods: a) closed-circuit (CC) operation, and b) charging-discharging (CD) operation. A type of buffer and its concentration were selected based on the literature (El-Din et al., 2011; Wang et al., 2016a). For both approaches, after feeding CHA, the biosensor was operated for 3 hours to reach steady-currents. In the first approach, the biosensor was operated under a CC mode, where the current is continuously being generated. When the steady-current was reached within 3 hours under the CC operation, maximum currents were recorded. Then, a calibration curve was established based on the maximum currents for different concentrations of CHA.

In the second approach, the operation of biosensor under a CD mode was implemented, where an open-circuit (electron charging) and a closed-circuit (electron discharging) operation were alternated using the potentiostat (see Fig. 3-1b). During an open-circuit operation, the electroactive microbes oxidize organic matters and accumulate captured electrons in the anode biofilms (Sim et al., 2018). When the system switched to a closed-circuit mode, the accumulated electrons from the anode biofilms are rapidly discharged, and transient peak currents are produced. According to Sim et al., (Sim et al., 2018), charging interval of 5-min (with 1-min discharging interval) resulted in the best MXC performance (i.e., R^2=0.99) compared to other charging intervals (vs. 1, 15, 30, and 40-min) for a complex organic substrate (i.e., municipal wastewater). We performed some preliminary experiments with different charging times (1, 5, and 15 minutes) to determine the appropriate charging time for our biosensor system (See Supporting Information). To avoid any interferences with other parameters, such as substrate limitation condition and salinity, CHA concentration of 300 mg COD/L was used with no addition of salinity. Briefly describing, 1-min charging time resulted in the lowest peak current (7.74±0.44 mA vs. 21.49±0.53 mA and 21.83±0.59 mA, which was ~3 times less than the maximum currents produced from 5-min and 15-min charging time). The peak current produced from 15-min charging time was similar to the peak current produced from 5-min charging time (See Supplementary). Also, it was evident that 1-min would be adequate for discharging biofilm for all conditions. Therefore, the selected charging (open-circuit) and discharging (close-circuit) times were 5 minutes and 1 minute, respectively. The currents were recorded at every 0.5 seconds using the potentiostat. The CD operation was repeated 20 times to ensure the reproducibility of results. Note that transient peak current is the maximum current produced during a charging-discharging cycle (see Fig. 1b), and the average of these transient peak

currents was used as the electrical signal in response to CHA concentration. Then, similar to the first approach, a calibration curve was established between the average transient peak currents and CHA concentrations for a comparison.

To study the effects of different salinity levels (0 - 3000 mg/L), the biosensor was operated for 180 minutes under the CC mode to allow the start of oxidation followed by an 18-minute CD operation. Salinity ranges were selected based on OSPW's salinity values (335 - 2881 mg/L) reported in the literature (Pouliot et al., 2013). Since sodium and chloride ions have been identified as the major source of salinity in OSPW (Zhang, 2016), NaCl was used to represent salinity in this study. In terms of selecting different temperatures, Larrosa-Guerrero et al., (2010) have reported the differences in current outputs of the MXCs working between 20 to 35°C were almost negligible. However, they have found MXCs operating below 15°C significantly reduced the current outputs (28.77 mA/m^2 to 1.71 mA/m^2). Therefore, the effects of different temperatures (13.5±0.3°C and room temperature, 20±1°C were selected) on the sensitivity of biosensor were also investigated under both moderate (500 mg NaCl/L) and extreme (3000 mg NaCl/L) salinity levels. For experiments at 13.5°C, the temperature was maintained using ice packs. Considering that typical alkalinity of OSPW ranges from 600 to 800 mg/L (6 to 8 mmol/L) as $CaCO_3$ (El-Din et al., 2011; Wang et al., 2016a), the bicarbonate buffer concentration was always fixed at 7 mmol/L. For studying the effect of different salinity levels and temperature, we performed CD cycles in triplicate.

3-2.3 Analytical methods

Chemical oxygen demand (COD) concentrations were measured using HACH reagent kits (HACH, Loveland, Co, USA). Conductivity and pH were measured using an electrical

conductivity/temperature meter (Extech EC100, ITM Instruments INC., Edmonton, AB, Canada) and a benchtop pH meter (Accumet AR15, Fisher Scientific, Pittsburgh, PA, USA), respectively. The current outputs generated by the biosensor were recorded every 5 min during a CC operation and 0.5 seconds during a CD operation using the potentiostat and the data were stored on a desktop PC. Microbial community analysis for pre-enriched biofilms was performed using 16S rRNA gene sequencing. The detailed protocol of DNA extraction and microbial community characterization in the literature (2018) was used in this study.

3-2.4 Statistical analysis

P-values were calculated using Tukey Pairwise Comparisons at 95% Confidence in Minitab 19. This statistical analysis was applied to the salinity and temperature tests under the charging-discharging mode.

3-3. Results and discussion

3-3.1 Characterization of the microbial community

Fig. 3-2 shows the bacterial community distribution of pre-enriched biofilms at phylum and genus levels.

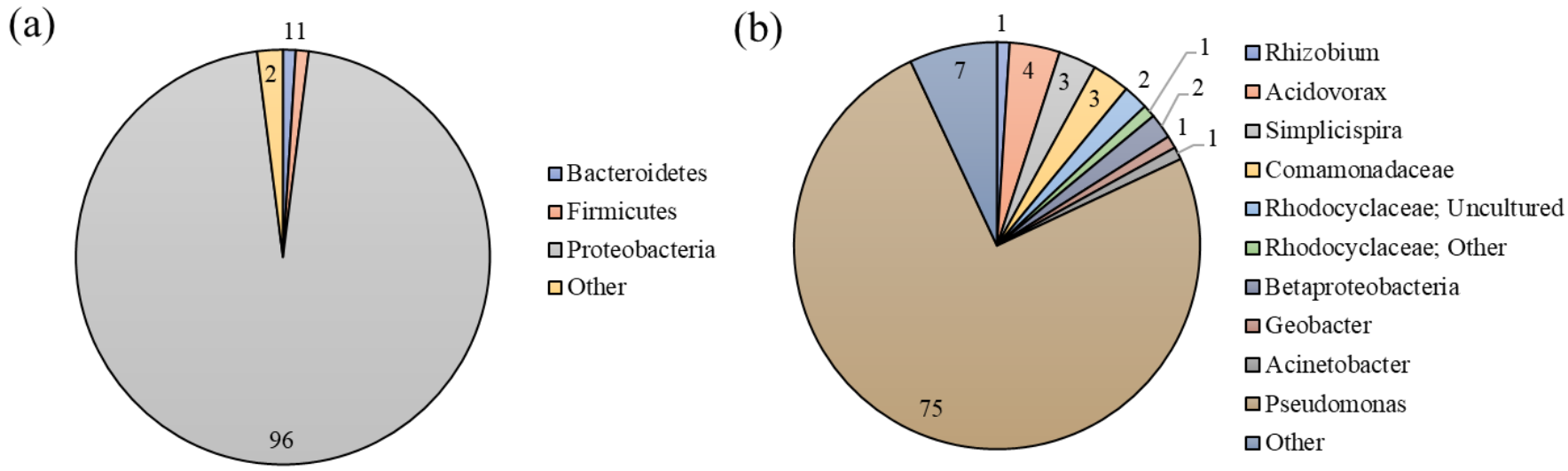

Figure 3-2. The relative abundance of bacterial communities at (a) phylum, and (b) genus level.

At the phylum level, bacterial species in pre-enriched biofilms were primarily dominated by *Proteobacteria* (96%), while *Firmicutes* (1%) and *Bacteroidetes* (1%) were detected in relatively minor abundances (Fig. 3-2a). At the genus level, *Pseudomonas* was the most dominant (75%), followed by *Acidovorax* (4%), *Comamonadaceae* (3%), and *Simplicispira* (3%), all of them belong to phylum *Proteobacteria* (Fig. 3-2b). Members of *Geobacter*, *Rhizobium*, *Acinetobacter* genera comprised a relatively small portion of the microbial community. *Pseudomonas* and *Acidovorax* species have been reported to be indigenous microbes residing in oil sands tailings ponds (Yu et al., 2018). Notably, certain *Pseudomonas* species have been reported to be capable of degrading both model and commercial NA compounds from solution (Yu et al., 2018). Interestingly, *Pseudomonas* species are also frequently detected in anode biofilms in MXCs, and well known as electroactive bacteria for their EET capability (Boon et al., 2008; Yang et al., 2018). They can oxidize various organic compounds, which can be coupled with the reduction of insoluble electron acceptors. *Pseudomonas* can also produce conductive nanowires to facilitate EET (Maruthupandy et al., 2015). However, the abundance of *Geobacter* sp., the most well-known electroactive bacteria, was very low. Previous studies suggested that *Acidovorax, Comamonadaceae, Simplicispira, and Acinetobacter* might be capable of generating an electrical current in MXCs (Mei et al., 2017; Sciarria et al., 2019; Timmers et al., 2012), while there was no substantial evidence on their EET capability. Thus, our results suggest a possible syntrophic partnership between CHA-degrading (*Pseudomonas*) and electroactive microbes (e.g.; *Acidovorax*). Considering the dominance of *Pseudomonas* species in biofilms as well as their capability of degrading NA compounds and facilitating EET, they might have played a dual role in biosensing CHA.

3-3.2 Calibration of biosensor

3-3.2.1 Continuous closed-circuit operation

Initially, the calibration of the sensor was performed based on the current generation under continuous CC operation. The detailed results provided in the Supplementary Information. The current generated immediately without any lag phase after the addition of the fresh CHA medium and reached a steady-state within 3 hours. The current generation at different CHA concentrations exhibited random and scattered trends, where inconsistencies were found when locating for the steady currents. For instance, steady currents produced from 50 and 100 mg COD/L of CHA were found between 1-2 hours, whereas 150, 200, and 250 mg COD/L showed the steady currents after 2.5 hours. The steady currents produced from 50, 100, 150, 200, and 250 mg COD/L of CHA were 0.153±0.007, 0.154±0.004, 0.169±0.004, 0.197±0.003, and 0.177±0.002 mA, respectively. A corresponding calibration curve was constructed based on the steady currents from the CC operation (see Supplementary Information). In general, the steady currents produced from the CC operation did not demonstrate a clear linear relationship with the CHA concentrations (coefficient of determination, R^2=0.64). Thus, a satisfactory calibration curve could not be obtained from the continuous CC operation. Thus, our first calibration method had suggested that the CC operation of MXC may not be the best suitable to measure different CHA concentrations in aqueous solution. For instance, the measurement of analyte concentrations in MXC biosensor would depend on the difference in steady currents; hence, larger output currents are required for better sensitivity and higher precision of analysis. During CC operation, steady currents from this biosensor varied within a small range (0.153-0.197 mA) for different CHA concentrations. A previous study also reported low current (<0.3 mA) generation during biodegradation of a cyclic NA model compound (trans- 4-methyl-1-

cyclohexane carboxylic acid) (Labrada & Nemati, 2017). Furthermore, oxidation of complex organic compounds in wastewater would require syntrophic interactions between fermentative and electroactive microbes, which could also lead to lower electrical response as well as fluctuations in electrical response from MXCs at different substrate concentrations (Gao et al., 2017; Sim et al., 2018). Alternatively, due to the capacitive nature of bioanode, MXCs could produce substantially higher output currents under consecutive open and closed-circuit alternation operation (i.e., CD mode) (Wang et al., 2016b). Hence, we further investigated whether such an approach could be used to enhance the sensitivity of MXC biosensor for CHA concentrations detection.

3-3.2.2 Charging-discharging operation

Fig. 3-3a-e shows the generation of current at different CHA concentrations under repetitive CD cycles.

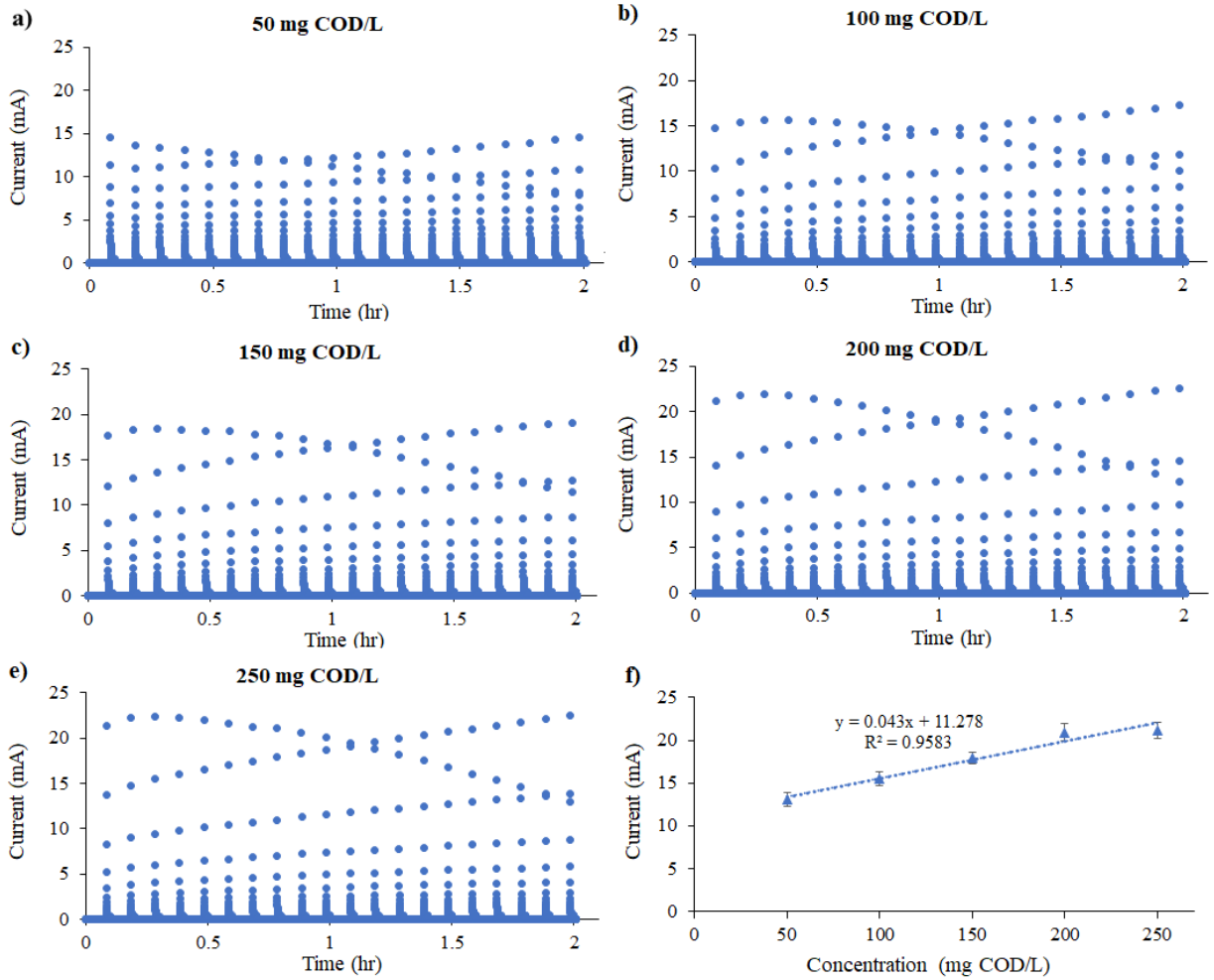

Figure 3-3. a-e) Current profile (mA) versus time (hr) under charging-discharging cycles of CHA oxidation after a 3-hour standing period; f) Calibration curve of average transient peak currents from charging-discharging cycles (mA) versus CHA concentration (mg COD/L).

The transient peak currents were produced during discharging cycles; yielded a similar trend for each CHA concentration. The average transient peak currents produced from 50, 100, 150, 200, and 250 mg COD/L of CHA were 13.1±0.80, 15.5±0.82, 17.9±0.66, 20.9±0.99, and 21.2±0.97 mA, respectively. Thus, following the increase of CHA concentration, the average peak currents increased and saturated at a high CHA concentration >200 mg COD/L. The difference in the transient peak currents for 200 and 250 mg COD/L was almost negligible (p-value=0.976), indicating substrate saturation of microbial metabolism. The transient peak currents produced from the CD operation resulted in a linear relationship between CHA concentrations and the peak currents (R^2=0.96) (Fig. 3-3f). Transient peak currents were approximately two order magnitudes higher than that observed during CC operation. Thus, the CD operation ultimately led to the high precision calibration of the biosensor. In a previous study, Sim et al. (2018) suggested that cumulative coulombs (i.e., accumulated charge during open circuit) from CD operation of an MXC biosensor could be correlated with 5-d biochemical oxygen demand (BOD_5) concentrations in complex wastewater like domestic sewage. While our results suggested that transient peak currents generated from CD operation could be directly used for measuring CHA concentrations in aqueous solution.

For a practical field-scale application, a biosensor should be able to provide a quick measurement of NA concentrations. For this purpose, we compared calibration curves based on the average peak currents from different CD times of 18, 60, 90, and 120 minutes (see Supplementary Information). Interestingly, the calibration plots obtained from different CD times were comparable (see Supplementary Information). Also, larger CD times (i.e., 60-120 minutes) showed significant fluctuations as the transient peak currents were increasing and decreasing. Such fluctuations could be attributed to differences between kinetic features of

fermentative and electroactive microbes, which warrant further investigation. Nonetheless, an 18-minute CD operation time, which was quick and stable, was adopted for further experiments.

3-3.3 Impact of environmental parameters on the sensitivity of the biosensor

3-3.3.1 Effects of salinity

Fig. 3-4a shows calibration plots obtained at different salinity levels.

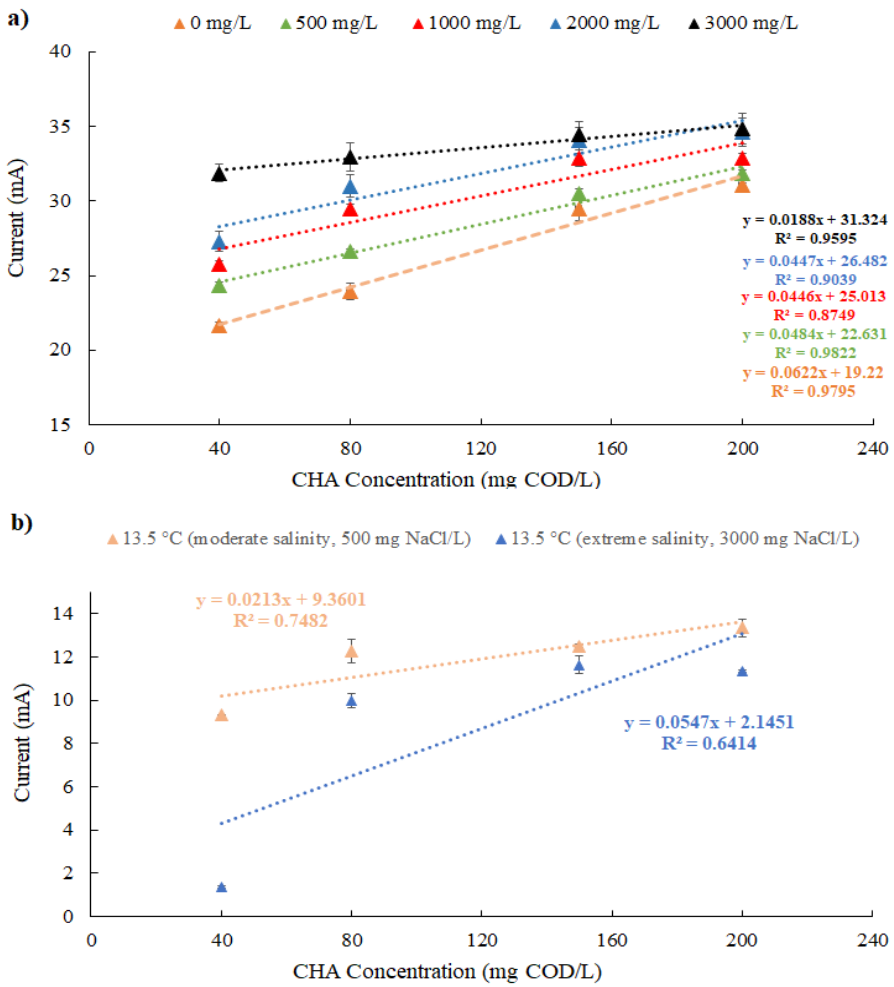

Figure 3-4. Calibration curves constructed using 18-min charging-discharging operation a) CHA concentration vs. current at different salinity levels with fixed bicarbonate concentration of 7 mM (at 20°C); b) CHA concentration vs. current constructed by lowering temperature to 13.5°C at two different salinity conditions.

The detailed results from CD operation under different salinity levels can be found in the Supplementary Information. As shown in Figure 4-4a, an increase in salinity levels led to increased transient peak currents. For instance, at 40 mg COD/L of CHA, the increase in salinity level from 0 to 3000 mg NaCl/L considerably increased the transient peak currents from 21.62±0.26 to 31.89±0.59 mA (p-value=0.017, see Supplementary Information). This might result from the increased solution conductivity (see Supplementary Information) at high salinity levels, which can facilitate anodic electron transport due to enhanced counter ions transport at lowered internal resistance (Tremouli et al., 2017). In contrast, switching to extreme salinity level (3000 mg NaCl/L) at high CHA concentrations (150 and 200 mg COD/L) led to very little changes in transient peak currents as the substrate saturation of microbial metabolism had been reached. Nonetheless, calibration curves at different salinity levels showed linear relationships between the CHA concentrations and transient peak currents (R^2=0.87-0.98), suggesting that MXC biosensor can be applied under wide salinity levels (335 - 2881 mg/L) reported for OSPW (Pouliot et al., 2013). As recently summarized by Grattieri and Minteer (Grattieri & Minteer, 2018), previous studies have demonstrated enhanced current output from MXCs by increasing salinity content to a certain level (Huang et al., 2010; Liu et al., 2005). However, a high salinity level (e.g., ~80 g/L NaCl), could inhibit anodic microbial communities and decrease performance of MXCs (Huang et al., 2010; Miller & Oremland, 2008)). In this study, the biosensor was not adversely impacted by introducing the highest salinity content reported for OSPW. However, the differences in slopes in linear regression equations indicated that the biosensor would be very sensitive to changes in salinity levels. Especially, for low CHA

concentration measurement, salinity effects need to be carefully considered for biosensor calibration.

3-3.3.2 Effects of lowering the temperature

The bioanode kinetics are known to be highly sensitive to temperature changes (Rousseau et al., 2020); therefore, the sensitivity of biosensor was examined by decreasing the temperature from 20°C to 13.5°C at low and extreme salinity conditions. Figure 4-4b shows calibration curves developed at 13.5°C under different salinity levels (500 and 3000 mg/L). The decrease in temperature led to a noticeable reduction in the transient peak currents. At moderate salinity level (500 mg/L), the average transient peak current significantly dropped from 24.31±0.25 mA (20°C) to 9.32±0.04 mA (13.5°C) at a low CHA concentration of 40 mg COD/L (p-value=0.016). Also, differences in the transient peak currents decreased with the decreasing CHA concentrations (p-value=0.019). For example, the differences in the transient peak currents between 20°C and 13.5°C was 18.52 mA (31.87-13.35 mA) for 200 mg COD/L, while the difference was 14.99 mA (24.31-9.32 mA) for 40 mg COD/L. Several studies reported detrimental effects of high salinity levels on MEC performance and further suggested that maintaining an optimum salinity would be critical for bioanode kinetics (Camacho et al., 2017; Tremouli et al., 2017). As discussed earlier, at 20°C, the increase in salinity levels led to an increase in transient peak currents from the biosensor, particularly at low CHA concentrations. However, at 13.5°C, the increase in salinity levels had a detrimental effect on the produced transient peak currents. At extreme salinity conditions, a slight decrease in transient peak currents was found for CHA concentrations of 80, 150, and 200 mg COD/L and interestingly, a significant decrease in transient peak currents was found for CHA concentration of 40 mg

COD/L. For instance, for CHA concentrations of 80 - 200 mg COD/L, the transient peak currents only droped from 13.35 to 11.34 mA at the most, however, the transient peak currents dropped from 9.32 to 1.34 mA for CHA concentration of 40 mg COD/L (see Supplementary Information). In general, the increase in salinity can decrease internal resistance in MECs (Jannelli et al., 2017; Lefebvre et al., 2012), while the decrease in temperature can increase internal resistance (Larrosa-Guerrero et al., 2010; Li et al., 2013). Specifically, in Figure 4-4b, lowering the temperature played a significant role at an extreme salinity condition at a low substrate concentration (i.e., 40 mg COD/L). This result is maybe due to exposing the electroactive bacteria to an over-excessive salinity level, and low substrate concentration and low temperature, in which, an unfavorable metabolic condition for these bacteria was established. However, further in-depth research will be needed to understand the complex interactions among salinity, temperature, and NA concentrations. Overall, our results suggested that the anode biofilms enriched at 20°C would be susceptible to a complex interaction between salinity and temperature.

3-3.4 Significance of results

Our results demonstrated that the MXC biosensor could be further developed for the rapid detection of naphthenic acid compounds. The existing methods available for analysis of mining-related NAs are time-intensive and expensive. The development of MXC-biosensor can provide a cost-effective solution for real-time monitoring of NAs, which will partially alleviate the need for off-site analysis of a large number of samples by oil sands producer companies. Additionally, MXC biosensors can be used for the early detection of OSPW seepage into surface and groundwater. All these aspects are also significant from an economic standpoint, as early

detection of NAs release to the environment can significantly reduce the cost of restoring environmental quality. Although our preliminary experiment used synthetic water samples containing only CHA as a carbon source, there are other organic compounds, including hydrocarbons, BTEX (benzene, toluene, ethylbenzene, and xylene), and phenols, present in OSPW (Zhang, 2016). Therefore, the next phase of this study will focus on understanding the interactions among various naphthenic acid compounds, other organic compounds/toxicants, various environmental parameters, and their impact on the sensitivity of the MXC biosensor.

3-4. Conclusions

Herein, an MXC biosensor is proposed for the quantification of NAs concentration in OSPW. A typical concentration-dependent electrical response (R^2=0.64) to a model NA compound (i.e., CHA) was observed under the CC operation of the biosensor for <3 hours, suggesting an excellent potential for rapid measurement of NAs concentrations. The CD operation of biosensor provided enhanced sensitivity and high precision calibration (R^2=0.96) for CHA concentration measurement. Furthermore, the results highlighted that changes in salinity levels and water temperature could potentially interfere with the biosensor response. In short, the results obtained from this study demonstrated an initial proof-of-concept of MXC biosensor's applicability for the rapid quantification of NAs in OSPW. For further development, the detection of NAs in real OSPW, long-term stability, and interference of various environmental parameters and conditions will be explored in future research.

3-5. References

Afzal, A., Drzewicz, P., Martin, J.W., El-Din, M.G. 2012. Decomposition of cyclohexanoic acid by the UV/H2O2 process under various conditions. *Science of the total environment*, **426**, 387-392.

Allen, E.W. 2008. Process water treatment in Canada's oil sands industry: I. Target pollutants and treatment objectives. *Journal of Environmental Engineering and Science*, **7**(2), 123-138.

Barrow, M.P., Peru, K.M., Fahlman, B., Hewitt, L.M., Frank, R.A., Headley, J.V. 2015. Beyond Naphthenic Acids: Environmental Screening of Water from Natural Sources and the Athabasca Oil Sands Industry Using Atmospheric Pressure Photoionization Fourier Transform Ion Cyclotron Resonance Mass Spectrometry. *J Am Soc Mass Spectrom*, **26**(9), 1508-21.

Boon, N., Aelterman, P., Clauwaert, P., De Schamphelaire, L., Vanhaecke, L., De Maeyer, K., Höfte, M., Verstraete, W., Rabaey, K. 2008. Metabolites produced by Pseudomonas sp. enable a Gram-positive bacterium to achieve extracellular electron transfer. *Applied Microbiology and Biotechnology*, **77**(5), 1119-1129.

Camacho, J.V., Romero, L.R., Marchante, C.F., Morales, F.F., Rodrigo, M.R. 2017. The salinity effects on the performance of a constructed wetland-microbial fuel cell. *Ecological engineering*, **107**, 1-7.

Choi, J., Liu, Y. 2014. Power generation and oil sands process-affected water treatment in microbial fuel cells. *Bioresource technology*, **169**, 581-587.

Davila, D., Esquivel, J., Sabate, N., Mas, J. 2011. Silicon-based microfabricated microbial fuel cell toxicity sensor. *Biosensors and Bioelectronics*, **26**(5), 2426-2430.

Dhar, B.R., Gao, Y., Yeo, H., Lee, H.-S. 2013. Separation of competitive microorganisms using anaerobic membrane bioreactors as pretreatment to microbial electrochemical cells. *Bioresource technology*, **148**, 208-214.

Drzewicz, P., Perez-Estrada, L., Alpatova, A., Martin, J.W., Gamal El-Din, M. 2012. Impact of peroxydisulfate in the presence of zero valent iron on the oxidation of cyclohexanoic acid and naphthenic acids from oil sands process-affected water. *Environmental science & technology*, **46**(16), 8984-8991.

El-Din, M.G., Fu, H., Wang, N., Chelme-Ayala, P., Pérez-Estrada, L., Drzewicz, P., Martin, J.W., Zubot, W., Smith, D.W. 2011. Naphthenic acids speciation and removal during petroleum-coke adsorption and ozonation of oil sands process-affected water. *Science of the Total Environment*, **409**(23), 5119-5125.

Gao, Y., Ryu, H., Rittmann, B.E., Hussain, A., Lee, H.-S. 2017. Quantification of the methane concentration using anaerobic oxidation of methane coupled to extracellular electron transfer. *Bioresource technology*, **241**, 979-984.

Grattieri, M., Minteer, S.D. 2018. Microbial fuel cells in saline and hypersaline environments: advancements, challenges and future perspectives. *Bioelectrochemistry*, **120**, 127-137.

Han, X., Scott, A.C., Fedorak, P.M., Bataineh, M., Martin, J.W. 2008. Influence of molecular structure on the biodegradability of naphthenic acids. *Environmental science & technology*, **42**(4), 1290-1295.

Headley, J.V., Peru, K.M., Barrow, M.P. 2016. Advances in mass spectrometric characterization of naphthenic acids fraction compounds in oil sands environmental samples and crude oil—a review. *Mass spectrometry reviews*, **35**(2), 311-328.

Huang, J., Sun, B., Zhang, X. 2010. Electricity generation at high ionic strength in microbial fuel cell by a newly isolated Shewanella marisflavi EP1. *Applied microbiology and biotechnology*, **85**(4), 1141-1149.

Jannelli, N., Nastro, R.A., Cigolotti, V., Minutillo, M., Falcucci, G. 2017. Low pH, high salinity: Too much for microbial fuel cells? *Applied energy*, **192**, 543-550.

Jiang, Y., Ulrich, A.C., Liu, Y. 2013. Coupling bioelectricity generation and oil sands tailings treatment using microbial fuel cells. *Bioresource technology*, **139**, 349-354.

Kaur, A., Kim, J.R., Michie, I., Dinsdale, R.M., Guwy, A.J., Premier, G.C., Centre, S.E.R. 2013. Microbial fuel cell type biosensor for specific volatile fatty acids using acclimated bacterial communities. *Biosensors and Bioelectronics*, **47**, 50-55.

Labrada, G.V., Nemati, M. 2017. Microbial Fuel Cell Bioreactors for Treatment of Waters Contaminated by Naphthenic Acids. *Frontiers International Conference on Wastewater Treatment and Modelling*. Springer. pp. 303-307.

Larrosa-Guerrero, A., Scott, K., Head, I., Mateo, F., Ginesta, A., Godinez, C. 2010. Effect of temperature on the performance of microbial fuel cells. *Fuel*, **89**(12), 3985-3994.

Leclair, L.A., Pohler, L., Wiseman, S.B., He, Y., Arens, C.J., Giesy, J.P., Scully, S., Wagner, B.D., van den Heuvel, M.R., Hogan, N.S. 2015. In vitro assessment of endocrine disrupting potential of naphthenic acid fractions derived from oil sands-influenced water. *Environmental science & technology*, **49**(9), 5743-5752.

Lefebvre, O., Tan, Z., Kharkwal, S., Ng, H.Y. 2012. Effect of increasing anodic NaCl concentration on microbial fuel cell performance. *Bioresource Technology*, **112**, 336-340.

Li, L., Sun, Y., Yuan, Z., Kong, X., Li, Y. 2013. Effect of temperature change on power generation of microbial fuel cell. *Environmental technology*, **34**(13-14), 1929-1934.

Liu, H., Cheng, S., Logan, B.E. 2005. Power generation in fed-batch microbial fuel cells as a function of ionic strength, temperature, and reactor configuration. *Environmental science & technology*, **39**(14), 5488-5493.

Lovley, D.R., Nevin, K.P. 2011. A shift in the current: new applications and concepts for microbe-electrode electron exchange. *Current opinion in Biotechnology*, **22**(3), 441-448.

Mahaffey, A., Dubé, M. 2016. Review of the composition and toxicity of oil sands process-affected water. *Environmental Reviews*, **25**(1), 97-114.

Martin, J.W. 2015. The Challenge: Safe release and reintegration of oil sands process-affected water. *Environmental toxicology and chemistry*, **34**(12), 2682-2682.

Maruthupandy, M., Anand, M., Maduraiveeran, G., Beevi, A.S.H., Priya, R.J. 2015. Electrical conductivity measurements of bacterial nanowires from Pseudomonas aeruginosa. *Advances in Natural Sciences: Nanoscience and Nanotechnology*, **6**(4), 045007.

McQueen, A.D., Kinley, C.M., Hendrikse, M., Gaspari, D.P., Calomeni, A.J., Iwinski, K.J., Castle, J.W., Haakensen, M.C., Peru, K.M., Headley, J.V., Rodgers, J.H., Jr. 2017. A risk-based approach for identifying constituents of concern in oil sands process-affected water from the Athabasca Oil Sands region. *Chemosphere*, **173**, 340-350.

Mei, X., Xing, D., Yang, Y., Liu, Q., Zhou, H., Guo, C., Ren, N. 2017. Adaptation of microbial community of the anode biofilm in microbial fuel cells to temperature. *Bioelectrochemistry*, **117**, 29-33.

Miller, L.G., Oremland, R.S. 2008. Electricity generation by anaerobic bacteria and anoxic sediments from hypersaline soda lakes. *Extremophiles*, **12**(6), 837-848.

Pouliot, R., Rochefort, L., Graf, M.D. 2013. Fen mosses can tolerate some saline conditions found in oil sands process water. *Environmental and experimental botany*, **89**, 44-50.

Reinardy, H.C., Scarlett, A.G., Henry, T.B., West, C.E., Hewitt, L.M., Frank, R.A., Rowland, S.J. 2013. Aromatic naphthenic acids in oil sands process-affected water, resolved by GCxGC-MS, only weakly induce the gene for vitellogenin production in zebrafish (Danio rerio) larvae. *Environmental science & technology*, **47**(12), 6614-6620.

Ripmeester, M.J., Duford, D.A. 2019. Method for routine "naphthenic acids fraction compounds" determination in oil sands process-affected water by liquid-liquid extraction in dichloromethane and Fourier-Transform Infrared Spectroscopy. *Chemosphere*, **233**, 687-696.

Ross, M.S., Pereira, A.d.S., Fennell, J., Davies, M., Johnson, J., Sliva, L., Martin, J.W. 2012. Quantitative and qualitative analysis of naphthenic acids in natural waters surrounding the Canadian oil sands industry. *Environmental science & technology*, **46**(23), 12796-12805.

Rousseau, R., Etcheverry, L., Roubaud, E., Basséguy, R., Délia, M.-L., Bergel, A. 2020. Microbial electrolysis cell (MEC): Strengths, weaknesses and research needs from electrochemical engineering standpoint. *Applied Energy*, **257**, 113938.

Sciarria, T.P., Arioli, S., Gargari, G., Mora, D., Adani, F. 2019. Monitoring microbial communities' dynamics during the start-up of microbial fuel cells by high-throughput screening techniques. *Biotechnology Reports*, **21**, e00310.

Sim, J., Reid, R., Hussain, A., Lee, H.-S. 2018. Semi-continuous measurement of oxygen demand in wastewater using biofilm-capacitance. *Bioresource Technology Reports*, **3**, 231-237.

Sun, J.-Z., Peter Kingori, G., Si, R.-W., Zhai, D.-D., Liao, Z.-H., Sun, D.-Z., Zheng, T., Yong, Y.-C. 2015. Microbial fuel cell-based biosensors for environmental monitoring: a review. *Water Science and Technology*, **71**(6), 801-809.

Timmers, R.A., Rothballer, M., Strik, D.P., Engel, M., Schulz, S., Schloter, M., Hartmann, A., Hamelers, B., Buisman, C. 2012. Microbial community structure elucidates performance of Glyceria maxima plant microbial fuel cell. *Applied microbiology and biotechnology*, **94**(2), 537-548.

Tremouli, A., Martinos, M., Lyberatos, G. 2017. The effects of salinity, pH and temperature on the performance of a microbial fuel cell. *Waste and biomass valorization*, **8**(6), 2037-2043.

Wang, C., Klamerth, N., Messele, S.A., Singh, A., Belosevic, M., Gamal El-Din, M. 2016a. Comparison of UV/hydrogen peroxide, potassium ferrate(VI), and ozone in oxidizing the organic fraction of oil sands process-affected water (OSPW). *Water Research*, **100**, 476-485.

Wang, Y., Wen, Q., Chen, Y., Yin, J., Duan, T. 2016b. Enhanced performance of a microbial fuel cell with a capacitive bioanode and removal of Cr (VI) using the intermittent operation. *Applied biochemistry and biotechnology*, **180**(7), 1372-1385.
Yang, Y., Zhou, H., Mei, X., Liu, B., Xing, D. 2018. Dual-edged character of quorum sensing signaling molecules in microbial extracellular electron transfer. *Frontiers in microbiology*, **9**.
Yu, D., Bai, L., Zhai, J., Wang, Y., Dong, S. 2017. Toxicity detection in water containing heavy metal ions with a self-powered microbial fuel cell-based biosensor. *Talanta*, **168**, 210-216.
Yu, X., Lee, K., Ma, B., Asiedu, E., Ulrich, A.C. 2018. Indigenous microorganisms residing in oil sands tailings biodegrade residual bitumen. *Chemosphere*, **209**, 551-559.
Zakaria, B.S., Barua, S., Sharaf, A., Liu, Y., Dhar, B.R. 2018. Impact of antimicrobial silver nanoparticles on anode respiring bacteria in a microbial electrolysis cell. *Chemosphere*, **213**, 259-267.
Zhang, Y. 2016. Development and application of Fenton and UV-Fenton processes at natural pH using chelating agents for the treatment of oil sands process-affected water.

Chapter 4 – Impact of salt and polycyclic aromatic hydrocarbons on the response of a microbial electrochemical biosensor applied for a mixture of naphthenic acids

The applicability of MXC biosensor on a model naphthenic acid was proven in Chapter 3. However, there are many different species of naphthenic acids along with other organic compounds, such as polycyclic aromatic hydrocarbons present in real OSPW. Hence, this study evaluates the applicability of MXC biosensors on the mixtures of naphthenic acids (known as the commercial naphthenic acid). Long-term exposures to salinity on the anode biofilm and the overall performance of MXC biosensor was also investigated. Furthermore, we examine the effect of polycyclic aromatic hydrocarbons on the biosensor's response.

This paper is being prepared for submission to a peer-reviewed journal.

4-1. Introduction

Alberta (Canada) holds one of the largest oil sands deposits across the globe (Allen, 2008). Due to such available and recoverable oil in Northern Alberta, the oil sands industries are currently conducting surface mining operations and producing a large volume of oil sands process-affected water (OSPW) via their hot water bitumen extraction process (Barrow et al., 2015). This OSPW contains various organic and inorganic compounds, such as suspended solids, various complex organic compounds, unrecovered bitumen and hydrocarbons, salts, and trace metals (El-Din et al., 2011; Mahaffey & Dubé, 2016). Because of the "zero-discharge" policy regulated by the Province of Alberta, OSPW is stored in engineered on-site settling basins called "oil sands tailing ponds" (Allen, 2008). To date, approximately 1 billion m^3 of OSPW are stored in the oil sands tailing ponds in Northern Alberta (Martin, 2015). Hence, the management of this large volume of OSPW is important and became one of the major environmental challenges faced by oil sands-related industries (Allen, 2008). Especially, the presence of various water-soluble organics in OSPW adversely affects the aquatic ecosystem and wildlife (McQueen et al., 2017).

Previous studies also have confirmed that the OSPW toxicity is associated with the presence of various naphthenic acids (NAs) that are natural components of petroleum (El-Din et al., 2011; Mahaffey & Dubé, 2016). More importantly, the potential NA intrusion from the oil sands tailings ponds into the surrounding water bodies (e.g., surface water and groundwater) became a major concern due to potential ecological risks (Fennell & Arciszewski, 2019). Many studies revealed the androgenic and estrogenic activities of the NAs and suggested that exposures to NAs can result in severe human health impacts, such as disrupting the human reproductive system (Leclair et al.,

2015; Reinardy et al., 2013). Therefore, NA concentrations have been routinely monitored in various water matrices, such as in OSPW and both surface and ground waters (Fennell & Arciszewski, 2019; Ripmeester & Duford, 2019; Ross et al., 2012). However, there are several drawbacks when using commonly-used analytical techniques (e.g., Fourier transform infrared spectroscopy, gas chromatography-mass spectrometry, high-performance liquid chromatography) (Headley et al., 2016) for field measurements of NAs. These commonly-used analytical methods are known to be time-consuming, expensive, and samples need to be sent to an analytical laboratory (Ripmeester & Duford, 2019). Also, no single absolute analytical method exists for the detection and quantification of mining-related NAs (Headley et al., 2016). Hence, the implementation of a low-cost, fast, and on-site analytical method for rapid detection and quantification of NAs will greatly address such analytical challenges.

To date, microbial electrochemical cell (MXC)-based biosensors have demonstrated great potential to be the next-generation real-time environmental monitoring tool (Davila et al., 2011; Kaur et al., 2013; Yu et al., 2017). Thus, MXC biosensors can be a suitable option for the determination of NA concentrations in OSPW. The MXC biosensors rely on using anode or cathode biofilms of electroactive bacteria, which serve as the biorecognition element (Sun et al., 2015). The electrons produced from microbial oxidation of organic analytes are transferred to the intermediate redox carriers and then, they further move to the anode electrode by the extracellular electron transfer process (Lovley & Nevin, 2011). The electrons are finally carried to the terminal electron acceptor (e.g., cathode) through an external circuit driven by the potential gradient between the two electrodes. Thus, MXC biosensors can continuously produce electrical signals in response to the presence of targeted organic analytes, where the levels of produced electrical

signals depend on the concentrations of organic electron donors (Kaur et al., 2013). Further details on the basic mechanism and fundamentals of MXC biosensors' operation can be found elsewhere (Adekunle, 2018; Do et al., 2020; Jiang et al., 2018; Sun et al., 2015; Zhou et al., 2017). Also, MXC biosensors' size can be miniaturized as small as μL-scales (Davila et al., 2011; Xiao et al., 2020), which is greatly beneficial for fabrication costs. Due to such advantages, MXC biosensors have been extensively studied for monitoring microbial activities, organics, and other contaminants in various water matrices (Do et al., 2020; Jiang et al., 2018; Sun et al., 2015).

Regarding the degradation of NAs under anaerobic conditions, a few studies have investigated the NAs degradation in MXCs (Choi & Liu, 2014; Jiang et al., 2013; Labrada & Nemati, 2017). However, the complete biodegradation of NAs and high current generation from MXCs was not achievable. Instead, rather than targetting OSPW treatment, MXCs can be more suitable as a biosensing tool for quantifying NA concentrations. Our previous study has revealed the applicability of MXC biosensors on a single model NA compound (cyclohexane carboxylic acid) (Chung et al., 2020). However, because OSPW does not only contain a single NA compound and it also contains other organic matters, such as polycyclic aromatic hydrocarbons (PAHs) (Folwell et al., 2016a; Siddique et al., 2006). Therefore, further investigation on the effect of NA mixture and PAHs on the performance of MXC biosensor are required to bring this idea to step forward towards field applications.

Therefore, this study evaluates the applicability of the MXC biosensor for the quantification of NA mixture in water samples. Also, the present study reveals how PAHs interfere with the signal output. We first confirmed whether the MXC biosensor could produce stable signal output when the commercial NAs (a mixture of NAs; referred to as 'CNA' in this chapter) are dosed, in

terms of precision, time-efficiency, sensitivity, and reproducibility, similar to our previous study (Chung et al., 2020). Secondly, we introduced different salt content and observed the effect on the MXC biosensor applied for the NA mixture. Finally, we explored the effects of different PAH concentrations and how they interfere with the MXC biosensor's current output. To the best of the authors' knowledge, this work is the first to prove that MXC biosensor could be applied for the detection of commercial NA mixture under a complex water matrix (e.g., presence of PAHs).

4-2. Materials and Methods

4-2.1 Microbial electrochemical biosensor

A dual-chamber plexiglass-fabricated MXC biosensor was used in this study**.** The biosensor consisted of an anode and a cathode (filled with tap water) separated by an anion exchange membrane (AMI-7001, Membranes International Inc., USA). The anode chamber was filled with a medium containing NA mixture (or CNA) and PAHs depending on the targeted results and experiments. High-density carbon fibers (2293-A, 24A Carbon Fiber, Fibre Glast Development Corp., Ohio, USA) integrated with a stainless-steel frame with a surface area of 122.57 cm^2 and a stainless-steel mesh (T304, McMaster-Carr, USA) were used as the anode and the cathode, respectively. Because this MXC biosensor is still in a developing stage, fairly larger working volumes of an anode (80 mL) and a cathode (40 mL) were selected to eliminate the issues of microbubble interference, which are experienced by small scales MXCs (e.g., μL) (Fraiwan et al., 2013; Yang et al., 2016). An Ag/AgCl reference electrode (MF-2052, Bioanalytical System Inc., USA) was used in this study and it was placed < 1 cm away from the anode electrode. Throughout the entire experiment, anode potential was poised at -0.2 V vs. standard hydrogen electrode (SHE) using a potentiostat system (Squidstat Prime, Admiral Instruments, Arizona, USA). The anolyte

was continuously mixed at a rate of 250 rpm using a magnetic mixer. Finally, we ensured that the anode chamber was operated under an anaerobic environment by purging nitrogen gas, and the extended gas outlet tubes from both chambers were placed in a jar filled with tap water to avoid further intrusions of oxygen molecules.

The MXC biosensor was initially inoculated with pre-enriched biofilms collected from a mother MXC reactor that was originally inoculated with matured fine tailings (MFT) from oil sands tailings pond located in Northern Alberta and fed with a mixture of acetate and various model naphthenic acids (e.g., cyclohexane carboxylic acid, cyclohexane butyric acid, cyclopentane carboxylic acid, etc.). After completion of our previous study (Chung et al., 2020), the MXC biosensor was fed with CNA (petroleum product, a mixture of alkylated cyclopentane carboxylic acids, $C_{10}H_{18}O_2$, Lot #: BCBS3204V, Aldrich Chemistry) containing medium for ~6 months until it reaches a steady-state (e.g., produce a stable current). The detailed composition of the trace minerals used in the medium can be found in the literature (Dhar et al., 2013). The average pH value of 8.1±0.2 was maintained throughout the experiments, which falls into the typical OSPW pH range (e.g., 7.8 – 8.5) (Zhang, 2016). After reaching steady-state current in repetitive fed-batch cycles, experiments were performed for biosensor calibration and studying the effects of salinity levels and PAHs on biosensor's sensitivity. All the experimental runs were performed in a batch mode. The cleaning of the anode chamber and recovery of anode biofilm were done through a methodology similar to the literature (e.g., only the carbon source was replaced with CNA) (Chung et al., 2020). All other details can be found in our previous study (Chung et al., 2020).

4-2.2 Experiments

Initially, the calibration of the biosensor was performed with different CNA concentrations (10 – 80 mg COD/L) with a fixed bicarbonate buffer concentration of 7 mmol/L. A type of buffer and its concentration were selected based on the literature (El-Din et al., 2011; Wang et al., 2016). The optimal calibration method, the charging-discharging (CD) cycles were chosen based on the results from our previous study (Chung et al., 2020). Briefly describing the CD cycle, it operates based on the alternation between an open-circuit (electron charging) and a closed-circuit (electron discharging). First, the MXC biosensor is operated using an open-circuit operation, where the electroactive bacteria (EAB) oxidize organic matter and accumulate captured electrons in the anode biofilms (Sim et al., 2018). Then, the system is switched to a closed-circuit mode, where the accumulated electrons from the anode biofilms are rapidly discharged and create a transient peak current (per CD cycle). Justification of selecting a charging time of 5-min and a discharging time of 1-min is discussed in the literature (Chung et al., 2020) and the standing period of >1.5 h was chosen based on our result (see Supplementary Information). Then, a calibration curve was established between the average transient peak currents and CNA concentrations. The closed-circuit operation was implemented to rapidly observe the effect of different salt content. Throughout the entire experiment, we performed CD cycles in triplicate. The same approach was used during the experiments observing the effects of different salinity levels and PAHs. A small amount of acetate medium (25 mM) (10 – 20 mL) was used for the recovery process whenever the MXC biosensor was greatly inhibited (e.g., producing significantly low stable current output, <0.5 mA) (see Supplementary Information).

To study the effects of different salinity levels (0 – 1500 mg/L), the biosensor (with NA mixture) was first operated for >3 h under the closed-circuit operation to observe the differences in maximum current output. After a long-term (>10 batch cycles) exposure to 1500 mg/L of salt content, the MXC biosensor was greatly inhibited (e.g., significantly low stable current output (< 0.5 mA) with a long start of oxidation period (>1.25 h)) (Fig. 1a). Hence, we did not investigate salinity higher than 1500 mg/L to avoid permanent damage to the anode biofilm. Since sodium and chloride ions have been identified as the major source of salinity in OSPW (Zhang, 2016), NaCl was used to represent salinity in this study. After all, a calibration curve (with the introduction of salinity) has been constructed using the method described above for a comparison.

To observe the effects of PAHs, 2-methylnaphalene (2-MN) and pyrene were chosen as the model compounds to represent the total PAH content in OSPW (Folwell et al., 2016a; Folwell et al., 2016b). BTEX (benzene, toluene, ethylbenzene, and xylene), short- and long-chained alkanes were excluded for our experiment because BTEX can be easily volatilized, and short and long-chained alkanes can be degraded under methanogenic conditions in OSPW (Folwell et al., 2016a; Siddique et al., 2006). Based on our analysis and aforementioned literature, a concentration of 120 mg COD/L for 2-MN and pyrene, and a range of 30 – 240 mg COD/L of CNA was selected to partially mimic the real OSPW scenario. Due to such low solubility of pyrene in water, only 30 mg COD/L was identified as a soluble form. Hence, 30 mg COD/L of pyrene was used for this test. After all, calibration curves (control and PAH conditions) were constructed for comparison.

The details of experimental methodology are illustrated in Fig. 4-1.

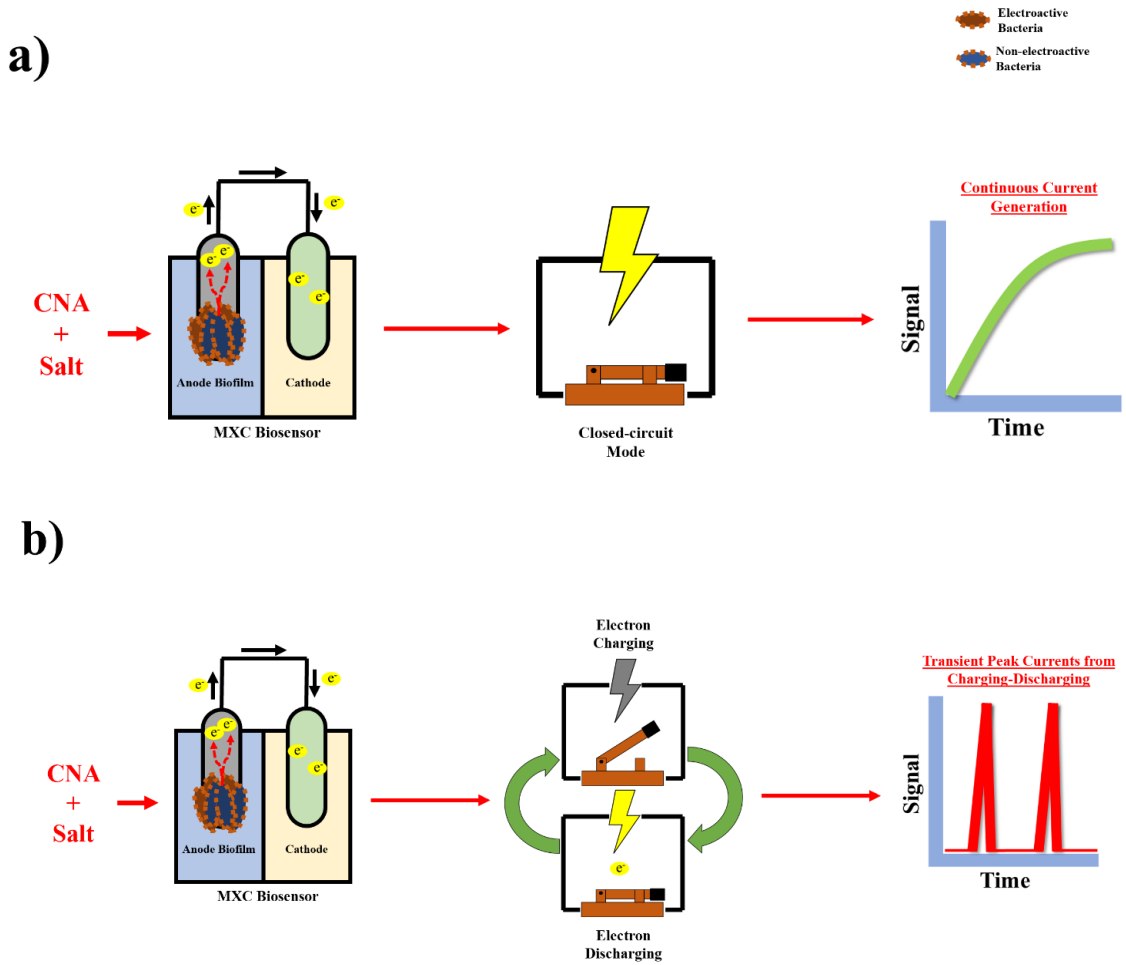
a)
Electroactive Bacteria
Non-electroactive Bacteria
CNA + Salt
e⁻
Anode Biofilm
Cathode
MXC Biosensor
Closed-circuit Mode
Continuous Current Generation
Signal
Time
b)
CNA + Salt
e⁻
Anode Biofilm
Cathode
MXC Biosensor
Electron Charging
Electron Discharging
Transient Peak Currents from Charging-Discharging
Signal
Time

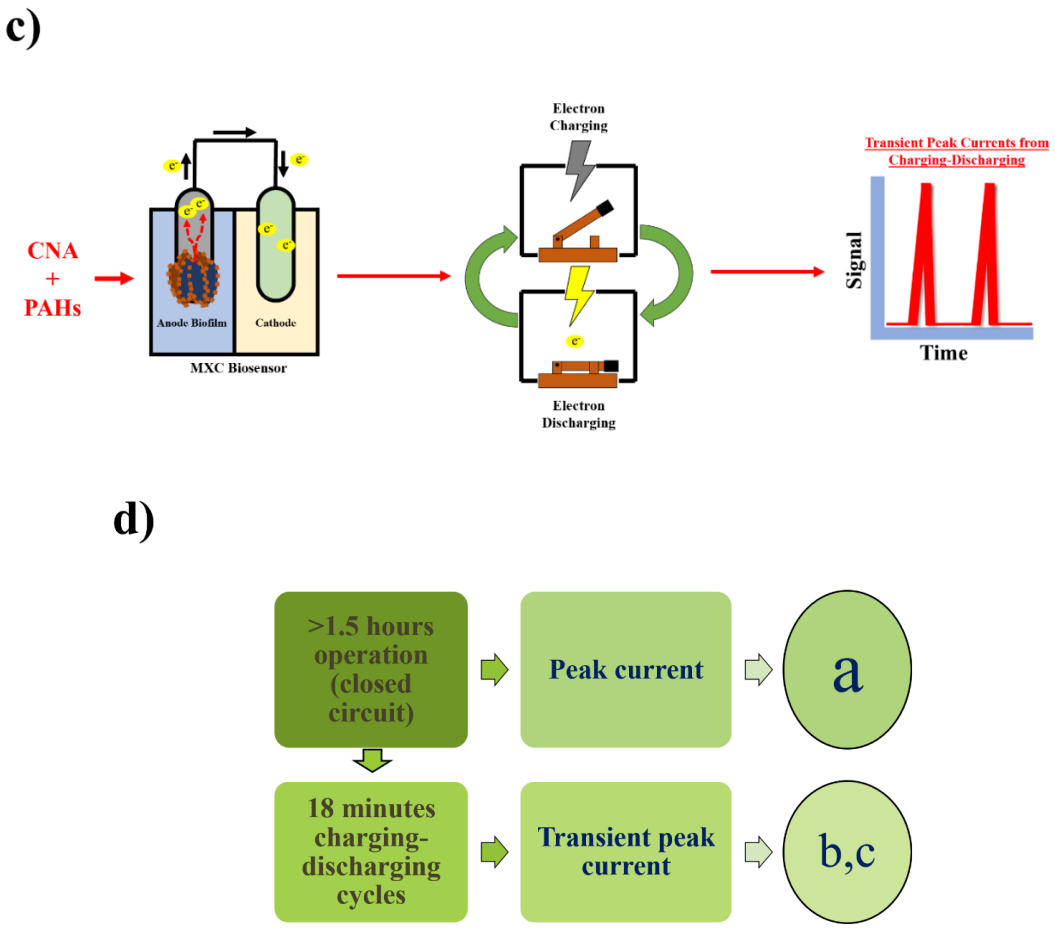

Figure 4-1. Descriptions of the methodology of the experiments using commercial NA (a mixture of NAs) as a carbon source: a) MXC biosensor operated with presence of salt content under closed-circuit mode; b) MXC biosensor operated with presence of salt

content under charging-discharging mode; c) MXC biosensor operated with presence of PAHs under charging-discharging mode; d) a flowchart describing the pathways of current production (e.g., closed-circuit operation in Fig. 4-1a and charging discharging operation in Fig. 4-1b,c).

4-2.3 Analytical methods

Chemical oxygen demand (COD) concentrations were measured using HACH reagent kits (HACH, Loveland, Co, USA). Conductivity and pH were measured using an electrical conductivity/temperature meter (Extech EC100, ITM Instruments INC., Edmonton, AB, Canada) and a benchtop pH meter (Accumet AR15, Fisher Scientific, Pittsburgh, PA, USA), respectively. The current outputs generated by the biosensor were recorded every 0.5 seconds during a CD operation using the potentiostat and the data were stored on a desktop PC.

4-3. Results and discussion

4-3.1 Current productions from commercial NAs in presence of various salinity levels

Current generation from the MXC biosensor using CNA as a carbon source under closed-circuit (CC, methodology described in Fig. 4-1a) mode and the constructed calibration curve from CD operations (methodology described in Fig. 4-1b) are shown in Fig. 4-2 (individual CD operation is provided in Supplementary Information). The MXC biosensor was operated for >3 h to observe the impact of different salinity levels (0 – 1500 mg/L) using the closed-circuit operation to rapidly observe the effects (Fig. 4-2a). As described in Fig. 1a, the maximum current output significantly decreased from 256.0±1.8 μA (control) to 112.7±3.8 (300 mg/L), 90.5±1.6 (500 mg/L), 82.8±0.5 (1000 mg/L), and 45.6±0.6 (1500 mg/L) μA when different salt contents were introduced. This was contradicting our previous findings using a single model NA compound (cyclohexane carboxylic acid) as a carbon source described in Chung et al. (2020). The hypothesis behind this is discussed later. After introducing a salt content of 1500 mg/L, the MXC biosensor was greatly inhibited demonstrated by a significantly low maximum current generation (e.g., 45.6±0.6 μA) as well as a relatively longer start of oxidation period (>1.25 h). Thus, to eliminate permanent damage

to the anode biofilm, increasing salinity level beyond >1500 mg/L was avoided unlike our previous study with a single model NA compound (Chung et al., 2020).

To amplify the impact of salinity on the response of MXC biosensor applied for NA mixture, the biosensor was enriched with the lowest possible salt content (e.g., 1500 mg/L) chosen from our results from closed-circuit operation (Fig. 4-2a). After a complete enrichment (e.g., when both maximum current and stable current are identical >3 batch cycles) with 1500 mg/L salinity level, CD operations have been implemented after >1.5 h of the standing period (described in Supplementary Information).

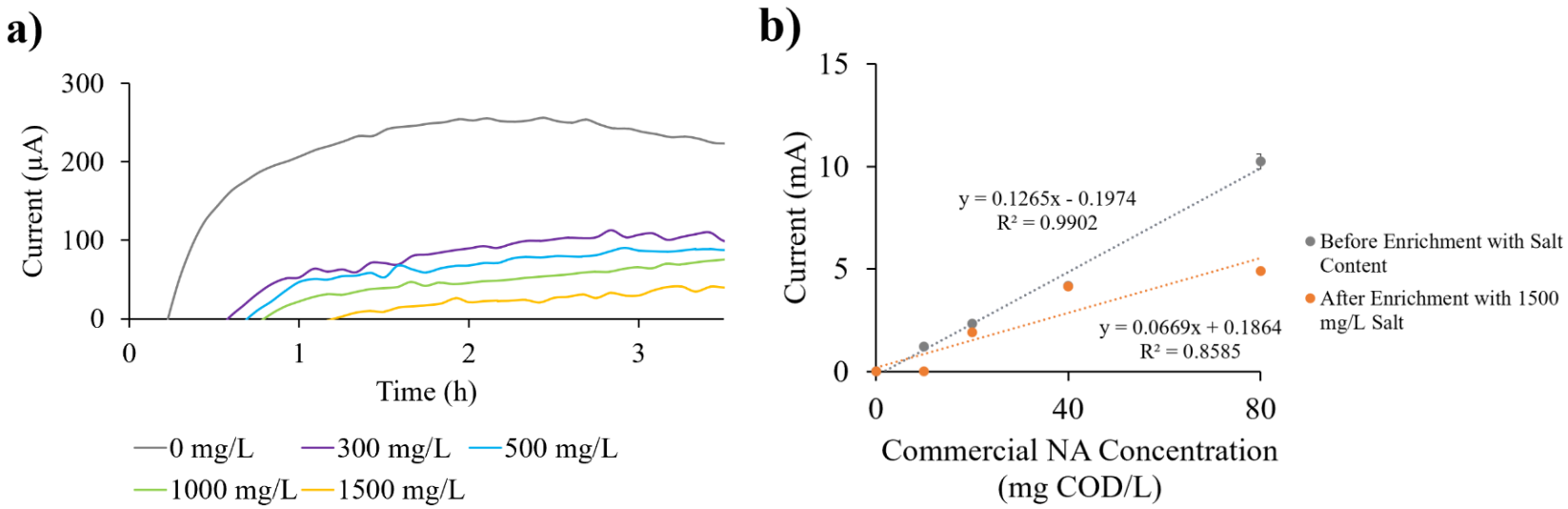

Figure 4-2. Currents produced from commercial NAs (CNA) with various salt contents (NaCl): a) continuous closed-circuit (CC) operation with 0 – 1500 mg/L salinity; and b) a calibration curve from charging-discharging (CD) operation with 0 and 1500 mg/L salinity.

As shown in Fig. 4-2b, two calibration curves were constructed from two different conditions: (i) before enrichment with salt content (e.g., control, no introduction of salt content during the enrichment); and (ii) after enrichment with salt content (e.g., long-term exposures to salt where the salt content was only dosed during the enrichment process, not during the construction of a calibration curve). The average transient peak currents for the control were 1.22±0.04, 2.34±0.03, 4.18±0.06, and 10.24±0.36 mA for CNA concentrations of 10, 20, 40, and 80 mg COD/L, respectively. On the other hand, the average transient peak currents dropped to 0±0, 1.92±0.11, 4.14±0.06, and 4.91±0.08 mA for 10, 20, 40, and 80 mg COD/L (CNA concentrations), respectively, when the MXC biosensor was enriched with a salt content of 1500 mg/L. The calibration curve from the control test results (Fig. 4-2b) indicated that the MXC biosensor can be applied for the detection of NA mixture as low as 10 mg COD/L and potentially, lower NA concentrations after further adjustment. Additionally, a very strong linear relationship was found between the concentration of CNA and the current output from CD operations (e.g., $R^2 = 0.99$). However, when the MXC biosensor was exposed to salt content for a long time (>10 batch cycles), the performance of the MXC biosensor was greatly hindered. Compared with the control (e.g., no salt dosage), the sensitivity decreased shown by the reduction in the detection range (e.g., 10 – 80 mg COD/L to 20 – 40 mg COD/L), meaning the biosensor was unable to provide readings lower than 20 mg COD/L and higher than 40 mg COD/L. This was confirmed by the no current output when 10 mg COD/L of CNA was dosed and the saturation (e.g., no change in current output) after dosing >40 mg COD/L of CNA.

As described in a review article (Grattieri & Minteer, 2018), many studies have shown higher current generation from MXCs by aggravating the salinity level to a certain concentration

(Huang et al., 2010; Liu et al., 2005) including our previous study (Chung et al., 2020). This is potentially due to the increase in solution conductivity at higher salinity levels, which can facilitate anodic electron transport due to enhanced counter ions transport at lowered internal resistance described in literature (Chung et al., 2020; Tremouli et al., 2017). On the other hand, a fairly high salt content (e.g., ~80 g/L NaCl, meaning high osmotic concentrations) could inhibit anodic microbial communities and decrease the performance of MXCs (Huang et al., 2010; Miller & Oremland, 2008). The inhibition of an anode biofilm can potentially be due to the dehydration, where the water exits the cellular membrane resulting in cell death (Grattieri & Minteer, 2018; Mille et al., 2002). In addition, the when bioreactor system, such as MXCs has a long-term exposure to a salt content, halophilic microbes (e.g., halotolerant bacteria) can grow (Grattieri & Minteer, 2018) and potentially compete with the EABs for COD in our MXC biosensor. For instance, Arulazhagan and Vasudevan (2011) reported that halotolerant bacteria are capable of reducing 66% of total COD and degrading >88% of PAHs (e.g., naphthalene, etc.) in their study. Thus, the non-electroactive halotolerant bacteria can potentially grow in our MXC biosensor, which may have contributed to the degradation of CNAs (e.g., similar structures to PAHs), decreasing the available organics (e.g., CNAs) for EABs to transfer electrons (Fig. 4-1b). Hence, these could be the reason why our biosensor was adversely impacted by introducing the salinity content (300 – 1500 mg/L, within the salinity range reported for OSPW). However, further microbial analysis would be needed to confirm this. Nonetheless, the result indicated that the biosensor could potentially be inhibited when detecting the NA mixture in a mild-saline water matrix.

4-3.2 Recovery of the biosensor from long term exposures to salt

After the CNA experiments with long-term exposure (>10 batch cycles) to a high salinity level (1500 mg/L), we performed a recovery of the biosensor using acetate (e.g., multiple batch cycles until steady-state is reached) (see Supplementary Information). Fig. 4-3a illustrates the duplicate results of CC operation with CNA (300 mg COD/L) after the recovery of the biosensor (long-term exposure to salts) with acetate medium.

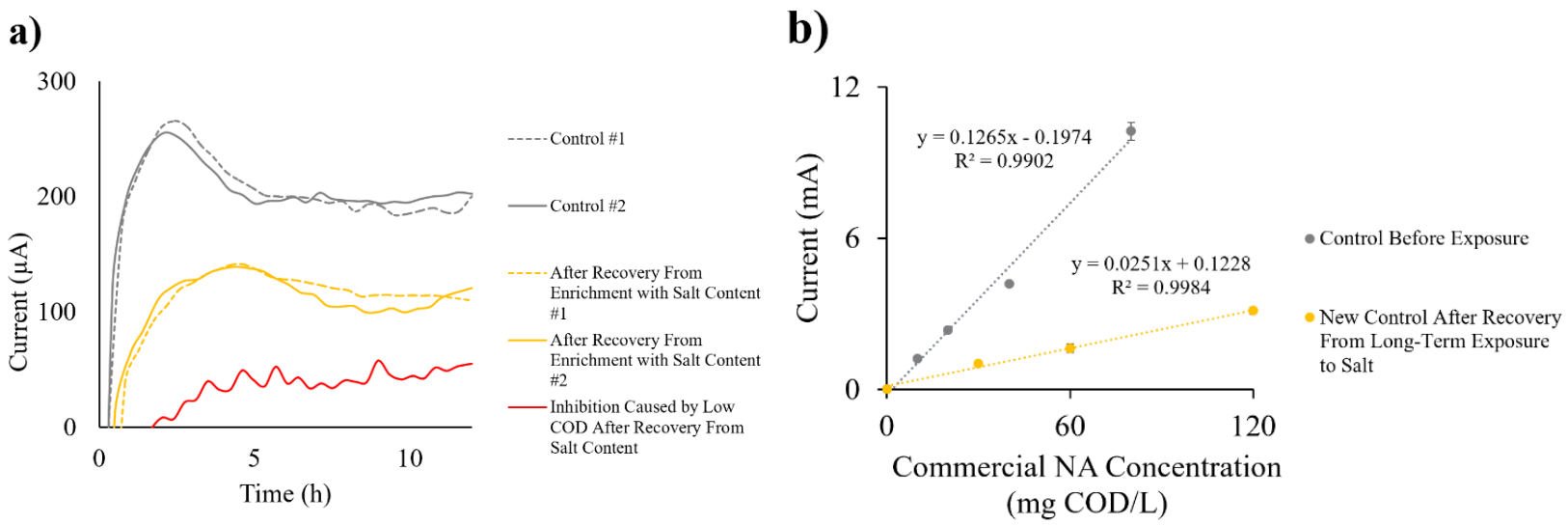

Figure 4-3. Results related to the recovery of MXC biosensor: a) recovery of MXC biosensor using 25 mM acetate; and b) a new control calibration curve after the recovery of the biosensor. A control curve before exposure to salinity was added for comparison.

As illustrated in Fig. 4-3a, 100% recovery of the MXC biosensor was not possible. The maximum current and the stable current before the long-term exposures to 1500 mg/L salt were 260.4±5.0 and 201.9±1.7 μA, respectively. However, after the recovery of the biosensor after long-term exposures to the salt content, both maximum current and stable current did not recover to the original state (140.0±1.0 and 120.7±1.0 μA, respectively). Additionally, the recovered MXC biosensor was further inhibited (red curve in Fig. 4-3a) when it was exposed to low COD concentrations (e.g., dosing <60 mg COD/L during the construction of a calibration curve in Fig. 4-3b). Furthermore, when the calibration curve was established after the recovery process, the sensitivity (e.g., current output) of the biosensor significantly dropped indicated by the decrease in the linear slope (the indication of current output) from 0.1265x to 0.0251x (Fig. 4-3b). The average transient peak currents were 1.02±0.02, 1.62±0.17, 3.14±0.14, and 6.13±0.15 mA for 30, 60, 120, and 240 mg COD/L after the recovery with acetate medium. Similar to the discussion in section 3.1, this finding indicated that the long-term exposures to a salt content could lead to irreversible inhibition of anode biofilm, and ultimately hindering the overall performance of the biosensor applied to the NA mixture. Therefore, the elimination of the salt content from the water matrix containing the NA mixture can potentially increase the sensitivity of the MXC biosensor. Also, looking into the analysis of microbial communities will be required to fully understand the reasons behind why the biosensor is hindered by long-term exposures to salt content.

4-3.2 Polycyclic aromatic hydrocarbons and their effects on current output

Fig. 4-4 illustrates the impact of different model PAH compounds on the MXC's current output (methodology is described in Fig. 4-1c). To only observe the effect of PAHs on the response of the biosensor applied for the detection of CNA, salt contents were not introduced in this experiment.

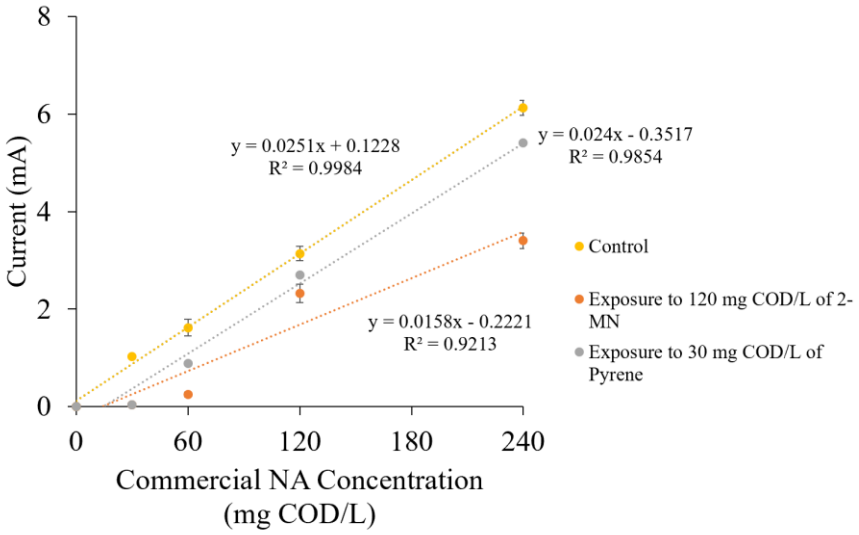

Figure 4-4. A graph illustrating the interference of model PAH compounds on the response of MXC biosensor operated with CNA as a carbon source.

Overall, both 2-MN and pyrene negatively impacted MXC biosensor's performance. Starting with 2-MN (120 mg COD/L), the average transient peak currents were 0.04±0, 0.25±0.05, 2.32±0.18, and 3.40±0.16 mA for 30, 60, 120, and 240 mg COD/L of CNA concentrations, respectively, which were significantly less than the transient peak currents produced from control environment. Especially, the biosensor was not able to produce high currents when <60 mg COD/L CNA was dosed. However, the biosensor was capable of producing reasonable current outputs at higher concentrations of CNA (>120 mg COD/L). Thus, the effect of adding 2-MN was more severe at lower concentrations. On the other hand, pyrene (soluble COD of 30 mg/L) had a less detrimental effect compared with the results from 2-MN. This is potentially due to the low solubility of pyrene in water, giving significantly lower COD concentrations. However, similar to 2-MN, the introduction of pyrene led to a decrease in the average transient peak currents (e.g., 0.03±0.0, 0.89±0.19, 2.70±0.24, and 5.40±0.38 for CNA concentrations of 30, 60, 120, and 240 mg COD/L).

Hence, both PAH model compounds can greatly interfere with the signal output of the NA-detecting MXC biosensor. To improve the performance of this MXC biosensor, higher charging times can potentially be utilized in the future to achieve higher sensitivity.

4-4. Conclusions

An MXC biosensor was proposed in this study to investigate the impact of salinity and PAHs in water samples containing a commercial naphthenic acid (CNA). Overall, the MXC biosensor operated using CNA as a carbon source under CD mode still showed a very strong linear relationship (R^2 = 0.99 – 0.998 for control, R^2 = 0.86 – 0.99) even with the interferences caused by salinity and PAHs. In contrast to our previous study (with a single model compound), introducing salinity along with a mixture of NAs led to a decrease in current output, which implies that the anodic biofilm was inhibited. In addition, long-term exposures (e.g., >10 batch cycles) to salt content can partially inhibit the anode biofilm, in which, the background currents (e.g., original current) cannot fully-recover to the original state even with the recovery. Hence, more in-depth and comprehensive analysis, such as microbial community analysis, is required to fully understand the effect of salinity on NA-detecting MXC biosensors operated with a mixture of complex NAs. The model PAH compounds (2-MN and pyrene) had a detrimental effect on MXC biosensor's response. Especially, fairly high PAH concentration (120 mg COD/L) can significantly reduce the biosensor's sensitivity and current output (e.g., from 1.02 to 0.04 mA for CNA concentration of 30 mg COD/L and from 6.13 to 3.40 for CNA concentration of 240 mg COD/L). Therefore, modification in the calibration method (e.g., increasing the charging time) is required to further increase the MXC biosensor's sensitivity during its operations with the NA mixture. Ultimately, the results obtained from this study demonstrated that with further improvements, the MXC

biosensor can be applied for NA mixture in OSPW. For further development, the detection of NAs in real OSPW, including a more in-depth and comprehensive study (e.g., microbial communities), will be examined in future research.

4-5. References

Adekunle, A. 2018. Development of an Autonomous Biobattery/biosensor System for Remote Applications, McGill University Libraries.

Allen, E.W. 2008. Process water treatment in Canada's oil sands industry: I. Target pollutants and treatment objectives. *Journal of Environmental Engineering and Science*, **7**(2), 123-138.

Arulazhagan, P., Vasudevan, N. 2011. Biodegradation of polycyclic aromatic hydrocarbons by a halotolerant bacterial strain Ochrobactrum sp. VA1. *Marine pollution bulletin*, **62**(2), 388-394.

Barrow, M.P., Peru, K.M., Fahlman, B., Hewitt, L.M., Frank, R.A., Headley, J.V. 2015. Beyond Naphthenic Acids: Environmental Screening of Water from Natural Sources and the Athabasca Oil Sands Industry Using Atmospheric Pressure Photoionization Fourier Transform Ion Cyclotron Resonance Mass Spectrometry. *J Am Soc Mass Spectrom*, **26**(9), 1508-21.

Choi, J., Liu, Y. 2014. Power generation and oil sands process-affected water treatment in microbial fuel cells. *Bioresource technology*, **169**, 581-587.

Chung, T.H., Meshref, M.N., Dhar, B.R. 2020. Microbial electrochemical biosensor for rapid detection of naphthenic acid in aqueous solution. *Journal of Electroanalytical Chemistry*, 114405.

Davila, D., Esquivel, J., Sabate, N., Mas, J. 2011. Silicon-based microfabricated microbial fuel cell toxicity sensor. *Biosensors and Bioelectronics*, **26**(5), 2426-2430.

Dhar, B.R., Gao, Y., Yeo, H., Lee, H.-S. 2013. Separation of competitive microorganisms using anaerobic membrane bioreactors as pretreatment to microbial electrochemical cells. *Bioresource technology*, **148**, 208-214.

Do, M.H., Ngo, H.H., Guo, W., Chang, S.W., Nguyen, D.D., Liu, Y., Varjani, S., Kumar, M. 2020. Microbial fuel cell-based biosensor for online monitoring wastewater quality: A critical review. *Science of the Total Environment*, **712**, 135612.

El-Din, M.G., Fu, H., Wang, N., Chelme-Ayala, P., Pérez-Estrada, L., Drzewicz, P., Martin, J.W., Zubot, W., Smith, D.W. 2011. Naphthenic acids speciation and removal during petroleum-coke adsorption and ozonation of oil sands process-affected water. *Science of the Total Environment*, **409**(23), 5119-5125.

Fennell, J., Arciszewski, T.J. 2019. Current knowledge of seepage from oil sands tailings ponds and its environmental influence in northeastern Alberta. *Science of the total environment*.

Folwell, B.D., McGenity, T.J., Price, A., Johnson, R.J., Whitby, C. 2016a. Exploring the capacity for anaerobic biodegradation of polycyclic aromatic hydrocarbons and naphthenic acids by microbes from oil-sands-process-affected waters. *International Biodeterioration & Biodegradation*, **108**, 214-221.

Folwell, B.D., McGenity, T.J., Whitby, C. 2016b. Biofilm and planktonic bacterial and fungal communities transforming high-molecular-weight polycyclic aromatic hydrocarbons. *Applied and environmental microbiology*, **82**(8), 2288-2299.

Fraiwan, A., Sundermier, S., Han, D., Steckl, A., Hassett, D., Choi, S. 2013. Enhanced Performance of Micro-Electro-Mechanical-Systems (MEMS) Microbial Fuel Cells Using Electrospun Microfibrous Anode and Optimizing Operation. *Fuel Cells*, **13**(3), 336-341.

Grattieri, M., Minteer, S.D. 2018. Microbial fuel cells in saline and hypersaline environments: advancements, challenges and future perspectives. *Bioelectrochemistry*, **120**, 127-137.
Headley, J.V., Peru, K.M., Barrow, M.P. 2016. Advances in mass spectrometric characterization of naphthenic acids fraction compounds in oil sands environmental samples and crude oil—a review. *Mass spectrometry reviews*, **35**(2), 311-328.
Huang, J., Sun, B., Zhang, X. 2010. Electricity generation at high ionic strength in microbial fuel cell by a newly isolated Shewanella marisflavi EP1. *Applied microbiology and biotechnology*, **85**(4), 1141-1149.
Jiang, Y., Ulrich, A.C., Liu, Y. 2013. Coupling bioelectricity generation and oil sands tailings treatment using microbial fuel cells. *Bioresource technology*, **139**, 349-354.
Jiang, Y., Yang, X., Liang, P., Liu, P., Huang, X. 2018. Microbial fuel cell sensors for water quality early warning systems: Fundamentals, signal resolution, optimization and future challenges. *Renewable and Sustainable Energy Reviews*, **81**, 292-305.
Kaur, A., Kim, J.R., Michie, I., Dinsdale, R.M., Guwy, A.J., Premier, G.C., Centre, S.E.R. 2013. Microbial fuel cell type biosensor for specific volatile fatty acids using acclimated bacterial communities. *Biosensors and Bioelectronics*, **47**, 50-55.
Labrada, G.V., Nemati, M. 2017. Microbial Fuel Cell Bioreactors for Treatment of Waters Contaminated by Naphthenic Acids. *Frontiers International Conference on Wastewater Treatment and Modelling*. Springer. pp. 303-307.
Leclair, L.A., Pohler, L., Wiseman, S.B., He, Y., Arens, C.J., Giesy, J.P., Scully, S., Wagner, B.D., van den Heuvel, M.R., Hogan, N.S. 2015. In vitro assessment of endocrine disrupting potential of naphthenic acid fractions derived from oil sands-influenced water. *Environmental science & technology*, **49**(9), 5743-5752.
Liu, H., Cheng, S., Logan, B.E. 2005. Power generation in fed-batch microbial fuel cells as a function of ionic strength, temperature, and reactor configuration. *Environmental science & technology*, **39**(14), 5488-5493.
Lovley, D.R., Nevin, K.P. 2011. A shift in the current: new applications and concepts for microbe-electrode electron exchange. *Current opinion in Biotechnology*, **22**(3), 441-448.
Mahaffey, A., Dubé, M. 2016. Review of the composition and toxicity of oil sands process-affected water. *Environmental Reviews*, **25**(1), 97-114.
Martin, J.W. 2015. The Challenge: Safe release and reintegration of oil sands process-affected water. *Environmental toxicology and chemistry*, **34**(12), 2682-2682.
McQueen, A.D., Kinley, C.M., Hendrikse, M., Gaspari, D.P., Calomeni, A.J., Iwinski, K.J., Castle, J.W., Haakensen, M.C., Peru, K.M., Headley, J.V., Rodgers, J.H., Jr. 2017. A risk-based approach for identifying constituents of concern in oil sands process-affected water from the Athabasca Oil Sands region. *Chemosphere*, **173**, 340-350.
Mille, Y., Beney, L., Gervais, P. 2002. Viability of Escherichia coli after combined osmotic and thermal treatment: a plasma membrane implication. *Biochimica et Biophysica Acta (BBA)-Biomembranes*, **1567**, 41-48.
Miller, L.G., Oremland, R.S. 2008. Electricity generation by anaerobic bacteria and anoxic sediments from hypersaline soda lakes. *Extremophiles*, **12**(6), 837-848.
Reinardy, H.C., Scarlett, A.G., Henry, T.B., West, C.E., Hewitt, L.M., Frank, R.A., Rowland, S.J. 2013. Aromatic naphthenic acids in oil sands process-affected water, resolved by

GCxGC-MS, only weakly induce the gene for vitellogenin production in zebrafish (Danio rerio) larvae. *Environmental science & technology*, **47**(12), 6614-6620.
Ripmeester, M.J., Duford, D.A. 2019. Method for routine "naphthenic acids fraction compounds" determination in oil sands process-affected water by liquid-liquid extraction in dichloromethane and Fourier-Transform Infrared Spectroscopy. *Chemosphere*, **233**, 687-696.
Ross, M.S., Pereira, A.d.S., Fennell, J., Davies, M., Johnson, J., Sliva, L., Martin, J.W. 2012. Quantitative and qualitative analysis of naphthenic acids in natural waters surrounding the Canadian oil sands industry. *Environmental science & technology*, **46**(23), 12796-12805.
Siddique, T., Fedorak, P.M., Foght, J.M. 2006. Biodegradation of short-chain n-alkanes in oil sands tailings under methanogenic conditions. *Environmental science & technology*, **40**(17), 5459-5464.
Sim, J., Reid, R., Hussain, A., Lee, H.-S. 2018. Semi-continuous measurement of oxygen demand in wastewater using biofilm-capacitance. *Bioresource Technology Reports*, **3**, 231-237.
Sun, J.-Z., Peter Kingori, G., Si, R.-W., Zhai, D.-D., Liao, Z.-H., Sun, D.-Z., Zheng, T., Yong, Y.-C. 2015. Microbial fuel cell-based biosensors for environmental monitoring: a review. *Water Science and Technology*, **71**(6), 801-809.
Tremouli, A., Martinos, M., Lyberatos, G. 2017. The effects of salinity, pH and temperature on the performance of a microbial fuel cell. *Waste and biomass valorization*, **8**(6), 2037-2043.
Wang, C., Klamerth, N., Messele, S.A., Singh, A., Belosevic, M., Gamal El-Din, M. 2016. Comparison of UV/hydrogen peroxide, potassium ferrate(VI), and ozone in oxidizing the organic fraction of oil sands process-affected water (OSPW). *Water Research*, **100**, 476-485.
Xiao, N., Wu, R., Huang, J.J., Selvaganapathy, P.R. 2020. Development of a xurographically fabricated miniaturized low-cost, high-performance microbial fuel cell and its application for sensing biological oxygen demand. *Sensors and Actuators B: Chemical*, **304**, 127432.
Yang, W., Wei, X., Fraiwan, A., Coogan, C.G., Lee, H., Choi, S. 2016. Fast and sensitive water quality assessment: a μL-scale microbial fuel cell-based biosensor integrated with an air-bubble trap and electrochemical sensing functionality. *Sensors and Actuators B: Chemical*, **226**, 191-195.
Yu, D., Bai, L., Zhai, J., Wang, Y., Dong, S. 2017. Toxicity detection in water containing heavy metal ions with a self-powered microbial fuel cell-based biosensor. *Talanta*, **168**, 210-216.
Zhang, Y. 2016. Development and application of Fenton and UV-Fenton processes at natural pH using chelating agents for the treatment of oil sands process-affected water.
Zhou, T., Han, H., Liu, P., Xiong, J., Tian, F., Li, X. 2017. Microbial fuels cell-based biosensor for toxicity detection: A review. *Sensors*, **17**(10), 2230.

Chapter 5 – Conclusions and Recommendations

5-1. Conclusions

Major findings and highlights from this thesis research are summarized below:

- Overall, the detection and monitoring of NAs using an MXC biosensor was accomplished in this thesis study. The applicability of MXC biosensor on NAs has been verified using both single and complex model compounds (CHA, commercial NAs).
- The charging-discharging operation was determined to be the optimal calibration method over the closed-circuit operation for the detection of CHA. Under the continuous closed-circuit operation of MXC biosensor, electrical responses (peak currents) were fairly proportional ($R^2 = 0.64$) to the CHA concentrations ranging from 50 to 250 mg COD/L. However, the charging-discharging operation of biosensor significantly increased the peak currents by 90–124 folds higher than that observed for continuous closed-circuit operation. Besides, a linear relationship between model NA concentrations and the peak currents ($R^2 = 0.96$) was observed.
- The biosensor would be sensitive to salinity levels and temperature changes. For CHA, lowering the temperature (from room temperature to 13.5 ℃) significantly decreased the current output (e.g., 24.31 ± 0.25 mA to 9.32 ± 0.04 mA). On the other hand, the current output increased with increasing the salinity levels. The salinity content was found to be more effective (e.g., more noticeable differences in the current output) in lower concentrations of CHA (e.g., 40 – 80 mg COD/L). However, once the biosensor is calibrated, it can be used for the measurement of model NA concentrations.

- The current produced from commercial NAs (mixtures of alkylated cyclopentane carboxylic acid) is generally lower than the current produced from CHA using a charging-discharging time of 6 min after a stable current period.
- Long-term exposures (e.g., >10 batch cycles) of the salt content (e.g., NaCl) led to a decrease in the background currents (e.g., peak and stable currents), which implies partial inhibition of anode biofilm. Also, the background currents were not recoverable (e.g., after >5 cycles) even with the addition of acetate. After the long exposure of salt content, the detection limit was narrowed (e.g., 20 – 40 mg COD/L), in which, the MXC biosensor was unable to provide sensitive monitoring of commercial NAs below 20 mg COD/L and above 40 mg COD/L.
- PAHs (e.g., pyrene and 2-methylnaphthalene) can also greatly interfere with the current output and decrease the performance of MXC biosensor applied to CNA detection.

5-2. Recommendations

The results of this study demonstrated that with further development, MXC biosensors could be used as a simple bioanalytical tool for monitoring NA concentrations in OSPW. However, several challenges and drawbacks still have to be addressed before implementing the biosensor for field measurement of NAs. The recommendations for future studies are as follows:

- The applicability of MXC biosensor on real OSPW must be verified using real OSPW. A complex water matrix of OSPW (e.g., presence of other organic and inorganic compounds) may greatly interfere with the current output produced by only NAs.

- Introducing the salt content in the anolyte can significantly increase the current output during the biosensor operation. On the other hand, it can be detrimental to the anode biofilm in a long term. Hence, introducing a microbial desalination cell (MDC) to eliminate the salt content and allow the biosensor to solely focus on the detection of NAs. Successful research studies of such will bring this biosensor a step forward towards field-scale application.
- A comprehensive analysis of microbial communities should be implemented to clearly understand the effects of environmental parameters (e.g., salinity) and why they positively or negatively influence the current output of the MXC biosensor.
- The current output as a single signal processing may limit its application to selective monitoring of NAs. For instance, a certain current output does not mean a certain type of NA species is detected. Hence, developing a method for selective monitoring in the MXC biosensor is great of interest.
- Increasing sensitivity with commercial NAs determination should also be revisited. For instance, utilizing higher charging time should be further investigated to increase the current output produced by commercial NAs.
- Developing a method to reduce the time to stabilize the current output (e.g., enhance the bio-oxidation of NAs). For instance, using readily-biodegradable organics, such as acetate to produce the background current output can be a viable option. However, a decrease in sensitivity can be a trade-off. In this way, the MXC biosensor can be operated under continuous flow mode, where the NA concentrations can be measured every few minutes (e.g., <5 minutes).

Bibliography

Abdalrhman, A.S., Ganiyu, S.O., El-Din, M.G. 2019. Degradation kinetics and structure-reactivity relation of naphthenic acids during anodic oxidation on graphite electrodes. *Chemical Engineering Journal*, **370**, 997-1007.

Adekunle, A. 2018. Development of an Autonomous Biobattery/biosensor System for Remote Applications, McGill University Libraries.

Adekunle, A., Raghavan, V., Tartakovsky, B. 2017. Carbon source and energy harvesting optimization in solid anolyte microbial fuel cells. *Journal of Power Sources*, **356**, 324-330.

Adekunle, A., Raghavan, V., Tartakovsky, B. 2019a. A comparison of microbial fuel cell and microbial electrolysis cell biosensors for real-time environmental monitoring. *Bioelectrochemistry*, **126**, 105-112.

Adekunle, A., Raghavan, V., Tartakovsky, B. 2019b. On-line monitoring of heavy metals-related toxicity with a microbial fuel cell biosensor. *Biosensors and Bioelectronics*, **132**, 382-390.

Adekunle, A., Raghavan, V., Tartakovsky, B. 2019c. Real-Time Performance Optimization and Diagnostics during Long-Term Operation of a Solid Anolyte Microbial Fuel Cell Biobattery. *Batteries*, **5**(1), 9.

Afzal, A., Drzewicz, P., Martin, J.W., El-Din, M.G. 2012. Decomposition of cyclohexanoic acid by the UV/H2O2 process under various conditions. *Science of the total environment*, **426**, 387-392.

Ahad, J.M., Macdonald, R., Parrot, J., Yang, Z., Zhang, Y., Siddique, T., Kuznetsova, A., Rauert, C., Galarneau, E., Studabaker, W. 2020. Polycyclic aromatic compounds (PACs) in the Canadian environment: A review of sampling techniques, strategies and instrumentation. *Environmental Pollution*, 114988.

Ahmad, I., Weng, J., Stromberg, A., Hilt, J., Dziubla, T. 2019. Fluorescence based detection of polychlorinated biphenyls (PCBs) in water using hydrophobic interactions. *Analyst*, **144**(2), 677-684.

Ahn, Y., Schröder, U. 2015. Microfabricated, continuous-flow, microbial three-electrode cell for potential toxicity detection. *BioChip Journal*, **9**(1), 27-34.

Ali, J., Wang, L., Waseem, H., Djellabi, R., Oladoja, N., Pan, G. 2020. FeS@ rGO nanocomposites as electrocatalysts for enhanced chromium removal and clean energy generation by microbial fuel cell. *Chemical Engineering Journal*, **384**, 123335.

Allen, E.W. 2008. Process water treatment in Canada's oil sands industry: I. Target pollutants and treatment objectives. *Journal of Environmental Engineering and Science*, **7**(2), 123-138.

Al-Mamun, A., Ahmad, W., Baawain, M.S., Khadem, M., Dhar, B.R. 2018. A review of microbial desalination cell technology: configurations, optimization and applications. *Journal of Cleaner Production*, **183**, 458-480.

Arana, T.J., Gude, V.G. 2018. A microbial desalination process with microalgae biocathode using sodium bicarbonate as an inorganic carbon source. *International biodeterioration & biodegradation*, **130**, 91-97.

Arulazhagan, P., Vasudevan, N. 2011. Biodegradation of polycyclic aromatic hydrocarbons by a halotolerant bacterial strain Ochrobactrum sp. VA1. *Marine pollution bulletin*, **62**(2), 388-394.

Ayyaru, S., Dharmalingam, S. 2014. Enhanced response of microbial fuel cell using sulfonated poly ether ether ketone membrane as a biochemical oxygen demand sensor. *Analytica chimica acta*, **818**, 15-22.

Barrow, M.P., Peru, K.M., Fahlman, B., Hewitt, L.M., Frank, R.A., Headley, J.V. 2015. Beyond Naphthenic Acids: Environmental Screening of Water from Natural Sources and the Athabasca Oil Sands Industry Using Atmospheric Pressure Photoionization Fourier Transform Ion Cyclotron Resonance Mass Spectrometry. *J Am Soc Mass Spectrom*, **26**(9), 1508-21.

Barua, S., Zakaria, B.S., Chung, T., Hai, F.I., Haile, T., Al-Mamun, A., Dhar, B.R. 2019. Microbial electrolysis followed by chemical precipitation for effective nutrients recovery from digested sludge centrate in WWTPs. *Chemical Engineering Journal*, **361**, 256-265.

Barua, S., Zakaria, B.S., Dhar, B.R. 2018a. Development of a self-powered biosensor for real-time monitoring of naphthenic acids. *Canada's Oil Sands Innovation Alliance (COSIA) Innovation Summit*, Calgary, AB, Canada.

Barua, S., Zakaria, B.S., Dhar, B.R. 2018b. Development of bioelectrochemical sensing device for naphthenic acids. *53rd Central Canadian Symposium on Water Quality Research*, Toronto, ON, Canada.

Bian, B., Shi, D., Cai, X., Hu, M., Guo, Q., Zhang, C., Wang, Q., Sun, A.X., Yang, J. 2018a. 3D printed porous carbon anode for enhanced power generation in microbial fuel cell. *Nano Energy*, **44**, 174-180.

Bian, B., Wang, C., Hu, M., Yang, Z., Cai, X., Shi, D., Yang, J. 2018b. Application of 3D printed porous copper anode in microbial fuel cells. *Frontiers in Energy Research*, **6**, 50.

Bilal, M., Iqbal, H.M., Barceló, D. 2019. Persistence of pesticides-based contaminants in the environment and their effective degradation using laccase-assisted biocatalytic systems. *Science of The Total Environment*, **695**, 133896.

Boon, N., Aelterman, P., Clauwaert, P., De Schamphelaire, L., Vanhaecke, L., De Maeyer, K., Höfte, M., Verstraete, W., Rabaey, K. 2008. Metabolites produced by Pseudomonas sp. enable a Gram-positive bacterium to achieve extracellular electron transfer. *Applied Microbiology and Biotechnology*, **77**(5), 1119-1129.

Bown, J., Bianchini, M., Ligthart, M., du Payrat, C.N., Whitmore, J. 1987. Methods of prevention, detection and control of spillages in west European oil pipelines. *Quarterly journal of technical papers*, **1**.

Brandão, Y., Teodosio, J., Dias, F., Eustáquio, W., Benachour, M. 2013. Treatment of phenolic effluents by a thermochemical oxidation process (DiCTT) and modelling by artificial neural networks. *Fuel*, **110**, 185-195.

Brown, D.M., Bonte, M., Gill, R., Dawick, J., Boogaard, P.J. 2017. Heavy hydrocarbon fate and transport in the environment. *Quarterly Journal of Engineering Geology and Hydrogeology*, **50**(3), 333-346.

Busca, G., Berardinelli, S., Resini, C., Arrighi, L. 2008. Technologies for the removal of phenol from fluid streams: a short review of recent developments. *Journal of Hazardous Materials*, **160**(2-3), 265-288.

Cai, W., Lesnik, K.L., Wade, M.J., Heidrich, E.S., Wang, Y., Liu, H. 2019. Incorporating microbial community data with machine learning techniques to predict feed substrates in microbial fuel cells. *Biosensors and Bioelectronics*, **133**, 64-71.

Camacho, J.V., Romero, L.R., Marchante, C.F., Morales, F.F., Rodrigo, M.R. 2017. The salinity effects on the performance of a constructed wetland-microbial fuel cell. *Ecological engineering*, **107**, 1-7.

Cao, X., Yu, C., Wang, H., Zhou, F., Li, X. 2017. Simultaneous degradation of refractory organic pesticide and bioelectricity generation in a soil microbial fuel cell with different conditions. *Environmental technology*, **38**(8), 1043-1050.

Catal, T., Kul, A., Atalay, V.E., Bermek, H., Ozilhan, S., Tarhan, N. 2019. Efficacy of microbial fuel cells for sensing of cocaine metabolites in urine-based wastewater. *Journal of Power Sources*, **414**, 1-7.

Chauhan, A., Chakraborti, A.K., Jain, R.K. 2000. Plasmid-encoded degradation of p-nitrophenol and 4-nitrocatechol by Arthrobacter protophormiae. *Biochemical and biophysical research communications*, **270**(3), 733-740.

Chen, Z., Niu, Y., Zhao, S., Khan, A., Ling, Z., Chen, Y., Liu, P., Li, X. 2016. A novel biosensor for p-nitrophenol based on an aerobic anode microbial fuel cell. *Biosensors and Bioelectronics*, **85**, 860-868.

Cheng, M., Zeng, G., Huang, D., Lai, C., Xu, P., Zhang, C., Liu, Y. 2016. Hydroxyl radicals based advanced oxidation processes (AOPs) for remediation of soils contaminated with organic compounds: a review. *Chemical Engineering Journal*, **284**, 582-598.

Choi, J., Liu, Y. 2014. Power generation and oil sands process-affected water treatment in microbial fuel cells. *Bioresource technology*, **169**, 581-587.

Chouler, J., Cruz-Izquierdo, A., Rengaraj, S., Scott, J.L., Di Lorenzo, M. 2018. A screen-printed paper microbial fuel cell biosensor for detection of toxic compounds in water. *Biosensors and Bioelectronics*, **102**, 49-56.

Chouler, J., Di Lorenzo, M. 2019. Pesticide detection by a miniature microbial fuel cell under controlled operational disturbances. *Water Science and Technology*, **79**(12), 2231-2241.

Chu, N., Liang, Q., Hao, W., Jiang, Y., Liang, P., Zeng, R.J. 2020. Microbial electrochemical sensor for water biotoxicity monitoring. *Chemical Engineering Journal*, 127053.

Chung, T.H., Meshref, M.N., Dhar, B.R. 2020a. Microbial electrochemical biosensor for rapid detection of naphthenic acid in aqueous solution. *Journal of Electroanalytical Chemistry*, 114405.

Chung, T.H., Meshref, M.N., Hai, F.I., Al-Mamun, A., Dhar, B.R. 2020b. Microbial electrochemical systems for hydrogen peroxide synthesis: Critical review of process optimization, prospective environmental applications, and challenges. *Bioresource Technology*, 123727.

Colantonio, N., Kim, Y. 2016. Cadmium (II) removal mechanisms in microbial electrolysis cells. *Journal of hazardous materials*, **311**, 134-141.

Daghio, M., Tofalos, A.E., Leoni, B., Cristiani, P., Papacchini, M., Jalilnejad, E., Bestetti, G., Franzetti, A. 2018. Bioelectrochemical BTEX removal at different voltages: assessment of the degradation and characterization of the microbial communities. *Journal of hazardous materials*, **341**, 120-127.

Dai, Z., Xu, Z., Wang, T., Fan, Y., Liu, Y., Yu, R., Zhu, G., Lu, X., Li, B. 2019. In-situ oil presence sensor using simple-structured upward open-channel microbial fuel cell (UOC-MFC). *Biosensors and Bioelectronics: X*, **1**, 100014.

Davila, D., Esquivel, J., Sabate, N., Mas, J. 2011. Silicon-based microfabricated microbial fuel cell toxicity sensor. *Biosensors and Bioelectronics*, **26**(5), 2426-2430.

de Ramón-Fernández, A., Salar-García, M., Fernández, D.R., Greenman, J., Ieropoulos, I. 2020. Evaluation of artificial neural network algorithms for predicting the effect of the urine flow rate on the power performance of microbial fuel cells. *Energy*, **213**, 118806.

Dhar, B.R., Gao, Y., Yeo, H., Lee, H.-S. 2013. Separation of competitive microorganisms using anaerobic membrane bioreactors as pretreatment to microbial electrochemical cells. *Bioresource technology*, **148**, 208-214.

Dhar, B.R., Ryu, H., Santo Domingo, J.W., Lee, H.-S. 2016. Ohmic resistance affects microbial community and electrochemical kinetics in a multi-anode microbial electrochemical cell. *Journal of Power Sources*, **331**, 315-321.

Dhar, B.R., Sim, J., Ryu, H., Ren, H., Santo Domingo, J.W., Chae, J., Lee, H.-S. 2017. Microbial activity influences electrical conductivity of biofilm anode. *Water research*, **127**, 230-238.

Di Lorenzo, M., Thomson, A.R., Schneider, K., Cameron, P.J., Ieropoulos, I. 2014. A small-scale air-cathode microbial fuel cell for on-line monitoring of water quality. *Biosensors and Bioelectronics*, **62**, 182-188.

Do, M.H., Ngo, H.H., Guo, W., Chang, S.W., Nguyen, D.D., Liu, Y., Varjani, S., Kumar, M. 2020. Microbial fuel cell-based biosensor for online monitoring wastewater quality: A critical review. *Science of the Total Environment*, **712**, 135612.

Drzewicz, P., Perez-Estrada, L., Alpatova, A., Martin, J.W., Gamal El-Din, M. 2012. Impact of peroxydisulfate in the presence of zero valent iron on the oxidation of cyclohexanoic acid and naphthenic acids from oil sands process-affected water. *Environmental science & technology*, **46**(16), 8984-8991.

El-Din, M.G., Fu, H., Wang, N., Chelme-Ayala, P., Pérez-Estrada, L., Drzewicz, P., Martin, J.W., Zubot, W., Smith, D.W. 2011. Naphthenic acids speciation and removal during petroleum-coke adsorption and ozonation of oil sands process-affected water. *Science of the Total Environment*, **409**(23), 5119-5125.

Feng, Y., Barr, W., Harper Jr, W. 2013a. Neural network processing of microbial fuel cell signals for the identification of chemicals present in water. *Journal of environmental management*, **120**, 84-92.

Feng, Y., Harper Jr, W.F. 2013b. Biosensing with microbial fuel cells and artificial neural networks: laboratory and field investigations. *Journal of environmental management*, **130**, 369-374.

Fennell, J., Arciszewski, T.J. 2019. Current knowledge of seepage from oil sands tailings ponds and its environmental influence in northeastern Alberta. *Science of the total environment*.

Fingas, M. 2016. *Oil spill science and technology*. Gulf professional publishing.

Fingas, M., Brown, C. 2005. An update on oil spill remote sensors. *Proc. 28th Arctic and Marine Oil Spill Program (AMOP) Tech. Seminar*. pp. 7-9.

Fingas, M., Brown, C. 2014. Review of oil spill remote sensing. *Marine pollution bulletin*, **83**(1), 9-23.

Folwell, B.D., McGenity, T.J., Price, A., Johnson, R.J., Whitby, C. 2016a. Exploring the capacity for anaerobic biodegradation of polycyclic aromatic hydrocarbons and naphthenic acids by microbes from oil-sands-process-affected waters. *International Biodeterioration & Biodegradation*, **108**, 214-221.

Folwell, B.D., McGenity, T.J., Whitby, C. 2016b. Biofilm and planktonic bacterial and fungal communities transforming high-molecular-weight polycyclic aromatic hydrocarbons. *Applied and environmental microbiology*, **82**(8), 2288-2299.

Fraiwan, A., Sundermier, S., Han, D., Steckl, A., Hassett, D., Choi, S. 2013. Enhanced Performance of Micro-Electro-Mechanical-Systems (MEMS) Microbial Fuel Cells Using Electrospun Microfibrous Anode and Optimizing Operation. *Fuel Cells*, **13**(3), 336-341.

Freyman, M.C., Kou, T., Wang, S., Li, Y. 2020. 3D printing of living bacteria electrode. *Nano Research*, **13**(5), 1318-1323.

Friman, H., Schechter, A., Nitzan, Y., Cahan, R. 2012. Effect of external voltage on Pseudomonas putida F1 in a bio electrochemical cell using toluene as sole carbon and energy source. *Microbiology*, **158**(2), 414-423.

Gami, A., Shukor, M., Khalil, K.A., Dahalan, F., Khalid, A., Ahmad, S. 2014. Phenol and its toxicity. *Journal of Environmental Microbiology and Toxicology*, **2**(1), 11-24.

Gao, Y., Ryu, H., Rittmann, B.E., Hussain, A., Lee, H.-S. 2017. Quantification of the methane concentration using anaerobic oxidation of methane coupled to extracellular electron transfer. *Bioresource technology*, **241**, 979-984.

García-Mancha, N., Monsalvo, V., Puyol, D., Rodriguez, J., Mohedano, A. 2017. Enhanced anaerobic degradability of highly polluted pesticides-bearing wastewater under thermophilic conditions. *Journal of hazardous materials*, **339**, 320-329.

Geed, S., Shrirame, B., Singh, R., Rai, B. 2017. Assessment of pesticides removal using two-stage Integrated Aerobic Treatment Plant (IATP) by Bacillus sp. isolated from agricultural field. *Bioresource technology*, **242**, 45-54.

Gmurek, M., Olak-Kucharczyk, M., Ledakowicz, S. 2017. Photochemical decomposition of endocrine disrupting compounds–A review. *Chemical Engineering Journal*, **310**, 437-456.

Goering, R., Bowman, C., Koval, C., Noble, R., Ashley, M. 2000. Complexation structure and transport mechanism of 1, 5-hexadiene and 1-hexene through silver facilitated transport membranes. *Journal of Membrane Science*, **172**(1-2), 49-57.

Gonçalves-Filho, D., Silva, C.C.G., De Souza, D. 2020. Pesticides determination in foods and natural waters using solid amalgam-based electrodes: challenges and trends. *Talanta*, **212**, 120756.

Grattieri, M., Minteer, S.D. 2018. Microbial fuel cells in saline and hypersaline environments: advancements, challenges and future perspectives. *Bioelectrochemistry*, **120**, 127-137.

Guo, F., Liu, H. 2020. Impact of heterotrophic denitrification on BOD detection of the nitrate-containing wastewater using microbial fuel cell-based biosensors. *Chemical Engineering Journal*, 125042.

Han, X., Scott, A.C., Fedorak, P.M., Bataineh, M., Martin, J.W. 2008. Influence of molecular structure on the biodegradability of naphthenic acids. *Environmental science & technology*, **42**(4), 1290-1295.

Headley, J.V., Peru, K.M., Barrow, M.P. 2016. Advances in mass spectrometric characterization of naphthenic acids fraction compounds in oil sands environmental samples and crude oil—a review. *Mass spectrometry reviews*, **35**(2), 311-328.

Heidrich, E.S., Edwards, S.R., Dolfing, J., Cotterill, S.E., Curtis, T.P. 2014. Performance of a pilot scale microbial electrolysis cell fed on domestic wastewater at ambient temperatures for a 12 month period. *Bioresource technology*, **173**, 87-95.

Hennebel, T., Benner, J., Clauwaert, P., Vanhaecke, L., Aelterman, P., Callebaut, R., Boon, N., Verstraete, W. 2011. Dehalogenation of environmental pollutants in microbial electrolysis cells with biogenic palladium nanoparticles. *Biotechnology letters*, **33**(1), 89-95.

Huang, J., Sun, B., Zhang, X. 2010. Electricity generation at high ionic strength in microbial fuel cell by a newly isolated Shewanella marisflavi EP1. *Applied microbiology and biotechnology*, **85**(4), 1141-1149.

Huang, Q., Liu, Y., Dhar, B.R. 2020. A critical review of microbial electrolysis cells coupled with anaerobic digester for enhanced biomethane recovery from high-strength feedstocks. *Critical Reviews in Environmental Science and Technology*, 1-40.

Jaeel, A.J., Al-wared, A.I., Ismail, Z.Z. 2016. Prediction of sustainable electricity generation in microbial fuel cell by neural network: effect of anode angle with respect to flow direction. *Journal of Electroanalytical Chemistry*, **767**, 56-62.

Jafary, T., Al-Mamun, A., Alhimali, H., Baawain, M.S., Rahman, M.S., Rahman, S., Dhar, B.R., Aghbashlo, M., Tabatabaei, M. 2020. Enhanced power generation and desalination rate in a novel quadruple microbial desalination cell with a single desalination chamber. *Renewable and Sustainable Energy Reviews*, **127**, 109855.

Jafary, T., Daud, W.R.W., Ghasemi, M., Kim, B.H., Jahim, J.M., Ismail, M., Lim, S.S. 2015. Biocathode in microbial electrolysis cell; present status and future prospects. *Renewable and Sustainable Energy Reviews*, **47**, 23-33.

Jannelli, N., Nastro, R.A., Cigolotti, V., Minutillo, M., Falcucci, G. 2017. Low pH, high salinity: Too much for microbial fuel cells? *Applied energy*, **192**, 543-550.

Jensen, B.K., Arvin, E., Gundersen, A.T. 1988. Biodegradation of nitrogen-and oxygen-containing aromatic compounds in groundwater from an oil-contaminated aquifer. *Journal of contaminant hydrology*, **3**(1), 65-75.

Jha, M.N., Levy, J., Gao, Y. 2008. Advances in remote sensing for oil spill disaster management: state-of-the-art sensors technology for oil spill surveillance. *Sensors*, **8**(1), 236-255.

Jia, H., Yang, G., Ngo, H.-H., Guo, W., Zhang, H., Gao, F., Wang, J. 2017. Enhancing simultaneous response and amplification of biosensor in microbial fuel cell-based upflow anaerobic sludge bed reactor supplemented with zero-valent iron. *Chemical Engineering Journal*, **327**, 1117-1127.

Jiang, Y., Liang, P., Huang, X., Ren, Z.J. 2018a. A novel microbial fuel cell sensor with a gas diffusion biocathode sensing element for water and air quality monitoring. *Chemosphere*, **203**, 21-25.

Jiang, Y., Liang, P., Liu, P., Miao, B., Bian, Y., Zhang, H., Huang, X. 2017a. Enhancement of the sensitivity of a microbial fuel cell sensor by transient-state operation. *Environmental Science: Water Research & Technology*, **3**(3), 472-479.

Jiang, Y., Liang, P., Liu, P., Wang, D., Miao, B., Huang, X. 2017b. A novel microbial fuel cell sensor with biocathode sensing element. *Biosens Bioelectron*, **94**, 344-350.
Jiang, Y., Liang, P., Liu, P., Yan, X., Bian, Y., Huang, X. 2017c. A cathode-shared microbial fuel cell sensor array for water alert system. *International Journal of Hydrogen Energy*, **42**(7), 4342-4348.
Jiang, Y., Liang, P., Zhang, C., Bian, Y., Yang, X., Huang, X., Girguis, P.R. 2015. Enhancing the response of microbial fuel cell based toxicity sensors to Cu(II) with the applying of flow-through electrodes and controlled anode potentials. *Bioresour Technol*, **190**, 367-72.
Jiang, Y., Su, M., Li, D. 2014. Removal of sulfide and production of methane from carbon dioxide in microbial fuel cells–microbial electrolysis cell (MFCs–MEC) coupled system. *Applied biochemistry and biotechnology*, **172**(5), 2720-2731.
Jiang, Y., Ulrich, A.C., Liu, Y. 2013. Coupling bioelectricity generation and oil sands tailings treatment using microbial fuel cells. *Bioresource technology*, **139**, 349-354.
Jiang, Y., Yang, X., Liang, P., Liu, P., Huang, X. 2018. Microbial fuel cell sensors for water quality early warning systems: Fundamentals, signal resolution, optimization and future challenges. *Renewable and Sustainable Energy Reviews*, **81**, 292-305.
Jin, X., Angelidaki, I., Zhang, Y. 2016. Microbial Electrochemical Monitoring of Volatile Fatty Acids during Anaerobic Digestion. *Environ Sci Technol*, **50**(8), 4422-9.
Jin, X., Li, X., Zhao, N., Angelidaki, I., Zhang, Y. 2017. Bio-electrolytic sensor for rapid monitoring of volatile fatty acids in anaerobic digestion process. *Water research*, **111**, 74-80.
Jun, L.Y., Yon, L.S., Mubarak, N., Bing, C.H., Pan, S., Danquah, M.K., Abdullah, E., Khalid, M. 2019. An overview of immobilized enzyme technologies for dye and phenolic removal from wastewater. *Journal of Environmental Chemical Engineering*, **7**(2), 102961.
Kaur, A., Kim, J.R., Michie, I., Dinsdale, R.M., Guwy, A.J., Premier, G.C., Centre, S.E.R. 2013. Microbial fuel cell type biosensor for specific volatile fatty acids using acclimated bacterial communities. *Biosensors and Bioelectronics*, **47**, 50-55.
Kaur, A., Kim, J.R., Michie, I., Dinsdale, R.M., Guwy, A.J., Premier, G.C., Centre, S.E.R. 2013. Microbial fuel cell type biosensor for specific volatile fatty acids using acclimated bacterial communities. *Biosensors and Bioelectronics*, **47**, 50-55.
Khan, A., Salama, E.-S., Chen, Z., Ni, H., Zhao, S., Zhou, T., Pei, Y., Sani, R.K., Ling, Z., Liu, P. 2020. A novel biosensor for zinc detection based on microbial fuel cell system. *Biosensors and Bioelectronics*, **147**, 111763.
Kim, J., Kim, H., Kim, B., Yu, J. 2014. Computational fluid dynamics analysis in microbial fuel cells with different anode configurations. *Water science and technology*, **69**(7), 1447-1452.
Kim, M., Hyun, M.S., Gadd, G.M., Kim, H.J. 2007. A novel biomonitoring system using microbial fuel cells. *Journal of environmental monitoring*, **9**(12), 1323-1328.
Kokabian, B., Gude, V.G., Smith, R., Brooks, J.P. 2018. Evaluation of anammox biocathode in microbial desalination and wastewater treatment. *Chemical Engineering Journal*, **342**, 410-419.
Kumlanghan, A., Liu, J., Thavarungkul, P., Kanatharana, P., Mattiasson, B. 2007. Microbial fuel cell-based biosensor for fast analysis of biodegradable organic matter. *Biosensors and bioelectronics*, **22**(12), 2939-2944.

Labrada, G.V., Nemati, M. 2017. Microbial Fuel Cell Bioreactors for Treatment of Waters Contaminated by Naphthenic Acids. *Frontiers International Conference on Wastewater Treatment and Modelling*. Springer. pp. 303-307.

Larrosa-Guerrero, A., Scott, K., Head, I., Mateo, F., Ginesta, A., Godinez, C. 2010. Effect of temperature on the performance of microbial fuel cells. *Fuel*, **89**(12), 3985-3994.

Lazzarini Behrmann, I.C., Grattieri, M., Minteer, S.D., Ramirez, S.A., Vullo, D.L. 2020. Online self-powered Cr (VI) monitoring with autochthonous Pseudomonas and a bio-inspired redox polymer. *Analytical and Bioanalytical Chemistry*, 1-9.

Leclair, L.A., Pohler, L., Wiseman, S.B., He, Y., Arens, C.J., Giesy, J.P., Scully, S., Wagner, B.D., van den Heuvel, M.R., Hogan, N.S. 2015. In vitro assessment of endocrine disrupting potential of naphthenic acid fractions derived from oil sands-influenced water. *Environmental science & technology*, **49**(9), 5743-5752.

Lefebvre, O., Tan, Z., Kharkwal, S., Ng, H.Y. 2012. Effect of increasing anodic NaCl concentration on microbial fuel cell performance. *Bioresource Technology*, **112**, 336-340.

Lesnik, K.L., Liu, H. 2017. Predicting microbial fuel cell biofilm communities and bioreactor performance using artificial neural networks. *Environmental science & technology*, **51**(18), 10881-10892.

Li, F., Zheng, Z., Yang, B., Zhang, X., Li, Z., Lei, L. 2016. A laminar-flow based microfluidic microbial three-electrode cell for biosensing. *Electrochimica Acta*, **199**, 45-50.

Li, J., Hu, J., Yang, C., Pu, W., Hou, H., Xu, J., Liu, B., Yang, J. 2019. Enhanced detection of toxicity in wastewater using a 2D smooth anode based microbial fuel cell toxicity sensor. *RSC advances*, **9**(15), 8700-8706.

Li, L., Sun, Y., Yuan, Z., Kong, X., Li, Y. 2013. Effect of temperature change on power generation of microbial fuel cell. *Environmental technology*, **34**(13-14), 1929-1934.

Liang, P., Duan, R., Jiang, Y., Zhang, X., Qiu, Y., Huang, X. 2018. One-year operation of 1000-L modularized microbial fuel cell for municipal wastewater treatment. *Water research*, **141**, 1-8.

Liao, C., Wu, J., Zhou, L., Li, T., Du, Q., An, J., Li, N., Wang, X. 2018. Optimal set of electrode potential enhances the toxicity response of biocathode to formaldehyde. *Sci Total Environ*, **644**, 1485-1492.

Lin, S., Lu, Y., Ye, B., Zeng, C., Liu, G., Li, J., Luo, H., Zhang, R. 2020b. Pesticide wastewater treatment using the combination of the microbial electrolysis desalination and chemical-production cell and Fenton process. *Frontiers of Environmental Science & Engineering*, **14**(1), 12.

Liu, B., Lei, Y., Li, B. 2014. A batch-mode cube microbial fuel cell based "shock" biosensor for wastewater quality monitoring. *Biosens Bioelectron*, **62**, 308-14.

Liu, B., Zhai, H., Liang, Y., Ji, M., Wang, R. 2019. Increased power production and removal efficiency of polycyclic aromatic hydrocarbons by plant pumps in sediment microbial electrochemical systems: A preliminary study. *Journal of hazardous materials*, **380**, 120896.

Liu, C., Thompson, J.A., Bau, H.H. 2011a. A membrane-based, high-efficiency, microfluidic debubbler. *Lab on a Chip*, **11**(9), 1688-1693.

Liu, H., Cheng, S., Logan, B.E. 2005. Power generation in fed-batch microbial fuel cells as a function of ionic strength, temperature, and reactor configuration. *Environmental science & technology*, **39**(14), 5488-5493.
Liu, Z., Liu, J., Zhang, S., Xing, X.-H., Su, Z. 2011b. Microbial fuel cell based biosensor for in situ monitoring of anaerobic digestion process. *Bioresource technology*, **102**(22), 10221-10229.
Logan, B.E. 2008. *Microbial fuel cells*. John Wiley & Sons.
Logan, B.E., Call, D., Cheng, S., Hamelers, H.V., Sleutels, T.H., Jeremiasse, A.W., Rozendal, R.A. 2008. Microbial electrolysis cells for high yield hydrogen gas production from organic matter. *Environmental science & technology*, **42**(23), 8630-8640.
Logan, B.E., Wallack, M.J., Kim, K.-Y., He, W., Feng, Y., Saikaly, P.E. 2015. Assessment of microbial fuel cell configurations and power densities. *Environmental Science & Technology Letters*, **2**(8), 206-214.
López-Hincapié, J.D., Picos-Benítez, A.R., Cercado, B., Rodríguez, F., Rodríguez-García, A. 2020. Improving the configuration and architecture of a small-scale air-cathode single chamber microbial fuel cell (MFC) for biosensing organic matter in wastewater samples. *Journal of Water Process Engineering*, **38**, 101671.
Lovley, D.R., Nevin, K.P. 2011. A shift in the current: new applications and concepts for microbe-electrode electron exchange. *Current opinion in Biotechnology*, **22**(3), 441-448.
Mahaffey, A., Dubé, M. 2016. Review of the composition and toxicity of oil sands process-affected water. *Environmental Reviews*, **25**(1), 97-114.
Martin, J.W. 2015. The Challenge: Safe release and reintegration of oil sands process-affected water. *Environmental toxicology and chemistry*, **34**(12), 2682-2682.
Maruthupandy, M., Anand, M., Maduraiveeran, G., Beevi, A.S.H., Priya, R.J. 2015. Electrical conductivity measurements of bacterial nanowires from Pseudomonas aeruginosa. *Advances in Natural Sciences: Nanoscience and Nanotechnology*, **6**(4), 045007.
Massaglia, G., Gerosa, M., Agostino, V., Cingolani, A., Sacco, A., Saracco, G., Margaria, V., Quaglio, M. 2017. Fluid dynamic modeling for microbial fuel cell based biosensor optimization. *Fuel Cells*, **17**(5), 627-634.
Mei, X., Xing, D., Yang, Y., Liu, Q., Zhou, H., Guo, C., Ren, N. 2017. Adaptation of microbial community of the anode biofilm in microbial fuel cells to temperature. *Bioelectrochemistry*, **117**, 29-33.
Menzie, C.A., Potocki, B.B., Santodonato, J. 1992. Exposure to carcinogenic PAHs in the environment. *Environmental science & technology*, **26**(7), 1278-1284.
Mille, Y., Beney, L., Gervais, P. 2002. Viability of Escherichia coli after combined osmotic and thermal treatment: a plasma membrane implication. *Biochimica et Biophysica Acta (BBA)-Biomembranes*, **1567**, 41-48.
Miller, L.G., Oremland, R.S. 2008. Electricity generation by anaerobic bacteria and anoxic sediments from hypersaline soda lakes. *Extremophiles*, **12**(6), 837-848.
Modin, O., Wilén, B.-M. 2012. A novel bioelectrochemical BOD sensor operating with voltage input. *Water research*, **46**(18), 6113-6120.
Moon, H., Chang, I.S., Kang, K.H., Jang, J.K., Kim, B.H. 2004. Improving the dynamic response of a mediator-less microbial fuel cell as a biochemical oxygen demand (BOD) sensor. *Biotechnology letters*, **26**(22), 1717-1721.

Morris, J.M., Jin, S., Crimi, B., Pruden, A. 2009. Microbial fuel cell in enhancing anaerobic biodegradation of diesel. *Chemical Engineering Journal*, **146**(2), 161-167.
Mossmark, F., Hultberg, H., Ericsson, L.O. 2008. Recovery from groundwater extraction in a small catchment area with crystalline bedrock and thin soil cover in Sweden. *Science of the total environment*, **404**(2-3), 253-261.
Na, C.-J., Yoo, M.-J., Tsang, D.C., Kim, H.W., Kim, K.-H. 2019. High-performance materials for effective sorptive removal of formaldehyde in air. *Journal of hazardous materials*, **366**, 452-465.
Nandimandalam, H., Gude, V.G. 2019. Indigenous biosensors for in situ hydrocarbon detection in aquatic environments. *Marine Pollution Bulletin*, **149**, 110643.
Nikhil, B., Pawan, J., Nello, F., Pedro, E. 2016. Introduction to biosensors. *Essays in Biochemistry*, **60**(1), 1-8.
Palma, E., Daghio, M., Tofalos, A.E., Franzetti, A., Viggi, C.C., Fazi, S., Papini, M.P., Aulenta, F. 2018. Anaerobic electrogenic oxidation of toluene in a continuous-flow bioelectrochemical reactor: Process performance, microbial community analysis, and biodegradation pathways. *Environmental Science: Water Research & Technology*, **4**(12), 2136-2145.
Patil, S., Harnisch, F., Schröder, U. 2010. Toxicity response of electroactive microbial biofilms—a decisive feature for potential biosensor and power source applications. *ChemPhysChem*, **11**(13), 2834-2837.
Peixoto, L., Min, B., Martins, G., Brito, A.G., Kroff, P., Parpot, P., Angelidaki, I., Nogueira, R. 2011. In situ microbial fuel cell-based biosensor for organic carbon. *Bioelectrochemistry*, **81**(2), 99-103.
Peres, L.C., Trapido, E., Rung, A.L., Harrington, D.J., Oral, E., Fang, Z., Fontham, E., Peters, E.S. 2016. The deepwater horizon oil spill and physical health among adult women in Southern Louisiana: the women and their children's health (WaTCH) study. *Environmental health perspectives*, **124**(8), 1208-1213.
Philamore, H., Rossiter, J., Walters, P., Winfield, J., Ieropoulos, I. 2015. Cast and 3D printed ion exchange membranes for monolithic microbial fuel cell fabrication. *Journal of Power Sources*, **289**, 91-99.
Pouliot, R., Rochefort, L., Graf, M.D. 2013. Fen mosses can tolerate some saline conditions found in oil sands process water. *Environmental and experimental botany*, **89**, 44-50.
Prévoteau, A., Clauwaert, P., Kerckhof, F.-M., Rabaey, K. 2019. Oxygen-reducing microbial cathodes monitoring toxic shocks in tap water. *Biosensors and Bioelectronics*, **132**, 115-121.
Pv, H., Sj, W., de Solla, S., Ja, H., Slj, H., Jl, P., Pj, T., Berthiaume, A., Langlois, V. 2020. Polycyclic aromatic compounds (PACs) in the Canadian environment: The challenges of ecological risk assessments. *Environmental Pollution*, 115165.
Qi, X., Liu, P., Liang, P., Hao, W., Li, M., Huang, X. 2019. Dual-signal-biosensor based on luminescent bacteria biofilm for real-time online alert of Cu (II) shock. *Biosensors and Bioelectronics*, **142**, 111500.
Rasmussen, M., Minteer, S.D. 2015. Long-term arsenic monitoring with an Enterobacter cloacae microbial fuel cell. *Bioelectrochemistry*, **106**, 207-212.

Raut, N., O'Connor, G., Pasini, P., Daunert, S. 2012. Engineered cells as biosensing systems in biomedical analysis. *Analytical and bioanalytical chemistry*, **402**(10), 3147-3159.

Raza, W., Lee, J., Raza, N., Luo, Y., Kim, K.-H., Yang, J. 2019. Removal of phenolic compounds from industrial waste water based on membrane-based technologies. *Journal of industrial and engineering chemistry*, **71**, 1-18.

Reddy, A.V.B., Moniruzzaman, M., Aminabhavi, T.M. 2019. Polychlorinated biphenyls (PCBs) in the environment: Recent updates on sampling, pretreatment, cleanup technologies and their analysis. *Chemical Engineering Journal*, **358**, 1186-1207.

Reinardy, H.C., Scarlett, A.G., Henry, T.B., West, C.E., Hewitt, L.M., Frank, R.A., Rowland, S.J. 2013. Aromatic naphthenic acids in oil sands process-affected water, resolved by GCxGC-MS, only weakly induce the gene for vitellogenin production in zebrafish (Danio rerio) larvae. *Environmental science & technology*, **47**(12), 6614-6620.

Ripmeester, M.J., Duford, D.A. 2019. Method for routine "naphthenic acids fraction compounds" determination in oil sands process-affected water by liquid-liquid extraction in dichloromethane and Fourier-Transform Infrared Spectroscopy. *Chemosphere*, **233**, 687-696.

Ross, M.S., Pereira, A.d.S., Fennell, J., Davies, M., Johnson, J., Sliva, L., Martin, J.W. 2012. Quantitative and qualitative analysis of naphthenic acids in natural waters surrounding the Canadian oil sands industry. *Environmental science & technology*, **46**(23), 12796-12805.

Rousseau, R., Etcheverry, L., Roubaud, E., Basséguy, R., Délia, M.-L., Bergel, A. 2020. Microbial electrolysis cell (MEC): Strengths, weaknesses and research needs from electrochemical engineering standpoint. *Applied Energy*, **257**, 113938.

Rozendal, R.A., Leone, E., Keller, J., Rabaey, K. 2009. Efficient hydrogen peroxide generation from organic matter in a bioelectrochemical system. *Electrochemistry Communications*, **11**(9), 1752-1755.

Ruiz, Y., Ribot-Llobet, E., Baeza, J.A., Guisasola, A. 2015. Conditions for high resistance to starvation periods in bioelectrochemical systems. *Bioelectrochemistry*, **106**, 328-334.

Santoro, C., Mohidin, A.F., Grasso, L.L., Seviour, T., Palanisamy, K., Hinks, J., Lauro, F.M., Marsili, E. 2016. Sub-toxic concentrations of volatile organic compounds inhibit extracellular respiration of Escherichia coli cells grown in anodic bioelectrochemical systems. *Bioelectrochemistry*, **112**, 173-177.

Sciarria, T.P., Arioli, S., Gargari, G., Mora, D., Adani, F. 2019. Monitoring microbial communities' dynamics during the start-up of microbial fuel cells by high-throughput screening techniques. *Biotechnology Reports*, **21**, e00310.

Seo, J.-S., Keum, Y.-S., Li, Q.X. 2009. Bacterial degradation of aromatic compounds. *International journal of environmental research and public health*, **6**(1), 278-309.

Shen, J., Feng, C., Zhang, Y., Jia, F., Sun, X., Li, J., Han, W., Wang, L., Mu, Y. 2012. Bioelectrochemical system for recalcitrant p-nitrophenol removal. *Journal of hazardous materials*, **209**, 516-519.

Shen, Y., Wang, M., Chang, I.S., Ng, H.Y. 2013. Effect of shear rate on the response of microbial fuel cell toxicity sensor to Cu (II). *Bioresource technology*, **136**, 707-710.

Si, R.-W., Zhai, D.-D., Liao, Z.-H., Gao, L., Yong, Y.-C. 2015. A whole-cell electrochemical biosensing system based on bacterial inward electron flow for fumarate quantification. *Biosensors and Bioelectronics*, **68**, 34-40.

Siddique, T., Fedorak, P.M., Foght, J.M. 2006. Biodegradation of short-chain n-alkanes in oil sands tailings under methanogenic conditions. *Environmental science & technology*, **40**(17), 5459-5464.

Sim, J., Reid, R., Hussain, A., An, J., Lee, H.-S. 2018a. Hydrogen peroxide production in a pilot-scale microbial electrolysis cell. *Biotechnology Reports*, **19**, e00276.

Sonawane, J.M., Ezugwu, C.I., Ghosh, P.C. 2020. Microbial fuel cell-based biological oxygen demand sensors for monitoring wastewater: State-of-the-art and practical applications. *ACS sensors*, **5**(8), 2297-2316.

Stein, N.E., Hamelers, H.M., van Straten, G., Keesman, K.J. 2012a. On-line detection of toxic components using a microbial fuel cell-based biosensor. *Journal of Process Control*, **22**(9), 1755-1761.

Stein, N.E., Hamelers, H.V., Buisman, C.N. 2010. Stabilizing the baseline current of a microbial fuel cell-based biosensor through overpotential control under non-toxic conditions. *Bioelectrochemistry*, **78**(1), 87-91.

Stein, N.E., Hamelers, H.V., Buisman, C.N. 2012b. The effect of different control mechanisms on the sensitivity and recovery time of a microbial fuel cell based biosensor. *Sensors and Actuators B: Chemical*, **171**, 816-821.

Stein, N.E., Hamelers, H.V., Buisman, C.N. 2012c. Influence of membrane type, current and potential on the response to chemical toxicants of a microbial fuel cell based biosensor. *Sensors and Actuators B: Chemical*, **163**(1), 1-7.

Sun, H., Angelidaki, I., Wu, S., Dong, R., Zhang, Y. 2019a. The potential of bioelectrochemical sensor for monitoring of acetate during anaerobic digestion: Focusing on novel reactor design. *Frontiers in microbiology*, **9**, 3357.

Sun, H., Zhang, Y., Wu, S., Dong, R., Angelidaki, I. 2019b. Innovative operation of microbial fuel cell-based biosensor for selective monitoring of acetate during anaerobic digestion. *Science of the Total Environment*, **655**, 1439-1447.

Sun, J.-Z., Peter Kingori, G., Si, R.-W., Zhai, D.-D., Liao, Z.-H., Sun, D.-Z., Zheng, T., Yong, Y.-C. 2015. Microbial fuel cell-based biosensors for environmental monitoring: a review. *Water Science and Technology*, **71**(6), 801-809.

Sung, J.H., Shuler, M.L. 2009. Prevention of air bubble formation in a microfluidic perfusion cell culture system using a microscale bubble trap. *Biomedical microdevices*, **11**(4), 731-738.

Sungpet, A., Pimsert, A., Jiraratananon, R., Way, J. 2002. Facilitated transport of unsaturated hydrocarbons through crosslinked-poly (sulfonated styrene). *Chemical Engineering Journal*, **87**(3), 321-328.

Tan, Y.C., Kharkwal, S., Chew, K.K.W., Alwi, R., Mak, S.F.W., Ng, H.Y. 2018. Enhancing the robustness of microbial fuel cell sensor for continuous copper(II) detection against organic strength fluctuations by acetate and glucose addition. *Bioresour Technol*, **259**, 357-364.

Theodosiou, P., Greenman, J., Ieropoulos, I.A. 2020. Developing 3D-Printable Cathode Electrode for Monolithically Printed Microbial Fuel Cells (MFCs). *Molecules*, **25**(16), 3635.

Timmers, R.A., Rothballer, M., Strik, D.P., Engel, M., Schulz, S., Schloter, M., Hartmann, A., Hamelers, B., Buisman, C. 2012. Microbial community structure elucidates performance of Glyceria maxima plant microbial fuel cell. *Applied microbiology and biotechnology*, **94**(2), 537-548.

Torres, C.I., Lee, H.-S., Rittmann, B.E. 2008. Carbonate species as OH− carriers for decreasing the pH gradient between cathode and anode in biological fuel cells. *Environmental science & technology*, **42**(23), 8773-8777.

Tran, P.H.N., Luong, T.T.T., Nguyen, T.T.T., Nguyen, H.Q., Van Duong, H., Kim, B.H. 2015. Possibility of using a lithotrophic iron-oxidizing microbial fuel cell as a biosensor for detecting iron and manganese in water samples. *Environmental Science: Processes & Impacts*, **17**(10), 1806-1815.

Tremouli, A., Martinos, M., Lyberatos, G. 2017. The effects of salinity, pH and temperature on the performance of a microbial fuel cell. *Waste and biomass valorization*, **8**(6), 2037-2043.

Tront, J.M., Fortner, J., Plötze, M., Hughes, J., Puzrin, A.M. 2008. Microbial fuel cell biosensor for in situ assessment of microbial activity. *Biosensors and Bioelectronics*, **24**(4), 586-590.

Tsuda, H., Hagiwara, A., Shibata, M., Ohshima, M., Ito, N. 1982. Carcinogenic effect of carbazole in the liver of (C57BL/6N× C3H/HeN) F1 mice. *journal of the National Cancer Institute*, **69**(6), 1383-1389.

Tucci, M., Bombelli, P., Howe, C.J., Vignolini, S., Bocchi, S., Schievano, A. 2019. A storable mediatorless electrochemical biosensor for herbicide detection. *Microorganisms*, **7**(12), 630.

Uría, N., Sánchez, D., Mas, R., Sánchez, O., Muñoz, F.X., Mas, J. 2012. Effect of the cathode/anode ratio and the choice of cathode catalyst on the performance of microbial fuel cell transducers for the determination of microbial activity. *Sensors and Actuators B: Chemical*, **170**, 88-94.

Velasquez-Orta, S.B., Werner, D., Varia, J.C., Mgana, S. 2017. Microbial fuel cells for inexpensive continuous in-situ monitoring of groundwater quality. *Water Res*, **117**, 9-17.

Vesvikar, M.S., Al-Dahhan, M. 2005. Flow pattern visualization in a mimic anaerobic digester using CFD. *Biotechnology and Bioengineering*, **89**(6), 719-732.

Wagner, R.C., Regan, J.M., Oh, S.-E., Zuo, Y., Logan, B.E. 2009. Hydrogen and methane production from swine wastewater using microbial electrolysis cells. *water research*, **43**(5), 1480-1488.

Wallace, S., de Solla, S., Head, J., Hodson, P., Parrott, J., Thomas, P., Berthiaume, A., Langlois, V. 2020. Polycyclic aromatic compounds (PACs) in the Canadian environment: Exposure and effects on wildlife. *Environmental Pollution*, 114863.

Wang, C., Klamerth, N., Messele, S.A., Singh, A., Belosevic, M., Gamal El-Din, M. 2016a. Comparison of UV/hydrogen peroxide, potassium ferrate(VI), and ozone in oxidizing the organic fraction of oil sands process-affected water (OSPW). *Water Research*, **100**, 476-485.

Wang, X., Gao, N., Zhou, Q. 2013. Concentration responses of toxicity sensor with Shewanella oneidensis MR-1 growing in bioelectrochemical systems. *Biosensors and Bioelectronics*, **43**, 264-267.

Wang, Y., Wen, Q., Chen, Y., Yin, J., Duan, T. 2016b. Enhanced performance of a microbial fuel cell with a capacitive bioanode and removal of Cr (VI) using the intermittent operation. *Applied biochemistry and biotechnology*, **180**(7), 1372-1385.

Webster, D.P., TerAvest, M.A., Doud, D.F., Chakravorty, A., Holmes, E.C., Radens, C.M., Sureka, S., Gralnick, J.A., Angenent, L.T. 2014. An arsenic-specific biosensor with genetically engineered Shewanella oneidensis in a bioelectrochemical system. *Biosensors and Bioelectronics*, **62**, 320-324.

Weelink, S.A., Van Eekert, M.H., Stams, A.J. 2010. Degradation of BTEX by anaerobic bacteria: physiology and application. *Reviews in Environmental Science and Bio/Technology*, **9**(4), 359-385.

Willie, M., Esler, D., Boyd, W.S., Molloy, P., Ydenberg, R.C. 2017. Spatial variation in polycyclic aromatic hydrocarbon exposure in Barrow's goldeneye (Bucephala islandica) in coastal British Columbia. *Marine Pollution Bulletin*, **118**(1-2), 167-179.

Wu, D., Li, L., Zhao, X., Peng, Y., Yang, P., Peng, X. 2019b. Anaerobic digestion: a review on process monitoring. *Renewable and Sustainable Energy Reviews*, **103**, 1-12.

Wu, L.-C., Tsai, T.-H., Liu, M.-H., Kuo, J.-L., Chang, Y.-C., Chung, Y.-C. 2017. A Green microbial fuel cell-based biosensor for in situ chromium (VI) measurement in electroplating wastewater. *Sensors*, **17**(11), 2461.

Wu, M., Xu, X., Lu, K., Li, X. 2019c. Effects of the presence of nanoscale zero-valent iron on the degradation of polychlorinated biphenyls and total organic carbon by sediment microbial fuel cell. *Science of The Total Environment*, **656**, 39-44.

Xiao, N., Selvaganapathy, P.R., Wu, R., Huang, J.J. 2020a. Influence of wastewater microbial community on the performance of miniaturized microbial fuel cell biosensor. *Bioresource technology*, **302**, 122777.

Xiao, N., Wu, R., Huang, J.J., Selvaganapathy, P.R. 2020b. Development of a xurographically fabricated miniaturized low-cost, high-performance microbial fuel cell and its application for sensing biological oxygen demand. *Sensors and Actuators B: Chemical*, **304**, 127432.

Xing, F., Xi, H., Yu, Y., Zhou, Y. 2020. A sensitive, wide-ranging comprehensive toxicity indicator based on microbial fuel cell. *Science of The Total Environment*, **703**, 134667.

Xu, Z., Liu, B., Dong, Q., Lei, Y., Li, Y., Ren, J., McCutcheon, J., Li, B. 2015. Flat microliter membrane-based microbial fuel cell as "on-line sticker sensor" for self-supported in situ monitoring of wastewater shocks. *Bioresource Technolology*, **197**, 244-51.

Xu, Z., Liu, Y., Williams, I., Li, Y., Qian, F., Zhang, H., Cai, D., Wang, L., Li, B. 2016. Disposable self-support paper-based multi-anode microbial fuel cell (PMMFC) integrated with power management system (PMS) as the real time "shock" biosensor for wastewater. *Biosensors and Bioelectronics*, **85**, 232-239.

Xue, Y., Lu, S., Fu, X., Sharma, V.K., Mendoza-Sanchez, I., Qiu, Z., Sui, Q. 2018. Simultaneous removal of benzene, toluene, ethylbenzene and xylene (BTEX) by CaO2 based Fenton system: Enhanced degradation by chelating agents. *Chemical Engineering Journal*, **331**, 255-264.

Yang, G.-X., Sun, Y.-M., Kong, X.-Y., Zhen, F., Li, Y., Li, L.-H., Lei, T.-Z., Yuan, Z.-H., Chen, G.-Y. 2013. Factors affecting the performance of a single-chamber microbial fuel cell-type biological oxygen demand sensor. *Water science and technology*, **68**(9), 1914-1919.
Yang, K., Ji, M., Liang, B., Zhao, Y., Zhai, S., Ma, Z., Yang, Z. 2020. Bioelectrochemical degradation of monoaromatic compounds: Current advances and challenges. *Journal of Hazardous Materials*, 122892.
Yang, W., Wei, X., Fraiwan, A., Coogan, C.G., Lee, H., Choi, S. 2016. Fast and sensitive water quality assessment: a μL-scale microbial fuel cell-based biosensor integrated with an air-bubble trap and electrochemical sensing functionality. *Sensors and Actuators B: Chemical*, **226**, 191-195.
Yang, Y., Wang, Y.-Z., Fang, Z., Yu, Y.-Y., Yong, Y.-C. 2018. Bioelectrochemical biosensor for water toxicity detection: generation of dual signals for electrochemical assay confirmation. *Analytical and bioanalytical chemistry*, **410**(4), 1231-1236.
Yang, Y., Zhou, H., Mei, X., Liu, B., Xing, D. 2018. Dual-edged character of quorum sensing signaling molecules in microbial extracellular electron transfer. *Frontiers in microbiology*, **9**.
Yao, S., Meyer, A., Henze, G. 1991. Comparison of amperometric and UV-spectrophotometric monitoring in the HPLC analysis of pesticides. *Fresenius' journal of analytical chemistry*, **339**(4), 207-211.
Yi, Y., Xie, B., Zhao, T., Li, Z., Stom, D., Liu, H. 2019a. Effect of external resistance on the sensitivity of microbial fuel cell biosensor for detection of different types of pollutants. *Bioelectrochemistry*, **125**, 71-78.
Yi, Y., Xie, B., Zhao, T., Liu, H. 2018. Comparative analysis of microbial fuel cell based biosensors developed with a mixed culture and Shewanella loihica PV-4 and underlying biological mechanism. *Bioresource technology*, **265**, 415-421.
Yi, Y., Xie, B., Zhao, T., Qian, Z., Liu, H. 2019b. Effect of control mode on the sensitivity of a microbial fuel cell biosensor with Shewanella loihica PV-4 and the underlying bioelectrochemical mechanism. *Bioelectrochemistry*, **128**, 109-117.
Yi, Y., Xie, B., Zhao, T., Qian, Z., Liu, H. 2020. The effect of anode hydrodynamics on the sensitivity of microbial fuel cell based biosensors and the biological mechanism. *Bioelectrochemistry*, **132**, 107351.
You, J., Preen, R.J., Bull, L., Greenman, J., Ieropoulos, I. 2017. 3D printed components of microbial fuel cells: Towards monolithic microbial fuel cell fabrication using additive layer manufacturing. *Sustainable Energy Technologies and Assessments*, **19**, 94-101.
Yu, D., Bai, L., Zhai, J., Wang, Y., Dong, S. 2017. Toxicity detection in water containing heavy metal ions with a self-powered microbial fuel cell-based biosensor. *Talanta*, **168**, 210-216.
Yu, D., Zhang, H., Bai, L., Fang, Y., Liu, C., Zhang, H., Li, T., Han, L., Yu, Y., Yu, H. 2020b. Visual detection of the toxicity of wastewater containing heavy metal ions using a microbial fuel cell biosensor with a Prussian blue cathode. *Sensors and Actuators B: Chemical*, **302**, 127177.
Yu, X., Lee, K., Ma, B., Asiedu, E., Ulrich, A.C. 2018. Indigenous microorganisms residing in oil sands tailings biodegrade residual bitumen. *Chemosphere*, **209**, 551-559.

Zakaria, B.S., Barua, S., Sharaf, A., Liu, Y., Dhar, B.R. 2018. Impact of antimicrobial silver nanoparticles on anode respiring bacteria in a microbial electrolysis cell. *Chemosphere*, **213**, 259-267.

Zakaria, B.S., Dhar, B.R. 2019. Progress towards catalyzing electro-methanogenesis in anaerobic digestion process: Fundamentals, process optimization, design and scale-up considerations. *Bioresource technology*, 121738.

Zakaria, B.S., Dhar, B.R. 2020. An intermittent power supply scheme to minimize electrical energy input in a microbial electrolysis cell assisted anaerobic digester. *Bioresource Technology*, 124109.

Zeng, S., Gan, N., Weideman-Mera, R., Cao, Y., Li, T., Sang, W. 2013. Enrichment of polychlorinated biphenyl 28 from aqueous solutions using Fe3O4 grafted graphene oxide. *Chemical engineering journal*, **218**, 108-115.

Zeng, X., Borole, A.P., Pavlostathis, S.G. 2016. Inhibitory effect of furanic and phenolic compounds on exoelectrogenesis in a microbial electrolysis cell bioanode. *Environmental science & technology*, **50**(20), 11357-11365.

Zhang, C., Li, Y., Shen, H., Shuai, D. 2020. Simultaneous coupling of photocatalytic and biological processes: A promising synergistic alternative for enhancing decontamination of recalcitrant compounds in water. *Chemical Engineering Journal*, 126365.

Zhang, D., Wang, Y., Li, C., Zhang, X. 2019. Polychlorinated biphenyl detection in organic solvents with paper-based analytical devices. *Environmental Technology*, 1-6.

Zhang, H., Yuan, X., Xiong, T., Wang, H., Jiang, L. 2020b. Bioremediation of co-contaminated soil with heavy metals and pesticides: influence factors, mechanisms and evaluation methods. *Chemical Engineering Journal*, 125657.

Zhang, J. 1997. Designing a cost-effective and reliable pipeline leak-detection system. *Pipes and Pipelines International*, **42**(1), 20-26.

Zhang, S., You, J., An, N., Zhao, J., Wang, L., Cheng, Z., Ye, J., Chen, D., Chen, J. 2018. Gaseous toluene powered microbial fuel cell: Performance, microbial community, and electron transfer pathway. *Chemical Engineering Journal*, **351**, 515-522.

Zhang, X., Xia, X., Ivanov, I., Huang, X., Logan, B.E. 2014. Enhanced activated carbon cathode performance for microbial fuel cell by blending carbon black. *Environmental science & technology*, **48**(3), 2075-2081.

Zhang, Y. 2016. Development and application of Fenton and UV-Fenton processes at natural pH using chelating agents for the treatment of oil sands process-affected water.

Zhao, L., Deng, J., Hou, H., Li, J., Yang, Y. 2019a. Investigation of PAH and oil degradation along with electricity generation in soil using an enhanced plant-microbial fuel cell. *Journal of Cleaner Production*, **221**, 678-683.

Zhao, L., Wang, C., Gu, H., Yue, C. 2018. Market incentive, government regulation and the behavior of pesticide application of vegetable farmers in China. *Food Control*, **85**, 308-317.

Zhao, T., Xie, B., Yi, Y., Liu, H. 2019b. Sequential flowing membrane-less microbial fuel cell using bioanode and biocathode as sensing elements for toxicity monitoring. *Bioresource Technolology*, **276**, 276-280.

Zhou, T., Han, H., Liu, P., Xiong, J., Tian, F., Li, X. 2017. Microbial fuels cell-based biosensor for toxicity detection: A review. *Sensors*, **17**(10), 2230.
Zhou, Y., Tang, L., Liu, Z., Hou, J., Chen, W., Li, Y., Sang, L. 2017b. A novel anode fabricated by three-dimensional printing for use in urine-powered microbial fuel cell. *Biochemical Engineering Journal*, **124**, 36-43.
Zhu, X., Ni, J. 2009. Simultaneous processes of electricity generation and p-nitrophenol degradation in a microbial fuel cell. *Electrochemistry Communications*, **11**(2), 274-277.
Zou, S., Qin, M., Moreau, Y., He, Z. 2017. Nutrient-energy-water recovery from synthetic sidestream centrate using a microbial electrolysis cell-forward osmosis hybrid system. *Journal of Cleaner Production*, **154**, 16-25.

Appendix

Supplementary Information: Figures

Chapter 3 – SI Figures

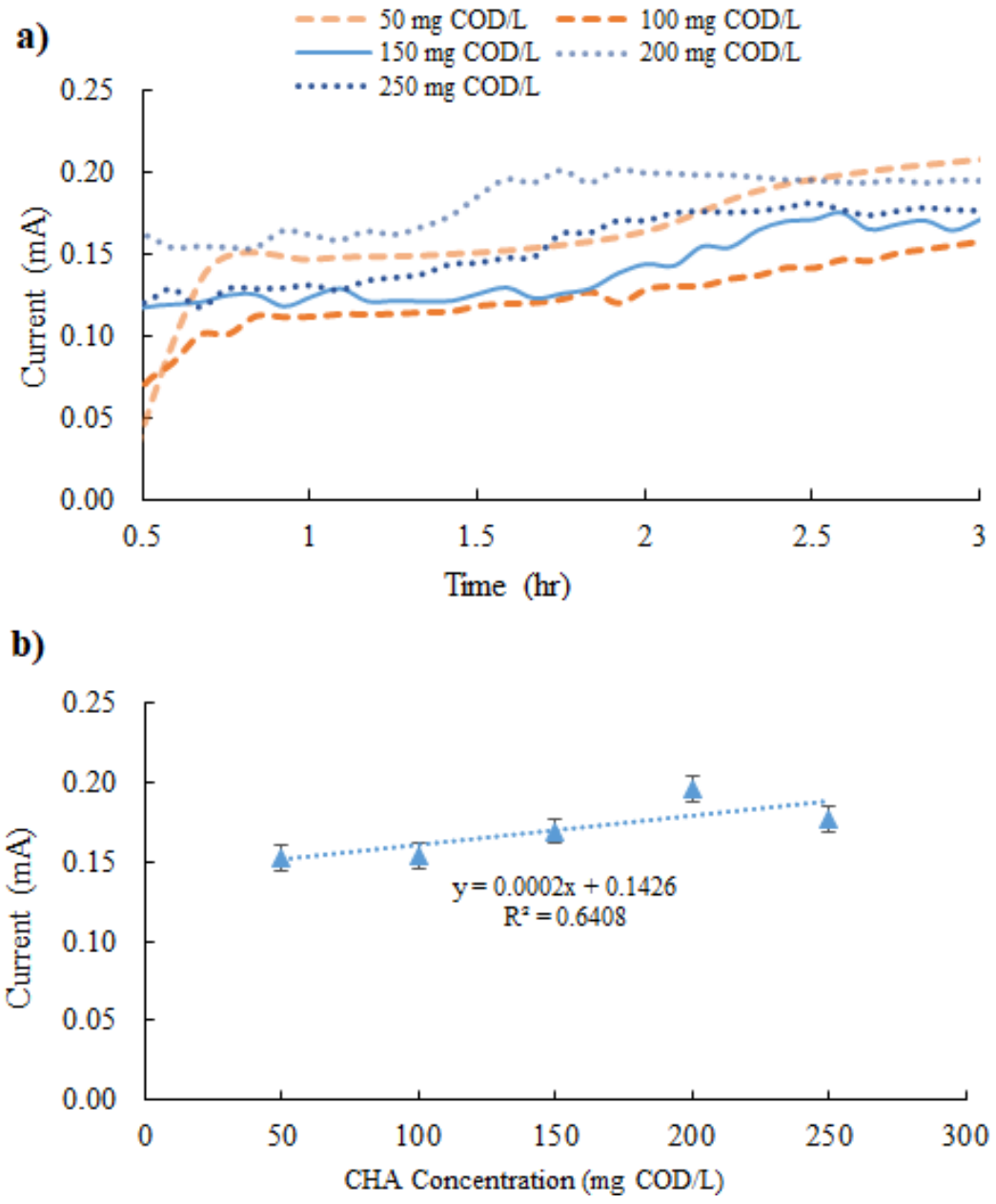

Figure S-1. a) Current profile (mA) versus time (hr) under a closed-circuit operation for the oxidation of CHA; b) Calibration curve of average currents from closed-circuit operations (mA)

versus CHA concentration (mg COD/L). Note steady current regions (changes in current less than 0.005 mA) were different among different CHA concentrations (e.g., 50 mg COD/L: between 1- and 1.5-hour mark. 100 mg COD/L: at ~3-hour mark. 150 mg COD/L: at ~2.5-hour mark. 200 mg COD/L >: between 2.5 and 3-hour mark).

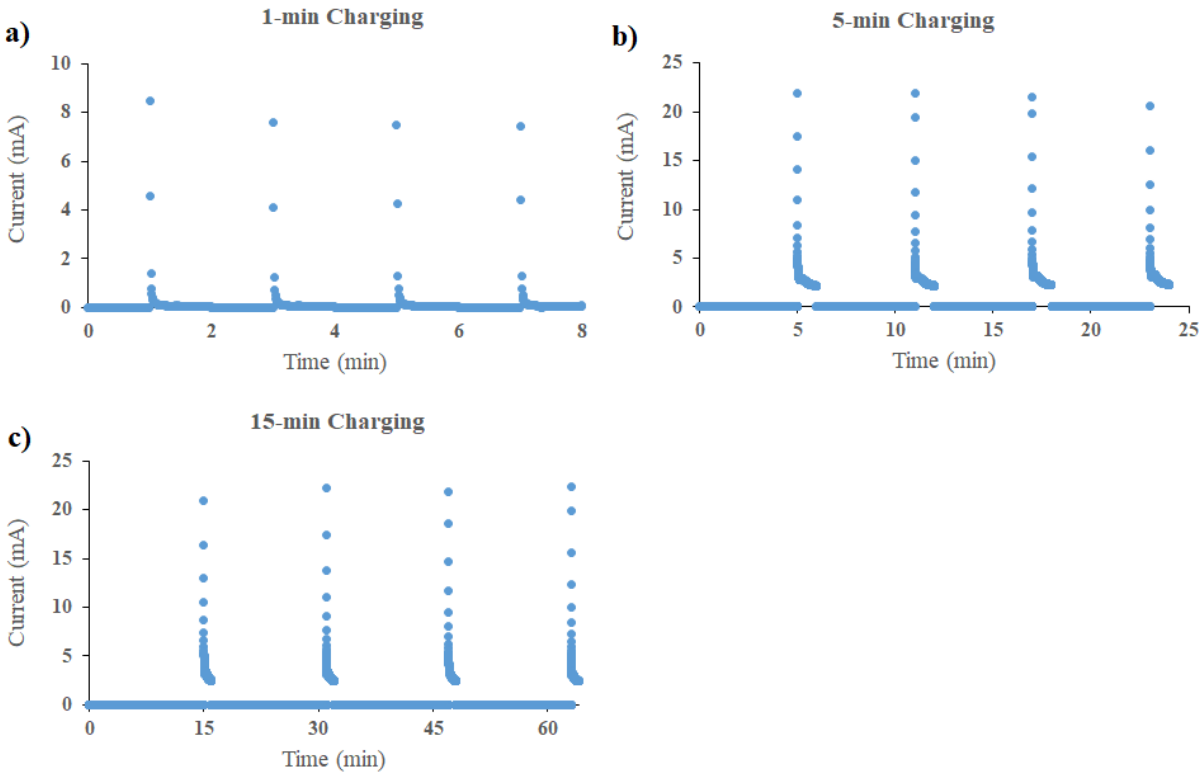

Figure S-2. Experimental results of different charging times for this MXC biosensor system a) 1 minute; b) 5 minutes; c) 15 minutes, with CHA concentrations of 300 mg COD/L, bicarbonate concentrations of 7 mmol/L, and 0 mg/L of salinity.

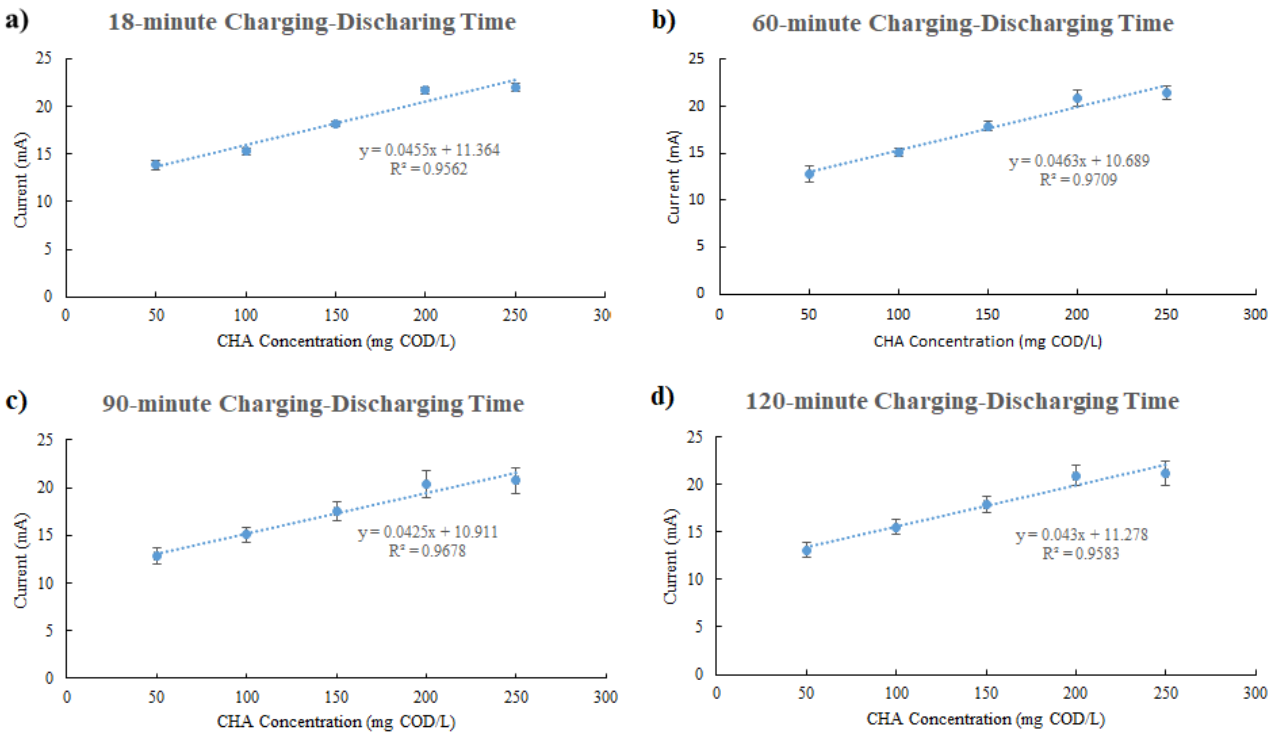

Figure S-3. Calibration curves constructed using charging-discharging operations for a) 18-minute; b) 60-minute; c) 90-minute; d) 120-minute charging-discharging time.

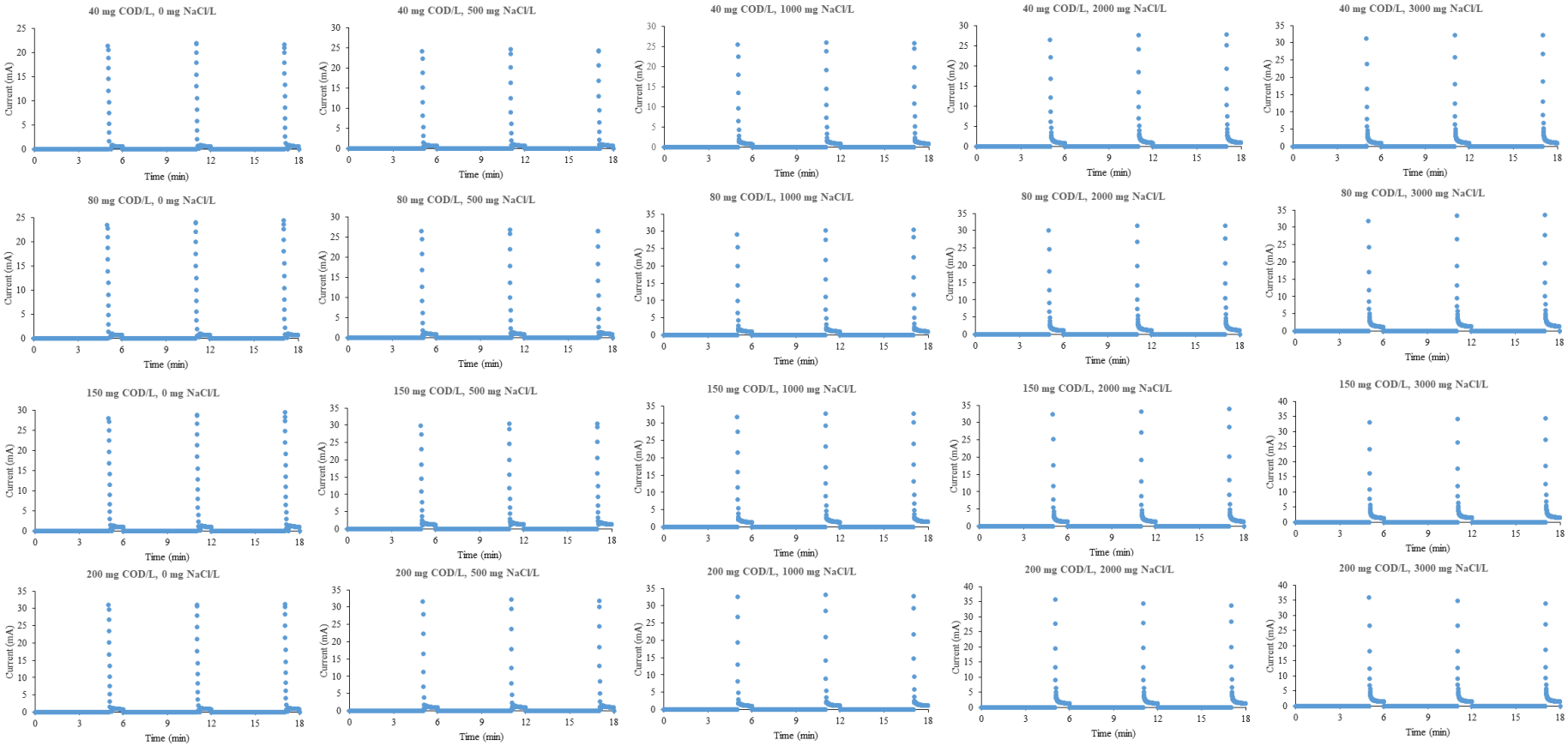

Figure S-4. CHA Charging-discharging curves produced from different salinity levels (0 – 3000 mg/L).

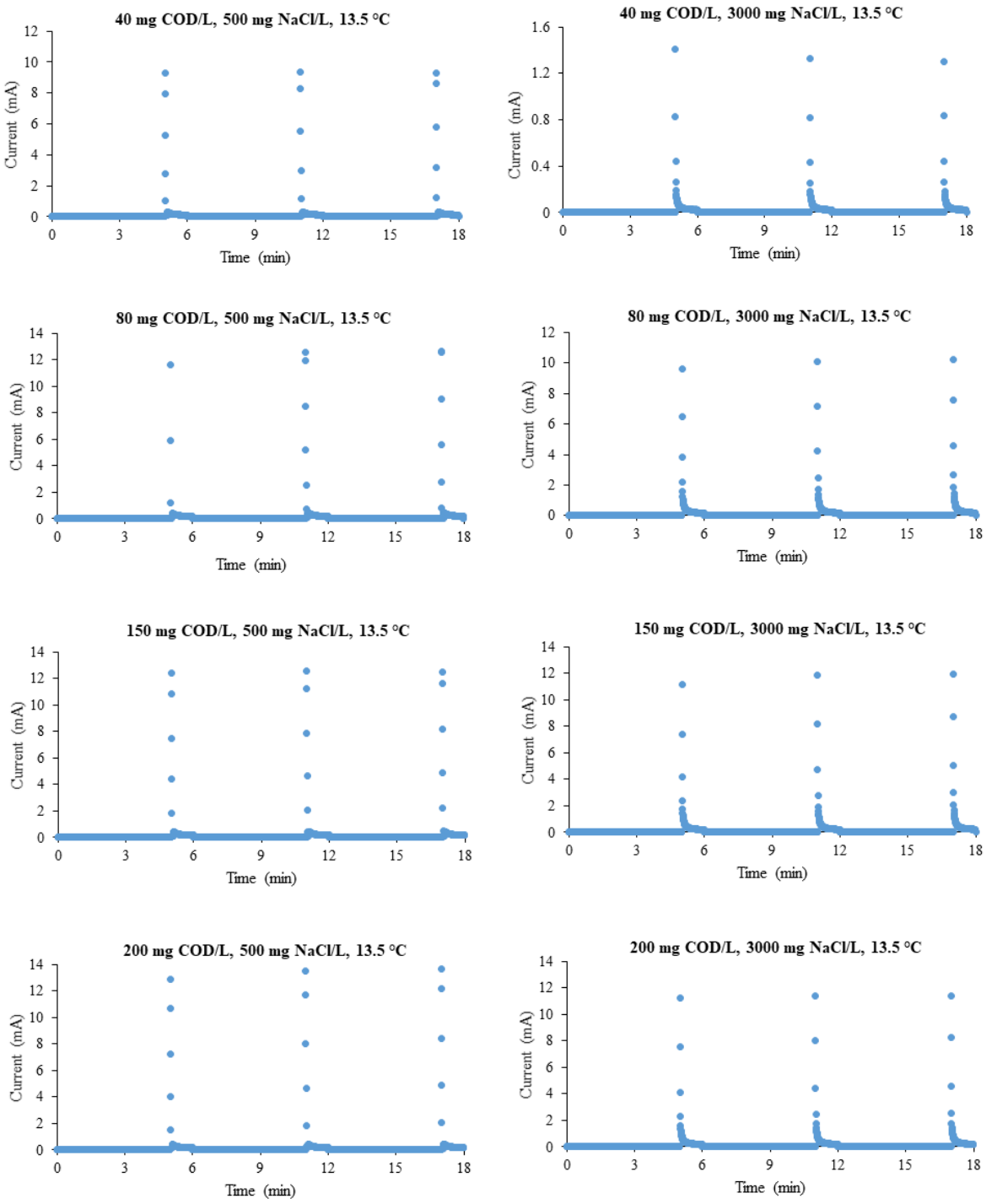

Figure S-5. CHA Charging-discharging curves produced from lowering temperature under a moderate (500 mg/L) and an extreme salinity (3000 mg/L) condition.

Chapter 4 – SI Figures

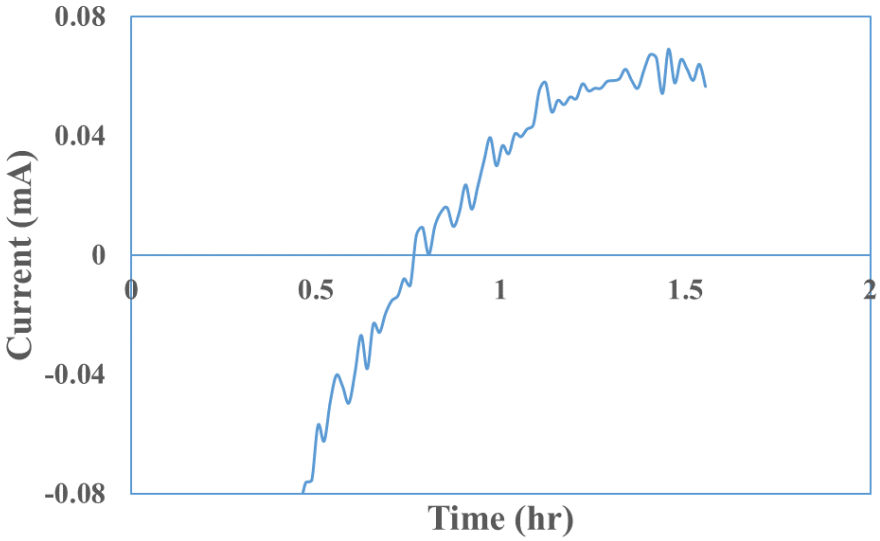

Figure S-6. Example of a commercial NAs batch cycle showing a stable current at >1.5 hours after a complete enrichment using commercial NAs as sole carbon source.

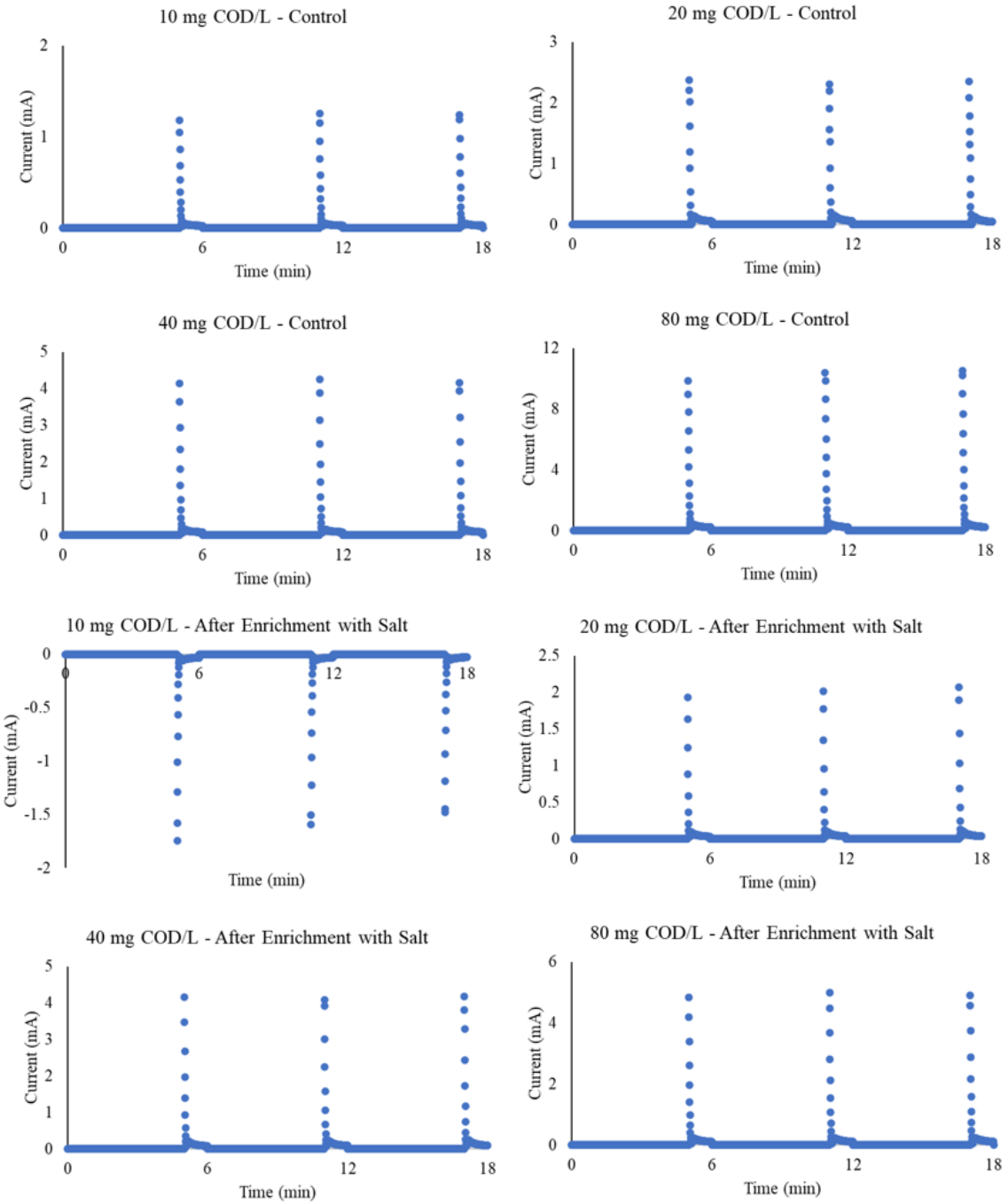

Figure S-7. Charging-discharging curves produced from before enrichment using salt content (control) and after enrichment using salt content (1500 mg/L) using commercial NAs (10 – 80 mg COD/L) as carbon source.

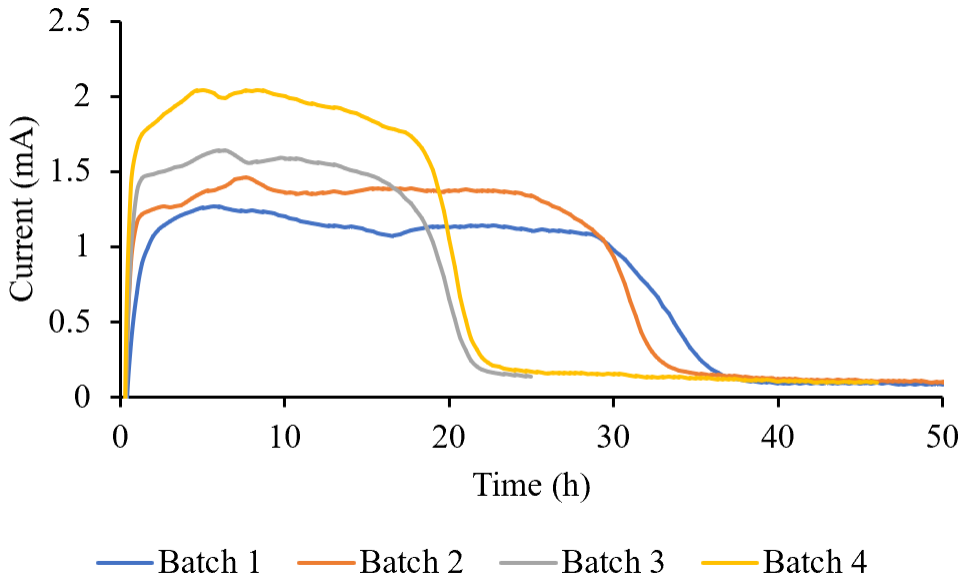

Figure S-8. Recovery of MXC biosensor after long-term exposures (salinity enrichment) of salt content using 10mL Acetate (25 mM).

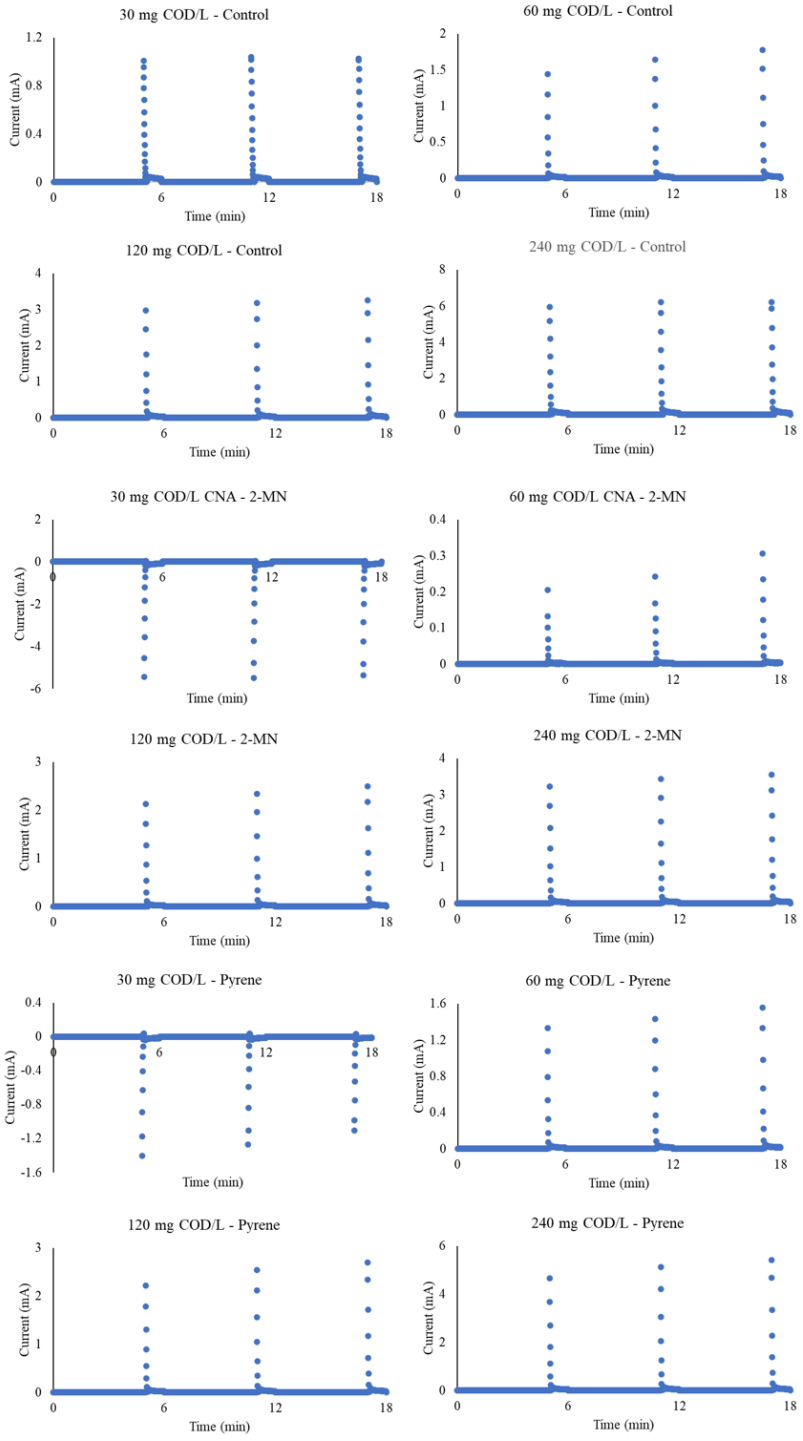

Figure S-9. Charging-discharging curves produced from PAHs (2-MN, 120 mg COD/L and pyrene, 30 mg COD/L) using commercial NAs (30 – 240 mg COD/L) as carbon source.

Supplementary Information: Tables

Chapter 3 – SI Tables

Table S-1. Data of the conductivity values for MFC-biosensor operated in 18-min charging-discharging operation with 7 mmol/L bicarbonate buffer concentration and different NaCl levels.

	Conductivity (mS/cm)				
	Salinity level (NaCl concentration)				
CHA Concentration	0 mg/L	500 mg/L	1000 mg/L	2000 mg/L	3000 mg/L
40 mg COD/L	0.76	1.76	2.71	4.53	6.32
80 mg COD/L	0.75	1.73	2.69	4.46	6.31
150 mg COD/L	0.74	1.69	2.55	4.51	6.13
200 mg COD/L	0.74	1.71	2.60	4.47	6.12

Table S-2. Data of the p-values for salinity and temperature tests.

Experiments	p-values	Significant? (if p-values < 0.05)
Different Salinity Level (0-3000 mg/L) at 20°C	0.017	Yes
Temperature 13.5°C (moderate, 500 mg/L vs. extreme, 3000 mg/L salinity)	0.33	No
Temperature 20.0°C (moderate, 500 mg/L vs. extreme, 3000 mg/L salinity)	0.0053	Yes
500 mg NaCl/L Salinity (13.5°C vs. 20°C)	0.049	Yes
3000 mg NaCl/L Salinity (13.5°C vs. 20°C)	0.28	No